

# 博士論文

**Study on Thermal Performance and Design Optimization of a  
Composite Double-circulation Trombe Wall System Assisted with  
Temperature-controlled DC Fans**

DCファンを用いた複合二重循環式トロンプウォールシ  
ステムの冷暖房負荷削減効果と最適化に関する研究

2022年6月

朱悦玮

ZHU YUEWEI



# **Study on Thermal Performance and Design Optimization of a Composite Double-circulation Trombe Wall System Assisted with Temperature-controlled DC Fans**

## **ABSTRACT**

As the global population grows, energy consumption and environmental issues are a growing concern worldwide. Not only do large buildings need to be considered for energy efficiency, but smaller buildings such as individual homes are also being incorporated into national energy efficiency programs.

This study focuses on an improved method for Trombe walls: installing insulated panels on the inside and using vents at the top and bottom to connect the inner and outer air layers to the interior space. Temperature-controlled DC fans are installed in the upper vent to steadily control air circulation, forming a composite Trombe wall system with dual circulation of the inner and outer air layers. The composite double-circulation Trombe wall system is then analyzed and optimized to achieve the best energy efficiency and indoor thermal comfort.

The structure of the thesis is as follows.

Chapter 1 is the background and purpose of the study. The current status of global energy use and demand as well as Japan's energy and environmental policies are presented, illustrating the role and prospects of passive buildings in the contemporary energy context.

Chapter 2 is a literature review of Trombe wall systems, detailing the basic principles and classification of Trombe walls, and providing a detailed review and summary of existing application strategies for composite Trombe walls and summer Trombe walls. It also summarizes the commonly used optimization parameters of the Trombe wall system and the metrics used for evaluation.

Chapter 3 is the methodology of the study, including the introduction of the actual measurement and simulation software and methods. In this study, the simulation software THERB for HAM was mainly used to compare the results with those of the real measurements and to conduct subsequent optimization experiments.

Chapter 4 is a basic study of the composite double-circulation Trombe wall system. First, the actual measured data are analyzed and compared with the simulation results to verify the feasibility of the software. The simulation software is used to compare the classical Trombe wall house and the composite double-circulation Trombe wall house, and it is found that the double-circulation Trombe wall has better energy efficiency, but still has limitations in terms of solar collector efficiency. Then parameters such as glass performance, fan efficiency, interior wall material and thickness were selected to study the effect of energy consumption of composite double-circulation

Trombe wall system. It is found that the use of winter insulating LOW-E double glazing, higher fan rate, and interior walls with higher thermal resistance can lead to higher efficiency of the composite double-circulation Trombe wall system, which can save about 52.3% of the thermal load after optimization than before optimization again.

Chapter 5 discusses the effect of the glazing surface ratio in the optimized composite Trombe wall system. Temperature and PMV-PPD are used as the main evaluation criteria for indoor thermal comfort, and indoor energy consumption is compared. It was found that the larger the proportion of glazing surface in the optimized composite Trombe wall system, the higher the energy efficiency, but at the same time the more likely the indoor overheating phenomenon. Under experimental conditions, the indoor overheating phenomenon is eliminated when the ratio of glass surface to indoor area is below 0.4.

Chapter 6 discusses the utilization of the composite double-circulation Trombe wall system in summer. The first part focuses on the effect of the ventilation pattern, where the ventilation of air from the interior to the exterior through the air layer of the Trombe wall system is more beneficial to the interior cooling in summer. The second part discusses the effect of thermal storage wall materials, comparing concrete materials, concrete combined with PCM materials in different locations and water walls to investigate the thermal performance and thermal comfort in summer and winter. The study found that PCM not only improves energy efficiency, with a total annual load reduction of 18.3% compared to concrete, but also improves indoor thermal comfort.

Chapter 7 presents the conclusion and discussion of this study and future work.

This paper presents an improved composite Trombe wall system that is simple and inexpensive to build. It is simple to use even in small buildings such as houses. From the environmental and economic point of view, it can reduce the air conditioning load in Kitakyushu, Japan or other hot summer and cold winter regions and can make a significant contribution to the global environment.

*Key words: Solar energy; Trombe wall; Thermal performance; Energy consumption; Thermal comfort*

# Study on Thermal Performance and Design Optimization of a Composite Double-circulation Trombe Wall System Assisted with Temperature-controlled DC Fans

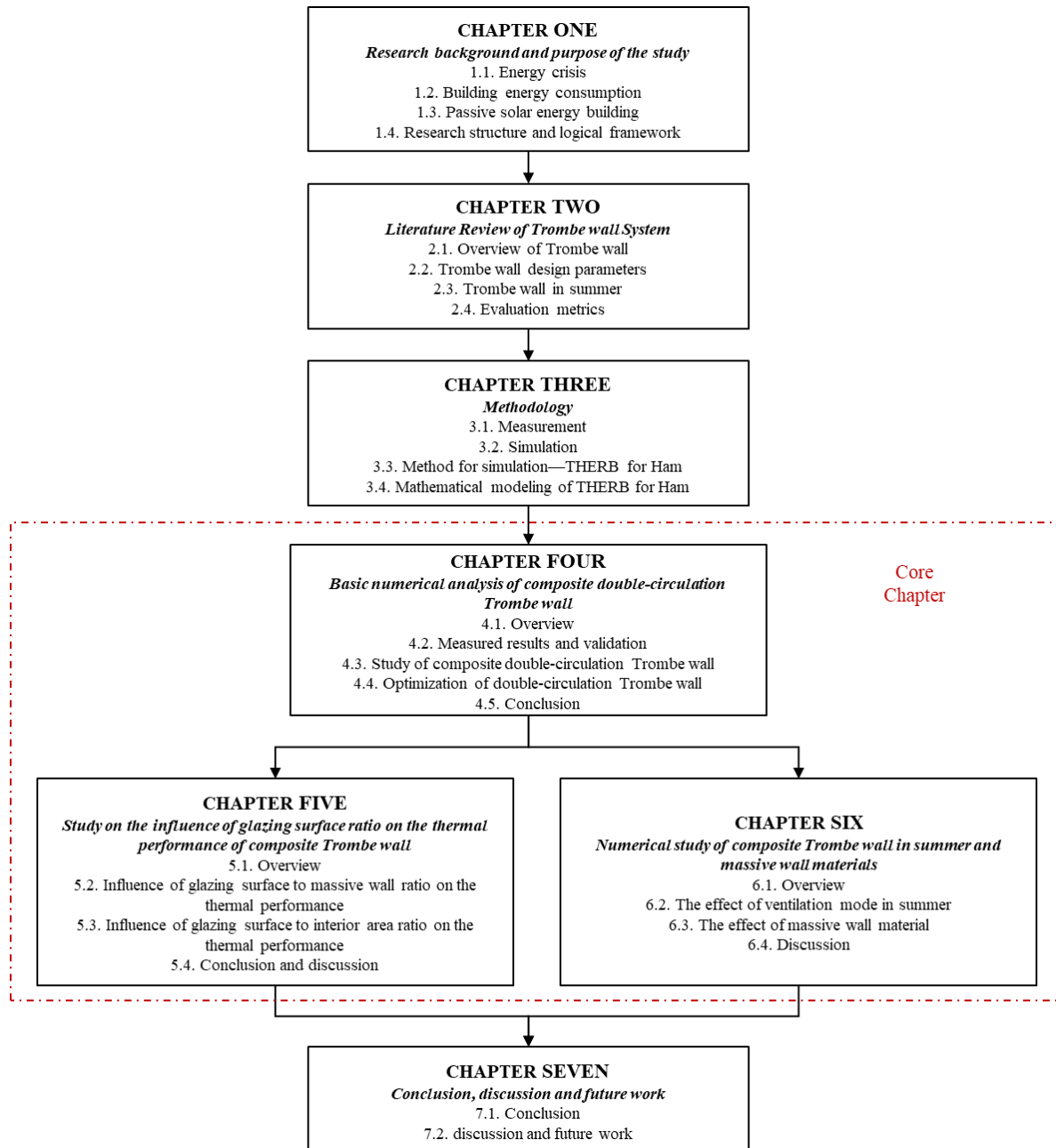


# TABLE OF CONTENTS

<b>ABSTRACT .....</b>	<b>I</b>
-----------------------	----------

<b>STRUCTURE OF THIS PAPER.....</b>	<b>III</b>
-------------------------------------	------------

## **CHAPTER ONE: RESEARCH BACKGROUND AND PURPOSE OF THE STUDY**

1.1 Energy crisis.....	1-1
1.1.1 Global energy .....	1-1
1.1.2 Japan energy.....	1-2
1.2 Building energy consumption .....	1-4
1.3 Passive solar energy building.....	1-4
1.4 Research structure and logical framework.....	1-6
1.4.1 Research purpose and core content.....	1-6
1.4.2 Chapter content overview and related instructions .....	1-8
Reference .....	1-10

## **CHAPTER TWO: LITERATURE REVIEW OF TROMBE WALL SYSTEM**

2.1 Overview of Trombe wall .....	2-1
2.1.1. Classical Trombe wall.....	2-1
2.1.2. Trombe wall classification .....	2-2
2.1.3. Composite Trombe wall .....	2-3
2.2 Trombe wall design parameters.....	2-8
2.2.1. Glazing properties .....	2-9
2.2.2. Massive wall area.....	2-10
2.2.3. Ventilation and air flow in vents.....	2-11
2.2.4. Shading devices.....	2-11

2.2.5. Channel depth.....	2-11
2.2.6. Window effects.....	2-11
2.2.7. Climate effects.....	2-12
2.2.8. Massive wall material properties.....	2-12
2.3 Trombe wall in summer .....	2-16
2.4 Evaluation metrics.....	2-18
2.4.1. Temperature.....	2-18
2.4.2. Energy .....	2-19
2.4.3. Efficiency .....	2-19
2.4.4. Auxiliary energy cost .....	2-19
2.4.5. Life cycle assessment.....	2-20
2.4.6. Payback period.....	2-20
2.4.7. Indoor environment.....	2-20
Reference .....	2-20

### **CHAPTER THREE: METHODOLOGY**

3.1. Measurement.....	3-1
3.1.1. Reference house description .....	3-1
3.1.2. Measuring tool .....	3-2
3.1.3. Weather station.....	3-4
3.2. Simulation.....	3-6
3.2.1. Numerical Model for Validation-reference house .....	3-6
3.2.2. Numerical Model for optimization-Composite Trombe wall house.....	3-9
3.2.3. Weather and location description .....	3-11
3.3. Method for simulation—THERB for Ham .....	3-12
3.3.1. Conductive Heat Transfer .....	3-13

3.3.2. Radiant heat transfer .....	3-14
3.3.3. Incident solar radiation.....	3-14
3.3.4. Ventilation .....	3-15
3.3.5. Conductive Moisture Transfer.....	3-15
3.3.6. Control of space conditioning .....	3-15
3.3.7. Flow Chart .....	3-15
3.4. Mathematical modeling of THERB for Ham.....	3-17
3.4.1. Mathematical modeling of PCM.....	3-17
3.5.2. Additional mathematical modeling .....	3-18
Reference .....	3-19

### **CHAPTER THREE: BASIC NUMERICAL ANALYSIS OF COMPOSITE DOUBLE-CIRCULATION TROMBE WALL**

4.1. Overview.....	4-1
4.2. Measured results and validation.....	4-1
4.2.1. Analysis of actual measurement results .....	4-1
4.2.2. Validation of simulation results.....	4-5
4.3. Study of composite double-circulation Trombe wall .....	4-11
4.3.1. Introduction.....	4-11
4.3.2. Result .....	4-16
4.4. Optimization of double-circulation Trombe wall.....	4-24
4.4.1. The effect of glazing surface properties .....	4-25
4.4.2. The effect of DC fan rates .....	4-33
4.4.3. The effect of inner wall properties .....	4-40
4.4.4. The effect of massive wall properties.....	4-52
4.4.5. Comprehensive optimization considerations.....	4-59

4.5. Conclusion .....	4-62
Reference .....	4-64

**CHAPTER FIVE: STUDY ON THE INFLUENCE OF GLAZING SURFACE RATIO ON THE THERMAL PERFORMANCE OF COMPOSITE TROMBE WALL**

5.1 Overview.....	5-1
5.2. Influence of glazing surface to massive wall ratio on the thermal performance.....	5-3
5.2.1. PMV-PPD description of the optimized composite double-circulation Trombe wall system .....	5-3
5.2.2. Influence of glazing surface to massive wall ratio on the thermal performance.....	5-8
5.3. Influence of glazing surface to interior area ratio on the thermal performance .....	5-15
5.4. Conclusion and discussion.....	5-25
References.....	5-26

**CHAPTER SIX: NUMERICAL STUDY OF COMPOSITE TROMBE WALL IN SUMMER AND MASSIVE WALL MATERIALS**

6.1 Overview.....	6-1
6.2. The effect of ventilation mode in summer .....	6-1
6.2.1. Optimized composite Trombe wall system in summer .....	6-1
6.2.2. The effect of different ventilation mode.....	6-6
6.3. The effect of massive wall material .....	6-19
6.3.1. The effect of massive wall material in summer.....	6-23
6.3.2. The effect of massive wall material in winter .....	6-26
6.3.3. Conclusion .....	6-36
6.4. Discussion.....	6-38
Reference .....	6-39

**CHAPTER 7: CONCLUSION, DISCUSSION AND FUTURE WORK**

7.1 Conclusion ..... 7-1

7.2. Discussion and future work..... 7-2

# *Chapter 1*

## ***RESEARCH BACKGROUND AND PURPOSE OF THE STUDY***



**CHAPTER ONE: RESEARCH BACKGROUND AND PURPOSE OF THE STUDY**

*RESEARCH BACKGROUND AND PURPOSE OF THE STUDY*..... 1-1

1.1 Energy crisis..... 1-1

    1.1.1 Global energy ..... 1-1

    1.1.2 Japan energy..... 1-2

1.2 Building energy consumption ..... 1-4

1.3 Passive solar energy building..... 1-4

1.4 Research structure and logical framework..... 1-6

    1.4.1 Research purpose and core content ..... 1-6

    1.4.2 Chapter content overview and related instructions ..... 1-8

Reference ..... 1-10



## 1.1 Energy crisis

The widespread use of fossil energy sources such as oil, coal and natural gas has driven the rapid development of the world economy. From the three technological revolutions to the present, fossil energy has always been the basis of a country's economic development, and energy plays an irreplaceable role in industrial production as well as in people's productive life. However, fossil energy, as a non-renewable energy source, is gradually depleting under the increasing energy demand of human beings. As the development and utilization of other renewable resources cannot completely replace fossil energy, countries are also intensifying their struggle for energy control, and the competition related to this is becoming more and more intense. Nuclear energy, though, is one of the most promising future energy sources for mankind. However, nuclear power plants produce high- and low-level radioactive waste, have lower thermal efficiency, and emit more waste heat into the environment than general fossil fuel power plants, resulting in more serious thermal pollution. Moreover, the investment cost of nuclear power plants is large and the technical requirements are high, so only a few countries in the world have nuclear power plants. It cannot be widely used in the global human production life.

### 1.1.1 Global energy

Global Energy and Climate Outlook (GECO) 2021 finds that the NDC and LTS pledges to stop global emissions growth over the next decades and lead to declining emissions until 2050. While delivering on these aims results in an increase of global mean temperature of 1.8 °C (current policies in excess of 3 °C), substantial further actions are needed to limit global warming to the Paris Agreement targets, to well below 2 °C and pursue efforts to 1.5 °C above preindustrial levels. To achieve this objective, net-zero greenhouse gas emissions have to be reached around the 2070s at the global level. Nevertheless, the announced LTS pledges could be a major step towards filling this gap, since an NDC-only scenario sees average temperature increases of 2.6 °C at the end of the century [1].

GECO 2021 analyses different plausible policy pathways and assesses their GHG emission and temperature implications<sup>2</sup>. Current policies stabilize emissions, however, only around 2040; hence, additional policies are needed to achieve the targets of the NDC-LTS pathway, which include the stated Nationally Determined Contributions and the Long-Term Climate Strategies announced by the UNFCCC parties. In the NDC-LTS pathway, emissions peak as early as 2023 and then stabilize by mid-century. Emission reductions in the power sector can contribute most towards realizing the emission targets, especially by reducing generation based on coal [2].

In the CurPol scenario, global final energy demand continues to rise, by an average of 1.1% per year over the period 2020-2030. In the CurPol scenario, energy consumption in developed countries

decreases slightly, while demand in developing countries increases. demand only slows down after 2030, growing by an average of 0.5% per year over 2030-2050[1]. For the NDC-LTS and 1.5°C-harmonization scenarios, where ambitious climate policies lead to a slowdown in the growth of final energy consumption after 2020. In the decade 2020-2030, the average annual growth rates are 0.6%/year and 0.3%/year, respectively. In the period 2030-2050, the deceleration intensifies, reaching negative growth of -0.5%/year and -0.8%/year in both scenarios, reaching 8.8 Gtoe and 8.1 Gtoe in 2050[2].

Beyond 2050 the NDC-LTS scenario shows global final energy demand rising again if no further climate policies are put in place, as mitigation once LTS targets are reached is outpaced by increasing economic growth. In the 1.5 °C-Uniform scenario, consumption remains stable after 2050, despite a growing global economy, stabilizing over 2050-2070 with an average growth of 0.2%/year, to reach 8.4 Gtoe in 2070.

At the same time, since the Covid-19 pandemic continues to impact global energy demand from 2019, a series of changes have taken place in the global energy demand. The 4% decline in global energy demand in 2020 is the largest decline since World War II and the largest absolute decline ever. Statistics for energy demand in 2021 highlight the ongoing impact of the pandemic on global energy use. Although the energy demand decreased by 1% in 2020, the power demand in 2021 increased at the fastest rate in more than 10 years [3].

The demand for renewable energy increased by 3% in 2020 and more than 8% in 2021, followed by a rebound in global carbon dioxide emissions, which rebounded by nearly 5% in 2021, close to the peak in 2018-2019[3].

### **1.1.2 Japan energy**

Japan was the tenth largest CO<sub>2</sub> emitter with 1091 Mt CO<sub>2</sub> in 2019. Primary energy demand is currently almost entirely satisfied by imported fossil fuels, as they account for more than 90% of the total, with an oil share of almost 40%. Since the 2013 peak, the decrease in Japan greenhouse gases emissions is essentially driven by nuclear plant restarts after the Fukushima catastrophe, as well as the gradual expansion of renewables and the reduction in primary energy demand. The latter has a key role to play in achieving climate targets because of the high population density of the country, and Japan has already seen decreasing energy consumption [2].

Japan's climate mitigation pathways imply substantial effort, mainly in power generation, shifting from coal and oil to gas, and mostly from fossil fuels to renewables. Nuclear plants account for a constant share of the electricity production and allow non-fossil generation to expand. Solar and wind represent 36% of the total in 2050. The increase in public transportation and in hybridization of private vehicles leads to a decrease in transport emissions until 2030. Afterwards, the effort is

diversified rather equitably in 2050 with the substantial increase of biofuels – mainly from the 2nd generation – and the electrification of the fleet. The progressive development of e-fuels also complements the mitigation.

In October 2020, the new Prime Minister of Japan declared that by 2050 Japan will aim to reduce greenhouse gas emissions to net-zero and to realize a carbon-neutral, decarbonized society. Despite all efforts, Japan remains heavily reliant on imported fossil fuels. In 2019, fossil fuels accounted for 88% of total primary energy supply (TPES), that is, its energy self-sufficiency rate is only about 12.1%, the sixth-highest share among ABBREVIATION for International Energy Agency (IEA) countries. Reaching carbon neutrality by 2050 requires steep emission reductions as early as possible and latest from 2030 onwards, and the quick implementation of a wide set of policies and measures. The Green Growth Strategy will have implications for the next Strategic Energy Plan that is currently under discussion, and which may include a revised 2030 energy mix [4]. As for the import of energy resource for Japan, the proportion of fossil fuels that imported from the other countries is summarized in Table 1.1. Of the mentioned, about 88% of oil is imported from the Middle East. In terms of coal, Japan is highly dependent on Australia. In terms of LNG, it is purchasing from diversified regions such as Australia, Asia, Russia and the Middle East.

**Table 1.1 Japan’s dependency on imports from overseas for fossil fuel resources**

Oil	99.7%
LNG	97.5%
Coal	99.3%

Since the 2011 East Japan earthquake, coupled with the timing of the nuclear leak at the Fukushima nuclear power plant, Japan's nuclear power generation has fallen sharply. The shutdown of nuclear power was compensated by increasing thermal power generation operations. As a result, fossil fuel power generation increased and peaked in 2014. Due to the shortage of resources in Japan, fossil fuels are dependent on overseas imports. As a result, the cost of power generation gradually increased after 2011, reaching 25.5 yen/kWh for household electricity in 2014. However, due to technological advances in renewable energy and subsidies from the FIT system, electricity generation from renewable energy also showed an upward trend after 2011, reaching 8.1% of total electricity generation in 2017. At the same time, electricity prices started to fall again due to the lowest marginal cost of renewables and reduced initial investments. Another factor that has affected electricity prices in recent years is the "surcharge" paid by electricity consumers. The surcharge has increased year by year, reaching about 23.2 yen/kWh so far in 2019.

## 1.2 Building energy consumption

With the growing of global population, energy consumption and environmental issues are now a growing concern worldwide. According to the World Energy Council, primary energy demand will double by 2050 [6].

The construction industry is the world's most energy-consuming, most of which is used in heating, ventilation and air conditioning systems (HVAC). There are two ways to define building energy consumption: one is building energy consumption in a broad sense, and the other is building energy consumption in a narrow sense. The former includes more indicators, including energy consumption in the production of building materials, indirect energy consumption such as building construction and energy consumption in the operation of various energy-using equipment in buildings. The narrow sense of building energy consumption refers specifically to the operational energy consumption of buildings, which is the energy consumption of equipment used in people's daily life, such as heating, cooling, air conditioning, lighting, etc. [7]. Building energy consumption for cooling and heating accounts for 18–73% of overall energy consumption. Heating energy consumption occupies 32–33% of the overall building energy consumption [8].

Japan's buildings consume more than 30% of its energy consumption [9] In recent years, standards for energy saving have been reviewed as the awareness of energy and global warming grows., measures for improving thermal insulation, energy generation, and efficient energy usage in houses are considered important. Their purpose is to realize a 10 % increase in the ratio of renewable energy per primary energy supply by 2020, through promoting solar energy and solar light [10]. The use of solar design for achieving thermal comfort inside a building is a growing concern over the building energy conservation [11]. The solar techniques can reduce yearly heating requirement by 25% [11]. The optimal architectural design strategies could save 63% to 76% of energy [12]. Japan has strengthened its efforts to improve energy consumption efficiency and achieved a reduction in energy consumption by about 62 million kl crude oil equivalent. The highest percentage of its planned abatement by 2030 is for households. The goal is to improve energy consumption efficiency by about 40%, to reach an all-time high level [5].

In the housing sector, with the aim of ensuring energy efficiency at the level of net Zero Energy Houses (ZEH) standards for new houses and buildings built after 2030, efforts are underway to make energy efficiency standards mandatory and raise those standard levels under the Act on the Improvement of Energy Consumption Performance of Buildings, as well as raise the “top-runner” standards in building materials and equipment [5].

## 1.3 Passive solar energy building

Solar energy is the most direct and simple clean energy that buildings can use. With the gradual

reduction of fossil energy and the increasingly serious energy crisis, passive buildings are gaining more and more attention due to their low, zero or even negative energy consumption, and more and more people are gradually recognizing passive building energy efficiency technology as the most reasonable and effective building energy saving technology [11]. The original intention of passive building is to minimize the energy consumption of winter heating and rely on measures such as thermal insulation and solar radiation to ensure a higher indoor temperature, while the current passive building refers to the analysis of local climate characteristics and geological environment features, comprehensive consideration of the building's body shape, layout, envelope structure, surrounding environment and other factors, making full use of climate and environmental resources without relying on external energy and mechanical equipment to achieve comfort of indoor directly heating in winter and cooling in summer [13], which is different from active buildings that rely on energy sources such as electricity and equipment such as air conditioning to achieve thermal comfort. [12, 13]

Passive solar technology can reduce annual heating demand by 25% [6]. Use a variety of construction equipment in buildings such as solar chimneys [14], solar roofs [15], Trombe walls, etc. OM solar is one of the cases, combining the characteristics of various passive solar houses and forming the unique Orange Mode.

OM solar system absorbs and stores heat through the air interlayer on the roof during the daytime in winter, and is carried by air currents to various heat storage bodies in the house for storage, and slowly releases heat from sunset to the next morning to maintain the room temperature [16]. Its basic structure is shown in the figure1.3.1. Winter system operation flow: The atmosphere enters from the bottom of the eaves, is heated by the solar energy absorbed by the roof, collects hot air in the ducts, and then is powered by the fan in the OM air treatment box, and the hot airflow is collected under the floor. It is finally sent into the room through the air outlets on both sides of the room. The heated air heats the concrete layer in the subfloor on one side and flows into the room on the other side. When the outdoor temperature drops at night, the heat storage concrete starts to slowly release heat into the room, so that the temperature of the whole room starts to rise from under the floor [17,18].

In summer, the roof air interlayer creates an insulation layer that can be used to produce hot water from the OM treatment tank on the one hand, and to remove waste heat directly from the room through the OM treatment tank on the other hand, so that the presence of the insulation layer can maintain a relatively low temperature in the room.

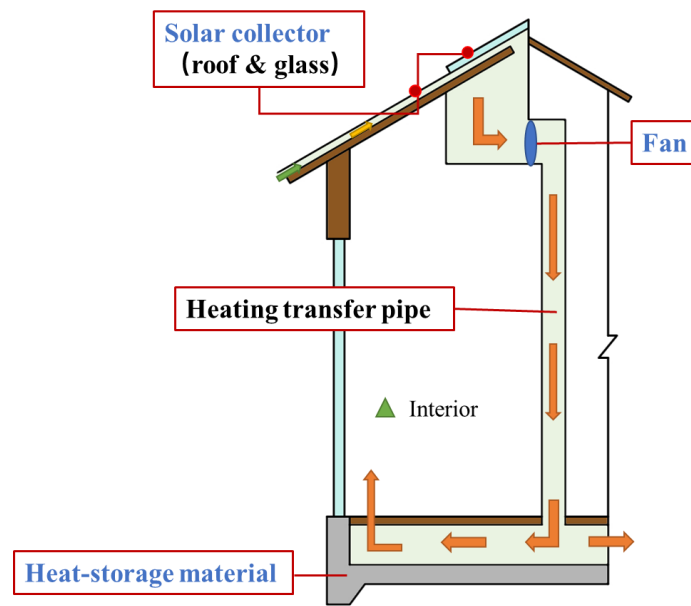


**Figure 1.3.1 OM solar system**

Among these devices, Trombe walls [19], which are called storage walls and solar heated walls (SHW), can coordinate the relationship between people and the natural environment and society, and because of its simple configuration, efficiency High, operating costs and other advantages have been widely used. In addition to environmental protection, the use of Trombe walls in buildings can reduce building energy consumption by up to 30% [20].

## 1.4 Research structure and logical framework

### 1.4.1 Research purpose and core content

In the context of global energy shortage and the promotion of net Zero Energy Houses in Japan, passive building using solar energy is the focus of this study. In this study, we study and research one of the Trombe wall of passive building technology: composite Trombe wall system, and focus on a new composite double-circulation Trombe wall system as figure 1.4.1. This new composite Trombe wall improves the efficiency of air exchange between the air layer in the Trombe wall system and the room in winter by connecting the air of the outer air layer to the room through the vent pipe as well, based on the traditional Trombe wall Michael.

The study first needed to verify the accuracy of the simulation software THERB for HAM in simulating the exchange between the air layer and the room air in the Trombe wall system. The new composite Trombe wall system will be compared with the HAM software to confirm its superiority in terms of energy efficiency. For the sake of its shortcomings, choose the direction and conditions of optimization. Using the control variable method to simulate and compare the selected optimization parameters, select the best optimization conditions from various aspects, conduct the

integration discussion. To achieve a high efficiency, some influencing factors must be considered when designing Trombe wall system in building, including Trombe wall design parameter (outer skin glazing properties, Trombe wall's area, channel depth, massive wall properties, shading devices), building parameters (construction materials, window effects), site parameters (solar radiation and orientation, wind speed and direction).

The study goes from superficial to deep, with comparative studies from various aspects. The study is not limited to the energy efficiency of the new Trombe wall in winter, but also includes a multi-dimensional evaluation of costing, thermal comfort and summer energy savings.

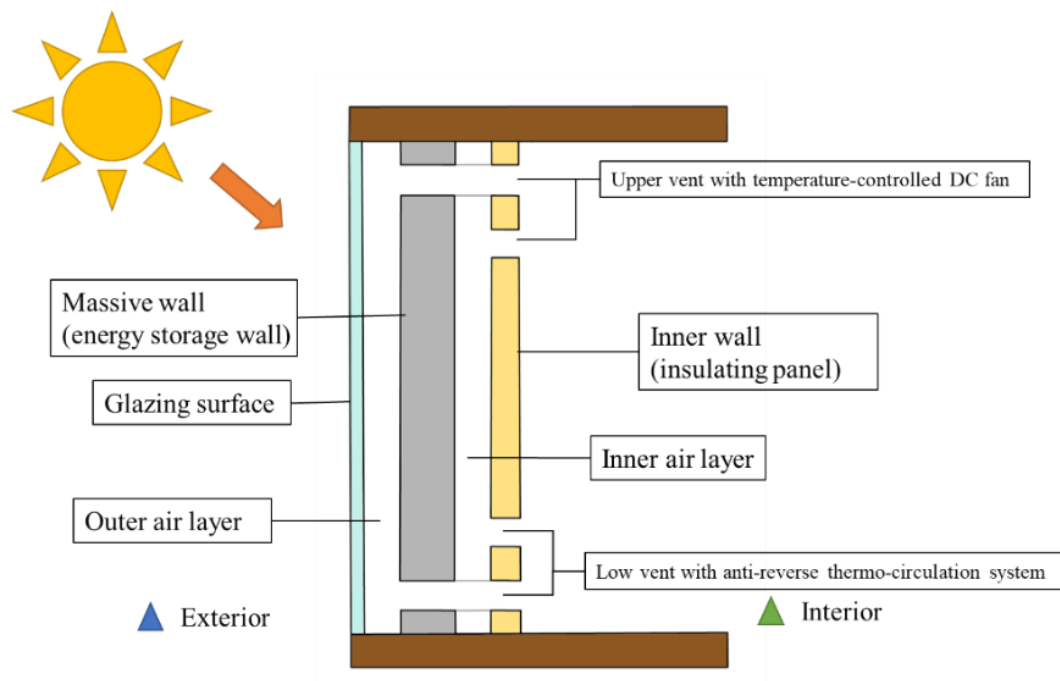


**Figure 1.4.1 The new composite Trombe wall**

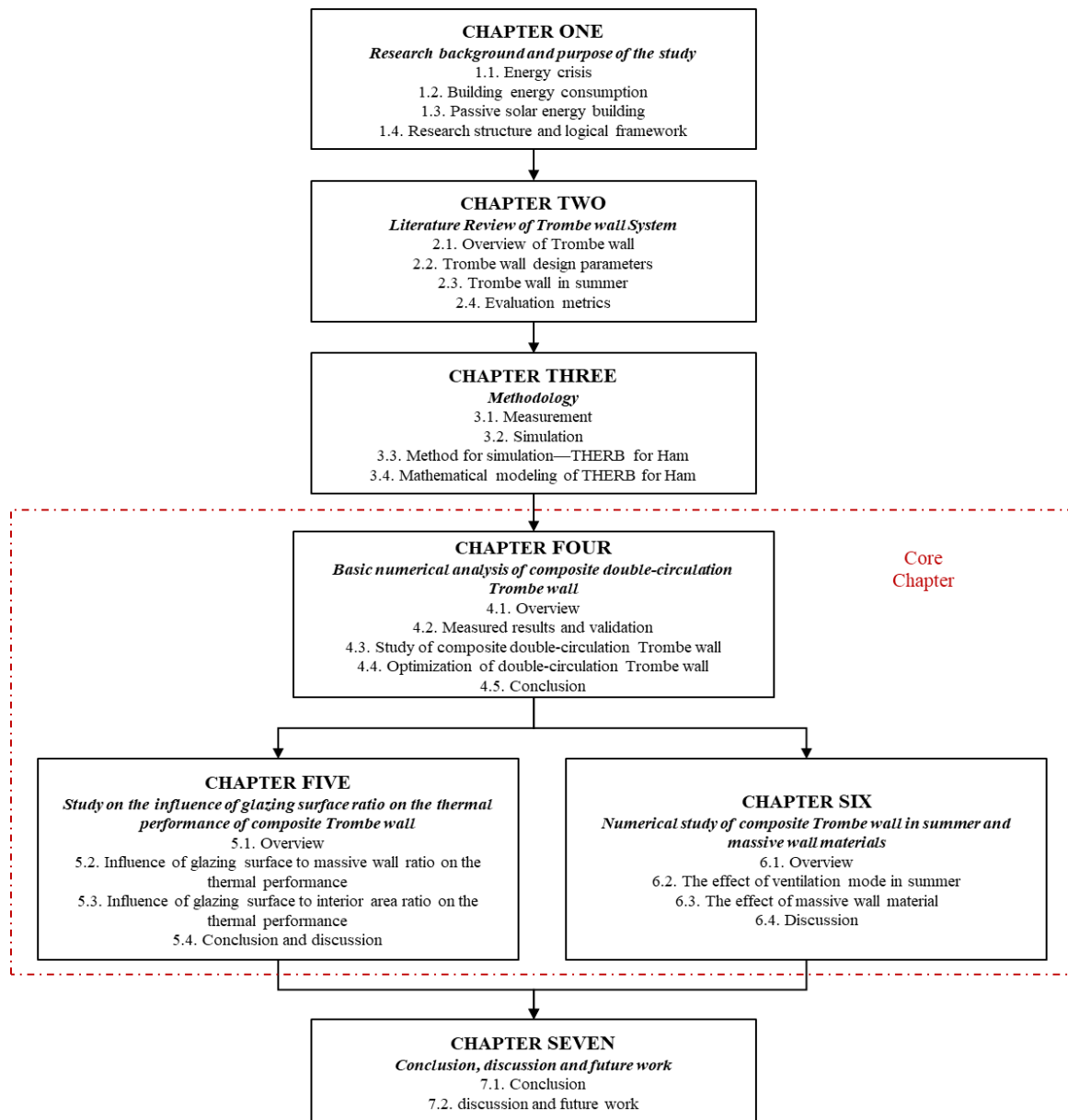


Figure 1.4.2 Framework

### 1.4.2 Chapter content overview and related instructions

In Chapter 1, Research Background and Purpose of the Study:

This Chapter gives the shortage of energy and the need for secure supply, the development of renewable energy is imperative. This chapter analyzes the global energy situation and the evolution of the global economy and energy under the COVID-19 epidemic. It summarizes the trends of renewable energy play. This is followed by a description of Japan's energy structure and dilemma, as well as the policies and goals adopted in recent years in response to energy demand. The independence of energy efficiency in small and medium-sized residential buildings and the

requirement for the development of new energy sources are analyzed, which demonstrates the role of passive buildings in the contemporary energy context. Finally, the research objectives and chapter structure of this paper are presented for the reader's reference.

In Chapter 2, Literature Review of Trombe wall System:

This chapter provides a detailed review of the application and development of Trombe wall systems. Section 2.1 reviews the fundamentals and classification of Trombe walls in general, and provides a detailed review and summary for existing composite Trombe walls, analyzing several existing variant forms. Section 2.2 reviews several variables that affect the efficiency of the Trombe wall system in existing studies and the related results are described. Section 2.3 reviews the application of the Trombe wall system in summer cooling chambers with the existing research results. Section 2.4 reviews the metrics used to evaluate the Trombe wall system, in particular temperature, load, cost, thermal comfort, etc.

In Chapter 3, Methodology:

The first part of this chapter describes the basic information about the buildings used for the real-world analysis and the tools used for the real-world measurements. The second part describes the basics of the digital model created by the simulation and the simulation environment, meteorological description, etc. The third part describes the simulation software THERB for HAM used. As well as the additional necessary calculation equations and software statements.

In Chapter 4, Basic numerical analysis of composite double-circulation Trombe wall:

This chapter first verifies the accuracy of the THERB for HAM software by comparing the actual measurement with the simulation experiment and used numerical simulations using THERB for HAM software to examine and compare the effective method of heat utilization of normal house, classic Trombe wall house and double-circulation Trombe wall house. Double-circulation Trombe wall was found to have a better ability to reduce heat load, but he had limitations in its own solar collector efficiency. Then used numerical simulations by the way of control variable, under the existing model and simulation conditions, we will select the wall material and thickness, glazing properties, ventilation as parameters to study the effect of double-circulation Trombe wall on building energy consumption. And the optimization conditions are combined to obtain a better composite optimization result.

In Chapter 5, Study on the influence of glazing surface ratio on the thermal performance of composite Trombe wall:

This chapter focuses on the optimal design of indoor thermal comfort for a composite double-circulation Trombe wall optimized for winter, mainly by adjusting the ratio of glazing surface to

reduce the storage of solar energy during daytime to achieve a lower peak indoor temperature. The thermal comfort of the interior is evaluated by temperature and PMV-PPD. In the first part, the effect of glazing surface to massive wall ratios on energy consumption and indoor thermal comfort is investigated. The second part investigates the effect of the ratio of floor area to energy consumption and indoor thermal comfort in a composite double-circulation Trombe wall system at the highest efficiency.

In Chapter 6, Numerical study of composite Trombe wall in summer and massive wall materials:

This chapter mainly discusses the utilization of composite double-circulation Trombe wall system in summer. And first part mainly studies the influence of ventilation mode. Another section discusses the effect of massive wall materials, a PCM with different section and water wall were selected and studied with concrete wall for summer and winter thermal performance and thermal comfort.

In Chapter 7, Conclusion, discussion and future work:

This chapter provides the conclusions and highlights the significance of the contribution. Further, composite double-circulation Trombe wall system recommendations based on the findings of this research have been suggested. At the end of the chapter, the limitations of the thesis and directions for future research have been proposed.

## Reference

- [1] Keramidas, K., Diaz Vazquez, A., Weitzel, M., Vandyck, T., Tamba, M., Tchung-Ming, S., Soria Ramirez, A., Krause, J., Van Dingenen, R., Chai, Q., Fu, S. and Wen, X. Global Energy and Climate Outlook 2019: Electrification for the low-carbon transition (2020).
- [2] Keramidas, K., Fosse, F., Díaz Vázquez, A., Dowling, P., Garaffa, R., Després, J., Russ, P., Schade, B., Schmitz, A., Soria Ramirez, A., Vandyck, T., Weitzel, M., Tchung-Ming, S., Diaz Rincon, A., Rey Los Santos, L., Wojtowicz, K. Global Energy and Climate Outlook 2021: Electrification for the low-carbon transition.
- [3] Global Energy Review 2021, <https://www.iea.org/reports/global-energy-review-2021>
- [4] Japan2021\_Energy Policy Review, <https://www.iea.org/reports/japan-2021>
- [5] Ministry of Economy, Trade and Industry, Agency for Natural Resources and Energy. JAPAN'S ENERGY 2019.
- [6] Chan, H.-Y.; Riffat, S. B.; Zhu, J., Review of passive solar heating and cooling technologies. Renewable and Sustainable Energy Reviews 2010, 14, (2), 781-789.
- [7] XIA, Xu; YANG, Qiao-xia; CHEN, Hai-ni. Indicator system of energy efficient technologies

evaluation of residential buildings in hot summer and cold winter regions of China. 2014.

[8] Ürge-Vorsatz, D.; Cabeza, L. F.; Serrano, S.; Barreneche, C.; Petrichenko, K., Heating and cooling energy trends and drivers in buildings. *Renewable and Sustainable Energy Reviews* 2015, 41, (Supplement C), 85-98.

[9] Lee, H.; Ozaki, A.; Lee, M., Energy saving effect of air circulation heat storage system using natural energy. *Building and Environment* 2017, 124, 104-117.

[10] Chel, A.; Nayak, J. K.; Kaushik, G., Energy conservation in honey storage building using Trombe wall. *Energy and Buildings* 2008, 40, (9), 1643-1650.

[11] Liu, Y. W.; Feng, W. In Integrating passive cooling and solar techniques into the existing building in South China, *Advanced Materials Research*, 2012; Trans Tech Publ: 2012; pp 3717-3720.

[12] Naboni, E.; Malcangi, A.; Zhang, Y.; Barzon, F., Defining The Energy Saving Potential of Architectural Design. *Energy Procedia* 2015, 83, 140-146.

[13] Song Q, Yang L, Yin B. Building for Climate: Passive Buildings[J]. *Central China Architecture*, 2014, (4): 11-15.

[13] Zhou B. Research on Passive Building Design Policy in Anhui Province and Simulation Verification Analysis. Diss. Anhui University of Architecture, 2015.

[14] Hami K, Draoui B, Hami O. The thermal performances of a solar wall. *Energy* 2012;39:11–6.

[15] Mazria, Edward (1979). *The Passive Solar Energy Book*. Emmaus, PA: Rodale Press. ISBN 0-87857-237-6.

[16] Li Y. An Overview of OM Solar Homes. *Refrigeration and Air Conditioning (Sichuan)* 2(2009):4.

[17] Youngjin C, Katsuya O, Kozo T, Makoto S, Masayuki M, Hyunwoo R, Seiji K, A Research of Detached Houses with Air-Based Solar System Intended to Full Solar Energy Use, GRAND RENEWABLE ENERGY 2014 Abstracts 27 July-1 August, 2014

[18] OM solar system. <https://omsolar.jp/technology/floor.php>

[19] Zhai XQ, Song ZP, Wang RZ. A review for the applications of solar chimneys in buildings. *Renew Sustain Energy Rev* 2011;15:3757–67.

[20] Fiaschi D, Bertolli A. Design and exergy analysis of solar roofs: a viable solution with esthetic appeal to collect solar heat. *Renew Energy* 2012;46:60–71.

## *Chapter 2*

# ***LITERATURE REVIEW OF TROMBE WALL SYSTEM***



## CHAPTER TWO: LITERATURE REVIEW OF TROMBE WALL SYSTEM

<i>LITERATURE REVIEW OF TROMBE WALL SYSTEM</i> .....	2-1
2.1 Overview of Trombe wall .....	2-1
2.1.1. Classical Trombe wall .....	2-1
2.1.2. Trombe wall classification .....	2-2
2.1.3. Composite Trombe wall .....	2-3
2.2 Trombe wall design parameters .....	2-8
2.2.1. Glazing properties .....	2-9
2.2.2. Massive wall area .....	2-9
2.2.3. Ventilation and air flow in vents .....	2-10
2.2.4. Shading devices .....	2-11
2.2.5. Channel depth .....	2-11
2.2.6. Window effects .....	2-11
2.2.7. Climate effects .....	2-12
2.2.8. Massive wall material properties .....	2-12
2.3 Trombe wall in summer .....	2-16
2.4 Evaluation metrics .....	2-18
2.4.1. Temperature .....	2-18
2.4.2. Energy .....	2-19
2.4.3. Efficiency .....	2-19
2.4.4. Auxiliary energy cost .....	2-19
2.4.5. Life cycle assessment .....	2-20
2.4.6. Payback period .....	2-20

2.4.7. Indoor environment.....	2-20
Reference .....	2-20

## 2.1 Overview of Trombe wall

### 2.1.1. Classical Trombe wall

Since 1881, when Edward Morse first proposed the idea of using solar energy in architecture [1,2], the discussion has never stopped. 1940, Fred Keck painted the walls black, making it possible to convert solar radiation into heat and accumulate it to heat rooms at night [3]. 1967 Felix Trombe and Jacques Michel designed and patented a low-rise apartment building which is known as the classic Trombe wall [4]. The Trombe Wall is a south-oriented energy storage wall with air layer and glazing surface [5-7]. The Trombe wall operational principle is that solar radiation heats a massive wall. A massive wall heats the air in the room by radiation and convective heat exchange. Air vents located in the upper and lower parts of the massive wall are used to ensure the necessary air circulation (Figure 2.1.1) [1,8].

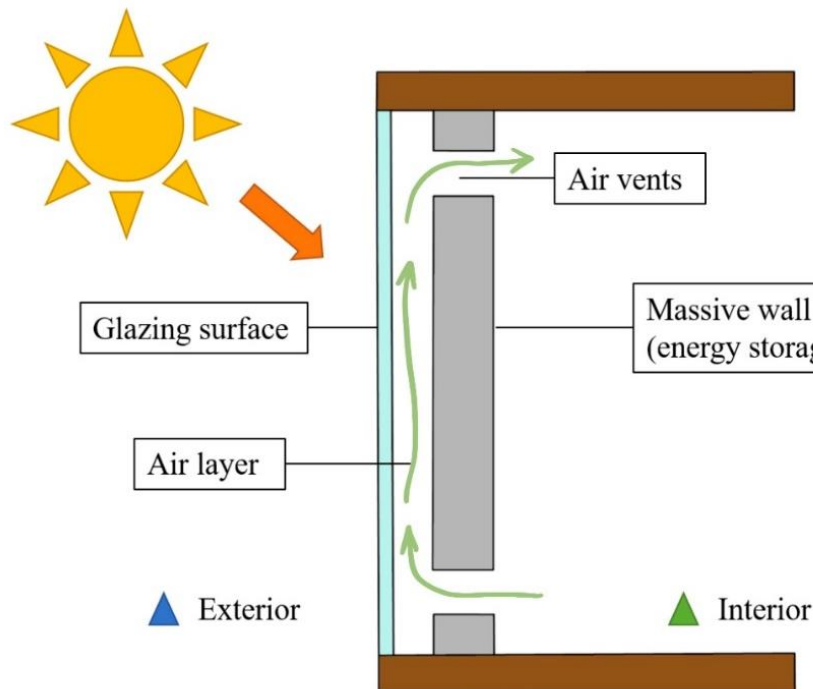


**Figure 2.1.1 A classic Trombe wall**

The classic Trombe wall uses the greenhouse effect of sunlight in the greenhouse to absorb solar radiation and utilize huge walls to absorb and store heat. Part of the energy is transmitted to the interior of the building (room) by conduction. At the same time, the lower temperature air enters the chamber from the room through the lower exhaust port of the wall, is heated by the wall and flows upward due to the buoyancy effect. The heated air then returns to the room through the upper exhaust vent of the wall. Therefore, the heat exchange between the Trombe wall and the indoor environment is transmitted through the wall, and partly through the ventilation of the vent. This simple structure

of the Trombe wall has the following disadvantages [9].

(1) Low thermal resistance (R). Mainly, it means that the massive wall part of the classical Trombe wall needs to be made of materials with better heat transfer and heat storage properties. Based on the calculation of the heat transfer coefficient of the envelope (K):

$$K = 1/R \quad (1)$$

The heat transfer coefficient is the reciprocal of the thermal resistance, and the higher the heat transfer coefficient the lower the thermal resistance of the material. During the night or during extended clouds, some heat flux is transferred from the inside to the outside, which results in excessive heat loss in the building [10].

(2) Reverse thermosiphon phenomenon. When the storage wall is cooler than the air in the venting layer, the air is cooled through the lower vent and reinjected into the chamber, especially during the cold season, thereby lowering the room temperature [11].

(3) Low aesthetic value [12]. Trombe wall to absorb solar radiation more efficiently, a transparent glass surface with a dark colored thermal storage wall needs to be exposed to the outside. The existing Trombe wall design is still in the aspect of thermal performance and environmental protection, and the aesthetic design has not been studied.

### 2.1.2. Trombe wall classification

Over time, Trombe walls have been modified to improve their efficiency. Depending on the main function of the Trombe walls utilized, they are divided into two types: a heated Trombe wall and a cooled Trombe wall. It will present seven different configurations of heated Trombe walls. [9,13]: (1) a classic Trombe wall; (2) a composite Trombe wall or Trombe–Michel wall; (3) a water Trombe wall; (4) a zigzag Trombe wall; (5) a solar trans-wall; (6) a fluidized Trombe wall; (7) a photovoltaic (PV) Trombe wall and (8) a phase changed material (PCM) Trombe wall. Different configurations of cooling-based types of Trombe wall will be introduced: (1) a ceramic evaporative cooling wall; (2) a classic Trombe wall and photovoltaic Trombe wall for cooling operation mode; and (3) a new designed Trombe wall in combination with solar chimney.

Among them, studies on Classic Trombe wall, Water Trombe wall, PCM Trombe wall, PV Trombe wall involved in both heating and cooling of room temperature. However, research on cooling room temperature in summer is relatively missing compared to heating in winter. The research on the application of phase change materials in Trombe wall system is gradually increasing in recent years. PCM is a material with a phase change is a substance with a high heat of fusion. It can accumulate and give off a large amount of thermal energy, when its state is changed. There are two types of PCM materials: organic and inorganic. Inorganic materials include salt hydrates and

their derivatives. Organic materials include paraffin and fatty acids. Such materials are more thermally stable. There is no corrosion and overcooling. However, these materials are highly flammable and have low thermal conduction. The details of this kind of Trombe wall will be described in the following section.

Figure 2.1.2 illustrates a summary of the above classification.

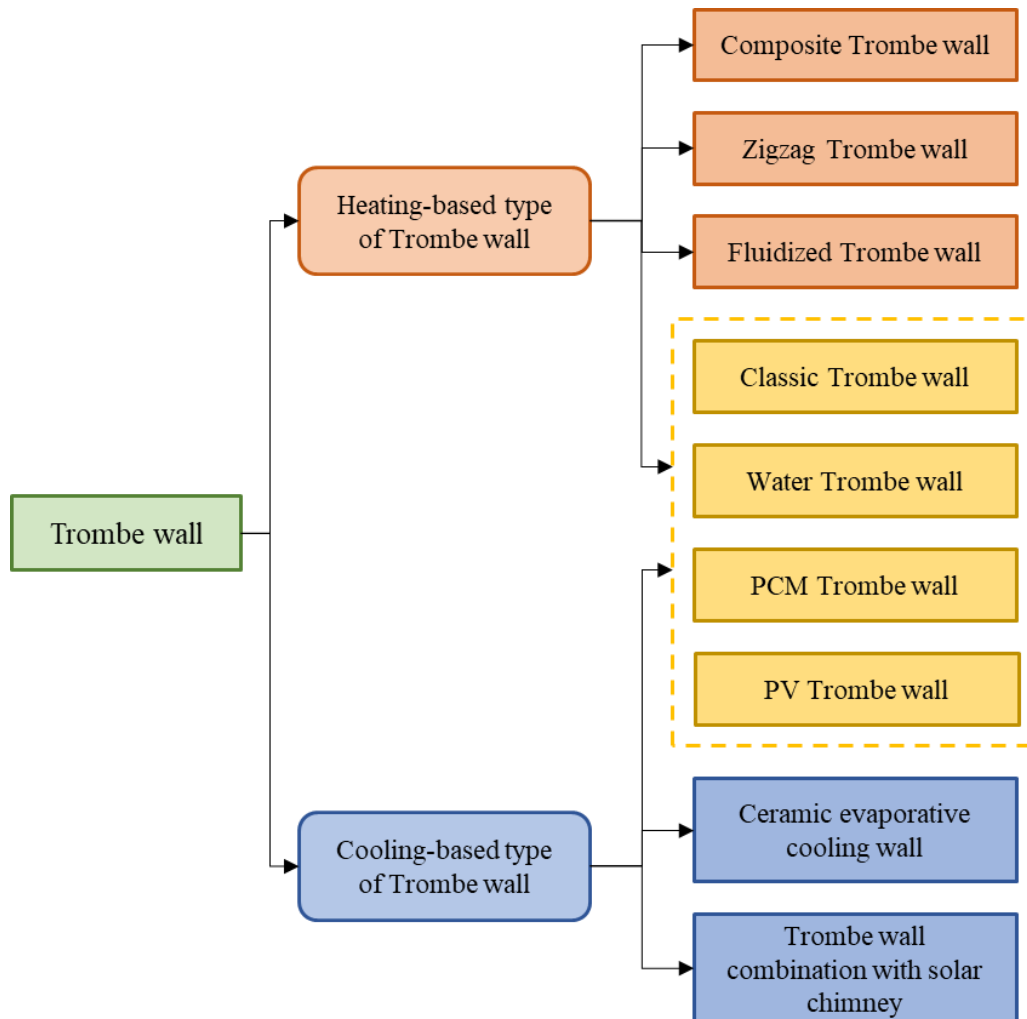


**Figure 2.1.2 Classification of Trombe wall**

### 2.1.3. Composite Trombe wall

The composite Trombe wall, which is also known as the Trombe–Michel wall [14,15], is one type of Trombe wall, which consists of several different layers. These layers include a glazing surface, a massive wall, a non-ventilated air layer, a ventilated air layer and an insulating panel (Figure 2.1.3). Composite Trombe walls are considered a remedy for two deficiencies of Trombe walls: heat loss during cloudy winter days and undesired heat inputs during hot weather [16].

The principle of the composite Trombe wall is as follows. The first layer is a transparent glazing surface, which allows most of the solar beams to pass through into the Trombe wall system. thus, the massive wall absorbs part of the acquired solar energy and heats it up. the massive wall stores and transfers part of the absorbed energy to the inner air layer. This energy is transferred to the room by convection through the ventilation channels. The insulation panels are used to prevent heat loss from the room through the massive wall and glazing surface. In addition, a small portion of the energy is transferred from the wall into the room by conduction. These free solar gains must be distinguished from direct solar gains.

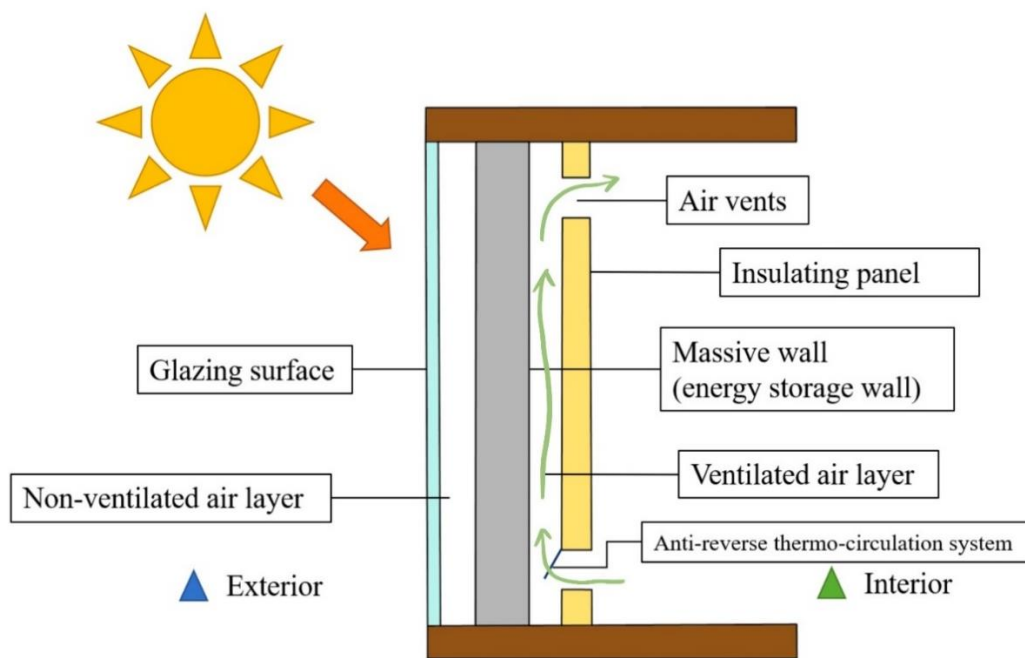


**Figure 2.1.3 A composite Trombe wall**

The advantages of Composite Trombe Wall are as follows. The user can control the rate of heating by controlling the airflow into the ventilation channels. Since the wall and the ventilation channels are insulated, the thermal resistance of the Composite Trombe Wall is very high. Shen et al. in France, compared the classical Trombe wall with the composite Trombe wall by software TRNSYS and validation by experiential test to know about the composite Trombe Wall efficiency [11,17]. The results showed that composite Trombe wall performs better during heating seasons, particularly in cold or cloudy climates [17].

However, it still has the following shortcomings:

(1) In clear weather, the heat flux from the classical Trombe wall is several orders of magnitude higher than from the composite Trombe wall [21].

(2) The wall requires a mechanism to prevent reverse thermo-circulation, which occurs when the massive wall becomes colder than the ambient air of the building’s internal space [18].

(3) In severe climatic conditions, the temperature difference can be quite large. As a result, moisture can form within massive wall. In addition, massive wall produces condensation on the surface due to moisture. If proper moisture barrier and waterproofing of insulating panel are neglected, then mold may appear on the insulating panel. This situation has a significant impact on the indoor climate [19].

To improve the composite Trombe wall for some of the above problems, Leonardo A et al. [20] Trombe–Michel wall with a vertical storage system. The results showed that the addable Trombe wall could reduce energy demand and winter firewood consumption by nearly 33%, with a 5°C increase in indoor temperature in the better case scenario measured during the cold season. Kecheng Y et al. [21] proposes a flue composite wall (FCW) to improve energy efficiency by recovering waste heat from the exhaust smoke from the Kang. Simulation results show Simulation results show that better thermal performance is achieved when the ratio of insulation to flue is 2, the thickness of the flue baffle is 20-50 mm, and the thickness of the flue is 20-50 mm. The thermal performance is better when the thickness is 20-50mm and the flue gas flow rate is 1.15m/s-1.55m/s. Double-layer Trombe wall with temperature-controlled DC fans designed by MA. Q et al. [22] that have two ventilated air cavities (Figure 2.1.4). In heating seasons, the indoor temperature increased by a maximum of 2.9 C with the double-layer Trombe wall. The outer-ventilated air layer temperature (T-ext) is higher from 10:00 to 18:00, at other times the temperature of the inner-ventilated air layer (T-int) is higher. T-ext and T-int are higher than T-room (Figure 2.1.5). In order to warm the room in the non-air-conditioned, it is effective to supply air from outer-ventilated and inner-ventilated air layer together [23].

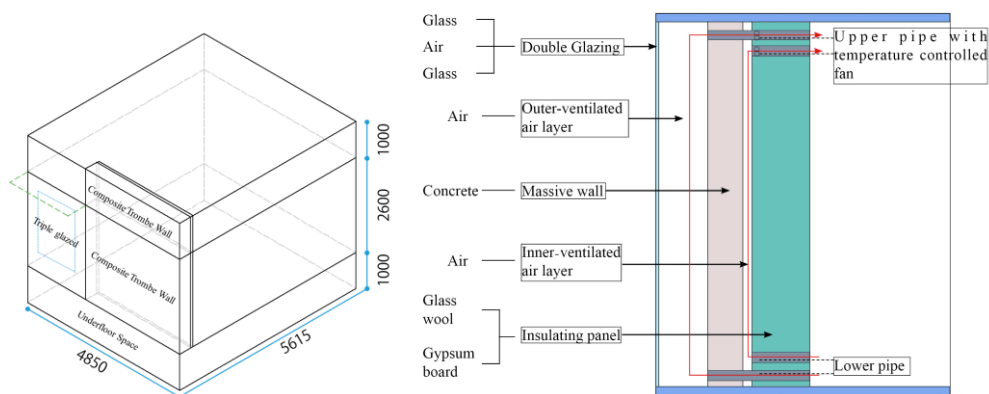
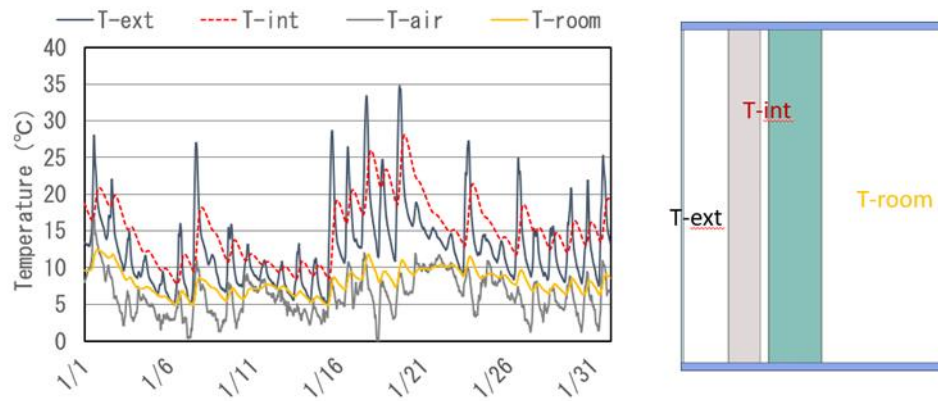


Figure 2.1.4 A double-layer Trombe wall with temperature-controlled DC fans [22]



**Figure 2.1.5 Indoor temperature of a double-layer Trombe wall in January**

Chen et al. [24,25] proposed a new type of composite Trombe wall with a porous absorber (Figure 2.1.6). In this type of wall, the added porous absorber acts as a thermal storage buffer that initially absorbs solar heat and then distributes it to the air in the channel or thermal storage wall. In addition, this porous component acts as a semi-thermal insulator, increasing the thermal resistance of the Trombe wall and preventing heat loss during cloudy days or at night when there is no solar radiation [35]. Liqun Z et al. [26] propose a composite Trombe wall, which combines a water wall and a conventional Trombe wall (Figure 2.1.7). Under certain conditions, the thermal efficiency of the water keel wall is 3.3% higher than that of the conventional keel wall. Under low irradiation conditions, its efficiency is 7.2% higher than that of a conventional Trombe wall. Under simulated conditions, the results show that the water Trombe wall can reduce the heat loss by 31% at night compared to the conventional Trombe wall.

Enghok L et al [27] studies a composite solar wall with latent storage designed to heat rooms during the heating season. The result indicates that the solar wall incorporating a PCM does not in the case release any more energy in the room to be heated (Figure 2.1.8). it was determined that the total stored energy from the external surface corresponds to 35.8% of the incident solar energy radiating the vertical facade. 60.8% of this energy is released into the room to be heated, which is equivalent to 21.8% of the incident solar energy.

Luo C et al [28] investigate a new solar PCM storage wall technology, namely a dual-channel and thermal-insulation-in-the-middle type solar PCM storage wall system (figure 2.1.9), which has the following four independent functions: passive solar heating, insulation, thermal insulation and passive cooling. The four independent functions of passive solar heating, thermal insulation, thermal insulation and passive cooling provide the flexibility to respond to the climate requirements of the building during different seasons of the year.

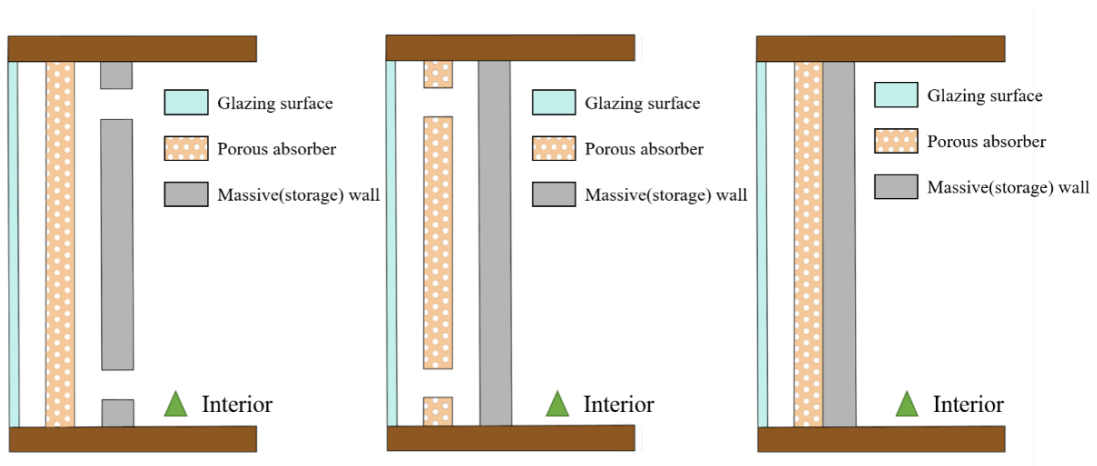


**Figure 2.1.6 Trombe wall with a porous absorber**

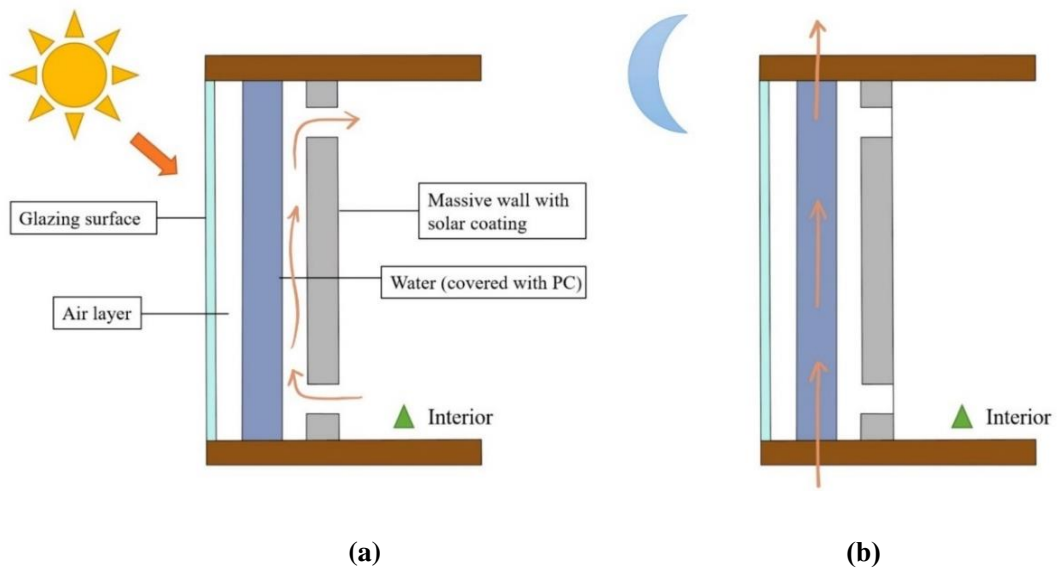


**Figure 2.1.7 A composite water Trombe wall: (a) The principle of water Trombe wall at daytime. (a) The principle of water Trombe wall at night-time.**

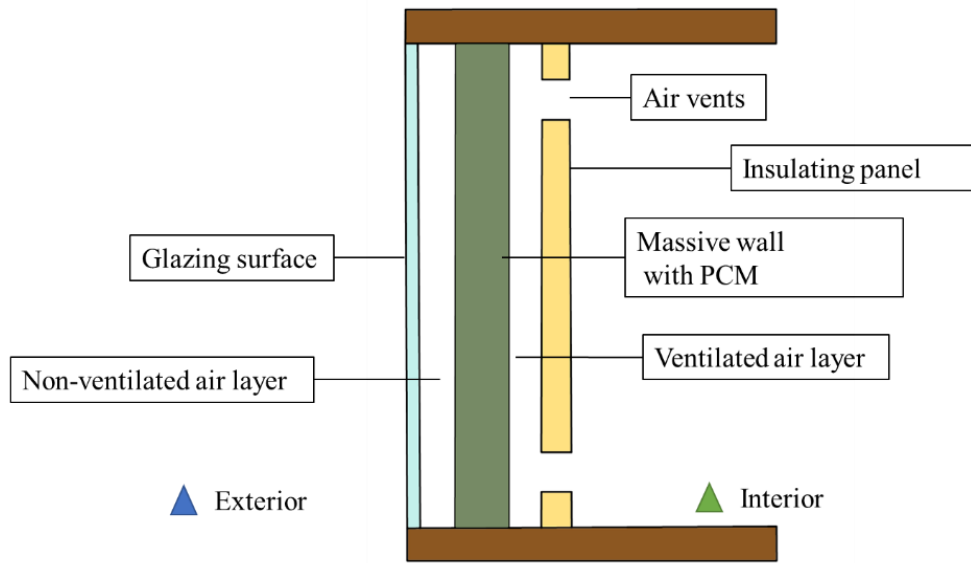


**Figure 2.1.8 A composite Trombe wall with PCM**

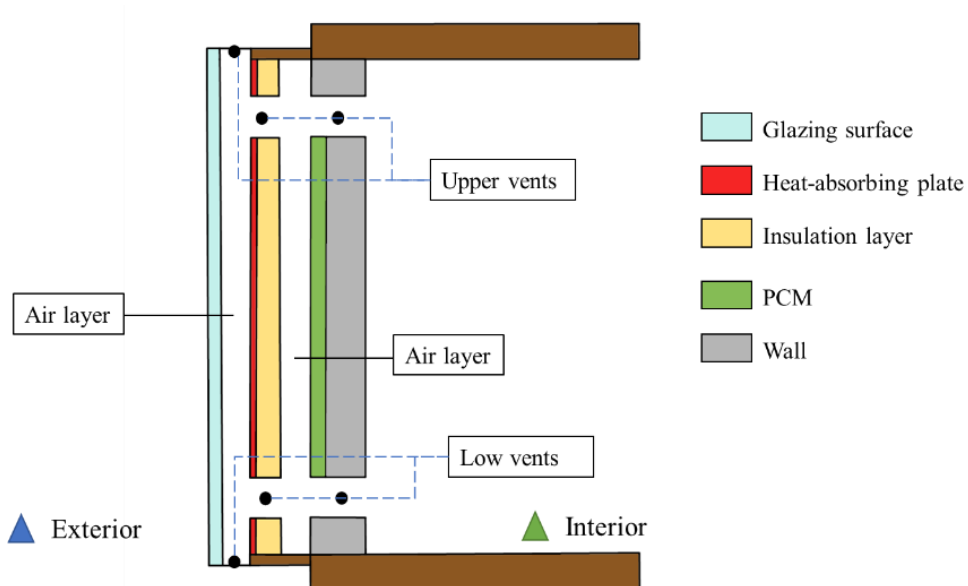


**Figure 2.1.9 A dual-channel and thermal-insulation-in-the-middle type solar PCM storage wall system.**

## 2.2 Trombe wall design parameters

To achieve a high efficiency, some influencing factors must be considered when designing Trombe wall system in building, including Trombe wall design parameter (outer skin glazing properties, Trombe wall's area, channel depth, massive wall properties, shading devices), building parameters (construction materials, window effects), site parameters (solar radiation and orientation, wind speed and direction).

### 2.2.1. Glazing properties

Glazing properties, such as the materials, the thickness, the number of glazing layers and window-to-wall ratios not only influence the amount of solar radiation that is either reflected, absorbed or transmitted but also affect the heat loss between the inter-space and outside environment [1]. Therefore, considering the influence of different glazing properties is of importance in Trombe wall design phase. During the cooling season, the favorable number of glazing layers design for a Trombe wall depends on the climate conditions of the building site.

Basak K et al. [9,29] compared the energy performance of single-glazed, double-glazed and a-Si translucent Photovoltaic (PV) modules on a Trombe wall. It was found that the double glazing had higher thermal insulation performance at night and in the evening. Higher thermal insulation performance was found in the evening. The temperature in the air ducts in the PV module section was lower than in the double and single glazed sections due to the lower solar radiation transmission in the PV module section. Another set of experiments were conducted by Irshad K et al. [9,30] conducted in Malay-sia, examining different photovoltaic glazing types (i.e., PV Single Glazing, PV Double glazing, PV Double glazing filled with gas (Argon)) comparing. Zhou L et al. [26] proposed a composite Trombe wall which combines the water wall with the traditional Trombe wall. The results show that water Trombe wall which replaced the glass surface with water can reduce the heat loss by 31% compared to Trombe wall. And Azhar A et al. [31] studied practical investigation about effect of a glass cover on the efficiency of the Photovoltaic/Trombe wall. The highest recorded thermal efficiency value was 80% using a glass cover and 0.5% nanofluid. Arash P et al. [32] investigated the effect of different structural and spectral glass specifications. Physical properties had the greatest impact on increasing comfort periods (up to 32%) and reducing cooling periods (up to 35%).

### 2.2.2. Massive wall area

Some researches seem that the increase in Trombe wall area provided the decrease in heating energy demand, while we must also not forget that we are limited by the total south wall area of the building. Jaber et al. [33] performed another simulation study on a typical Jordanian residence, which was equipped with Trombe wall system. In this study, they investigated the effect of variable Trombe wall ratio ( $\alpha$ ), the percentage of Trombe wall area to the total south wall area, on building heating from thermal and economic points of view by using Life Cycle Cost (LCC) criterion. They found that the percentage of heating energy savings increased with the increasing of Trombe area ratio ( $\alpha$ ) firstly. When ( $\alpha$ )=20%, about 22.3% of heating auxiliary energy was saved annually. However, when  $\alpha$  exceeded the value of 37%, the percentage of heating energy savings kept at nearly steady values. Therefore, the optimum Trombe wall area ratio was 37%, which corresponded to 32.1% of heating auxiliary energy savings.

Briga-Sá et al. [34] used a calculation methodology for the Trombe wall based on International Organization for Standardization (ISO) 13790:2008(E), studied its behavior at 15 cm, 20 cm, 25 cm, 30 cm, 35 cm and 40 cm thicknesses. The obtained results show that in the heating season, if the Trombe wall is ventilated, the heat gain increases with the increase of the thickness of a massive wall. However, in the case of unventilated Trombe walls, the heat gain decreases when the thickness increases. The thicker the wall, the longer it takes for the heat to reach the interior. In this direction, Agrawal and Tiwari propose the optimal thickness of concrete Trombe walls to be 30-40 cm [35].

### 2.2.3. Ventilation and air flow in vents

Classical Trombe walls can be divided into two types: vented and unvented [36]. For vented Trombe walls, two heat circulation vents are installed at the top and bottom of the wall to aid heat circulation. These vents are designed to control heat losses. Heat loss occurs in the air space between the glass and the wall, by convection, conduction or radiation back to the atmosphere. The higher the temperature of the air space, the greater the heat loss. The efficiency of ventilated and unventilated Trombe walls has long been considered an important topic in passive energy research. The research group [37] also simulated a thermostatically controlled ventilation system in which the dampers close when the internal temperature of the building exceeds 24°C [37]. This approach was found to prevent overheating.

A group of Portuguese scientists conducted a simulation study using EnergyPlus software in three different climate zones in Portugal. The study aimed to determine the effect of vents on the efficiency of Trombe walls [38]. The size of the vent is an important parameter when designing a Trombe wall and depends on the solar savings fraction (SSF) [39]. In addition, external vents, which can be installed on the exterior of the Trombe wall, facilitate air circulation [49].

Also, the vents can be controlled by fans for forced air circulation. A thermal network computer simulation of a Trombe wall with thermostatically controlled fans was performed by Sebald et al. The thermostatically controlled fan started to operate when the temperature of the exterior wall exceeded 29 degrees Celsius. The results showed that the performance of the fan depends on parameters such as the thickness of the wall and the climate [41]. For example, the fan can increase the efficiency of a room with a 37 m<sup>2</sup> Trombe wall by 22% in Albuquerque, 20% in Santa Barbara, and 7% in Madison [41].

Li D et al. [42] studied the pattern of air flow rate in Trombe wall, when the wall height increases, the ascending rate of air velocity is increases. A combined solar chimney is proposed that integrates an inclined-roof solar chimney with a traditional Trombe wall by Liu H et al. [43] Briga-Sá et al. [44] suggested during the heating season, the air vents should be open when the solar radiation values exceed 100 W/m<sup>2</sup>.

Ji J et al. [45] applied Direct Current (DC) fans to the PV-Trombe Wall (PV-TW) for simulation and practical testing. It was found that the room temperature was significantly increased and the PV cells were cooled to some extent by applying the DC fan. The potential of PV-TW can be exerted by the assisted DC fan. Ma, Q. [22] investigated energy conservation in a concrete construction office building with a composite Trombe wall with a temperature-controlled DC fan for winter heating application. the ventilation rates of the fan were controlled at 40 m<sup>3</sup>/h. It is more efficient to have the fan start up when the ventilated air cavity temperature is 19°C if the operative temperature of the interior is maintained 20°C with air conditioning. [57] The effects of those fans that is turned on and off at different time were also investigated. It is best to supply air from inner-ventilated air layer in December, February and March. It is best to supply air from outer-ventilated air layer and inner-ventilated air layer together in November. In January, it is better to not supply air.

#### **2.2.4. Shading devices**

Heat loss during winter nights and excessive warming during hot summers are two disadvantages that limit the application of Trump walls. Shading devices are considered as simple techniques to solve these disadvantages, such as shades, roller blinds, blinds and cantilevers [47-49]. Furthermore, they demonstrated that the best Trump wall efficiency could be achieved by the combined use of overhanging and roller shades during hot summer days [50]. In addition, an experimental study conducted by Chen et al. during winter nights showed that the use of shading devices in the aisles is an effective way to improve the thermal performance of Trombe walls [51]. The use of shading devices should be adjusted during different seasons of the year. During the cooling season. Shading devices should be removed during the day to allow more solar radiation to reach the Trumbull wall. While during the hot summer season, the operation is reversed.

#### **2.2.5. Channel depth**

When considering the design of a Trombe wall, it is unavoidable to consider the channel located between the glass enclosure and the large external wall [52]. As the depth of the channel increases, the frictional pressure loss decreases, which leads to a decrease in the flow resistance and an increase in the mass flow rate [53]. When the depth increases to a certain value, the airflow state will change from a finite. Then backflow occurs at the exit of the Trombe wall. In addition, the excessive depth of the channel can lead to insufficient thickness of the large wall, which can cause structural safety problems [54].

#### **2.2.6. Window effects**

The thermo-siphon effect encourages top-down air flow in the room, however, due to the design of the windows, solar radiation can be directed to the interior floor or its adjacent walls. These walls are then heated and a bottom-up airflow occurs. As a result, the air flow in the room compared to

the absence of the window. Although the results suggest that higher efficiency can be achieved without the window [55], windows provide not only direct sunlight, but also beneficial daylight and visual contact with the outside world. In addition, the above study could not refer in detail to the effects of window size, ratio and location and so on [55].

### **2.2.7. Climate effects**

In general, the efficiency of Trombe walls increases with the level of solar radiation. The efficiency of Trombe walls is not only related to the level of solar radiation, but is also influenced by the orientation. In the northern hemisphere, the sun rises and sets slightly southward from east-west in winter, and slightly northward from east-west in summer. This slight angle depends on the time of year and the distance of the observer from the equator. In the Southern Hemisphere, all these directions are reversed. Thus, in the Northern Hemisphere, the most favourable directions for Trombe wall are due south, southeast, and southwest. In contrast, in the southern hemisphere it is due north, northeast, and northwest [56]. In addition, during the design phase of the Trombe wall, attention should be paid to the shading problems arising from the surrounding environment and from the buildings themselves in highly dense cities.

In addition to solar radiation, wind is a key natural stimulus affecting the thermal and airflow behaviour of Trombe walls, such as wind speed and direction. In general, the heat loss coefficient and wind pressure of glazing are related to the wind speed and direction, which mainly affect the thermal efficiency and ventilation rate of the Trombe wall.

### **2.2.8. Massive wall material properties**

To achieve a high efficiency, some influencing factors must be considered when designing Trombe wall system in building, including Trombe wall design parameter (outer skin glazing properties, Trombe wall's area, channel depth, massive wall properties, shading devices), building parameters (construction materials, window effects), site parameters (solar radiation and orientation, wind speed and direction).

The massive wall of the Trombe wall assumes the function of receiving and storing solar energy, and in the selection of massive wall materials, Stazi et al [57] studied three wall materials: concrete, brick and aerated concrete in the pre-use phase and use phase of the Trombe wall. The best overall performance was obtained for the wall using aerated concrete blocks considering the pre-use and use phases, which combines the low environmental impact of the production cycle with the high energy performance of the use phase [57].

In addition, Hassanain et al [58] studied the effect of various adobe materials on the efficiency of Trombe walls and found that different adobe materials produce different efficiencies. Increasing the weight and volume of a Trombe wall can increase its thermal storage capacity. However, this

increases the dead load of the building, which is considered to be a problem by structural engineers. To solve this problem, one of the possibilities is to use phase change materials (PCM) as a thermal storage medium [59-63]. PCM was first used for Trombe walls by Telkes et al. in 1978 [64]. PCM can store more energy in a relatively small volume and is lighter than ordinary building materials [65].

Moreover, according to an experimental study by Zalewski et al [66], the energy stored in PCM can be transferred to the room faster compared to concrete walls. The results showed that for bricks containing hydrated salts, the solar gain was restored to the room in 2 hours and 40 minutes, which is more than twice as short as for a 15 cm thick concrete wall. This may be an inconvenient situation if the wall is installed in an occupied dwelling to utilize the gain at the end of the day. Although this undesirable phenomenon does not seem to be annoying due to the low amount of energy stored in the PCM [66]. J. Koo et al [67] found that the maximum amount of heat storage in the wall panel is achieved when the average phase change temperature is close to the average room temperature. In order to expand the heat storage in PCM wall panels, the phase change temperature should be as low as possible.

According to a simulation study conducted by Rabani et al [68] on the indoor heating time of Trombe walls of different materials during non-sunny days. The results showed that Trombe walls made of paraffin wax could keep the room warm for about 9 hours compared to other materials. Similarly, Liu et al [69] found that the application of PCM can prolong the utilization time of solar chimneys, especially at night. Different types of PCM exhibit different thermal responses on the Trombe wall.

Bogdan M. Diaconu [70] proposed a new composite wall containing a double layer of PCM, where the outer layer of the wall consists of PCM, the middle layer of conventional insulation and the outer layer of high phase change temperature PCM. this wall structure model has a phase change in summer, which can effectively reduce the room temperature, and can act as a good insulation in winter. Winter and summer simulations of this room resulted in energy savings and reduced peak compound, and determined that the phase change temperature of PCM makes the highest energy savings. Pasupathy, A et al [71] examines in detail the concept of a two-layer PCM in order to achieve year-round thermal management in a passive manner. Zhang Y et al [72] also focused on double-layer phase change material walls. It is proposed that two PCMs with different phase change temperatures are filled into a multi-layer flat wall at the same time to form a double-layer PCM wall. When the two PCM layers are located in the middle of the wall, the temperature of the inner surface of the building envelope is the most stable, and the utilization rate of low phase change temperature PCM in winter and high phase change temperature PCM in summer are both 0~100%, which can make the wall maintain high thermal performance [72]. Similar, Zhu, Na, et al. [73] used TRNSYS software, simulated data show that the optimal phase change temperatures are 30°C and 18°C for

the exterior and interior PCM wall panels, respectively. The peak cooling and thermal loads of the PCM Trombe building are reduced by 9% and 15%, respectively, compared to the reference Trombe building. In summer, the indoor temperature of the PCM rooms was on average 3.28°C lower than that of the reference rooms.

Two types of PCM (paraffin and hydrated salt  $\text{CaCl}_2 \cdot 6\text{H}_2\text{O}$ ) were encapsulated in copper capsules with an aspect ratio of 0.76. The results showed that the 8-cm-thick hydrated salt storage wall showed the least variation compared to the 5-cm-thick paraffin wax, with room temperature fluctuating at a comfortable temperature of about 20°C [74]. In Japan, a group of scientists confirmed this result [75]. Khalifa and Abbas conducted a numerical study in Baghdad, Iraq, on an area heated by a south-facing Trombe wall with different storage materials (concrete, paraffin and hydrated salt  $\text{CaCl}_2 \cdot 6\text{H}_2\text{O}$ ) [79]. Chao. L [76] found in hot and humid summer regions of China that PCM TWS provided more effective thermal insulation performance than the common envelope and typical TWS. During the daytime, PCM TWS releases cold at a peak heat flow rate of -25.1 w/m<sup>2</sup>, while at night, it accumulates cold at a peak heat flow rate of 20.1 w/m<sup>2</sup>. Compared with typical TWS, PCM TWS achieves better induced ventilation, corresponding to a maximum room ventilation rate of 140 m<sup>3</sup>/h (31h<sup>-1</sup>) and a minimum value of 29 m<sup>3</sup>/h (6h<sup>-1</sup>). Compared to typical TWS, PCM TWS can significantly reduce the room air temperature by a maximum of 2.1°C and 5°C compared to a normal envelope.

**Table 2.1 Latent heat and melting points of some PCMs [77-82]**

<b>Material</b>	<b>Type</b>	<b>Melting Point(°C)</b>	<b>Latent heat of fusion (kJ/kg)</b>
RT21	Organic	21	134
Dimethyl sabacate	Organic	21	120-135
RT22	Organic	22	172
Polyglycol E600	Organic	22	127.2
S23	Inorganic	23	175
ClimSel C24	Inorganic	24	126
A24	Organic	24	124

CaCl <sub>2</sub> + MgCl <sub>2</sub> .6H <sub>2</sub> O	Eutectic	25	95
Micronal26	Organic	26	110
Micronal 5001	Organic	26	110
n-octadecane	Organic	27	243.5
RT27	Organic	27	184
Paraffin C18	Organic	28	244
RT28	Organic	28	245
CaCl <sub>2</sub> .6H <sub>2</sub> O	Inorganic	29	191
LiNO <sub>3</sub> .2H <sub>2</sub> O	Inorganic	30	296
RT31	Organic	31	165
n-nonadecane	Organic	31.8	160
A32	Organic	32	130
Na <sub>2</sub> CO <sub>3</sub> .10H <sub>2</sub> O	Inorganic	33	247
LiBr <sub>2</sub> .2H <sub>2</sub> O	Inorganic	34	124
FeCl <sub>3</sub> .6H <sub>2</sub> O	Inorganic	37	223
1-Tetradecanol	Organic	38	205
Camphenilone	Organic	39	205
Caprylone	Organic	40	259

RT42	Organic	42	174
S44	Inorganic	44	100
NH <sub>2</sub> CONH <sub>2</sub> + NH <sub>4</sub> NO <sub>3</sub>	Eutectic	46	95
n-eicosane	Organic	46.7	209
Na <sub>2</sub> HPO <sub>4</sub> .7H <sub>2</sub> O	Inorganic	48	281
S50	Inorganic	50	100
Mg(NO <sub>3</sub> ) <sub>3</sub> .6H <sub>2</sub> O + NH <sub>4</sub> NO <sub>3</sub>	Eutectic	52	125.5
Na(CH <sub>3</sub> COO).3H <sub>2</sub> O	Inorganic	58	226
Mg(NO <sub>3</sub> ) <sub>3</sub> .6H <sub>2</sub> O + MgCl <sub>2</sub> .6H <sub>2</sub> O	Eutectic	59	132.2
Palmitic acid	Organic	64	185.4
Polyglycol E6000	Organic	66	190
Stearic acid	Organic	69	202.5
ClimSel 70	Inorganic	70	396

---

### 2.3 Trombe wall in summer

Trombe walls are also used to cool the room temperature in summer. A classic summer principle of a Trombe wall is shown in the figure 2.3.1.

One type of cooling-based type of Trombe walls is the ceramic evaporative cooling wall [83] which employs an external reflective thermal blind to avoid direct solar gain. In particular, porous ceramic elements filled with clean water are used in the inner wall. Outside air enters through the slits in the lower part of the gap, while outside air enters the interior through its upper part. In hot

summer days, the slit acts as a cooling chamber to reduce the temperature of the outside air due to the direct evaporative cooling phenomenon [83].

Another type of Trombe wall based on cooling was developed on the basis of solar chimneys [13]. For mild climates, the cooling-based Trombe wall acts as a natural ventilation when the outdoor temperature is lower than the indoor temperature (Figure 2.3.2(a)). However, for hot climates, it acts as an insulating material to reduce the heat gain in the room when the outdoor temperature is higher than the indoor temperature (Figure 2.3.2(b)). Due to the lack of control over the energy supply of the storage wall, it risks overheating during hot summer days. To satisfy the thermal comfort and aesthetic values, PV panels and shading devices are mixed with this cooling-based Trombe wall, which is an alternative mode of operation for PV Trombe walls in summer [84].

Rabani et al. [85] conducted a study in a hot and dry area and proposed a new design of Trombe wall, which is a combination of Trombe wall and solar chimney. This innovative design eliminates the main drawback: the Trombe wall is useless during half of the year, while the solar chimney cannot generate air flow during the late hours of the day. In addition, unlike the traditional Trombe wall, where the absorber receives solar radiation from one direction, the new design of the Trombe wall channel allows the absorber to receive solar radiation from three directions (east, south, and west), resulting in an increase in channel temperature and mass flow rate within the channel. In addition, two air inlets equipped with a water spray system were used in order to reduce the air temperature and increase the humidity in the room. According to the experimental results [85], the use of the water jet system increased the thermal efficiency of the system by about 30%.

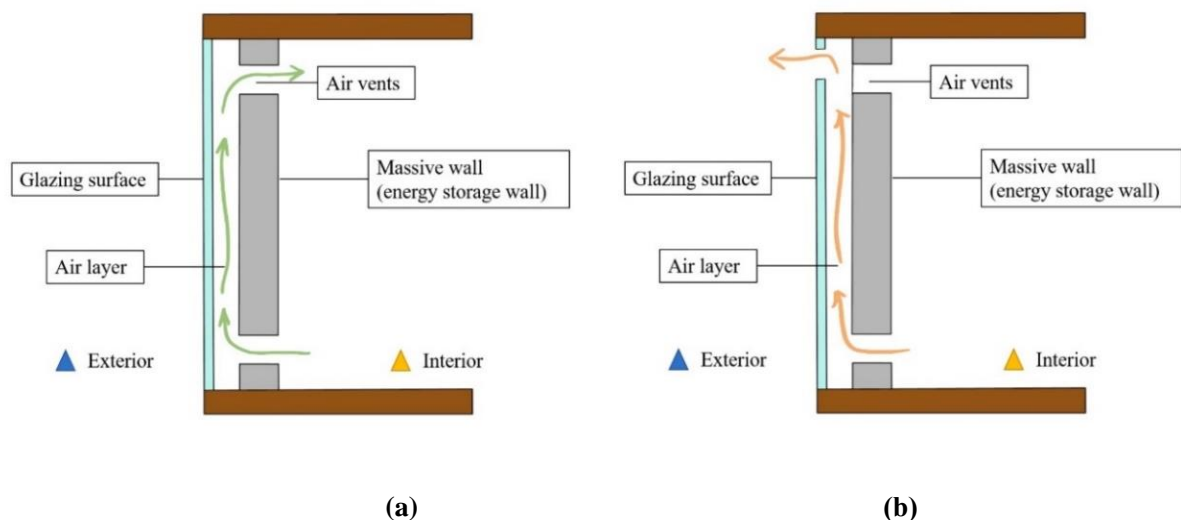


**Figure 2.3.1 Constructive diagram of a classical Trombe wall: (a)Winter mode (b)Summer mode**

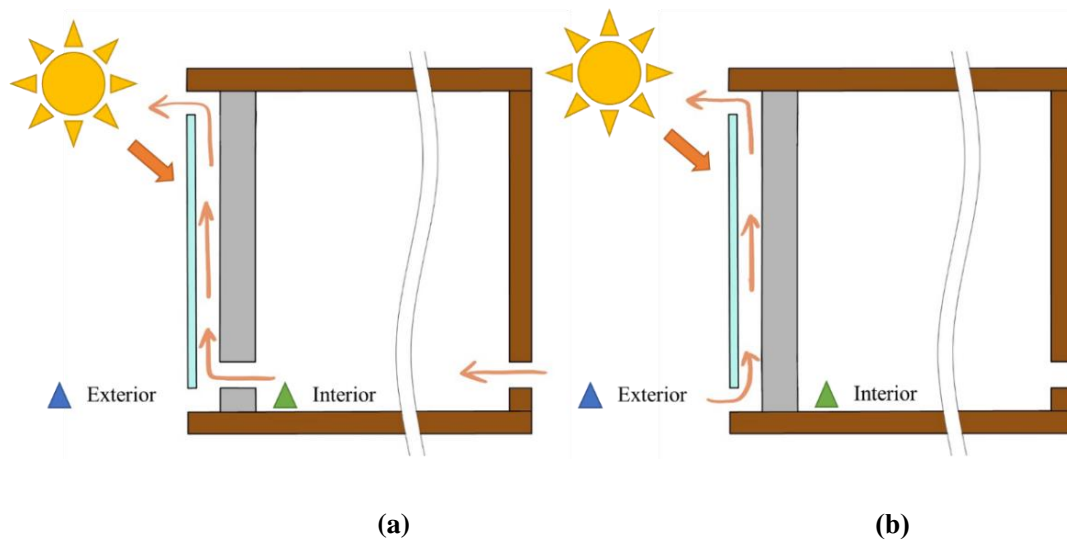


**Figure 2.3.2 A cooling-based type of Trombe wall operation mode:(a) natural ventilation mode (b) thermal insulation model.**

## 2.4 Evaluation metrics

### 2.4.1. Temperature

Temperature is the most commonly used parameter in the evaluation of Trombe walls [86]. It is also the basis for the calculation of other evaluation indicators of Trombe walls. The general temperature measurement includes the temperature of the inner and outer glass surfaces, the passage air, the inner and outer wall surfaces, the air inlets and outlets, and the interior. The performance of a Trombe wall can be reflected by the temperature of different aspects. For example, high temperatures of the passage air and air vents can indirectly indicate high efficiency of the Trombe wall. A high indoor temperature in winter can reflect a low heating load or a good thermal environment. In addition, there are some formal indicators for evaluating the performance of Trombe walls in terms of temperature fluctuations.

Thermal load levelling (TLL): This index is equal to the difference between the maximum and minimum of indoor temperature ( $T_{r \max}$  and  $T_{r \min}$ ) divided by their sum [87]:

$$TLL = \frac{T_{r \max} - T_{r \min}}{T_{r \max} + T_{r \min}} \quad (2)$$

In this equation, the numerator represents the degree of the indoor temperature fluctuation and the denominator reflects the basic value of such variation. A greater numerator and a smaller denominator indicate more fluctuation. Hence, TLL indicates the stability of the indoor temperature.

Decrement factor (f): It is defined as the ratio of temperature amplitude at the inside wall-surface to that at the outside wall-surface [92]:

$$f = \frac{T_{w \text{ inside max}} - T_{w \text{ inside min}}}{T_{w \text{ outside max}} - T_{w \text{ outside min}}} \quad (3)$$

Where  $T_{w \text{ inside max}}$ ,  $T_{w \text{ inside min}}$ ,  $T_{w \text{ outside max}}$ ,  $T_{w \text{ outside min}}$  are the maximum-temperature and minimum-temperature of inside and outside wall-surface, respectively. This index represents the temperature attenuation by the wall.

#### 2.4.2. Energy

The energy assessment of the Trombe Wall can be done from either an energy supply or energy demand perspective. Although energy supply and energy demand are usually related, they provide two opposing perspectives for assessing the Trombe wall [86].

For PV Trombe walls, power generation is also evaluated as an aspect of energy gain [88,89].

Energy load. This is also considered as the energy demand or energy consumption to maintain the indoor thermal environment after using the Trombe wall. It includes the heating load and cooling load in winter and summer, respectively. Building energy simulations can be used to obtain this energy load.

Solar Fraction. This metric contains information about the energy gain and energy load. It indicates the level of solar energy used for room heating. It can be expressed as the ratio of effective solar heating to the total heating demand [90,91].

#### 2.4.3. Efficiency

Since efficiency is a frequently used evaluation parameter for Trombe walls, and since heating is the main function of Trombe walls, this metric is often used to analyse the performance of Trombe wall [91].

Load reduction efficiency: Since the air circulation driven by Trombe wall via the upper and lower vents causes an air stratification in the indoor space, only a part of the entire heat gain from Trombe wall can be directly used to reduce the heating load [92].

Absorption-storing efficiency and dissipation efficiency: These two indexes convey opposite meaning. They respectively indicate the ability of a Trombe wall to absorb and store the heat from solar radiation during daytime, and to discharge this heat for the indoor room during night [58].

#### 2.4.4. Auxiliary energy cost

Auxiliary energy cost is a direct evaluation indicator of the operating cost of a building equipped with a Trombe wall, but it can also indirectly reflect the cost saving performance of a Trombe wall. This cost can be calculated by multiplying the consumption of auxiliary energy sources (e.g.

electricity, gas, oil, biomass) by their unit price. A lower value means more cost savings for Trombe walls. However, only a limited number of studies [75] have ever used this method.

#### **2.4.5. Life cycle assessment**

Life cycle assessment includes the phases of manufacturing, operation and disposal. Global warming potential, also known as CO<sub>2</sub> emissions, is used more than other indicators in the environmental assessment of Trombe walls, not only for life cycle analysis [93-195] but also for annual analysis [36,88]. GWP can be calculated by multiplying the energy consumption of a Trombe wall by its unit CO<sub>2</sub> emissions. And as a common economic analysis tool, Life cycle cost is often adopted to evaluate the cost of a building with Trombe wall.

#### **2.4.6. Payback period**

Payback period is also a common economic index used for Trombe wall analysis [86]. It represents the period when the accumulative operation-cost saving of Trombe wall can offset the additional investment of Trombe wall compared to a normal wall.

#### **2.4.7. Indoor environment**

Indoor thermal comfort is an aspect that cannot be ignored when assessing the performance of a Trombe wall, since the main task of this wall is to maintain a suitable indoor temperature for people. Both winter heating and summer overheating are important issues for the indoor thermal comfort of a Trombe wall. Indoor air quality (IAQ) is another aspect that has been studied in recent years since the development of air purifying Traub walls [96,97].

### **Reference**

- [1] Zhongting Hu; Wei He; Jie Ji; Shengyao Zhang, A review on the application of Trombe wall system in buildings, *Renewable and Sustainable Energy Reviews*, Volume 70, April 2017, Pages 976-987
- [2] Denzer A. The solar house: pioneering sustainable design. *Arts* 2013; 3:303–6
- [3] Daniel A. A house in the Sun: modern architecture and solar energy in the cold war. Oxford university press; 2016.
- [4] Mazria, Edward. *The Passive Solar Energy Book*. Emmaus, PA: Rodale Press.1979, ISBN 0-87857-237-6.
- [5] Chan, H.-Y.; Riffat, S. B.; Zhu, J., Review of passive solar heating and cooling technologies. *Renewable and Sustainable Energy Reviews* 2010, 14, (2), 781-789.
- [6] XIA, Xu; YANG, Qiao-xia; CHEN, Hai-ni. Indicator system of energy efficient technologies

- evaluation of residential buildings in hot summer and cold winter regions of China. 2014.
- [7] Üрге-Vorsatz, D.; Cabeza, L. F.; Serrano, S.; Barreneche, C.; Petrichenko, K., Heating and cooling energy trends and drivers in buildings. *Renewable and Sustainable Energy Reviews* 2015, 41, (Supplement C), 85-98.
- [8] Sergei, K., Shen, C., Jiang, Y. A review of the current work potential of a trombe wall. *Renewable and Sustainable Energy Reviews*, 2020, 130: 109947.
- [9] Omidreza Saadatian, K.Sopian, C.H.Lim, Nilofar Asim, M.Y.Sulaiman, Trombe walls: A review of opportunities and challenges in research and development, *Renewable and Sustainable Energy Reviews*, Volume 16, Issue 8, October 2012, Pages 6340-6351
- [10] Shen J, Lassue S, Zalewski L, Huang D. Numerical study of classical and composite solar walls by TRNSYS. *J Therm Sci* 2007;16:46–55.
- [11] Zalewski L, Lassue S, Duthoit B, Butez M. Study of Solar Walls — Validating a Simulation Model. 2002.
- [12] Ji J, Yi H, He W, Pei G. PV-trombe wall design for buildings in composite climates. *J Sol Energy Eng* 2007;129:431.
- [13] Saadatian O, Chin L, Sopian K, Salleh E, Ludin N. Solar walls: the neglected components of passive designs. *Advanced in Environment, Biotechnology and Biomedicine* 2012:120–6.
- [14] Ji J, Luo C, Chow T-T, Sun W, He W. Thermal characteristics of a building-integrated dual-function solar collector in water heating mode with natural circulation. *Energy* 2010;36:566–74.
- [15] Marinosci C, Strachan PA, Semprini G, Morini GL. Empirical validation and modelling of a naturally ventilated rain screen façade building. *Energy and Buildings* 2011;43:853–63.
- [16] Zhai XQ, Song ZP, Wang RZ. A review for the applications of solar chimneys in buildings. *Renew Sustain Energy Rev* 2011;15:3757–67.
- [17] ShenJ, Sp Lassue, Zalewski L, Huang D. Numerical study on thermal behavior of classical or composite Trombe solar walls. *Energy and Buildings* 2007;39:962–74.
- [18] Zalewski L, Joulin A, Lassue Sp, Dutil Y, Rousse D. Experimental study of small-scale solar wall integrating phase change material. *Solar Energy*. 2012.
- [19] Karaseva L. Quality of residential buildings. FSAEI of HE. Southern Federal University; 2019.
- [20] Agurto, L., Allacker, K., Fissore, A., Agurto, C., & De Troyer, F. (2020). Design and experimental study of a low-cost prefab Trombe wall to improve indoor temperatures in social

housing in the Biobío region in Chile. *Solar Energy*, 198, 704-721.

[21] Yu, K., Tan, Y., Zhang, T., Jin, X., Zhang, J., & Wang, X. (2019). Experimental and simulation study on the thermal performance of a novel flue composite wall. *Building and Environment*, 151, 126-139.

[22] Ma, Q.; Fukuda, H.; Kobatake, T.; Lee, M. Study of a Double-Layer Trombe Wall Assisted by a Temperature-Controlled DC Fan for Heating Seasons. *Sustainability* 2017, 9, 2179.

[23] MA, Qingsong, et al. Optimizing energy performance of a ventilated composite Trombe wall in an office building. *Renewable Energy*, 2019, 134: 1285-1294.

[24] Chen W, Liu W. Numerical analysis of heat transfer in a composite wall solar collector system with a porous absorber. *Appl Energy* 2004;78:137–49.

[25] Zhu N, Li S, Hu P, Lei F, Deng R. Numerical investigations on performance of phase change material Trombe wall in building. *Energy* 2019;187:116057.

[26] ZHOU, Liqun, et al. Investigation on the thermal performance of a composite Trombe wall under steady state condition. *Energy and Buildings*, 2020, 214: 109815.

[27] LEANG, Enghok, et al. Numerical and Experimental Investigations of Composite Solar Walls Integrating Sensible or Latent Heat Thermal Storage. *Applied Sciences*, 2020, 10.5: 1854.

[28] LUO, Chenglong, et al. Thermal feature of a modified solar phase change material storage wall system. *International Journal of Photoenergy*, 2018, 2018.

[29] Kundakci Koyunbaba B, Yilmaz Z. The comparison of Trombe wall systems with single glass, double glass and PV panels. *Renew Energy* 2012; 45:111–8.

[30] Irshad K, Habib K, Thirumalaiswamy N. Energy and cost analysis of photo voltaic Trombe wall system in tropical climate. *Energy Procedia* 2014; 50:71–8.

[31] Abed, A. A., Ahmed, O. K., Weis, M. M., Ahmed, A. K., Ali, Z. H. Influence of glass cover on the characteristics of PV/trombe wall with BI-fluid cooling. *Case Studies in Thermal Engineering*, 2021, 27: 101273.

[32] Pourghorban, A., Asoodeh, H. The impacts of advanced glazing units on annual performance of the Trombe wall systems in cold climates. *Sustainable Energy Technologies and Assessments*, 2022, 51: 101983.

[33] S. Jaber, S. Ajib, Optimum design of Trombe wall system in mediterranean region, *Sol Energy*, 85 (2011), pp. 1891-1898

- [34] Briga-Sá A, Martins A, Boaventura-Cunha J, Lanzinha JC, Paiva A. Energy performance of Trombe walls: adaptation of ISO 13790:2008(E) to the Portuguese reality. *Energy Build* 2014; 74:111–9.
- [35] Agrawal B, Tiwari GN. *Building integrated photovoltaic thermal systems: for sustainable developments*. London, United Kingdom: Royal Society of Chemistry;2011.
- [36] Abraham Y. A knowledge based CAAD system for passive solar architecture. *Renewable Energy*2009;34:769–79.
- [37] Balcomb JD, McFarland RD. Simple empirical method for estimating the performance of a passive solar heated building of the thermal storage wall type1978.
- [38] Ferreira J, Pinheiro M. In search of better energy performance in the Portuguese buildings—the case of the Portuguese regulation. *Energy Policy* 2011;39:7666–83.
- [39] Balcomb JD. *Passive solar buildings*. Hong Kong: MIT Press;1992.
- [40] Stepler R. *Trombe wall-retrofit*. Popular Science Bonnier Corporation 1980:140.
- [41] Sebald AV, Clinton JR, Langenbacher F. Performance effects of Trombe wall control strategies. *Solar Energy* 1979;23:479–87.
- [42] Du, L., Ping, L., Yongming, C. Study and analysis of air flow characteristics in Trombe wall. *Renewable Energy*, 2020, 162: 234-241.
- [43] Liu, H., Li, P., Yu, B., Zhang, M., Tan, Q., Wang, Y., Zhang, Y. Contrastive Analysis on the Ventilation Performance of a Combined Solar Chimney. *Applied Sciences*, 2022, 12.1: 156.
- [44] Briga-Sá, A., Paiva, A., Lanzinha, J. C., Boaventura-Cunha, J., & Fernandes, L. Influence of Air Vents Management on Trom-be Wall Temperature Fluctuations: An Experimental Analysis under Real Climate Conditions. *Energies*, 2021, 14.16: 5043.
- [45] Ji J, Yi H, Pei G, Jiang B, He W. Study of PV-Trombe wall assisted with DC fan. *Building and Environment* 42 (2007) 3529–3539
- [46] Ma, Q.; Fukuda, H.; Wei, X.; Hariyadi, A. Optimizing energy performance of a ventilated composite Trombe wall in an office building. Volume 134, April 2019, Pages 1285-1294
- [47] C. Ngô, J. Natowitz, *Our energy future: resources, alternatives and the environment*, John Wiley & Sons, New Jersey, United States (2012)
- [48] F. Stazi, A. Mastrucci, C. di Perna, The behaviour of solar walls in residential buildings with different insulation levels: an experimental and numerical study, *Energy Build*, 47 (2012), pp. 217-

- [49] X. Hong, W. He, Z. Hu, C. Wang, J. Ji, Three-dimensional simulation on the thermal performance of a novel Trombe wall with venetian blind structure, *Energy Build*, 89 (2015), pp. 32-38
- [50] M. Soussi, M. Balghouthi, A. Guizani, Energy performance analysis of a solar-cooled building in Tunisia: passive strategies impact and improvement techniques, *Energy Build*, 67 (2013), pp. 374-386
- [51] STAZI, Francesca; MASTRUCCI, Alessio; DI PERNA, Costanzo. Trombe wall management in summer conditions: An experimental study. *Solar Energy*, 2012, 86.9: 2839-2851.
- [52] B. Chen, X. Chen, Y.H. Ding, X. Jia, Shading effects on the winter thermal performance of the Trombe wall air gap: an experimental study in Dalian, *Renew Energy*, 31 (2006), pp. 1961-1971
- [53] DRAGIĆEVIĆ, S.; LAMBIC, M. Influence of constructive and operating parameters on a modified Trombe wall efficiency. *Archives of Civil and Mechanical Engineering*, 2011, 11.4: 825-838.
- [54] CHEN, Zheng D., et al. An experimental investigation of a solar chimney model with uniform wall heat flux. *Building and Environment*, 2003, 38.7: 893-906.
- [55] Sun, W., Ji, J., Luo, C., & He, W. (2011). Performance of PV-Trombe wall in winter correlated with south façade design. *Applied Energy*, 88(1), 224-231.
- [56] S. Jaber, S. Ajib, Optimum design of Trombe wall system in mediterranean region, *Sol Energy*, 85 (2011), pp. 1891-1898
- [57] Stazi F, Mastrucci A, Munafò P. Life cycle assessment approach for the optimization of sustainable building envelopes: an application on solar wall systems. *Build Environ* 2012;58:278–88.
- [58] Hassanain AA, Hokam EM, Mallick TK. Effect of solar storage wall on the passive solar heating constructions. *Energy Build* 2011;43:737–47.
- [59] Pielichowska K, Pielichowski K. Phase change materials for thermal energy storage. *Prog Mater Sci* 2014;65:67–123.
- [60] Tian Y, Zhao CY. A review of solar collectors and thermal energy storage in solar thermal applications. *Appl Energy* 2013;104:538–53.
- [61] Tyagi VV, Panwar NL, Rahim NA, Kothari R. Review on solar air heating system with and without thermal energy storage system. *Renew Sustain Energy Rev* 2012;16:2289–303.

- [62] Tyagi VV, Buddhi D. PCM thermal storage in buildings: a state of art. *Renew Sustain Energy Rev* 2007;11:1146–66.
- [63] Cabeza LF, Castellón C, Nogués M, Medrano M, Leppers R, Zubillaga O. Use of microencapsulated PCM in concrete walls for energy savings. *Energy Build* 2007;39:113–9.
- [64] Telkes M. Trombe wall with phase change storage material. *Proceedings of the 2nd National Passive Solar Conference*. Philadelphia, PA, USA; 1978.
- [65] Fiorito F. Trombe walls for lightweight buildings in temperate and hot climates. Exploring the use of phase-change materials for performances improvement. *Energy Procedia* 2012;30:1110–9.
- [66] Zalewski L, Joulin A, Lassue S, Dutil Y, Rouse D. Experimental study of small scale solar wall integrating phase change material. *Sol Energy* 2012;86:208–19.
- [67] Koo J , So H , Hong S W , et al. Effects of wallboard design parameters on the thermal storage in buildings[J]. *Energy and Buildings*, 2011, 43(8):1947-1951.
- [68] Rabani M, Kalantar V, Faghih AK, Rabani M, Rabani R. Numerical simulation of a Trombe wall to predict the energy storage rate and time duration of room heating during the non-sunny periods. *Heat Mass Transf* 2013;49:1395–404.
- [69] Li Y, Liu S. Experimental study on thermal performance of a solar chimney combined with PCM. *Appl Energy* 2014;114:172–8.
- [70] Bogdan M. Diaconu. Novel concept of composite phase change material wall system for year-round thermal energy savings[J]. *Energy and buildings*, 2010.10:1759-1772.
- [71] Pasupathy, A., and R. Velraj. Effect of double layer phase change material in building roof for year-round thermal management. *Energy and Buildings* 40.3 (2008): 193-203.
- [72] Zhang Yuan, Wu Zhiwei, Ge Fenghua, et al. Analysis of thermal performance of double-layer phase change material walls in hot summer and cold winter regions[J]. 2022(4).
- [73] Zhu, Na, et al. Numerical investigations on performance of phase change material Trombe wall in building. *Energy* 187 (2019): 116057.
- [74] Khalifa AJN, Abbas EF. A comparative performance study of some thermal storage materials used for solar space heating. *Energy Build* 2009;41:407–15.
- [75] Onishi J, Soeda H, Mizuno M. Numerical Study on a Low Energy Architecture Based Upon Distributed Heat Storage System. 2001.
- [76] LI, Chao; YANG, Xun; PENG, Kewen. Performance study of a phase change material Trombe

wall system in summer in hot and humid area of China. *Energy Reports*, 2022, 8: 230-236.

[77] OMARA, Adil AM; ABUELNUOR, Abuelnuor AA. Trombe walls with phase change materials: A review. *Energy Storage*, 2020, 2.6: e123.

[78] H. Akeiber, P. Nejat, M. Z. A. Majid, M. A. Wahid, F. Jomehzadeh, I. Z. Famileh, et al., "A review on phase change material (PCM) for sustainable passive cooling in building envelopes," *Renewable and Sustainable Energy Reviews*, vol. 60, pp. 1470-1497, 2016.

[79] P. Tatsidjodoung, N. Le Pierrès, and L. Luo, "A review of potential materials for thermal energy storage in building applications," *Renewable and Sustainable Energy Reviews*, vol. 18, pp. 327-349, 2013.

[80] Zhang, S.S.; Xia, L.; Jin, X. Research progress on phase change energy storage building walls. *Journal of Southeast University: Natural Sciences Edition*, 2015, 45.3: 612-618.

[81] J. Lizana, R. Chacartegui, A. Barrios-Padura, and J. M. Valverde, "Advances in thermal energy storage materials and their applications towards zero energy buildings: a critical review," *Applied Energy*, vol. 203, pp. 219-239, 2017.

[82] S. A. Memon, "Phase change materials integrated in building walls: A state of the art review," *Renewable and sustainable energy reviews*, vol. 31, pp. 870-906, 2014.

[83] Melero S, Morgado I, Neila FJ, Acha C. Passive evaporative cooling by porous ceramic elements integrated in a trombe wall. *Architecture & sustainable development (vol 2): 27th international conference on passive and low energy Architecture*. Presses univ. de Louvain. 2011. p. 267.

[84] Peng J, Lu L, Yang H, Han J. Investigation on the annual thermal performance of a photovoltaic wall mounted on a multi-layer façade. *Appl Energy* 2013;112:646–56.

[85] Rabani M, Kalantar V, Dehghan AA, Faghieh AK. Empirical investigation of the cooling performance of a new designed Trombe wall in combination with solar chimney and water spraying system. *Energy Build* 2015;102:45–57.

[86] Wang, D., Hu, L., Du, H., Liu, Y., Huang, J., Xu, Y., & Liu, J. (2020). Classification, experimental assessment, modeling methods and evaluation metrics of Trombe walls. *Renewable and Sustainable Energy Reviews*, 124, 109772.

[87] Taffesse F, Verma A, Singh S, Tiwari GN. Periodic modeling of semi-transparent photovoltaic thermal-trombe wall (SPVT-TW). *Sol Energy* 2016;135:265–73.

[88] Hu Z, He W, Ji J, Hu D, Lv S, Chen H, et al. Comparative study on the annual performance of

three types of building integrated photovoltaic (BIPV) Trombe wall system. *Appl Energy* 2017;194:81–93.

[89] Jovanovic J, Sun X, Stevovic S, Chen J. Energy-efficiency gain by combination of PV modules and Trombe wall in the low-energy building design. *Energy Build* 2017;152:568–76.

[90] Kara YA, Kurnuç A. Performance of coupled novel triple glass and phase change material wall in the heating season: an experimental study. *Sol Energy* 2012;86:2432–42.

[91] Yu Z, Ji J, Sun W, Wang W, Li G, Cai J, et al. Experiment and prediction of hybrid solar air heating system applied on a solar demonstration building. *Energy Build* 2014;78:59–65.

[92] de Gracia A, Navarro L, Castell A, Ruiz-Pardo A, Alvarez S, Cabeza LF. Experimental study of a ventilated facade with PCM during winter period. *Energy Build* 2013;58:324–32.

[93] Assefa G, Ambler C. To demolish or not to demolish: life cycle consideration of repurposing buildings. *Sustain Cities Soc* 2017;28:146–53.

[94] Zhang H, Shu H. A comprehensive evaluation on energy, economic and environmental performance of the trombe wall during the heating season. *J Therm Sci* 2019;28:1141–9.

[95] Struhala K, Cekon M, Slavik R. Life cycle assessment of solar façade concepts based on transparent insulation materials. *Sustain Times* 2018;10.

[96] Yu B, Li N, He W, Ji J, Zhang S, Chen H. Multifunctional solar wall for dehumidification, heating and removal of formaldehyde: Part 1. System description, preparation and performance of SiO<sub>2</sub>/TiO<sub>2</sub>adsorbent. *Build Environ* 2016;100:203–14.

[97] Yu B, He W, Li N, Zhou F, Shen Z, Chen H, et al. Experiments and kinetics of solar PCO for indoor air purification in PCO/TW system. *Build Environ* 2017;115: 130–46.

## *Chapter 3*

### ***METHODOLOGY***



## CHAPTER THREE: METHODOLOGY

<i>METHODOLOGY</i> .....	3-1
3.1. Measurement.....	3-1
3.1.1. Reference house description .....	3-1
3.1.2. Measuring tool .....	3-2
3.1.3. Weather station.....	3-4
3.2. Simulation.....	3-6
3.2.1. Numerical Model for Validation-reference house .....	3-6
3.2.2. Numerical Model for optimization-Composite Trombe wall house.....	3-9
3.2.3. Weather and location description .....	3-11
3.3. Method for simulation—THERB for Ham .....	3-12
3.3.1. Conductive Heat Transfer .....	3-13
3.3.2. Radiant heat transfer .....	3-14
3.3.3. Incident solar radiation.....	3-14
3.3.4. Ventilation .....	3-15
3.3.5. Conductive Moisture Transfer.....	3-15
3.3.6. Control of space conditioning .....	3-15
3.3.7. Flow Chart.....	3-15
3.4. Mathematical modeling.....	3-17
3.4.1. Mathematical modeling of PCM.....	3-17
3.5.2. Additional mathematical modeling .....	3-18
Reference .....	3-19



### 3.1. Measurement

#### 3.1.1. Reference house description

The reference house was a small building built for the experiments located in Kitakyushu, Japan (33.88, 130.70). The overall width of the reference house was 2.70 m and the depth was 2.785 m. The roof was sloping and the total height was 3.98 m (including foundation). The main structure material was Japanese fir (length 3000 mm, width 105 mm, and height 105 mm), with a 30 mm insulation layer inside and a galvalume steel plate as the outer enclosure structure. The interior floors, ceilings, and walls of the reference house were lined with insulation panels with a thermal conductivity of 0.036 W/mK. The structure of each part is shown in Table 3.1.

**Table 3.1 Material and structure of envelope of the reference house**

Construction	Material	Thickness (m)
Exterior wall	Styrofoam board	0.030
	Japanese fir	0.105
	galvalume steel plate	0.002
Floor	Styrofoam board	0.030
	Japanese fir	0.105
Roof/Ceiling	Styrofoam board	0.030
	Japanese fir	0.105
	galvalume steel plate	0.002
Ground	Soil	-----

The entire south elevation of the house was designed in a classic Trombe wall configuration; the massive wall was constructed of 100 mm thick concrete blocks with a total dimension of 2.63 m × 2.34 m. The outside of the concrete massive wall was covered with a layer of dark film, so as to improve the absorptivity of the massive wall. The glass layer of the Trombe wall was a single floor-to-ceiling glass window that could be opened. Figure 3.1.1(a) shows the south elevation of the reference house with the entire glazing surface belonging to the Trombe wall. The structure of each part is shown in Table 3.2. The reference house is not equipped with light-permeable windows, and Figure 3.1.1 shows the south elevation and interior of the house.

**Table 3.2 Material and structure of Trombe wall in reference house**

<b>Construction</b>	<b>Material</b>	<b>Thickness (m)</b>
Massive wall	Concrete brick	0.100
Air layer	Air	-----*
Glazing surface	Glass (Single layer)	0.003

\*The gap between massive wall and glazing surface is 0.210 m.



(a)



(b)

**Figure 3.1.1 The reference house: (a) The south elevation of the reference house (b) The massive wall of Trombe wall**

### 3.1.2. Measuring tool

**Indoor thermometer --Thermo Recorder TR-72wf:** The apparatus is manufactured by TandD and is used to measure the temperature and humidity of the indoor and air layers. It is also used to measure outdoor air temperature for proofreading. Measure and record temperature and humidity with these next generation cloud connectible data loggers.

Measurement Channels: temperature 2ch

Measurement Range: -40 to 110°C

Accuracy Avg:  $\pm 0.3^\circ\text{C}$

Logging Capacity: 8,000 data sets

Recording Intervals: 15 choices from 1 sec. to 60 min.

Operating Environment: Temperature: -10 to 60°C

Humidity: 90%RH or less (no condensation)

Dimensions: H:58mm × W:78mm × D:26mm

**Surface thermometer -- Thermo Recorder TR-71wf:** The apparatus is manufactured by TandD and is used to measure the temperature of the surface of walls. One machine can connect two sensors at the same time. Measure and record temperature with these next generation cloud connectible data loggers.

Measurement Channels: temperature 2ch

Measurement Range: -40 to 110°C

Accuracy Avg:  $\pm 0.3^\circ\text{C}$

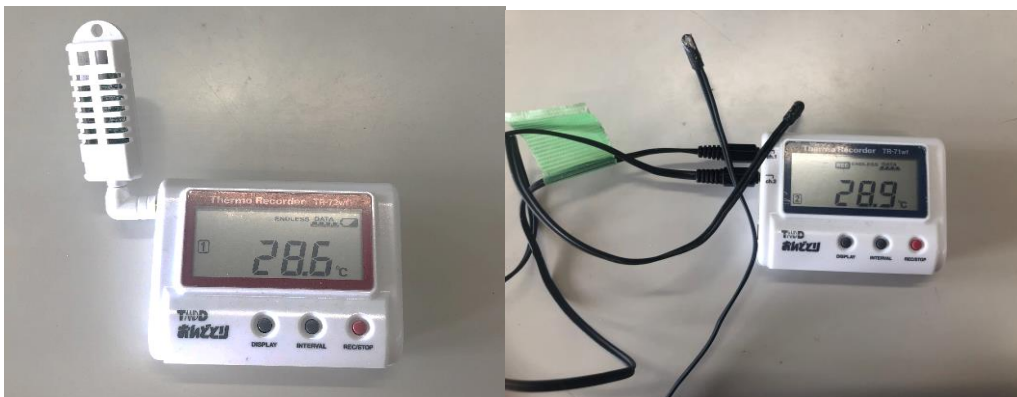
Logging Capacity: 8,000 data sets

Recording Intervals: 15 choices from 1 sec. to 60 min.

Operating Environment: Temperature: -10 to 60°C

Humidity: 90%RH or less (no condensation)

Dimensions: H:58mm × W:78mm × D:26mm



(a)

(b)

**Figure 3.1.2 Thermometer: (a) Thermo Recorder TR-72wf (b) Thermo Recorder TR-71wf**

The room temperature and air layer temperature were measured using the TR-72wf, and the massive wall interior and exterior surface temperatures were measured using the TR-71wf. The measurement points and their locations are indicated in Figure 3.1.2. The actual measurement experiment calibrated all thermometers and set them in the position as shown in Figure 3.1.3.

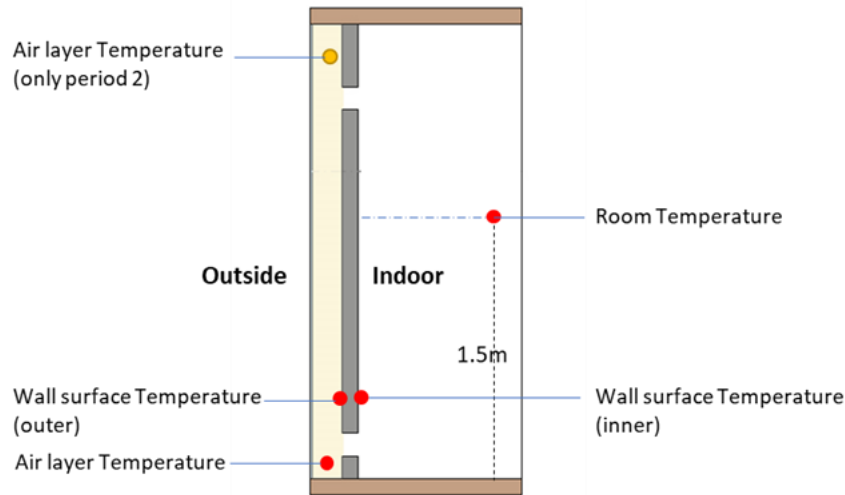


**Figure 3.1.3 Thermometers setting location**

### 3.1.3. Weather station

Weather Link-Davis Vantage Pro2 is used for the weather conditions near the coordinate position of the measured part: the surrounding temperature, humidity, wind speed, etc. A customizable station with a wide range of options and sensors to help professionals and hobbyists measure, monitor, and manage weather data. It can provide the highest level of accuracy, reliability and ruggedness. Specifically, can measure:

- Inside Temperature and Humidity
- Outside Temperature and Humidity
- Barometric Pressure
- Rainfall
- Detachable Wind Speed and Direction sensors
- Optional UV and Solar radiation sensors
- Optional additional temperature and humidity sensors

The weather station was set up at the neighboring location of the reference house during the actual measurement and verification phase, and simultaneously tested the local weather conditions

(air temperature, humidity, solar radiation, wind direction and speed, etc.) as well as the indoor temperature of the reference house every 10 min from 1 January to 13 January 2020. The outside temperature and solar radiation situation is shown in Figure 3.1.5 The outside humidity is shown in Figure 3.1.6.



**Figure 3.1.4 The picture of Davis Vantage Pro2 and Installation location**

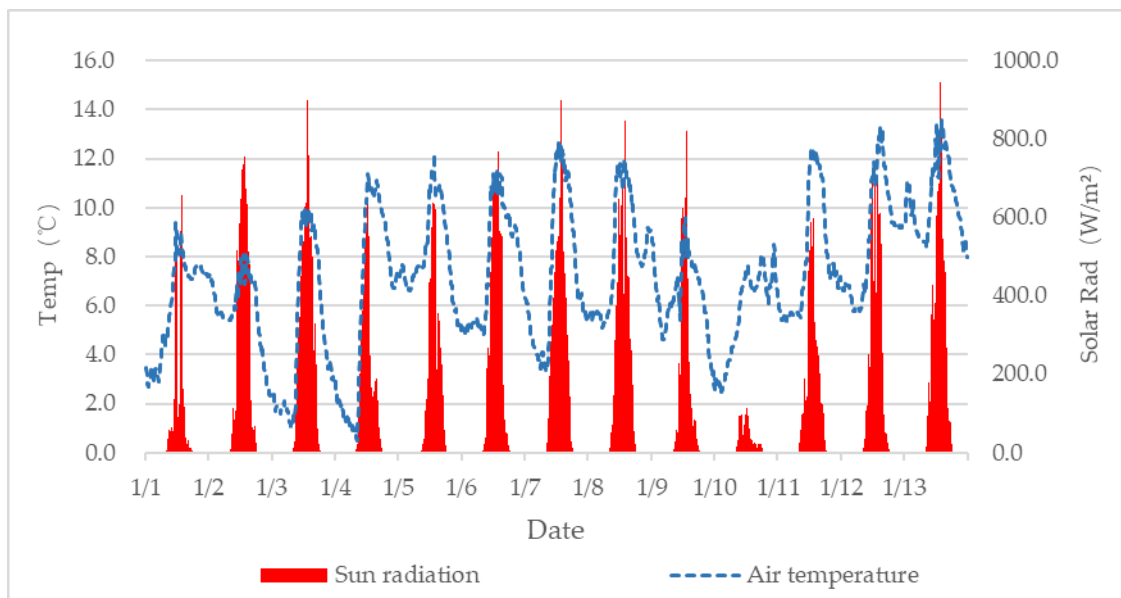


**Figure 3.1.5 The outside temperature and solar radiation measured from January 1st to January 13th in 2020.**

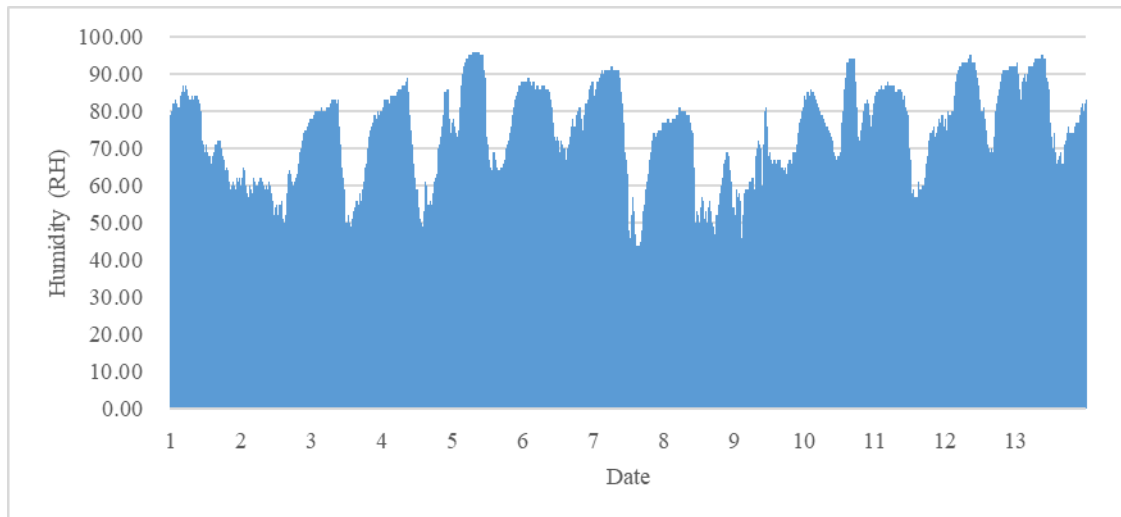


**Figure 3.1.6 The outside humidity measured from January 1st to January 13th in 2020.**

## 3.2. Simulation

### 3.2.1. Numerical Model for Validation-reference house

The validation simulation experiments are based on the reference room in the field to establish a digital model of equal size, and its mapping 3D model and Construction method of the Trombe wall and construction drawings of the exterior envelope of the wall is shown in Figure 3.2.1. Simplified explode model of experimental house simulation calculation is shown in Figure 3.2.2. The thermal performance parameters of each part of the material are shown in the following table 3.3, The 3d model shows the construction method of the main wooden structure, and the exposed part of the outer skin of the actual building is made of steel wave board as the outermost envelope, the same below.

**Table 3.3 Properties of each material**

<b>Material</b>	<b>Thickness (m)</b>	<b>Thermal Conductivity (W/m·K)</b>	<b>Density (kg/ m<sup>3</sup>)</b>	<b>Specific heat capacity (J/kg·K)</b>
Japanese fir	0.105	0.099	364.0	2150
Polystyrene foam	0.030	0.036	27.0	1100
Air layer	-----	0.022	1.2	1000

Galvalume steel plate	0.002	44.200	3690.0	196
Concrete	0.100	1.600	2200.0	840
Glass	0.003	0.780	2540.0	770

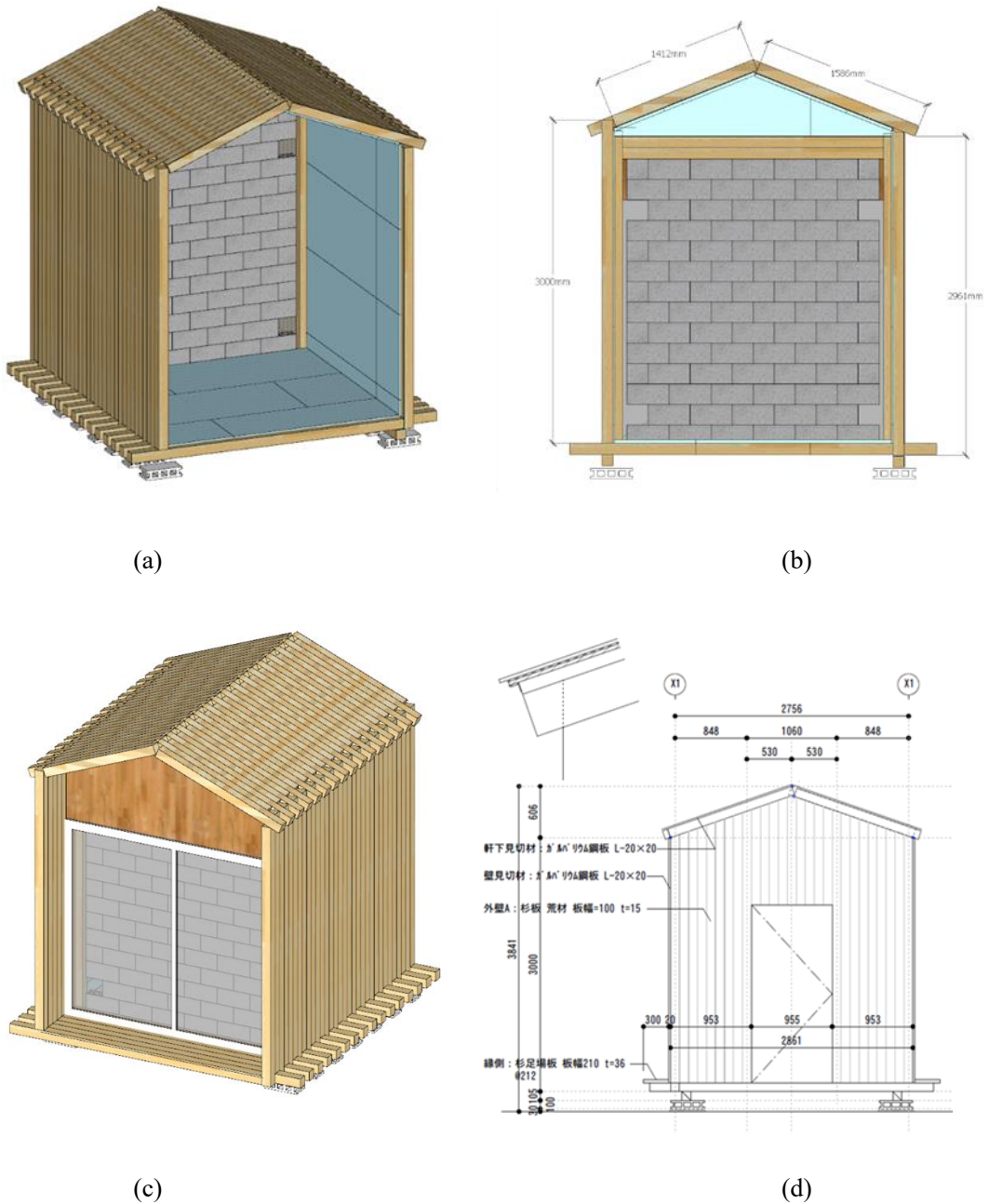
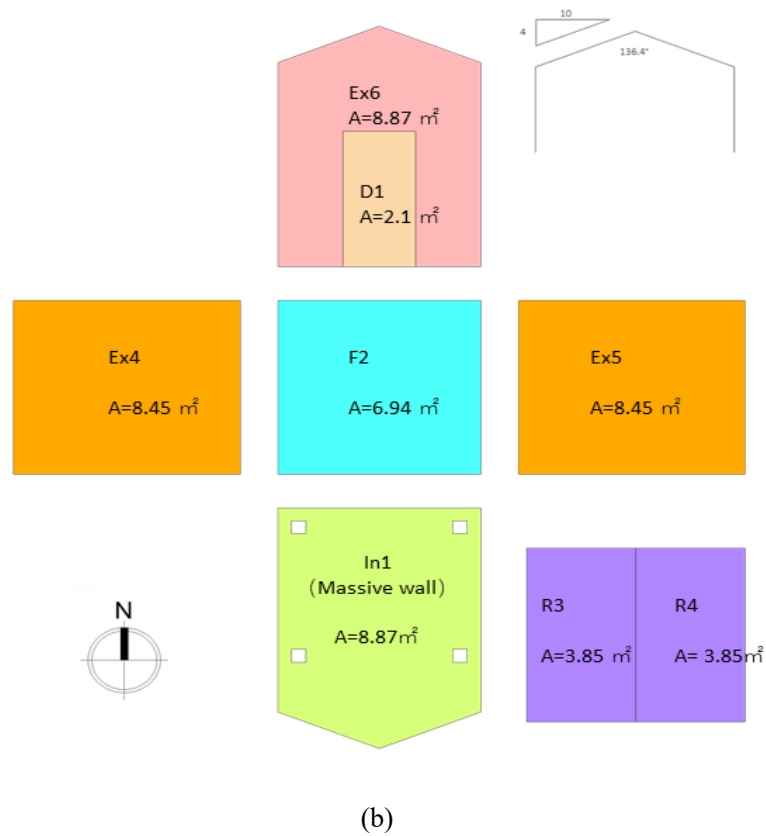
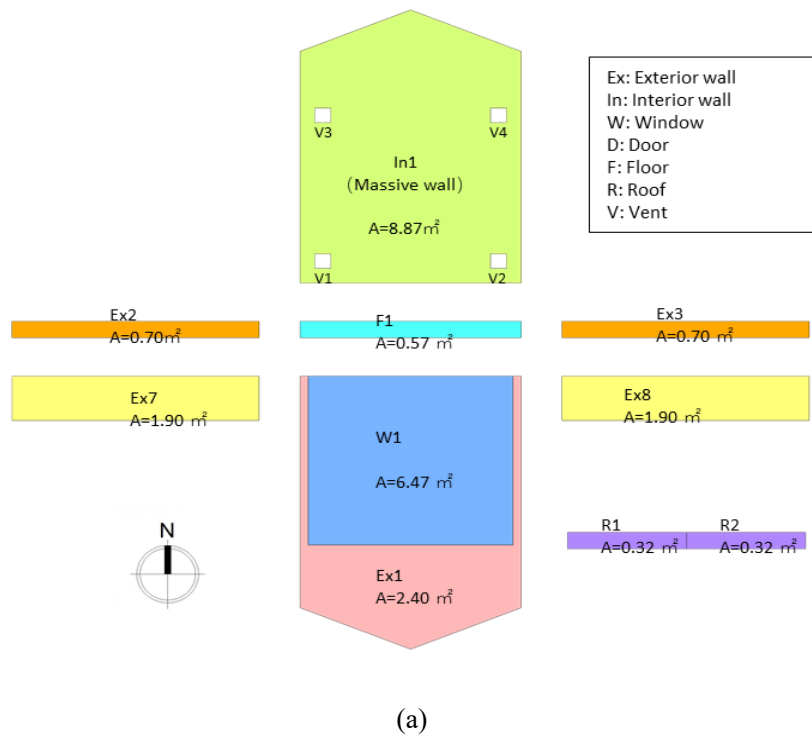


Figure 3.2.1 Reference house: (a) 3D model of sketch up (inside); (b) Trombe wall construction; (c) 3D model of sketch up (outside, South); (d) Construction drawings of the exterior envelope



**Figure 3.2.2 Simplified explode model of experimental house: (a) South part; (b) North part**

### 3.2.2. Numerical Model for optimization-Composite Trombe wall house

The structure of the numerical model for validation was the same as the reference room. There were still some disadvantages, such as a low thermal resistance and inverse thermo-siphon phenomena, which occur when the massive wall has a lower temperature than room temperature, particularly during the night in the cold season, when reversing the air circulation through the vents chills the room even more than the classic Trombe wall. Following these shortages, a composite double-circulation Trombe wall, which had an added interior wall made of insulating material (Styrofoam board), was constructed inside the classic wall. It had two ventilated air vents (between the wall and the glass, and between the wall and insulation) as shown in Figure 3.2.3 The use of a DC fan on the upper vents would control the thermal cycling of the indoor air and the air layer automatically according to the temperature of the ventilated air vents. simplified plan view of simulation calculation is shown in Figure 3.2.4. The material properties [1] are shown in Table 3.4 below.

Trombe wall system, which has a special feature that there is a circulating air exchange inside the system: hot air from above the air layer enters the room from the upper air chamber, while the opposite happens below. At the same time, the air temperature in the upper part of the air layer is slightly higher than in the lower part. Therefore, when designing the simulation model, it was considered to divide the air layer into two parts (with the middle set to "no material"), where the air above the air layer enters the room, and the air below the air layer enters the air layer from the room.

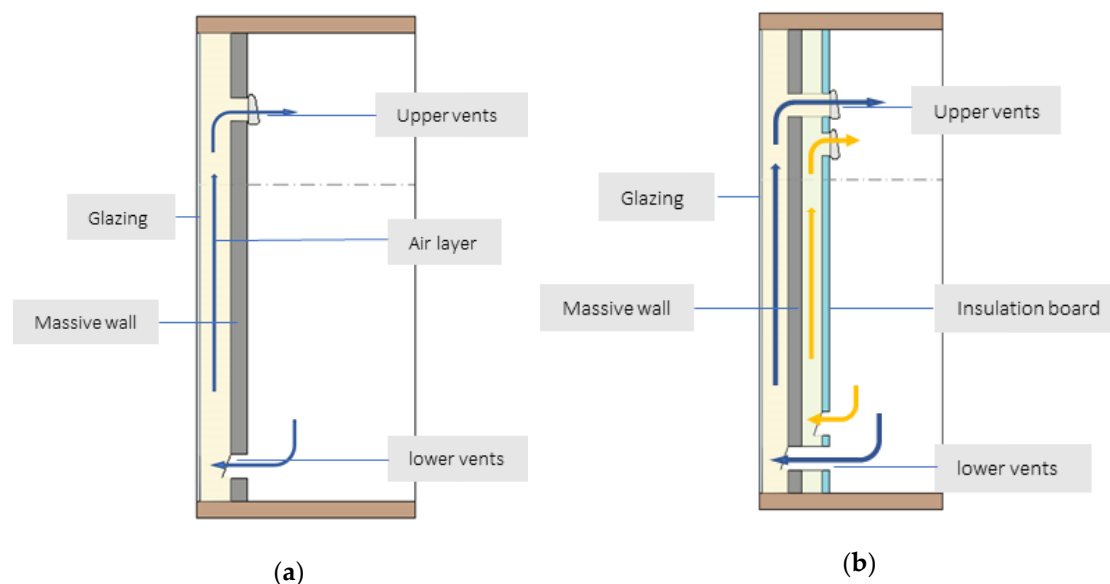


**Figure 3.2.3 Trombe wall section of the south elevation of the models: (a) The classical Trombe wall and its air circulation (b) The new type composite Trombe wall and its air circulation**

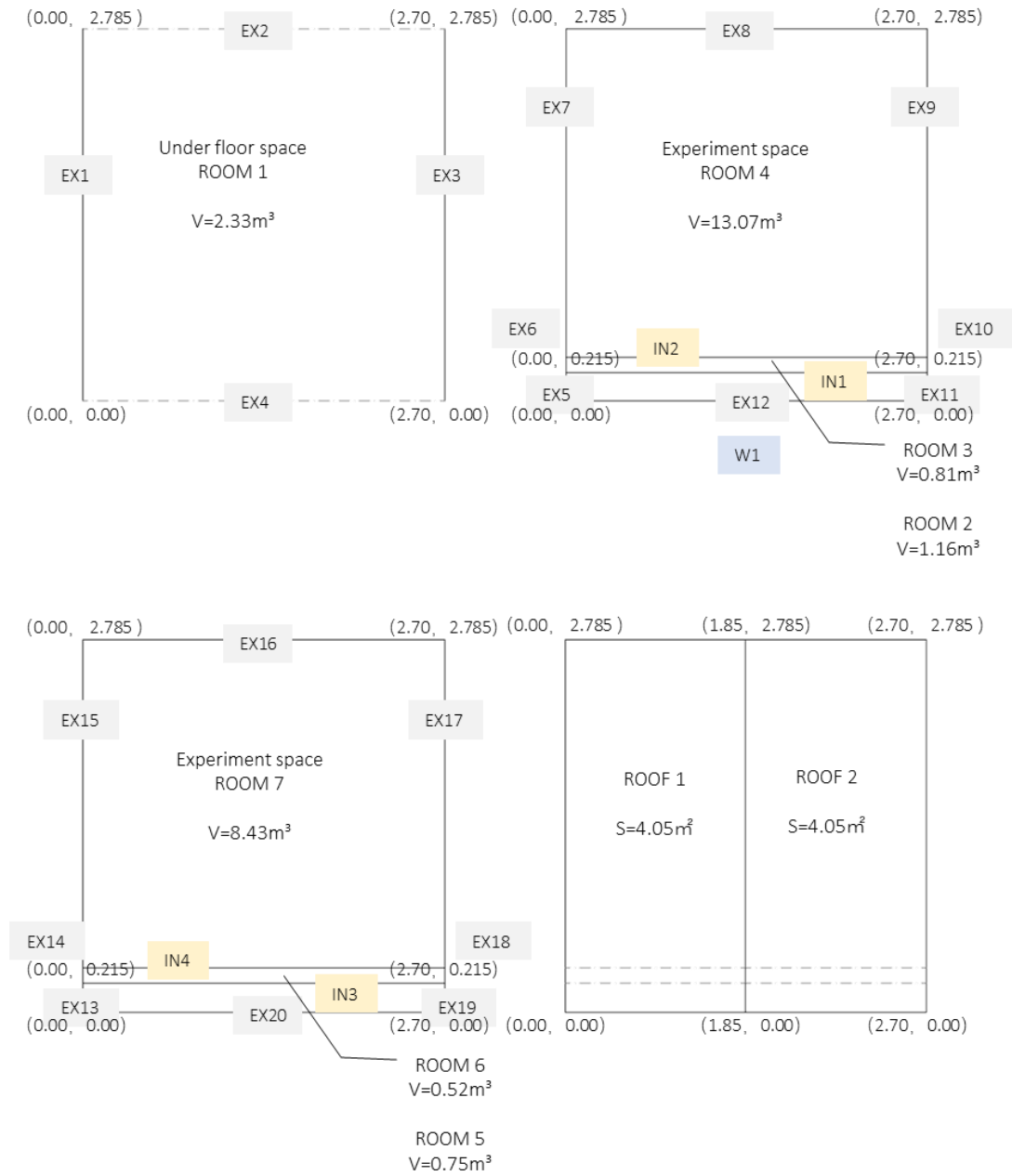


**Figure 3.2.4 Space divided of experimental house**

**Table 3.4 Material and structure of Trombe wall in reference house**

<b>Construction</b>	<b>Material</b>	<b>Thickness (m)</b>
Glazing surface	Glass (Single layer)	0.003
Outer air layer	Air	-----*
Massive wall	Concrete block	0.100
Inner air layer	Air	-----*
Insulation board	Polystyrene foam	0.06

\*The gap between massive wall and glazing surface is 0.210 m. The gap between glazing surface and insulation board is 0.15 m.

### 3.2.3. Weather and location description

The reference house for the measurements was located in Kitakyushu, Japan (33.88, 130.70). The climate of Kitakyushu is temperate humid, with quite cold winters and hot, moist, and rainy summers. According to the Japan Meteorological Agency (JMA), Kitakyushu is located in the northern part of Fukuoka. In winter, prevailing north westerly winds cause the advection of cold air from Siberia to Kyushu (North) and bring cloudy conditions to the area, although the amount of precipitation is small.

During the winter season (November to February), a Siberian High develops over Eurasia, while an Aleutian Low develops over the northern North Pacific, resulting in a winter pressure pattern with a high in the west and a low in the east. As a result, cold air will flow into the northern Kyushu area, resulting in many cloudy days, while areas on the leeward side of the mountainous region will have relatively clear days. On sunny mornings with high pressure, temperatures may drop and become cooler due to radiative cooling. Early June to mid-July is the rainy season, when the Pacific High strengthens and warm, moist air masses from the south collide with cooler air masses from the continent and the north, causing fronts to become stagnant. After the end of the rainy season, the Pacific High will bring clear skies and a hot midsummer. The hot days with daily maximum temperatures of 35°C or higher and tropical nights with night-time minimum temperatures of 25°C or higher will increase due to the strong solar radiation.

The meteorological data (air temperature, humidity, solar radiation, wind direction and speed, etc.) used for the year-round simulations used the meteorological standard year's data of the Automated Meteorological Data Acquisition System (AMeDAS) collected locally in Yahata

Kitakyushu (33.51, 130.44) closed to the reference house. The Extended AMeDAS Weather Data (EA Weather Data) is an all-Japan weather data compiled by supplementing missing weather data observed by the Japan Meteorological Agency's Area Meteorological Stations (AMeDAS), correcting data considered to be anomalous, and supplementing data for weather elements not observed by AMeDAS. EA weather data include hourly and daily values of 10 weather elements: local pressure, temperature, relative humidity, absolute humidity, total solar radiation, atmospheric radiation, wind direction, wind speed, precipitation, and sunshine duration.

Figure 3.2.5 compares the actual measured and nearest meteorological observation point outdoor temperatures in January of different years with those recorded on the 1st to 10th of the meteorological standard year. Although the daily weather conditions vary from year to year, the overall average temperatures are similar and fluctuations are roughly the same, so the weather standard year data for Kitakyushu can be used as a condition for predicting building loads.

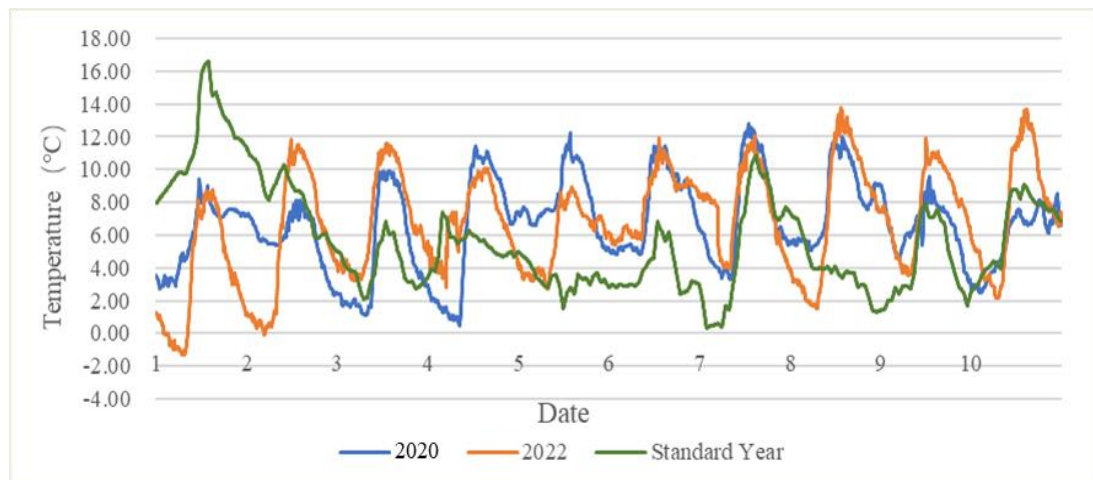


**Figure 3.2.5 Temperature comparison between field measurements and local meteorological observation points in January**

### 3.3. Method for simulation—THERB for Ham

This study uses the THERB for Ham software which was initially developed by Akihito Ozaki, to explore an effective method for utilizing the heat inside the solar space. According to the building input model, the room (space) can be arbitrarily divided into a living room (including underfloor, inter-floor space and stairwell) or an air layer. As described below, the convective heat transfer coefficient and the radiation heat transfer coefficient between the room temperature and the air layer are calculated differently.

In the default setting, the convective heat transfer coefficient is updated in each calculation step for each of the outer surface, inner surface and air layer (air layer and closed air layer) of the building. At this time, the dimensionless equation based on boundary layer theory or experimental rules is

applied to forced convection and natural convection. The main flow rate required to calculate the forced convection heat transfer coefficient is calculated from the experimental formula of the external wind direction and velocity of the outer surface of the building and the ventilation flow rate of the inner surface (in the open state of the window). Use the value divided by the equivalent cross section. Calculate the natural convective heat transfer coefficient of the interior surface of the building (window closed), divided into vertical and horizontal planes. In addition to the default settings, a functional equation of wind speed and wind speed of the external environment can be used based on experimental or experimentally based constant values.

The convective heat transfer coefficient of the inner surface may also be a functional equation based on the difference between the experimental surface temperature and the air temperature, or a constant value (constant throughout the day or only constant during air conditioning). The convective heat transfer coefficient of the air layer is in the default setting for each venting layer (forced convection or natural convection, depending on the flow rate) and the closed air layer applies a dimensionless equation, but can be set to a constant value. The characteristic of THERB for HAM are as follows [2]:

- (1) Comprehensive calculation of heat and moisture transfer and airflow
- (2) Prediction of the hygrothermal environment (temperature, humidity, predicted average value, standard effective temperature)
- (3) Temperature and humidity control or predictive average voting control
- (4) Considering the time variation of convective heat transfer and moisture transfer
- (5) The forced and natural heat transfer coefficient and moisture transfer coefficient of each component are calculated according to the dimensionless equation.
- (6) Strict geometric calculations for external and internal daylight and shading areas.
- (7) Multi-layer window model
- (8) Multiple reflections of solar radiation transmitted through windows
- (9) Nonlinearity of radiation heat transfer
- (10) Mutual radiation between internal surfaces
- (11) Efficient insulation structure and Network airflow model

### **3.3.1. Conductive Heat Transfer**

The finite difference method is applied to the model of one-dimensional transient thermal conduction of multi-layer walls. Regarding thermal conduction to the ground, the finite difference

method of two or three dimensions is applied to the previous calculation of the ground temperature and then the results are used as the input excitation for conductive calculation of the earthen floor and basement walls.

By default, the convective heat transfer coefficients are recalculated at every time step on all surfaces of the exterior, interior and cavities of buildings using dimensionless equations which are derived from either the profile method for boundary layer (based on the energy equation, the momentum equation and the fluid friction) or defined from the experimental findings according to natural or forced convection. Furthermore, the natural convective heat transfer coefficients are classified into either vertical or horizontal surfaces. It is possible to use the functional equations of the wind direction and velocity for the exterior convective heat transfer coefficients and the functional equations of the temperature difference between surface and room for the interior convective heat transfer coefficients. It is also possible to set constant heat transfer coefficients all day long or modify the coefficients to take into consideration air-conditioning time for every part of the building [2].

### **3.3.2. Radiant heat transfer**

On the exterior surfaces of the buildings, the standard method of using the radiant heat transfer coefficients and atmospheric radiation is applied. On the interior of buildings, instead of the general method (that is, the calculation of heat transfer between surface and indoor air and radiation between surfaces), the use of the long-wave absorption coefficient makes it possible to simulate a net absorption of radiant heat as a consequence of multiplex reflection among interior surfaces. Mutual radiation between the surfaces of cavities in walls and windows can also be calculated [2].

### **3.3.3. Incident solar radiation**

Incident solar radiation on the exterior and into the interior of buildings is divided into direct and diffuse solar radiation and calculated for all parts of the building in all directions using accurate geometric calculations of shaded and unshaded portions of the building by considering the influence of overhangs and wings. Isotropic model or anisotropic models can be chosen for diffuse solar radiation. Transmitted solar radiation is calculated by the multilayer window model and considers multiplex reflection (depending on an incidence angle of solar radiation) between not only the glazing layers but also between the window and interior shade at every time step. The multiplex reflection of both direct and diffuse solar radiation among interior surfaces including re-transmission of solar radiation from the inside to the outside through the windows is calculated by using the short-wave absorption coefficient. In addition, the absorption coefficients of long and short wave are applied to radiant heat emitted from lights and appliances, etc [2].

### **3.3.4. Ventilation**

The network airflow model integrating a thermal model with a plant model estimates natural and forced ventilation quantities of each zone (rooms and cavities) caused by air leakage, infiltration and mechanical ventilation. As for independent ventilated cavities in the walls, it is possible to estimate airflow quantities by hydrodynamic analysis as the solution to the equations of motion, energy and continuity. Constant ventilation quantities can be also set every hour for all zones [2].

### **3.3.5. Conductive Moisture Transfer**

Water Potential which is derived by applying the chemical potential of thermodynamics to moisture diffusion is used as the driving force of moisture transfer. This approach is proposed to be more accurate than other models based on physical properties such as vapour pressure. The model called P-model using water potential makes it possible to combine moisture transfer with heat transfer perfectly, and take into account internal energy and external forces such as gravity. The convective moisture transfer coefficients on all surfaces of the exterior, interior and cavities of buildings are calculated from the dimensionless Sherwood number, which is derived on the basis of the analogy between heat and mass transfer [2].

### **3.3.6. Control of space conditioning**

Control methods for space conditioning are classified into three types: heating, cooling, and simultaneous heating and cooling. By default, humidity control and temperature control are linked. Temperature and humidity set-point and ranges can be optionally set every hour. Moreover, the control of humidity is automatically performed in the case when the sensible temperature such as PMV is set as the set-point of air-conditioning [2].

### **3.3.7. Flow Chart**

Figure 3.3.1 shows the flow chart of THERB for HAM. One of the characteristics of THERB for HAM is that calculation nodes are automatically numbered for each room component or element and associated both temperature and humidity calculation.



### 3.4. Mathematical modeling

#### 3.4.1. Mathematical modeling of PCM

THERB for Ham is software written in Fortran language that allows editing and adding other computational models. In Chapter 6, special calculations need to be added due to the special nature of phase change materials (PCM).

In order to facilitate the simulation calculation in this paper, the mathematical models are reasonably simplified in the following: (1) All layers of the wall materials are isotropic media; (2)The heat transfer process through the wall the heat transfer process is one-dimensional; except for the phase change process in which the PCM (3) Except for the change of heat capacity of PCM during the phase change, all other thermal physical parameters are constant; (4) Ignore the convective heat transfer during the phase change of The convective heat transfer during the phase change of PCM layer is neglected; (5)The contact thermal resistance of the contact surface of each layer of the wall material is neglected. The contact thermal resistance of the contact surfaces of the wall materials is neglected.

The energy equation is as follows.

If  $T \leq T_s$

$$\rho_s C_{p,s} \frac{\partial T}{\partial t} = \lambda_s \frac{\partial^2 T}{\partial x^2} \quad (1)$$

If  $T_s < T \leq T_m$

$$\rho_s C_{p,s} \frac{\partial T}{\partial t} + \rho_m \frac{\partial C_{p,m} T}{\partial t} = \frac{\partial}{\partial x} \left( \lambda_m \frac{\partial T}{\partial t} \right) \quad (2)$$

If  $T_m \leq T < T_l$

$$\rho_l C_{p,l} \frac{\partial T}{\partial t} + \rho_m \frac{\partial C_{p,m} T}{\partial t} = \frac{\partial}{\partial x} \left( \lambda_m \frac{\partial T}{\partial t} \right) \quad (3)$$

If  $T > T_l$

$$\rho_l C_{p,l} \frac{\partial T}{\partial t} = \lambda_l \frac{\partial^2 T}{\partial x^2} \quad (4)$$

Where  $T_m = (T_s + T_l)/2$ ,  $C_p$  is the specific heat capacity,  $\rho$  is the density;  $T$  is the temperature;  $t$  is the time.  $\lambda$  is the thermal conductivity;  $x$  is the seating in the thickness direction. In the subscript,  $s$  is the solid phase,  $l$  is the liquid phase, and  $m$  is the melting period.



= 5390 (¥), Y = 15 years [5].

### Reference

[1] M. Kumar Kumaran, Architectural Institute of Japan, International Energy Agency Energy Conservation in Buildings and Community Systems IEA ANNEX 24 Heat, Air and Moisture Transfer Through New and Retrofitted Insulated Envelope Parts (Hamtie) Final Report Volume 3 TASK 3: Material Properties; Maruzen Publishing, Tokyo, Japan, 2001.10

[2] Ozaki, A.; Tsujimaru, T., Prediction of hygrothermal environment of buildings based upon combined simulation of heat and moisture transfer and airflow. Journal of the International Building Performance Simulation Association 2006, 16, (2), 30-37.

[3] Ozaki, A.; Watanabe, T.; Takase, S. In Simulation software of the hydrothermal environment of buildings based on detailed thermodynamic models, Proceedings of eSim 2004 Canadian Conference on Building Energy Simulation, 2004; 2004; pp 45-54.

[4] Electricity price. <https://denryoku-gas.jp/utility/kyuden/kwh-price>.

[5] Temperature-controlled DC fan price <http://kakaku.com/item/K0000913041>

## *Chapter 4*

# ***BASIC NUMERICAL ANALYSIS OF COMPOSITE DOUBLE-CIRCULATION TROMBE WALL***



**CHAPTER THREE: BASIC NUMERICAL ANALYSIS OF COMPOSITE DOUBLE-CIRCULATION TROMBE WALL**

*BASIC NUMERICAL ANALYSIS OF COMPOSITE DOUBLE-CIRCULATION TROMBE WALL*  
..... 4-1

4.1. Overview ..... 4-1

4.2. Measured results and validation ..... 4-1

4.2.1. Analysis of actual measurement results ..... 4-1

4.2.2. Validation of simulation results ..... 4-5

4.3. Study of composite double-circulation Trombe wall ..... 4-11

4.3.1. Introduction ..... 4-11

4.3.2. Result ..... 4-16

4.4. Optimization of double-circulation Trombe wall ..... 4-24

4.4.1. The effect of glazing surface properties ..... 4-25

4.4.2. The effect of DC fan rates ..... 4-33

4.4.3. The effect of inner wall properties ..... 4-40

4.4.4. The effect of massive wall properties ..... 4-52

4.4.5. Comprehensive optimization considerations ..... 4-59

4.5. Conclusion ..... 4-62

Reference ..... 4-64



## 4.1. Overview

With the promotion of highly insulated and sealed houses, central air conditioning systems that integrate ventilation, cooling and heating are gaining attention. In addition, solar thermal utilization is attracting attention as an effective means of reducing energy consumption for cooling/heating and hot water supply. Therefore, research and development of houses that combine central air conditioning systems and solar energy utilization are necessary for a comfortable thermal environment and energy conservation.

In this chapter, the actual measurements of an experimental house (33.88, 130.70) in Kitakyushu, Japan, are analyzed and compared with simulated experiments to verify the feasibility of THERB for HAM software for Trombe wall. Then the simulated numerical studies of a no-lighting house without Trombe wall (with and without windows), a classic Trombe wall room and a composite double-circulation Trombe wall room in this parametric environment are compared, and the energy performance and simulated air conditioning load values of these four types of houses in the heating season are explored. Focus on composite double-circulation Trombe wall system with temperature-controlled DC fan, to improve its thermal storage efficiency, basic factors such as insulation, fans, shading devices, vents, glass types, and materials and thickness of thermal storage walls are explored to optimize their performance.

## 4.2. Measured results and validation

### 4.2.1. Analysis of actual measurement results

The reference house for measurement is located in Kitakyushu, Japan (33.88, 130.70). The overall width of the house is 2.70m and the depth is 2.785m. The roof is sloping and the total height is 3.98m (including foundation). The main structure material is 105mm x 105mm x 3000mm Japanese fir, with 30mm insulation layer inside and galium steel plate as outer enclosure structure, single-glazed window. It is a classic Trombe wall house with a massive wall use concrete brick as the main material. The outer side of the concrete brick is laid with a black plastic film in order to improve the heat storage efficiency of the wall.

The actual measurement was carried out from January 1st to January 12th. No natural ventilation, and no forced ventilation in the wall by DC fan. The tool used for the measurement is Thermo Recorder TR-72wf and Thermo Recorder TR-71wf. Thermo Recorder TR-72wf is used for temperature of space. Thermo Recorder TR-71wf is used for temperature of surface. The measurement point is as shown in Figure 4.2.1. Where the room temperature and air layer temperature measurement points are near the center of the space, and the massive wall surface temperature is below the entire wall to the west.

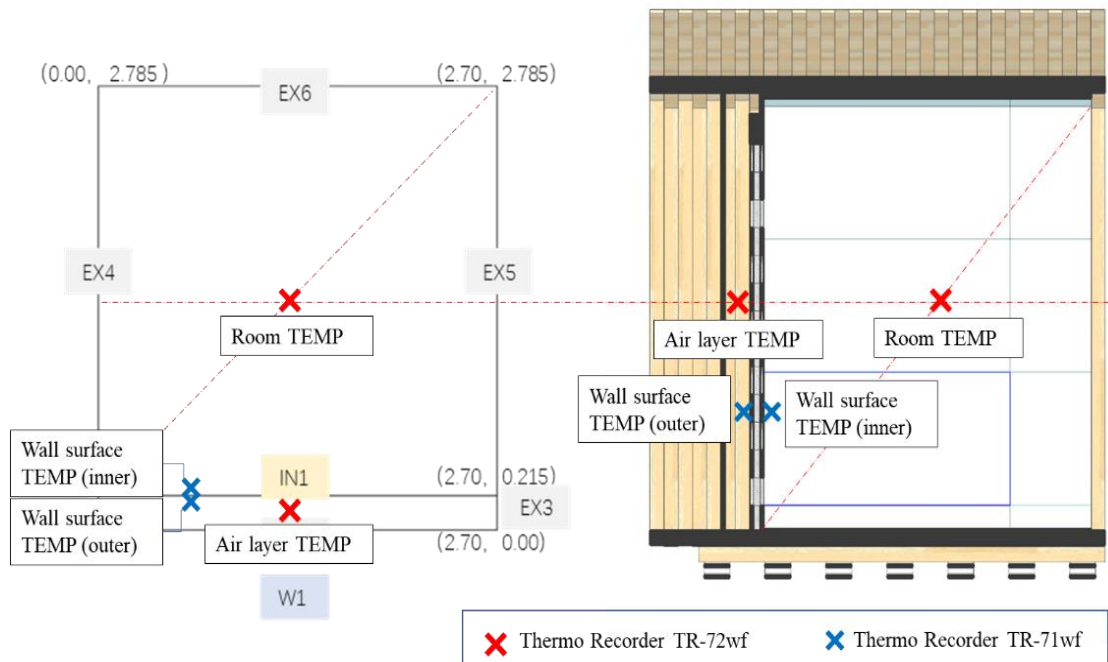


**Figure 4.2.1 The measurement point**

The experiment measured the temperature data at each measurement point every ten minutes. Figure 4.2.2 shows the measurements of space temperature versus outdoor temperature and solar radiation for the period from January 1st to January 12th, 2020. Where the solar radiation is the sum of the bar graph area, the larger the area within a single day, the higher the solar radiation. The comparison shows that indoor air temperature and air layer temperature fluctuate with the change of outdoor air temperature. However, in contrast, the law of change is more affected by solar radiation. It is observed that in general the air layer temperature is higher than the indoor temperature during the daytime. However, at the high point of solar radiation, the maximum temperature of the room will exceed the air layer temperature. The temperature of the air layer drops rapidly at night, and the air layer temperature drops to a level close to the outdoor temperature until the daily solar radiation production (i.e., before sunrise). Figure 4.2.3 shows the building space temperature and massive wall interior and exterior surface temperatures for the period from January 3rd to January 1th, 2020. During this period, the average outdoor temperature was 7.2°C, the average indoor temperature was 13.0°C, while the maximum indoor temperature was 32.6°C. The highest temperature point is the outside surface temperature of the massive wall. The temperature at the surface of the wall can exceed 35°C.

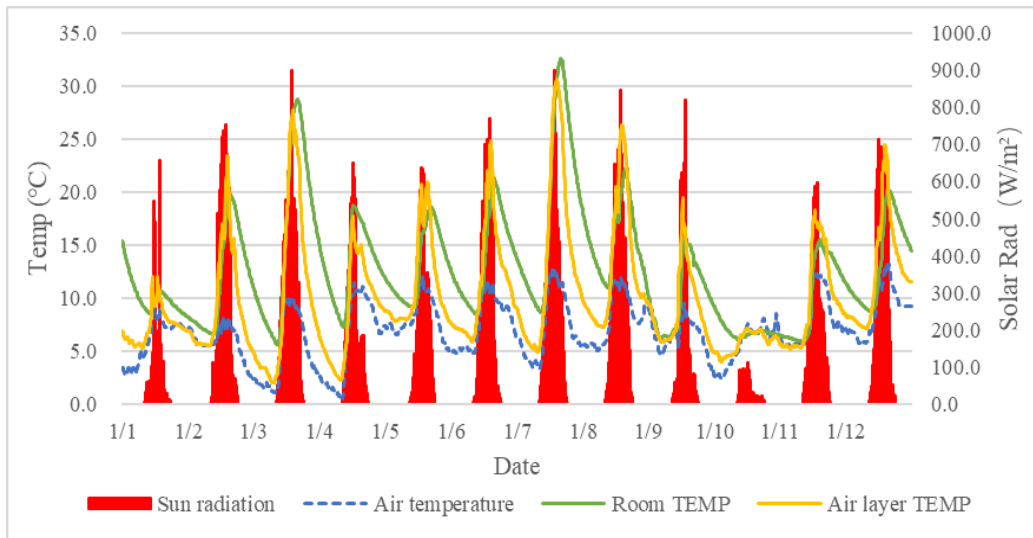


**Figure 4.2.2 The weather and temperature of reference house from January 1st to January 12th**

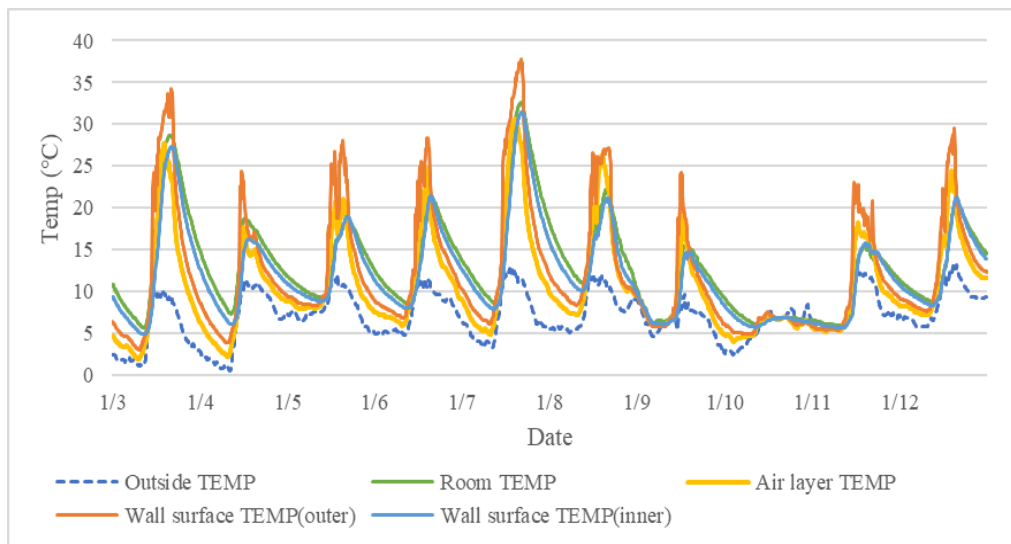


**Figure 4.2.3 The temperature of reference house from January 3rd to January 12th**

Figure 4.2.4 shows the data for one of the sunny days on January 7th. Where solar radiation is the area of the graph and outdoor temperature and indoor temperature are represented as bars. The graph reveals that the indoor temperature on that day can remain consistently greater than the outdoor temperature, with its maximum temperature difference exceeding 20° C. And from 12:00 noon to 22:00 at night, the indoor temperature can be maintained above 20°C. The highest temperature point is the outside surface temperature of the massive wall. the outside surface temperature of the massive wall has a similar trend to the temperature of the air layer, both starting to rise when solar radiation starts to be generated. On that day, there was a rapid increase in the outdoor surface temperature of

the massive wall around 11:00 a.m. It is speculated that this may be related to other weather factors (wind speed and direction, air humidity, etc.). the beginning of the decrease in the outdoor surface temperature of the massive wall started after a sudden brief cloudy period before sunset, and the temperature drop point of the air layer was higher than that of the wall surface temperature earlier. And the trend of indoor temperature change is similar to the trend of the indoor side surface temperature of the massive wall. In both cases, the temperature starts to increase slightly later than the air layer and the wall exterior side surface temperature. The wall surface temperature and the air layer temperature are not always higher than the indoor temperature. At night, due to the heat loss from the walls, their temperature drops faster than the indoor temperature and the actual temperature is even lower than the indoor temperature.

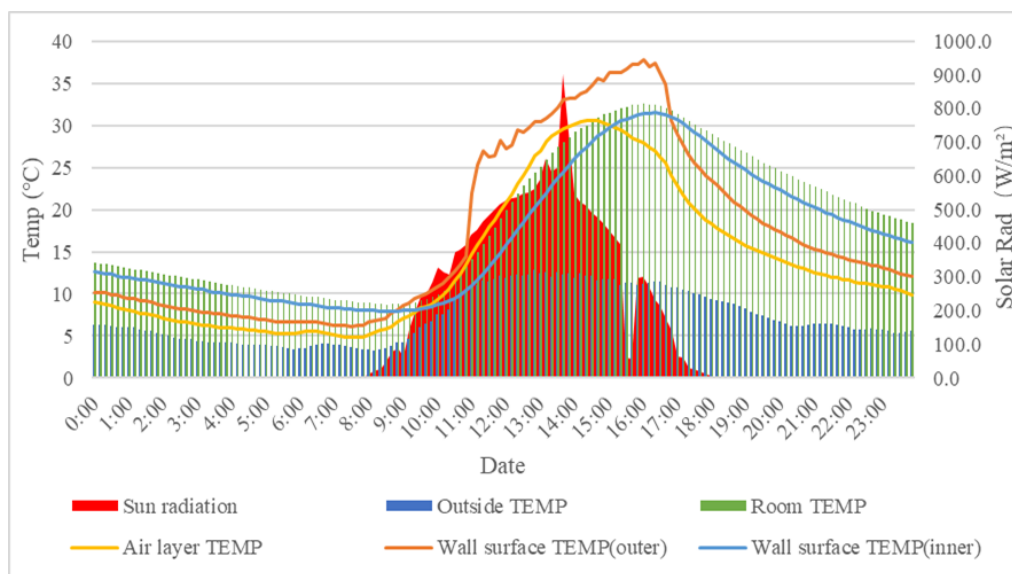


**Figure 4.2.4 The weather and temperature of reference house on January 7th**

January 10th was a non-sunny day with significantly less fluctuation in indoor temperature than a sunny day. Compared with January 7 (a sunny day), the average temperature on January 7th was 7.3°C, the average indoor temperature was 18.7°C, and the maximum room temperature was 32.6°C. The average outdoor temperature on January 10 was 5.71°C, the average indoor temperature was 6.9°C, and the maximum indoor temperature at night was 8.9°C. The actual outdoor temperature on January 10, is shown in Figure 3.2.5. That day was the same as January 10th: the indoor temperature followed the same trend as the temperature on the interior side of the wall, and the air layer temperature followed the same trend as the temperature on the exterior side of the wall. On that day, the outdoor temperature gradually increased from night to day. However, because the initial indoor temperature was higher than the outdoor one, the indoor temperature on that day gradually decreased to a level similar to the outdoor temperature. The air layer though received a small amount of solar radiation after sunrise and there was a slight increase in temperature. However, because the day was

cloudy and rainy, the solar radiation was extremely low, and the air layer lost a large amount of temperature the night before so the initial temperature itself was lower than the indoor temperature. Even if the air layer temperature and the outside surface temperature of the massive wall increased on that day, they could not reach the level that could heat the indoor temperature. Therefore, the use of Trombe wall system is closely related to solar radiation.

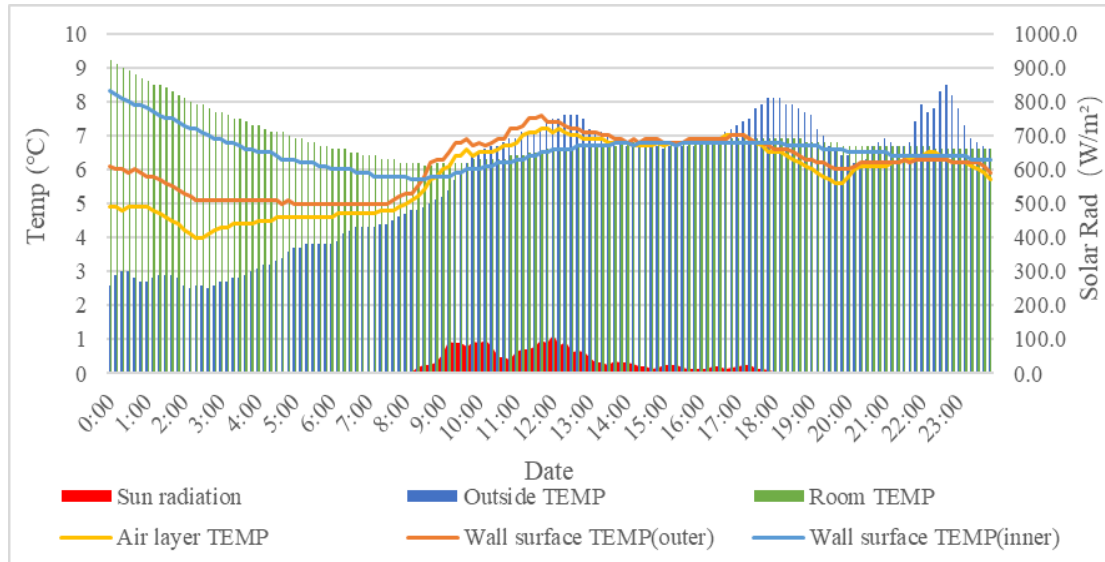


**Figure 4.2.5 The weather and temperature of reference house on January 10th**

#### 4.2.2. Validation of simulation results

In addition to analyzing the data, the other main purpose of the field measurements is to verify the accuracy of the simulation software and parameters to ensure that the subsequent simulation predictions are closer to the actual situation. The accuracy of the software Therb for HAM has been extensively verified in the simulation of ordinary houses, but there is not enough data to support it in the Trombe wall system, which has a special feature that there is a circulating air exchange inside the system: hot air from above the air layer enters the room from the upper air chamber, while the opposite happens below. The opposite happens below. At the same time, the air temperature in the upper part of the air layer is slightly higher than in the lower part. Therefore, when designing the simulation model, it was considered to divide the air layer into two parts (with the middle set to "no material"), where the air above the air layer enters the room, and the air below the air layer enters the air layer from the room. This configuration needs to be verified.

Figure 4.2.6 shows a basic flow chart for simulation result verification.

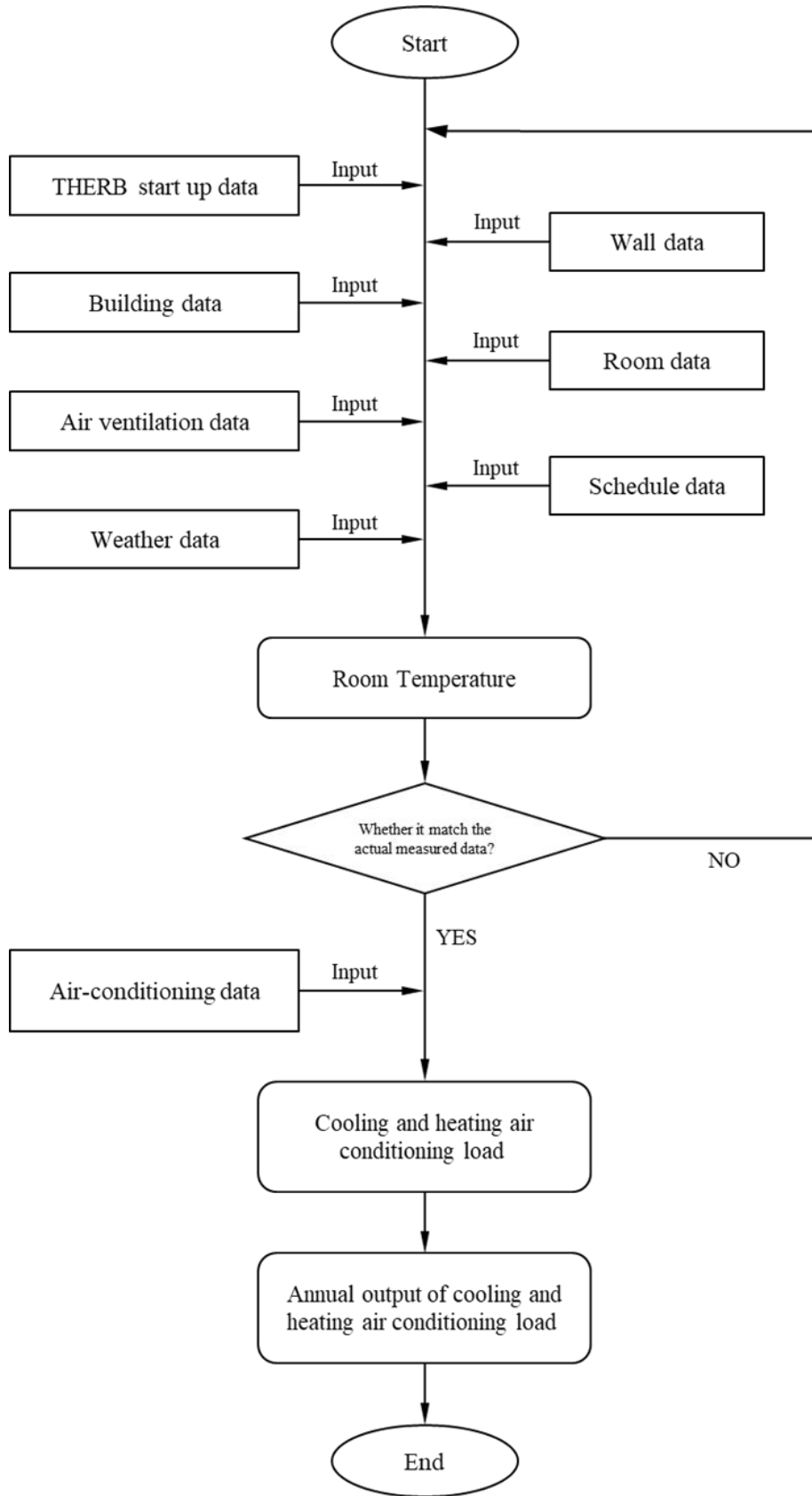
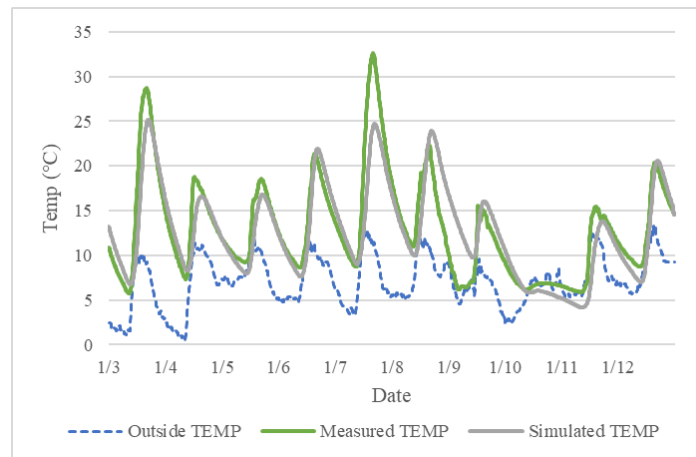
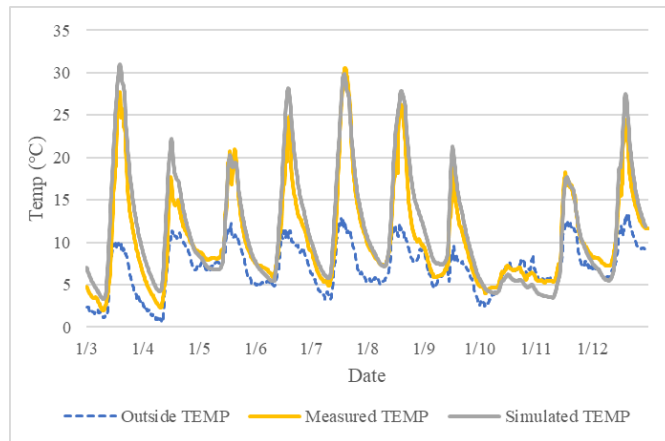


Figure 4.2.6 Basic flow chart for simulation result verification

Figure 4.2.7 shows the comparison of indoor temperature (room temperature) between the measured data and the simulated calculated data by THERB for Ham Software (every 10 minutes) from January 3th to January 12th. There was a relatively significant deviation from January 8 to January 9, but the simulated data and the measured data were in good overall agreement and almost consistent in terms of trend. Figure 4.2.8 shows the comparison of air layer temperature between the measured data and the simulated calculated data by THERB for Ham Software (every 10 minutes) from January 3th to January 12th. The simulated data and the measured data are in general agreement and the trend is also consistent. In contrast the measured data had more minor fluctuations at the daytime peak. The simulated data have a slight lag in the rate of decline during the temperature drop. Figure 4.2.9 shows the comparison of temperature of the outer surface of the massive wall chamber between the measured data and the simulated calculated data by THERB for Ham Software (every 10 minutes) from January 3th to January 12th. The simulated data are in general agreement with the measured data and are also consistent in terms of trend. Similar to the case of the air layer temperature, the measured data have more small fluctuations at the daytime peak. The simulated data lagged slightly in the rate of decline during the temperature drop. Figure 4.2.10 shows the comparison of temperature of the inner surface of the massive wall chamber between the measured data and the simulated calculated data by THERB for Ham Software (every 10 minutes) from January 3th to January 12th. Except for January 8, the simulated data peaks are biased high, but the basic trend is in good agreement.



**Figure 4.2.7 Comparison of room temperature between the measured data and the simulated**



**Figure 4.2.8 Comparison of air layer temperature between the measured data and the simulated**

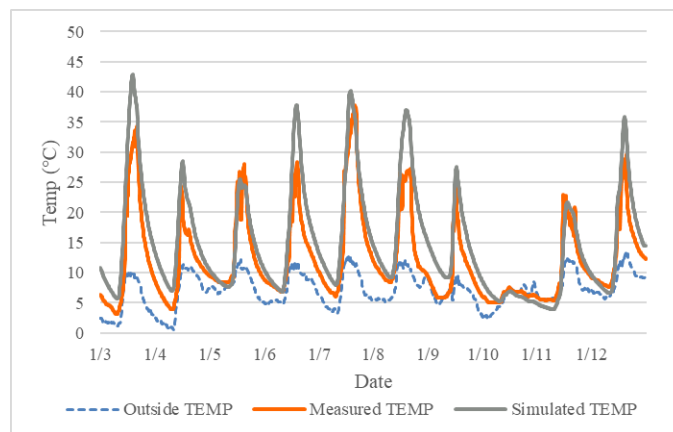


**Figure 4.2.9 Comparison of massive wall surface (outer) temperature between the measured data and the simulated**

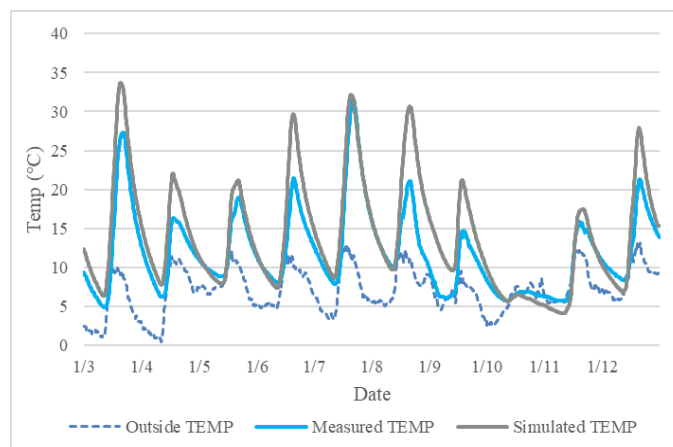


**Figure 4.2.10 Comparison of massive wall surface (inner) temperature between the measured data and the simulated**

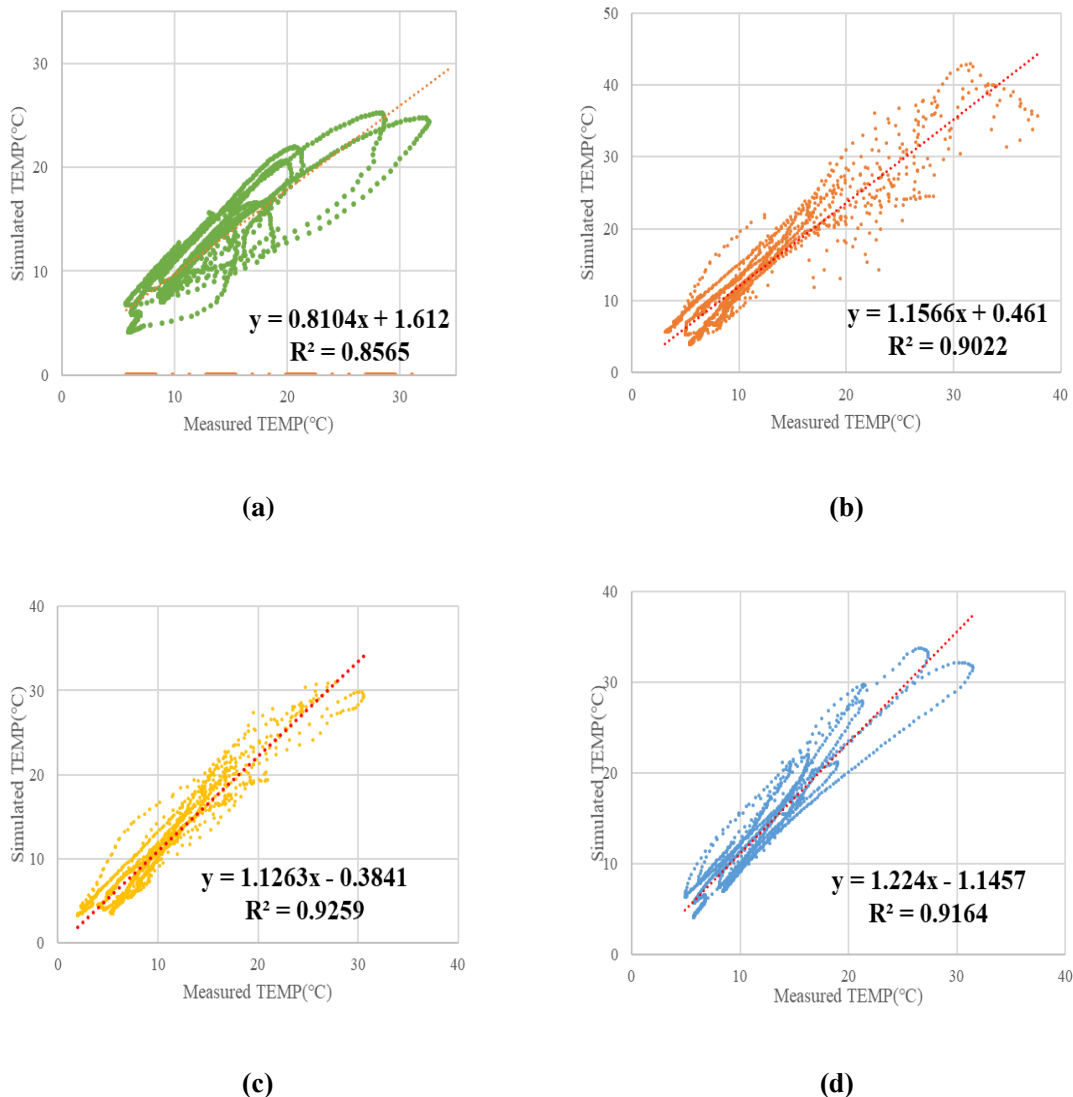


**Figure 4.2.11** Statistic of temperature between the measured data and the simulated: (a) Indoor temperature; (b) Massive wall surface (outer) temperature; (c) Air layer temperature; (d) Massive wall surface (inner) temperature

The comparison of simulated and measured results found that a relatively large gap occurred after sunset on January 9 for all parts except the air layer temperature. as well as the peak of simulated data would be higher than measured, and the changes were not prone to small and frequent fluctuations. The simulated results are overall slightly slower than the measured during the daily decrease in wall temperature. Possible causes of these errors are listed below:

(1) The internal circulation of the Trombe wall system in the reference cabin is caused by the temperature difference between the air layer and the room. The flowing air volume is different at each moment and the trend is different from day to day. However, even if the ventilation at each moment in the simulation parameters varies according to the time, the daily ventilation is fixed.

That is, when the solar radiation is higher than other days, the actual air circulation rate will increase at noon, while the ventilation in the simulation is consistent with other days, so that the room temperature will be lower than the actual measured temperature at that time.

(2) Inverse thermo-siphon phenomena: The actual reference house is not set up to perfectly prevent backflow, and the air layer is easily back flowed from the indoor air circulation at night. Same as the problem in (1), the simulation model cannot determine the air flow by the air temperature difference, so the model used for validation has all the air exchange between the air layer and the room set to 0 in the night-time setting. this may also be one of the reasons for the error.

(3) Material parameters can also cause some deviations: The thermal properties and other parameters of the materials used in the simulation are mainly obtained through information provided by the manufacturer or information recorded in general-purpose books, and are determined through repeated debugging, which may be different from the actual materials.

(4) While the simulations are "perfect environments" in terms of insulation performance, there is a possibility that additional heat loss may occur through deterioration of building materials, gaps between materials, or inadequate sealing. This is likely to result in a relatively rapid drop in temperature.

(5) Changes in external climate: Although weather conditions are measured at short intervals of only ten minutes, natural conditions may also change during this period, leading to errors in the results.

(6). The simulation time is not long enough. Due to the limitation of the data, the pre-assisted calculation time is only 1 day, and the inaccuracy of the initial conditions during the actual simulation will also affect the results.

However, the overall trend of the data is consistent and the simulated temperatures largely match the actual temperatures, which confirms the accuracy of the simulation software. In addition, in the subsequent simulations, for the air circulation between the layers of the Trombe wall system, the air flow of a DC fan with a temperature control device will be simulated in such a way that the air flow rate between the air layer and the room entering the room through the air chamber is constant when the fan is on, and the air exchange between the two spaces also stops when the fan stops operating. Therefore, the errors that occur in the actual measurement and verification phase due to the air flow rate can be avoided in the follow-up, theoretically.

Simulation experiment will use the control variable method, so we will continue to use the data from the experimental chalet and THERB for HAM software for the next simulation.

### **4.3. Study of composite double-circulation Trombe wall**

#### **4.3.1. Introduction**

Although the above experiments verify that the classic Trombe wall (CTW, the simplified space plane is shown in the figure 4.3.1) has an effect on winter indoor insulation, there are still some disadvantages, such as low thermal resistance, and inverse thermo-siphon phenomena.

Following these shortages, designed a new composite double-circulation Trombe wall (DLTW, the simplified space plane is shown in the figure 4.3.3) according to the classic Trombe house, which add an interior wall made of insulating material constructed inside the classic wall. It has two ventilated air vents (between the wall and the glass, between the wall and insulation). The heat was transferred into the interior by convection through the ventilated air vents. Temperature controlled DC fan installed in the vent. the use of DC fan would accelerate the thermal cycling of air interior and exterior automatically according to the temperature of the ventilated air vents. the ventilation rates of the fan were controlled at 40 m<sup>3</sup>/h. The characteristics of the double-circulation Trombe wall would be studied by comparing the dynamic thermal loads of the classical composite Trombe wall with temperature-controlled DC fan and the double-circulation Trombe wall with temperature-controlled DC fan.

The temperature sensing points of the temperature-controlled DC fan for the classic Trombe wall and the composite double-circulation Trombe wall are shown in the figure4.3.2 and figure4.3.4, respectively.

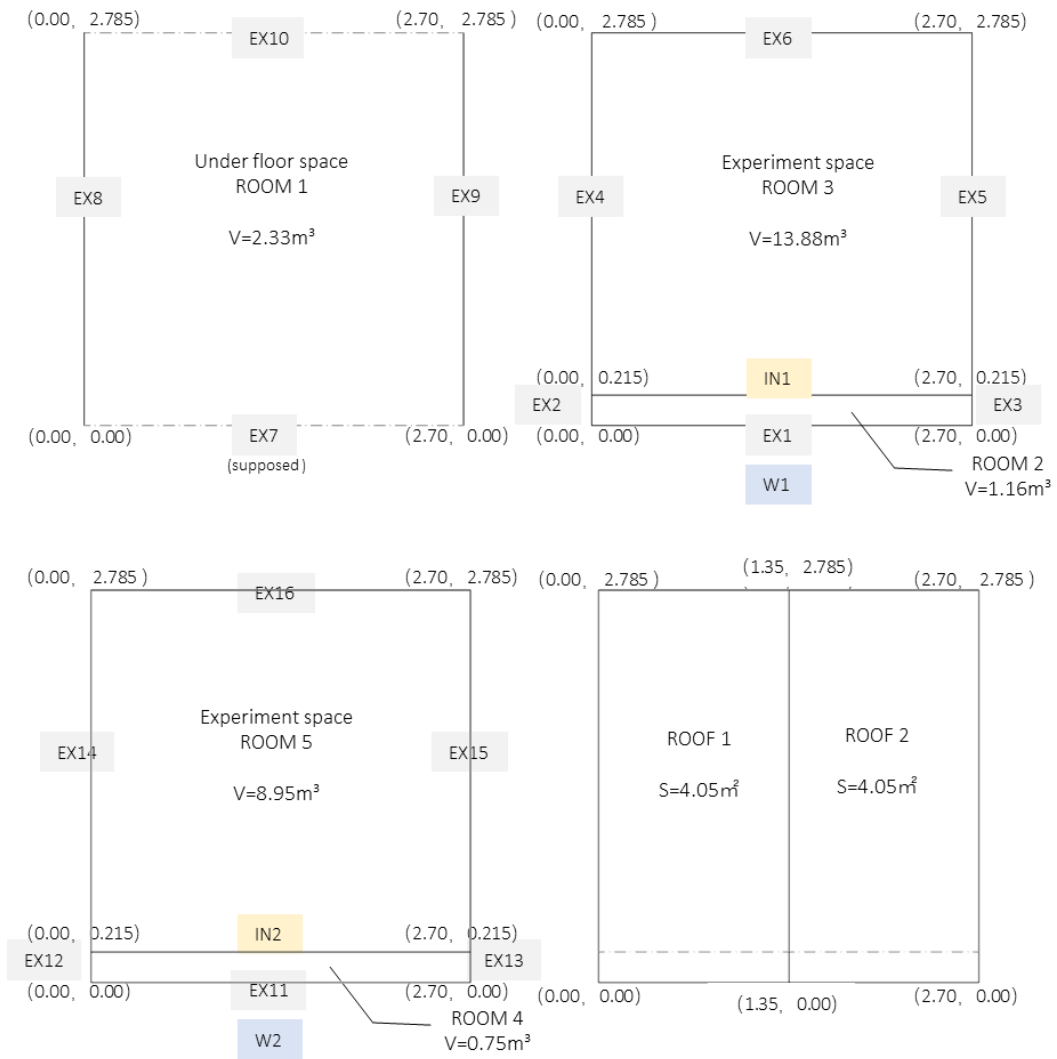


**Figure 4.3.1 Simplified space plan of classic Trombe wall house**

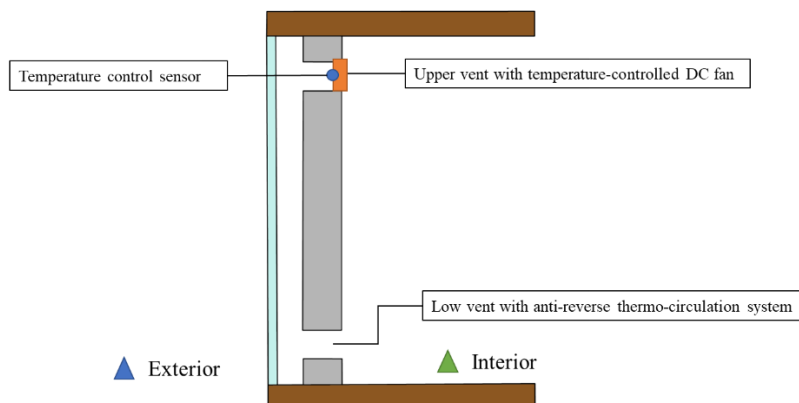


**Figure 4.3.2 Temperature sensing points of classic Trombe wall house**

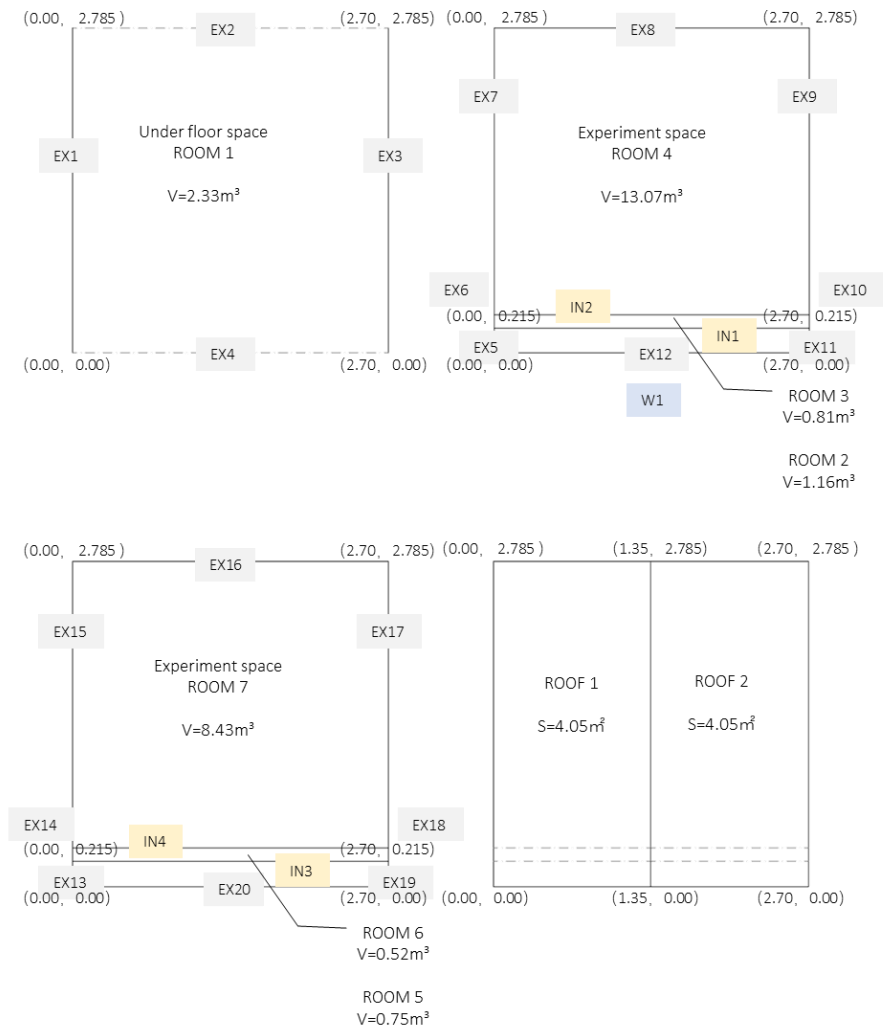


**Figure 4.3.3 Simplified space plan of composite double-circulation Trombe wall house**

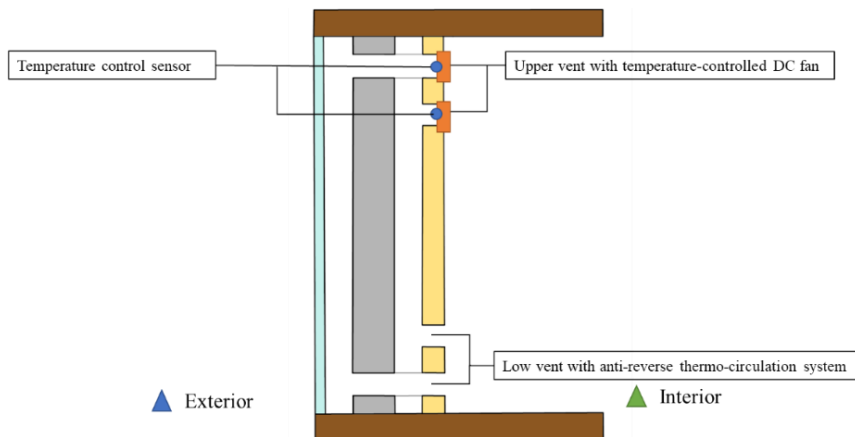


**Figure 4.3.4 Temperature sensing points of composite double-circulation Trombe wall house**

In addition to the classic Trombe wall house, as a comparison, there is one sunroom (only glazing surface on the south elevation) without Trombe wall (SR without TW) and one no-lighting house without Trombe wall (NH without TW). Except for the southern structure, the other enclosure structures are the same with overall width of the house is 2.70m and the depth is 2.785m. The roof is sloping and the total height is 3.98m. The main structure material is Japanese fir, with 30mm insulation layer inside and gallium steel plate as outer enclosure structure, single-glazed window. Figure 4.3.5 to Figure 4.3.6 shows the space divided and section of sunroom without Trombe wall (SR without TW) and no-lighting house without Trombe wall (NH without TW), respectively.

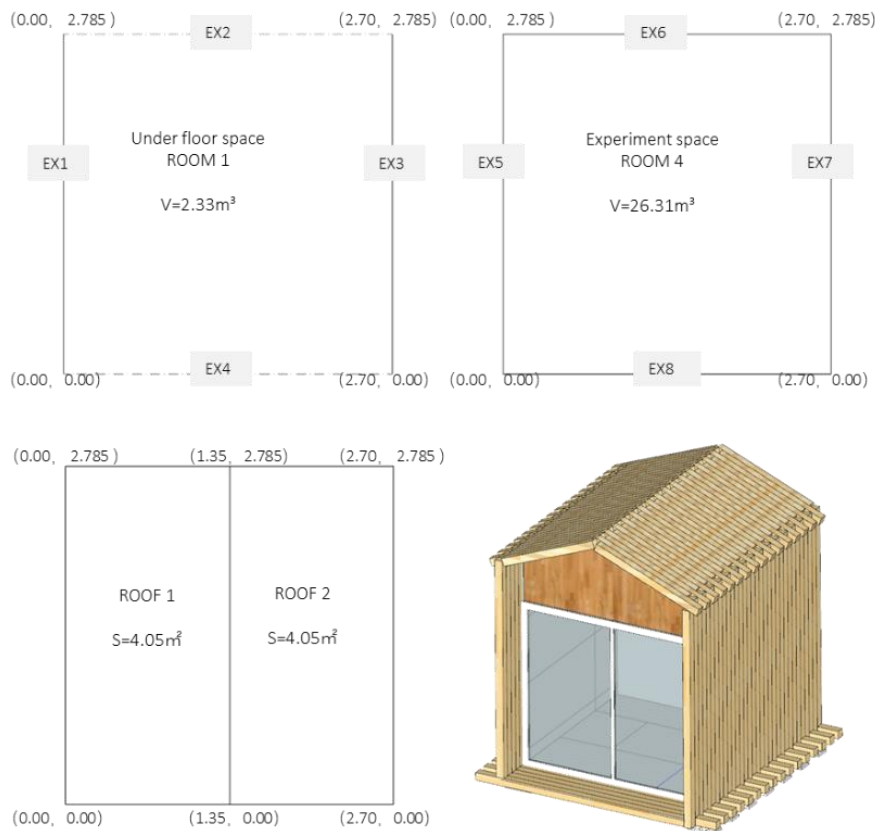


**Figure 4.3.5 Simplified space plan of sunroom without Trombe wall**

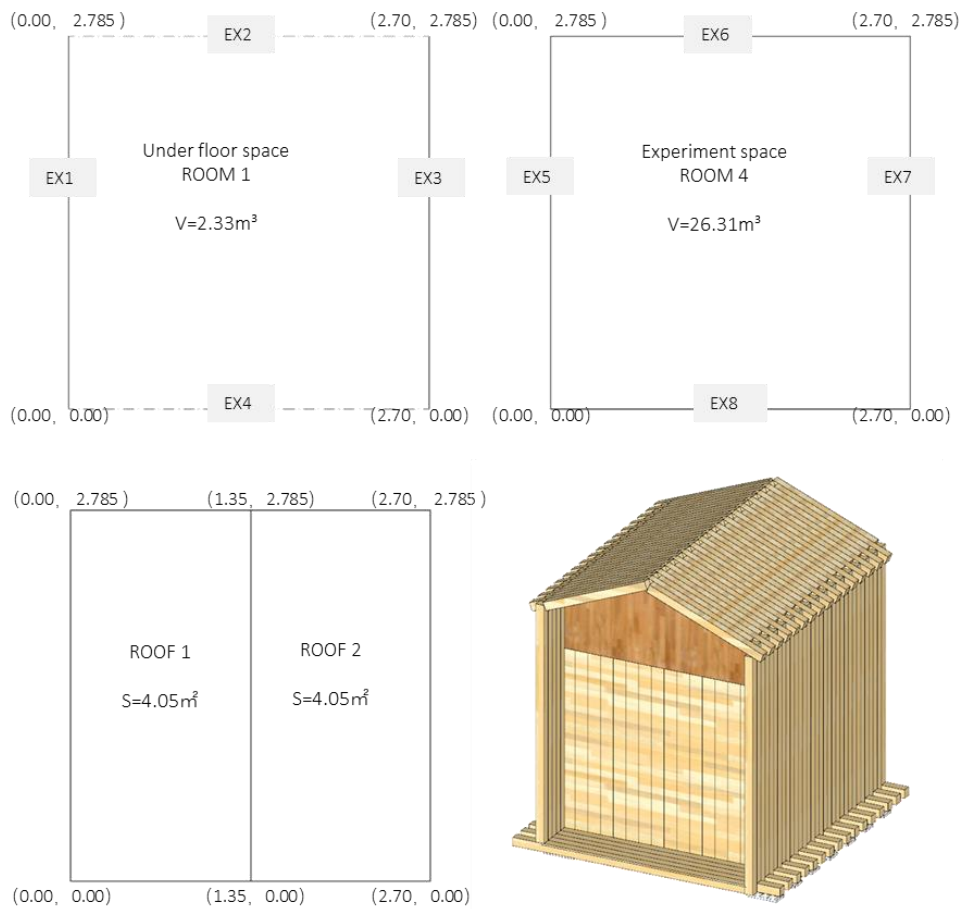


**Figure 4.3.6 Simplified space plan of no-lighting house without Trombe wall**

In order to obtain more accurate data and longer-term thermal data and air conditioning load data, the comparison simulation experiment used meteorological standard year data for the Yahata area in Kitakyushu, Japan, with an auxiliary time of 30 days to help calculate the start of the heating season from more accurate initial data.

The air conditioning heating season is from November 1 to March 31, and the setting temperature is unified to 20 degrees. There are three ways to use central air conditioning: an all-day air conditioning mode and two intermittent air conditioning modes: office mode and residential mode. Intermittent air conditioning is only turned on in the case of someone was using the room. All-day air conditioning: The air conditioning system is turned on for 24 hours (Figure 4.3.7).



**Figure 4.3.7 Air conditioning schedule of all-day mode**

Office mode: it simulates the activity time of general office workers, assuming that the working time is from 9:00 to 21:00, and the weekend is the same as the working day (Figure 4.3.8).



**Figure 4.3.8 Air conditioning schedule of office mode**

Residential mode: it simulates the time of people at home, assuming that they go out to work or entertain at 9:00 every day, back home at 18:00, and the air-conditioning operation time is from 18:00 to 9:00 am. (Figure 3.3.9).

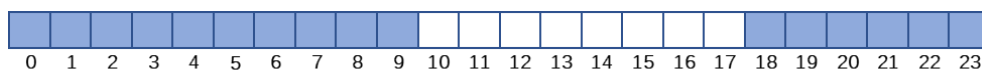


**Figure 4.3.9 Air conditioning schedule of residential mode**

Interior ventilation from the outside. For the time being, the increase in ventilation due to high indoor temperature or humidity is not considered. The air circulation has to meet only the necessary ventilation of 0.5 times/h. In the house with Trombe wall, the air circulation is achieved by DC forced ventilation between the air layer and the indoor space. 40m<sup>3</sup>/h, the ventilation temperature is controlled at 19°C, i.e. the temperature of the induction part is higher than 19°C, the DC fan runs and sends hot air into the room and opens the lower air hole by default to send cool air into the air layer.

#### 4.3.2. Result

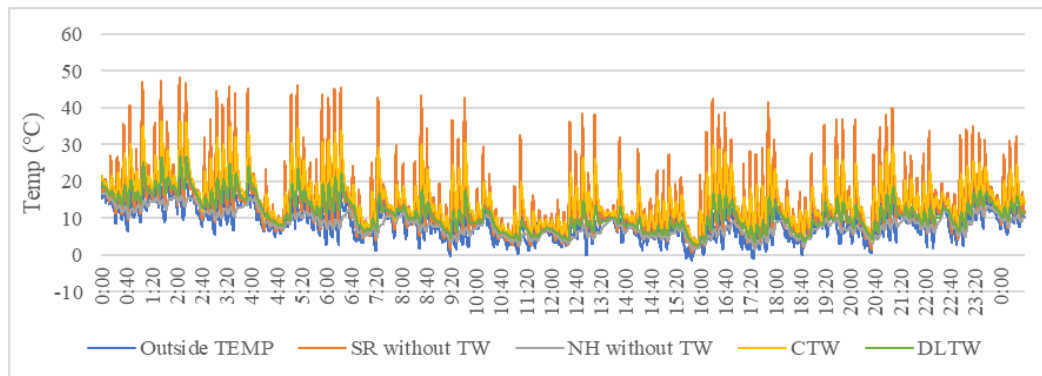
The indoor temperature in the no air conditioning state overall the heating season from November 1st to March 31st is shown in Figure 4.3.10. The results from the whole heating season show that the Sunroom without Trombe wall can reach high indoor temperatures during the day, with a maximum temperature of over 45°C without heating and additional external ventilation. But at night, the heat loss from the south side windows is very fast. The indoor temperature is very low at night and the house has a large temperature difference between day and night. The average room temperature is 14.7°C. If the comfortable temperature for human body is 18°C to 25°C, From Table 4.1, the proportion of suitable temperature time for no-lighting house with windows without air conditioning is 12.7%, and it should be noted that in this case there are more than 12.9% of time the temperature will exceed 25°C and 7.8% of time exceed 30°C.

No-lighting house without Trombe wall is not exposed to direct sunlight. and also has internal insulation on the south side, the indoor temperature does not fluctuate much, but it is difficult for this residence to use solar energy to heat the indoor air. The indoor temperature variation is

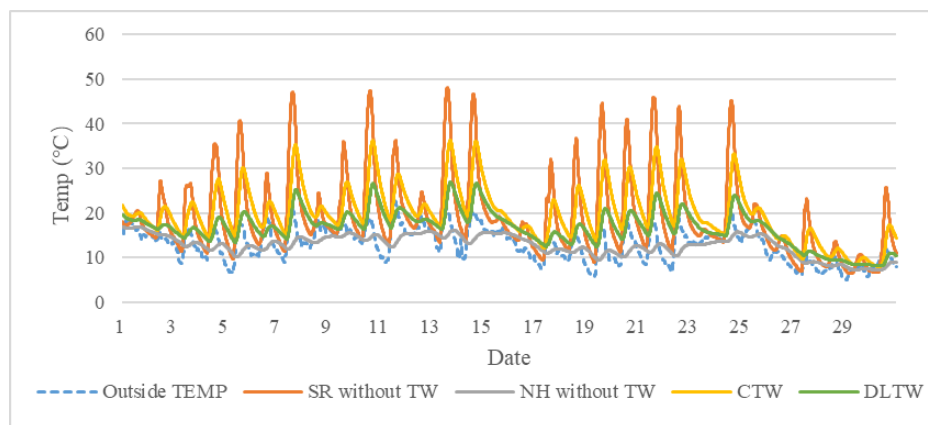
influenced by the temperature, the average room temperature is as low as 8.4°C and the temperature is always below 18°C.

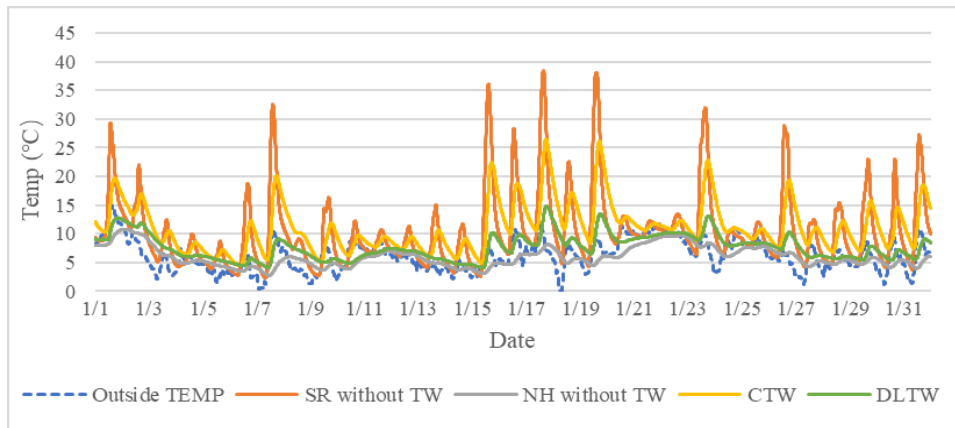
The classic Trombe wall house performs best without air conditioning. It can reach a higher average room temperature: 15.3°C. The maximum room temperature during the day can exceed 35°C. However, the heat loss of the huge walls is not small at night, so the temperature difference between day and night is also large. If the human comfort temperature is 18°C to 25°C, the proportion of suitable temperature time for a classic Traub wall house without air conditioning is 21.2%. In this case, there will be 8.5% of the time when the temperature exceeds 25°C and 2.3% of the time when it exceeds 30°C.

Composite double-circulation Trombe wall houses do not seem to have high room temperatures without air conditioning, but the room temperature can remain considerably higher than the outdoor temperature, and the maximum room temperature can exceed 20°C. Moreover, with the double wall, the heat loss at night is reduced and the temperature fluctuation is small, with an average room temperature of 11.3°C. If the human comfort temperature is 18°C to 25°C, the proportion of suitable temperature time for Composite double-circulation Trombe wall house without air conditioning is 9.2%.



**Figure 4.3.10 Indoor temperature with different types of houses in heating season**



**Figure 4.3.11 Indoor temperature with different types of houses in November****Figure 4.3.12 Indoor temperature with different types of houses in January****Table 4.1 Statistics of temperature of overall heating season**

	< 10°C	<18°C	18°C- 25°C	> 25°C	> 30°C
SR without TW	34.0%	74.4%	12.7%	12.9%	7.8%
NH without TW	70.9%	100%	0	0	0
CTW	20.1%	70.3%	21.2%	8.5%	2.3%
DLTW	45.1%	90.3%	9.2%	0.5%	0

The new modified composite double-circulation Trombe wall system did not perform better than the classic Trombe wall in terms of overall indoor temperature, especially in clear weather, the heat flux from the classical Trombe wall is several orders of magnitude higher than from the composite Trombe wall, is consistent with the description in [1,2]. However, after calculating the indoor air conditioning heat load. Figure 4.3.13 shows the heating load fluctuation of each house in different air conditioning mode in January. In the all-day air-conditioning mode, heating load of sunroom without Trombe wall is 296.60kwh, heating load of no-lighting house without Trombe wall is 213.87kwh, heating load of classical Trombe wall house is 203.29kwh, heating load of double-circulation Trombe wall house is 146.24kwh. In office mode, they are respectively 140.22kwh, 171.13kwh, 140.60kwh, 122.23kwh. In residential mode, they are respectively 277.51kwh, 187.54wh, 178.78wh, 131.40wh. The lowest air conditioning heat load in all air conditioning modes in the coldest month was composite double-circulation Trombe wall system, which differs from that seen from the temperature fluctuation curve.

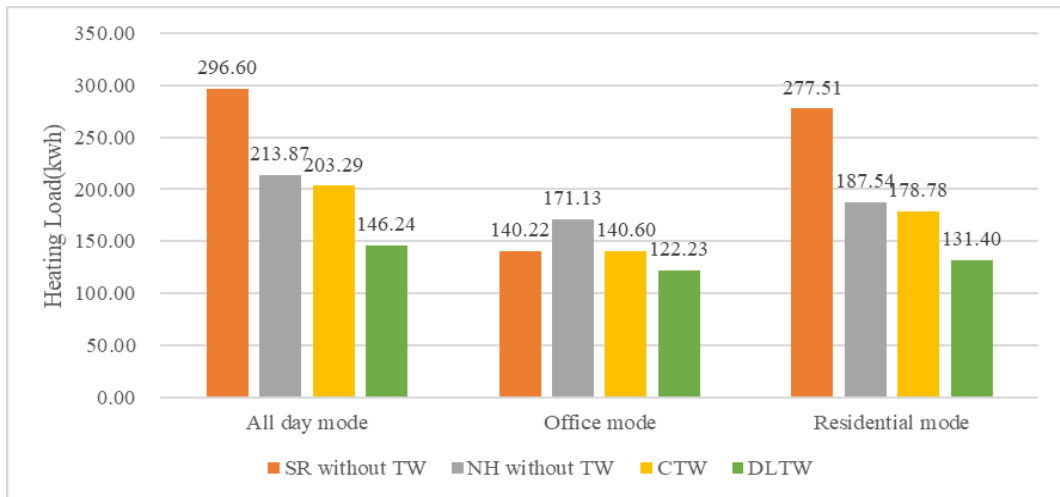


**Figure 4.3.12 Indoor temperature with different types of houses in January**

Based on the conjecture that the cause of the above results may be related to the magnitude of indoor air fluctuations, the equation based on two criteria for the evaluation of temperature fluctuations:

Thermal load levelling (TLL)

$$TLL = \frac{T_r \max - T_r \min}{T_r \max + T_r \min} \tag{1}$$

Thermal load levelling (f)

$$f = \frac{T_w \text{ inside max} - T_w \text{ inside min}}{T_w \text{ outside max} - T_w \text{ outside min}} \tag{2}$$

The results of the calculated indoor temperature changes and fluctuations for each month are shown in the table below, and the statistical box plots are shown in Figure 4.3.13. Combining the calculated values with the box distribution, the TLL values indicate the temperature fluctuation of the room itself, with the largest fluctuation in the sunroom and the smallest in the no-lighting house. the fluctuation of the composite double-circulation Trombe wall system is similar to that of the no-lighting house, and the classical Trombe wall system fluctuates more than composite double-circulation Trombe wall system, and in the coldest month, the difference between the two is more than 20%. And the f-value indicates the effect of indoor fluctuation with outdoor temperature fluctuation. It can be found that the temperature fluctuations of both sunroom and classic TW system exceed the outdoor temperature. f-value of no-lighting house basically stays around 0.5, and the f-value of composite double-circulation Trombe wall system decreases in the months when the temperature is smaller. From the box plot, the temperature distribution of no-lighting house is smaller than that of other kinds of houses because there is no additional active or passive system,

and the minimum temperature of sunroom exceeds that of the house with Trombe wall system by more than 5°C, and there are a large number of anomalies (i.e., overheating.) The fluctuation size of four different house objects from high to low is: sunroom, classic Trombe wall system, composite double-circulation Trombe wall system and no-lighting house. air conditioning load from high to low is: sunroom, no-lighting house classic Trombe wall system, composite double-circulation Trombe wall system (all-day mode and residential mode). After analysis, the factors influencing the indoor air conditioning load are not only the value of temperature but also its fluctuation.

**Table 4.2 Statistics of temperature of each month**

	°C	Outside TEMP	SR without TW	NH without TW	CTW	DLTW
November	TEMP-Ave	13.06	19.34	12.77	19.97	16.67
	TEMP-Max	22.7	48.21	16.91	36.21	26.85
	TEMP-Min	4.9	6.49	7.1	7.89	8.07
	TLL	-----	0.76	0.41	0.64	0.54
	f	-----	2.34	0.55	1.59	1.06
December	TEMP-Ave	8.77	15.52	8.33	16.22	11.96
	TEMP-Max	17.9	46.12	12.47	34.52	23.36
	TEMP-Min	-0.2	1.55	3.23	5.03	4.73
	TLL	-----	0.93	0.59	0.75	0.66
	f	-----	2.46	0.51	1.63	1.03
January	TEMP-Ave	6.22	10.63	6.01	11.63	7.66
	TEMP-Max	16.6	38.51	10.77	26.48	14.82
	TEMP-Min	0	2.35	2.75	4.41	3.99
	TLL	-----	0.88	0.59	0.71	0.58
	f	-----	2.18	0.48	1.33	0.65

	TEMP-Ave	6.04	12.99	5.94	13.42	8.65
February	TEMP-Max	17.6	42.29	9.92	29.95	16.73
	TEMP-Min	-1.7	0.59	1.57	3.04	2.8
	TLL	-----	0.97	0.73	0.82	0.71
	f	-----	2.16	0.43	1.39	0.72
	TEMP-Ave	9.45	15.28	8.68	15.62	11.28
March	TEMP-Max	19.5	39.93	13.28	29.61	18.47
	TEMP-Min	0.5	1.64	2.99	4.04	4.29
	TLL	-----	0.92	0.63	0.76	0.62
	f	-----	2.02	0.54	1.35	0.75

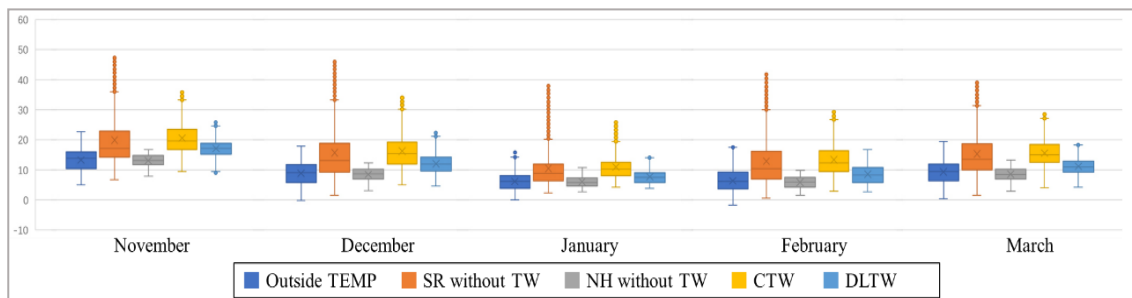


**Figure 4.3.13 Statistics of temperature without heating**

Two more typical days in winter were selected for comparison, a cold but sunny January 19 (Figure 4.3.14(a)) and a cold and cloudy February 4 (Figure 4.3.14(b)). The comparison revealed that, similar to the results of the temperature fluctuation and magnitude calculations, the indoor temperature of the house in classic Trombe wall system on a sunny day was consistently higher than the composite double-circulation Trombe wall system, but on a cloudy day, before sunrise, the indoor temperature in classic Trombe wall system dropped below composite double-circulation Trombe wall system. And comparing the indoor air conditioning load in the air conditioning on state, only the air conditioning load of classic Trombe wall system in the air conditioning on mode of office on a sunny day is lower than that of composite double-circulation Trombe wall system. the rest, regardless of the sunny day (Figure 4.3.15) or cloudy day (Figure 4.3.16), the best energy saving is achieved by composite double-circulation Trombe wall system.

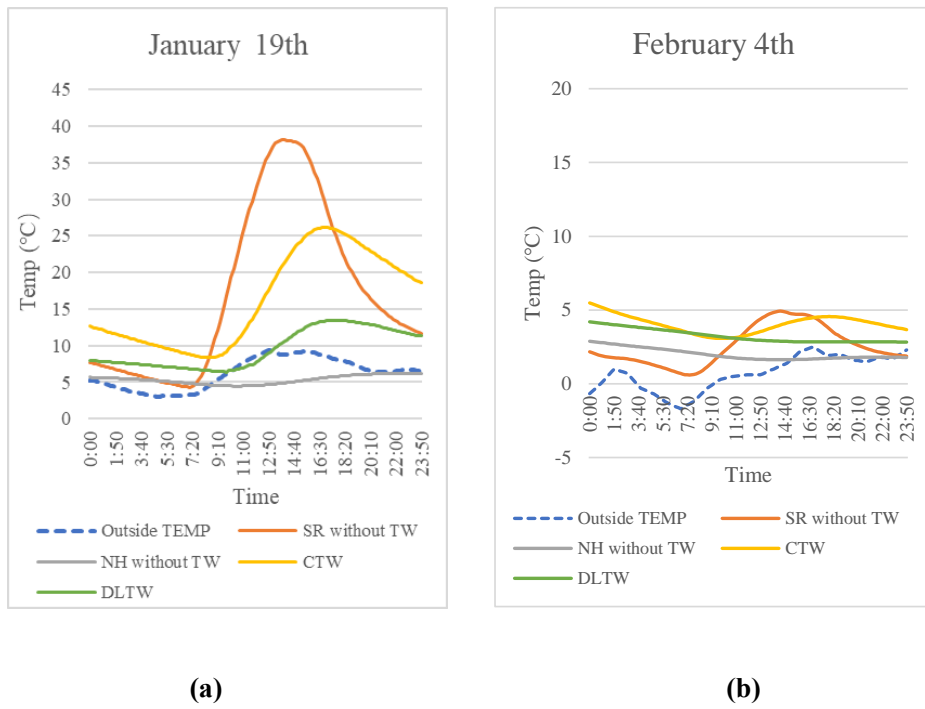


**Figure 4.3.14 Indoor temperature with different types of houses: (a) January 19<sup>th</sup> ;(b) February 4<sup>th</sup>**

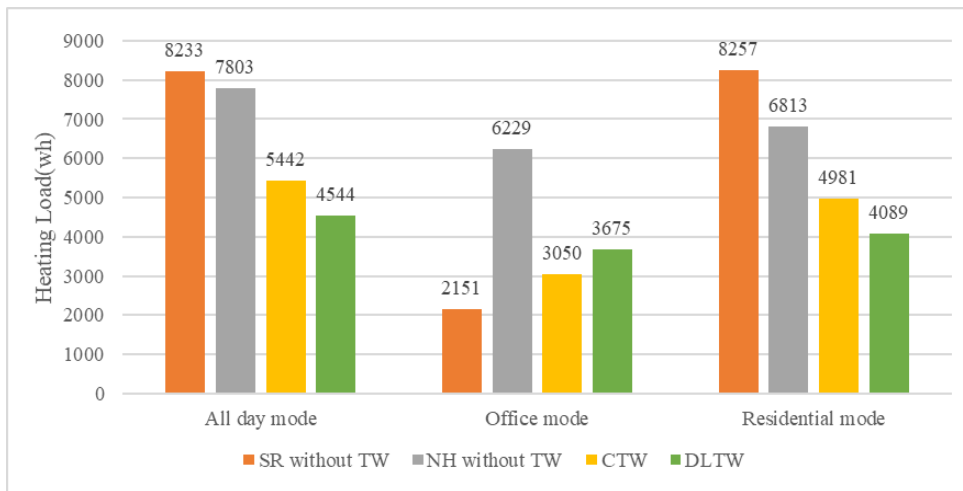


**Figure 4.3.15 Comparison of Air conditioning load with different types of houses on January 19<sup>th</sup>**

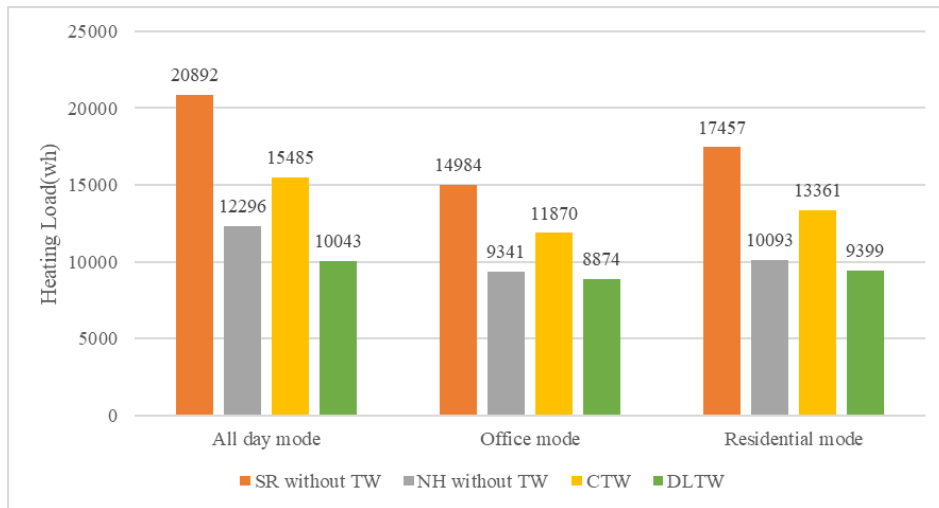


**Figure 4.3.16 Comparison of Air conditioning load with different types of houses on February 4th**

Fig. 3.4.22 shows the heating load fluctuation of each house in different air conditioning mode in whole heating season (5 months). In the all-day air-conditioning mode, heating load of no-lighting house with window is 1316.16kwh, heating load of no-lighting house without window is 954.89kwh, heating load of classical Trombe wall house is 882.06kwh, heating load of double-circulation Trombe wall house is 633.31kwh. In office mode, they are respectively 609.31kwh, 761.12kwh, 601.96kwh, 527.74kwh. In residential mode, they are respectively 1235.29kwh, 836.44kwh, 782.45kwh, 568.14kwh.

By comparing the indoor temperature, the thermal performance of the improved wall was not as good as expected. Although its indoor temperature is higher than the indoor temperature without Trombe wall, because of the lack of thermal radiation effect of the massive wall, the maximum indoor temperature in January can only reach about 15 °C without using with air conditioner. Its thermal performance is not as good as that of the classic Trombe wall.

However, the annual winter heat load calculated after using air conditioning is compared. It was found that the annual heat load of the improved composite double-circulation Trombe wall is 568.14 kwh, which is 27.3% less compared to the classic Trombe wall and 32.1% less compared to the case without Trombe wall. Therefore, the improved composite has the potential to be studied.

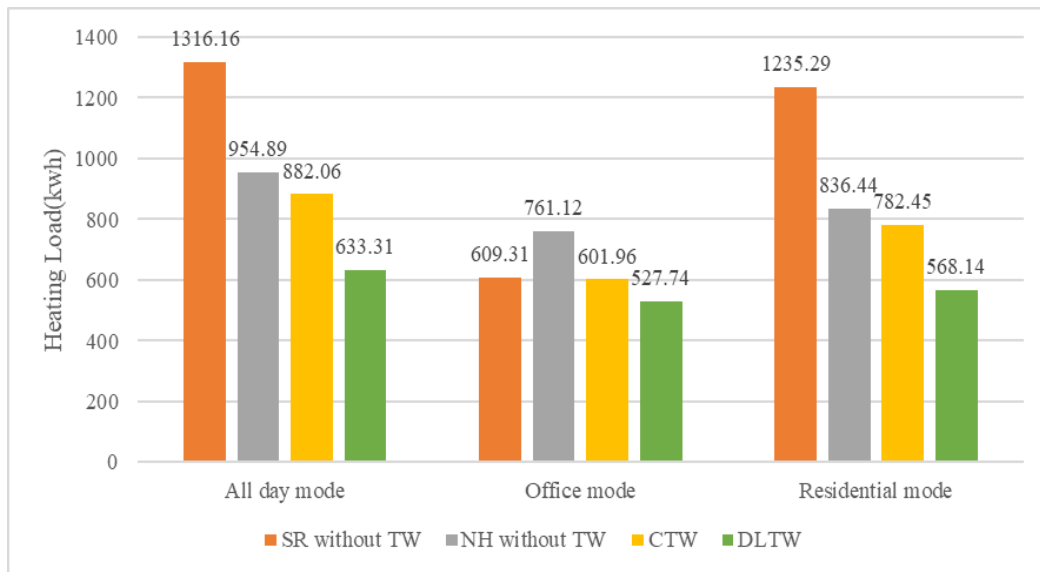


**Figure 4.3.12 Comparison of Air conditioning load with different types of houses all over heating season**

#### 4.4. Optimization of double-circulation Trombe wall

The previous section measured and simulated the thermal effects and the operation of the Trombe wall system. The previous section showed that the Trombe wall system can efficiently store and utilize solar energy and that the potential of the composite double-circulation Trombe wall is higher than that of the classical Trombe wall system with the assistance of a temperature-controlled DC fan. This section will use the THERB for HAM software. The composite double-circulation Trombe wall is further investigated. Trombe wall system is a sustainable and environmentally friendly building technology and in order to improve the thermal storage efficiency, some effects have to be taken into account. There are various components that may change the efficiency of Trombe walls such as insulation, fans, shading devices, vents, glazing type, material and thickness of massive wall, coating material and air cavity depth.

Under the existing model and simulation conditions, the simulation experiment will select wall material and thickness, glazing performance, and ventilation as parameters to study the effect of composite double-circulation Trombe wall on building energy consumption. The weather data in this section will continue to use the meteorological standard year data of Yahata area in Kitakyushu city. Temperature-controlled DC fan temperature control is set to 19°C, i.e., when the temperature of the induction section is higher than 19°C, the DC fan operates and hot air is sent into the room, and the lower air hole is opened by default to send cold air into the air layer for air circulation. The air conditioning heat load comparison in this section will be compared using the residential mode, which is turned on at 18:00 and off at 9:00 at night.

In the simulation phase, the variation of indoor temperature in the absence of air conditioning heating is first compared to determine whether a variable can be an influencing factor. After that, the air conditioning heat load in the residential mode air conditioning system is compared to explore whether the variable conditions can optimize the wall and reduce the building energy consumption.

#### 4.4.1. The effect of glazing surface properties

##### ① Introduction

The heat loss of exterior window and door glass is a major part of the energy consumption of buildings, accounting for more than 50% of the energy consumption of buildings. Relevant research data show that the heat transfer from the inner surface of the glass is dominated by radiation, accounting for 58%, which means that the heat loss should be reduced from changing the performance of the glass.

When using the building load as an energy saving evaluation criterion, the heat flow through the window (in this case, the transparent glazing surface of the Trombe wall) needs to be considered, and the heat flow calculation formula is as follows:

$$q_F = S_e \cdot S_f \cdot C_w \cdot C_n \cdot D_F \quad (3)$$

Where  $S_e$  is the shading factor of the glass,  $S_f$  is the shading factor of the window frame,  $C_w$  is the external shading factor of the window,  $C_n$  is the internal shading factor of the window, and  $D_F$  is the solar heat gain factor.

The total shading factor, which is related to the load, is positively related to the shading factor of the glass, the shading factor of the window frame, the external shading factor of the window, and the internal shading factor of the window. Because the simulation experiment simplifies the building modelling, the calculation basically only needs to consider the shading coefficient of glazing surface. In general, the greater the thickness of the glass, the smaller its shading coefficient  $S$ , and the smaller the heat flow lost at night, the more insulated it is.

One way is to use multi-layer insulating glass, which has a small heat transfer coefficient in winter and can effectively stop the temperature difference heat transfer at night. Also in summer, it can reduce solar radiation during the daytime.

Another more effective method is to suppress radiation from its inner surface. The radiation rate of ordinary float glass is as high as 0.84, and when coated with a silver-based low-radiation film, its radiation rate can be reduced to less than 0.15. Low-e coated glass (also known as low-e glass) coating layer has a high transmission of visible light and high reflection of medium and far infrared characteristics, so that it has excellent thermal insulation and good light transmission compared with

ordinary glass and traditional architectural coated glass. Therefore, the use of Low-E glass for building doors and windows can greatly reduce the transfer of heat from indoor to outdoor caused by radiation, achieving the ideal energy-saving effect.

But the heat through the glass is two-way, that is, heat can be transferred from indoor to outdoor, and vice versa. In winter, the indoor temperature is higher than the outdoor temperature, which requires insulation. Low-E glass can achieve the requirements of winter and summer, both thermal insulation and thermal insulation, to play the effect of environmental protection and low carbon. the LOW-E film surface location in 2 # or 3 # insulating glass heat transfer coefficient value is the smallest (outdoor for 1 # location, indoor for 4 # location, as shown in the f igure 4.4.2), that is the best thermal insulation performance.

And when considering the location of 2# or 3#, it is theoretically necessary to consider the shading coefficient of Low-E glass (Slowe), which is calculated by the following formula:

$$S_{lowe} = \frac{g}{\tau_s} \quad (4)$$

$$g = \tau_s + \sum_{i=1}^n q_{ini} \quad (5)$$

$$q_{ini} = \frac{A_i R_{outi}}{R_k} \quad (6)$$

$$R_{outi} = \frac{1}{h_{out}} + \sum_{k=2}^i R_k + \sum_{k=1}^{i-1} R_{gk} + \frac{1}{2} R_{gi} \quad (7)$$

Where  $g$  is the total solar transmittance ratio of the single glass,  $\tau_s$  is the direct solar transmittance ratio of the single glass,  $q_{ini}$  is the secondary heat transfer thermal effect of each layer of glass to the room,  $A_i$  is the direct solar absorption ratio of the  $i$ -th layer of glass, and  $h_{out}$  is the heat transfer coefficient of the outdoor surface of the glass.  $R_{outi}$  is the thermal resistance of the  $i$ -th layer of glass in the direction of the outside of the room,  $R_{gi}$  is the solid thermal resistance of the  $i$ -th layer of glass,  $R_{gk}$  is the  $k$ -th layer solid thermal resistance of the glass, and  $R_k$  is the thermal resistance of the  $k$ -th gas layer.

The above formula can be seen, if the coating surface on the 2 #, through the first glass, a large part of the near-infrared radiation is reflected off. Directly through the radiation is less. Absorption of heat due to the first piece of glass due to the outer surface (1 #) high radiation rate of the inner surface (2 #) low radiation rate, so more heat radiation to the outdoors, less radiation to the indoor hollow cavity, less heat to reach the second piece of glass makes the hollow glass to reach the hollow cavity and the second piece of glass less heat, and thus less heat transferred to the room, the final SC value is lower.

When the coating surface is on the 3#, most of the heat will pass through the first glass and reach

the insulating cavity and the second glass. 3# side reflects most of the near-infrared radiation but the radiation absorption of the glass and the film layer transfers heat to cause the second glass to heat up. The temperature of the second piece of glass is high. 3# side has low-E film layer, which leads to less heat radiation to the outside of the room, while 4# side has high emissivity, which leads to more heat radiation to the room resulting in higher shading coefficient SC for low-E film side in 3# side than in 2# side (Figure 4.4.3).

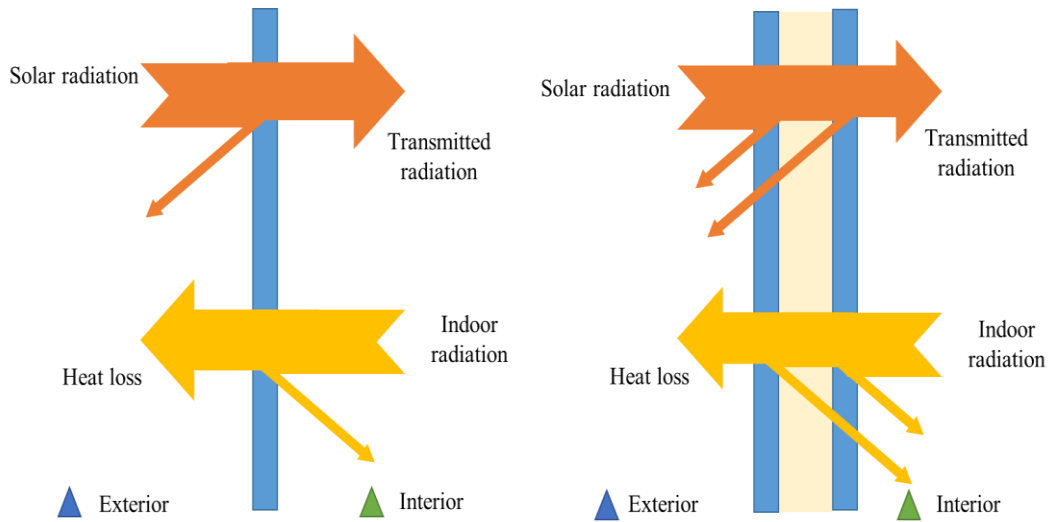


**Figure 4.4.1 Difference between single-glazed and double-glazed**

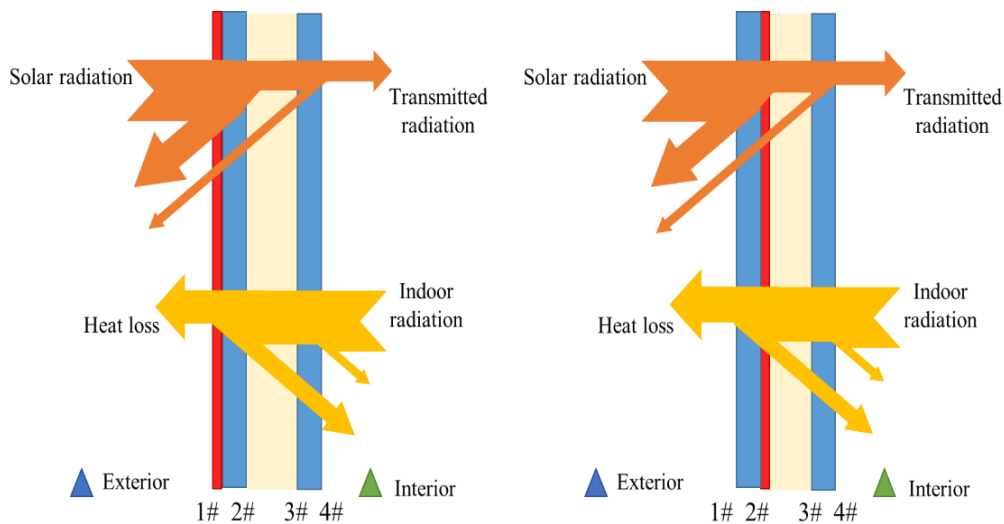


**Figure 4.4.2 The number of LOW-E film surface location**

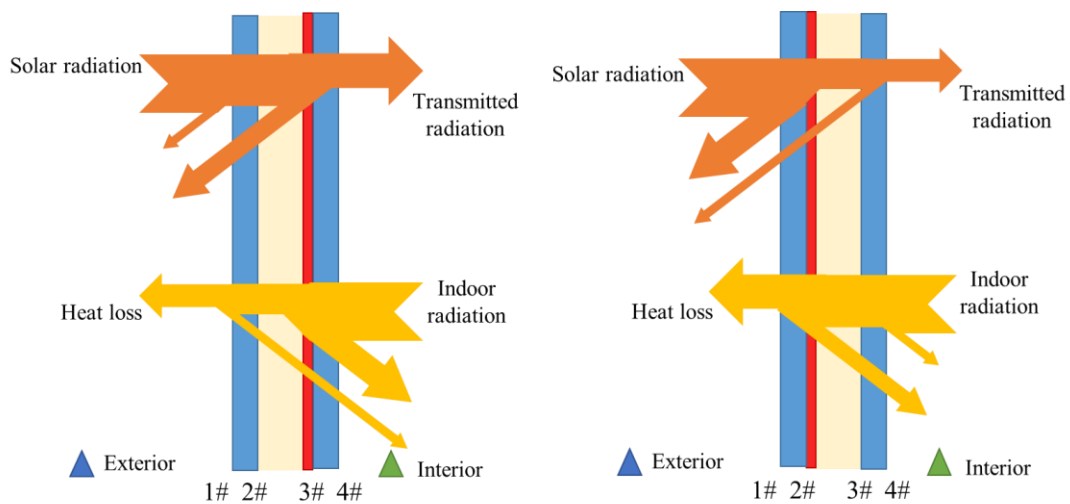


**Figure 4.4.3 Difference between 2# and 3# LOW-E film surface location**

## ② The effect of glazing surface properties

Because in the composite double-circulation Trombe wall system, the solar radiation through the glass does not act directly on the room, so it is difficult to judge the advantages and disadvantages of the composite double-circulation Trombe wall system by analyzing only the individual glass types, so in this part, we have selected Therefore, in this section, single-layer glass (initial control), double-circulation insulating glass, triple-layer insulating glass, Low-E glass with Low-E film at position 2# (2# Low-E) and Low-E glass with Low-E film at position 3# (3# Low-E) are selected for control analysis.

For a preliminary analysis of the indoor temperature variation without air conditioning throughout the year, the indoor temperature fluctuations for five different types of windows without heating are shown in Figure 4.4.4. Two representative months were also selected, the single-month temperature change curves of November, the warmest month in winter, and January, the coldest month (Figure 4.4.5 and Figure 4.4.6) From the figure, it can be seen that the highest indoor temperature collection and insulation performance without air conditioning is the double-glazed low-E glass with the low-e layer in #3 layer. Compared with single-pane glass, multi-pane glass can significantly improve the heat collection and insulation performance. And triple glazed windows have more air layers and are more effective. The winter performance of double-glazed low-E glass with low-e layer in #3 layer lies between double and triple glazing. The difference between the different glass types is more obvious in sunny daytime, and in the case of continuous rainy days, the difference in indoor air temperature of the composite double-circulation Trombe wall system with different glass types is not significant.

When comparing the heat load of November (Figure 4.4.7) with that of January (Figure 4.4.8)

after setting the indoor air conditioner to turn on at night, it was found that the comparison of the heat load of indoor air conditioner in the two winter months was consistent with the comparison of the temperature change in the month without air conditioning. The most energy-efficient glass is 3# Low-E, followed by triple insulating glass, 2# Low-E and double insulating glass, and the highest energy consumption is for single-pane glass. In November, compared with the heat load of 58.9 kwh for a single-glazed house, 3# Low-E, triple insulating glass, 2# Low-E and double insulating glass can save 63.7%, 49.9%, 45.0% and 34.8% respectively.

In January, compared to the heat load of 131.4 kwh for a single glazed house, 3# Low-E, triple insulated glass, 2# Low-E and double insulated glass can save 38.5%, 25.7%, 20.8% and 15.3%, respectively.

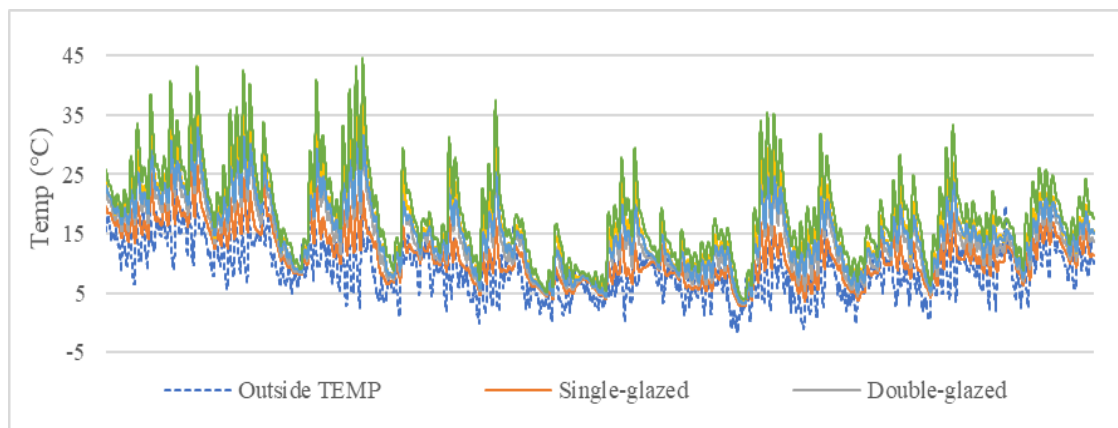


**Figure 4.4.4 Comparison of room temperature with different types of glazing without heating all over heating season**

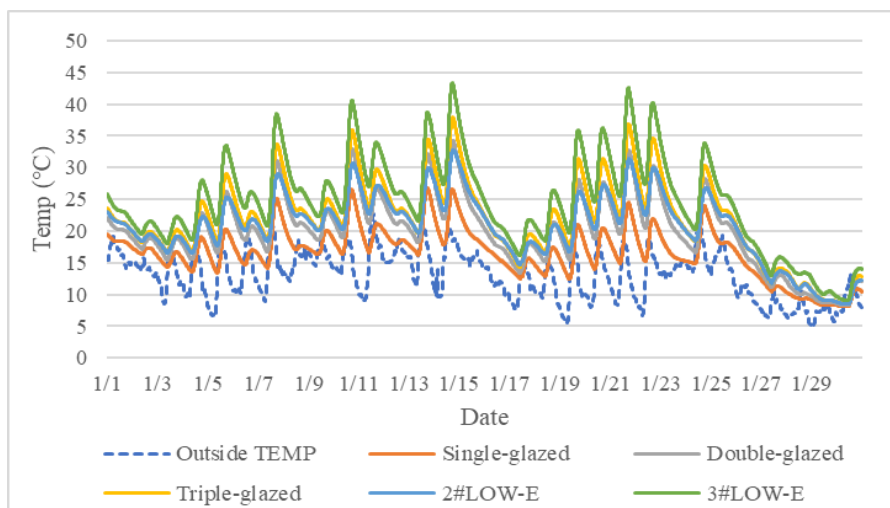


**Figure 4.4.5 Comparison of room temperature with different types of glazing without heating of November**

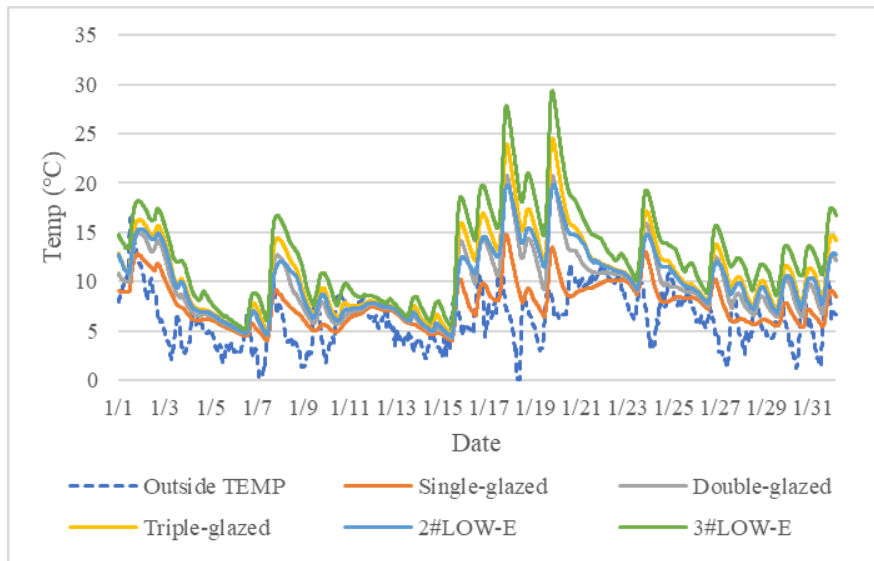


**Figure 4.4.6 Comparison of room temperature with different types of glazing without heating in January**

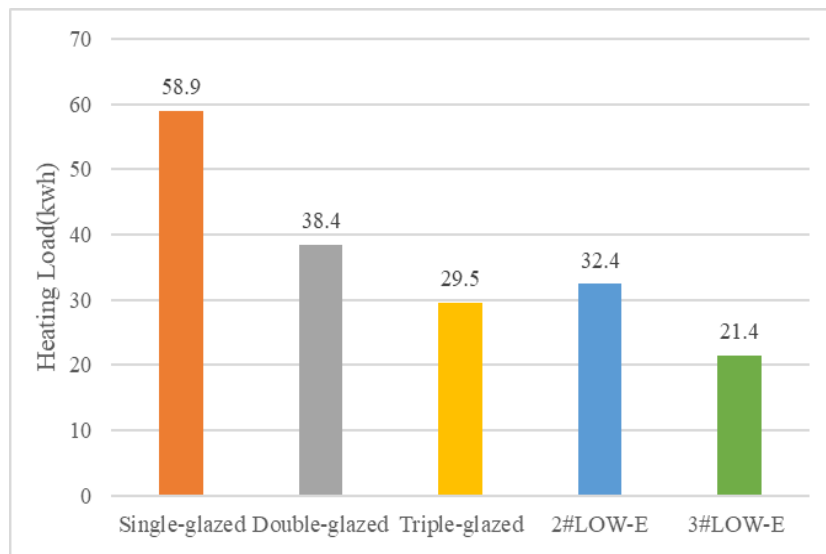


**Figure 4.4.7 Comparison of Air conditioning load with different types of glazing with heating in November**

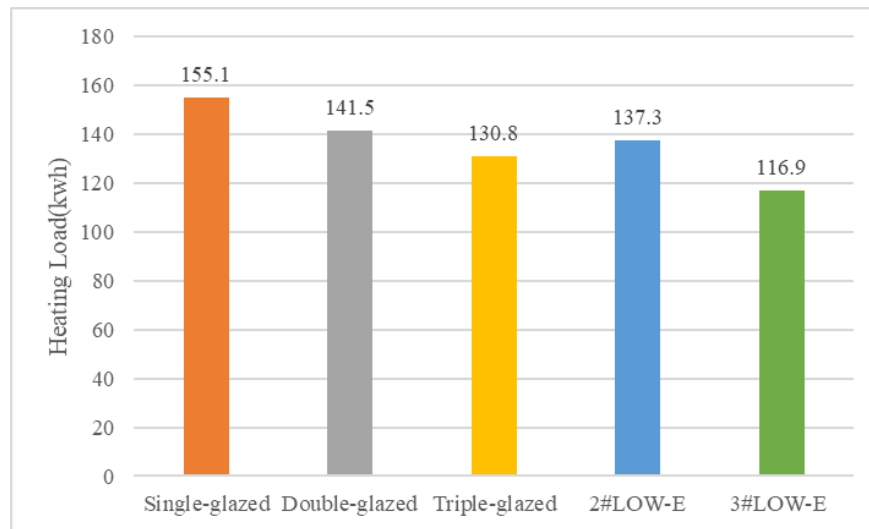


**Figure 4.4.8 Comparison of Air conditioning load with different types of glazing with heating in January**

A cold, sunny day, January 19 (shown as Figure 4.4.9), and the coldest, cloudy day of the year, February 4 (shown as Figure 4.4.10), were intercepted and compared. The results obtained are as follows.

On January 19, we can clearly compare that Low-E double-glazed windows are the best, and the indoor temperature can be increased by more than  $10^{\circ}\text{C}$  compared with single-glazed windows. The next best is triple glazing, which can increase the indoor temperature by more than  $7^{\circ}\text{C}$  compared with single glazing. In terms of daytime collection efficiency, the indoor temperature rise rate of multi-layer glass is also significantly higher than that of single-layer glass. The trend is similar for double and triple glazing, with 3# Low-E glass showing a higher rise rate than the others. Compared with the case of single-pane glass, 3#Low-E can save 55.9% of energy, while double-pane glass can save 24.2% and triple-pane glass can save 35.9% (). And the temperature change curve of 2#Low-E glass is smoother than other types of glass on sunny days intersecting with the curve of double glazing.

On February 4th, it was found that in the absence of solar radiation, the temperature in the room will continue to drop if air conditioning is not used. low-E double glazed windows have the fastest temperature drop at night because of the high initial temperature and the large temperature difference between inside and outside, and when the temperature drops to a certain level, the whole curve gradually stabilizes and the indoor temperature is higher than other types of windows. However, in general, the advantages of multi-layer glass are not well reflected in the absence of sufficient sunlight. on February 4, the difference in air-conditioning load between different types of windows was less than 0.1kwh(Figure 4.4.11).

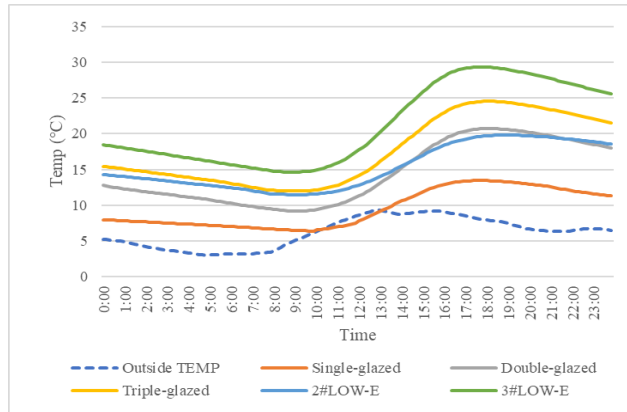


Figure 4.4.9 Indoor temperature with different types of glazing on January 19<sup>th</sup>

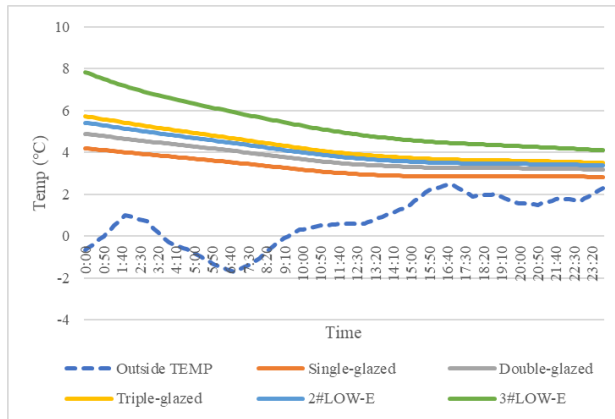


Figure 4.4. Indoor temperature with different types of glazing on February 4<sup>th</sup>

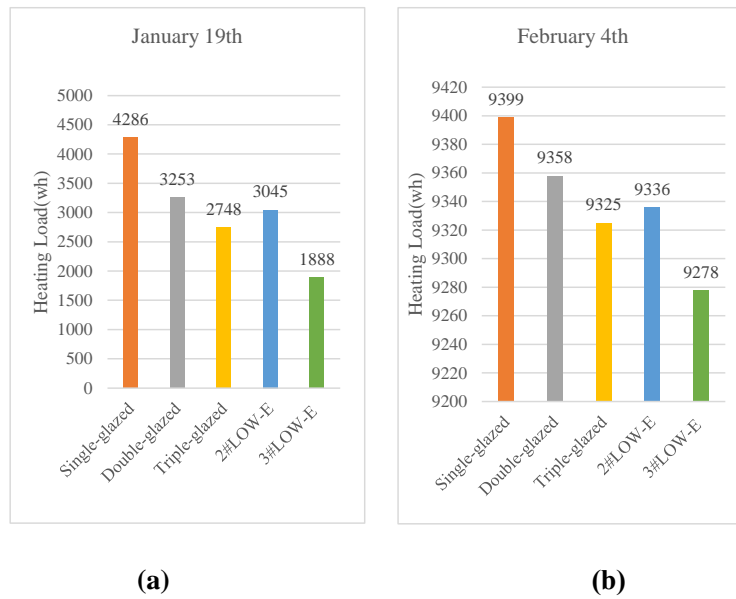
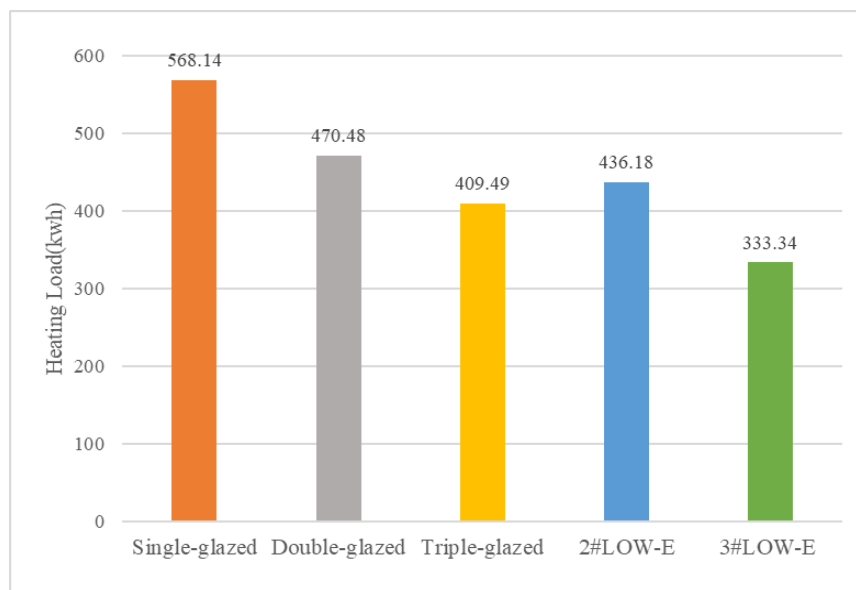


Figure 4.4.11 Comparison of Air conditioning load with different types of glazing: (a) on January 19<sup>th</sup>; (b) on February 4<sup>th</sup>

Through the above comparison of these time periods, a common conclusion can be drawn: the insulation performance of multi-layer glass is better than single-layer glass, and the more layers, the better the insulation performance, the use of Low-E glass can greatly reduce the heat transfer to the outdoors caused by indoor radiation, to achieve the expected energy-saving effect. The effect of 2#Low-E in winter is not as good as 3#Low-E. The overall energy efficiency of the composite double-circulation Trombe wall system with different glass types is ranked from good to bad as 3#Low-E, triple-layer glass, 2#Low-E, double-circulation glass and single-layer glass. The percentage of energy savings from double glazed, 2#Low-E, triple glazed and Low-E double glazed windows compared to single glazed windows throughout the heating season are 17.19%, 23.2%, 27.89% and 41.33%.

However, without increased outside air circulation, indoor temperatures can be too high during the day, requiring additional measures to reduce indoor temperatures. Also, the advantages of multi-pane glass do not work well in the absence of sufficient sunlight.



**Figure 4.4.12 Comparison of Air conditioning load with different types of glazing with heating all over heating season**

#### 4.4.2. The effect of DC fan rates

The DC fan set in the upper vents controls the rate of inner air circulation and outer air circulation, i.e., the rate of hot air transfer, for which no specific values have been calculated in previous studies of composite Trombe walls.

In the design of composite double-circulation Trombe wall, there are two holes at the top and bottom of both inner and outer walls, so a maximum of Two fans can be installed on each floor, and

the maximum actual ventilation capacity of each DC fan is  $70\text{m}^3/\text{h}$ , The ventilation volume of DC fan the experiment chosen as a reference adjustment range from  $0\text{ m}^3/\text{h}$  to  $70\text{ m}^3/\text{h}$ . Setting the fans at the two upper side vents, the limit case can obtain a ventilation volume of  $140\text{ m}^3/\text{h}$ . So, the numerical experiments simulated the air supply is simulated at  $20\text{ m}^3/\text{h}$ ,  $40\text{ m}^3/\text{h}$ ,  $70\text{ m}^3/\text{h}$ ,  $110\text{ m}^3/\text{h}$  and  $140\text{ m}^3/\text{h}$  respectively, and conducted with no forced ventilation as the control. At the same time, the temperature sensing point of both the upper and lower fans is set at  $19^\circ\text{C}$ , that is, only when the temperature of the outer air layer or the inner air layer is higher than  $19^\circ\text{C}$ , the fan will operate and send air to the room.

First, the study conducted a preliminary analysis of the indoor temperature change throughout the year when air conditioning is not used. From the Figure 4.4.13, it can be found that increasing the air circulation flow rate can effectively increase the indoor temperature. When the ventilation rate is  $140\text{ m}^3/\text{h}$ , the indoor temperature is kept at the highest without heating. And it can be tentatively judged that the higher the ventilation rate of indoor air circulation in this range, the higher the efficiency of Trombe wall.

More evident results are shown in the warmest month, November (Figure 4.4.14), and the coldest month, January (Figure 4.4.15), and the performance is consistent. It can also be found that on consecutive rainy days, the fan turns off making the indoor temperature tend to be the same due to the difficulty of the heat in the inner and outer air layers to rise by storing solar radiation. The energy consumption values with the room air conditioner turned on at night are also consistent with the temperature change pattern. In both warm November and cold January, the DC fan rate of up to  $140\text{ m}^3/\text{h}$  consumes the least energy in winter,  $49.9\text{ kwh}$  in November and  $118.3\text{ kwh}$  in January.  $41.2\%$  and  $19.0\%$  are saved respectively when the fan is turned off.

At the same time, observing the data, it can be found that the reduction in energy consumption decreases with each increase in fan rate, so it can be deduced that even if the DC fan rate is increased to  $140\text{ m}^3/\text{h}$  or more, the heat load saved will not be significantly increased. It is even possible that other problems may arise due to the high speed.

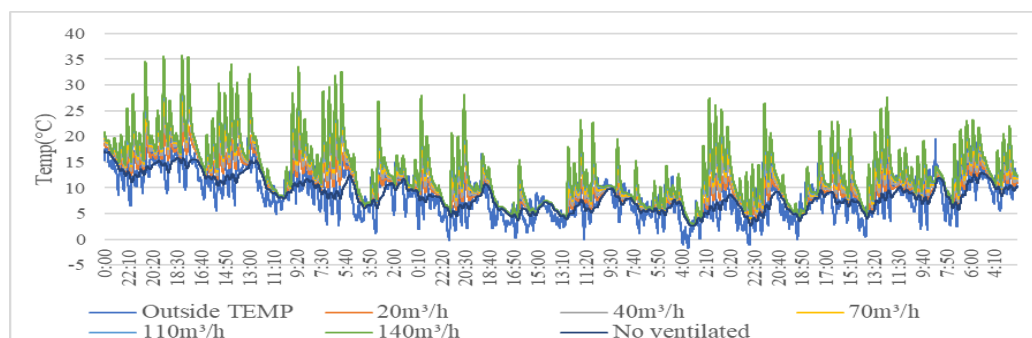


**Figure 4.4.13 Comparison of room temperature with different ventilation rates without**

**heating all over heating season**

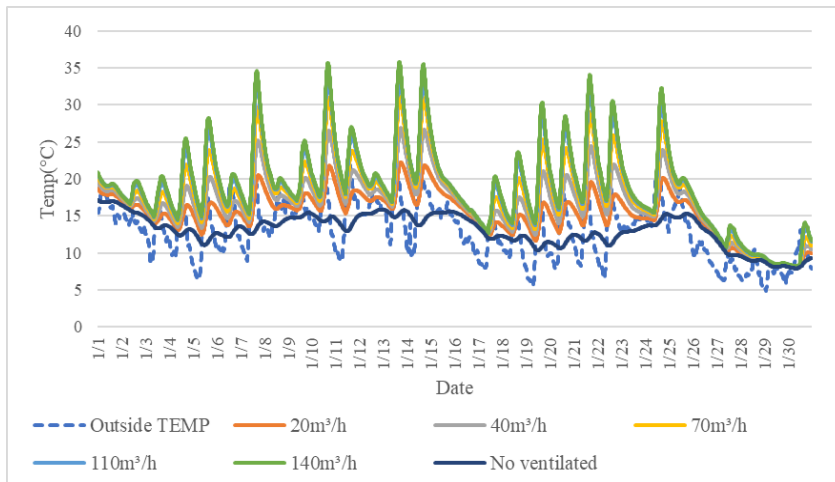


**Figure 4.4.14 Comparison of room temperature with different ventilation rates without heating in November**

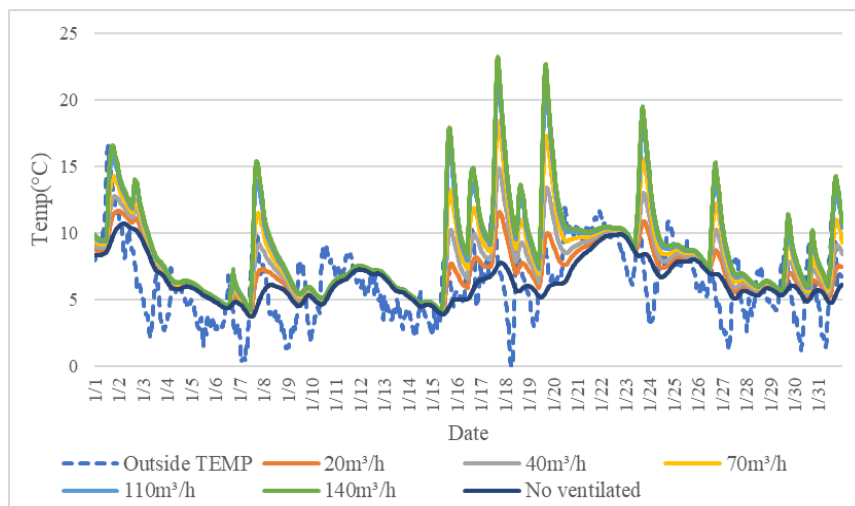


**Figure 4.4.15 Comparison of room temperature with different ventilation rates without heating in January**

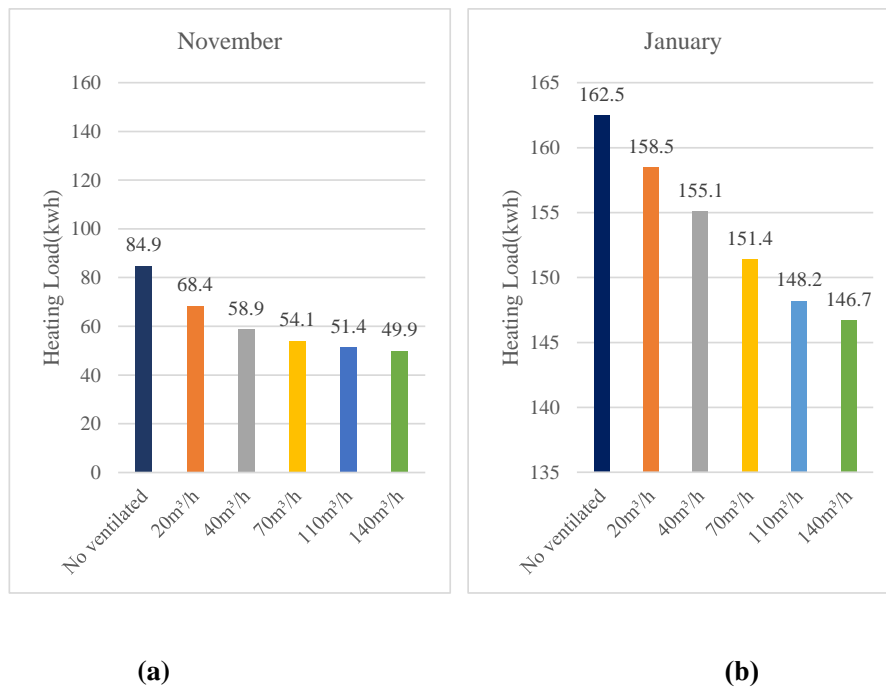


**Figure 4.4.16 Comparison of Air conditioning load with different types of DC fan rates:  
(a) November; (b) January**

By observing the indoor temperature change curve for different fan rates on a cold but high daytime solar radiation day, January 19, as shown in Figure 4.4.17, it can be learned that the higher the fan rate, the faster the indoor temperature increase. Without turning on the fan, i.e., the air circulation between the inner and outer air layers of the composite double-circulation Trombe wall and the room is stopped, it is difficult for the opaque house to obtain heat from the cold climate conditions, and the indoor temperature always remains at a low level. When the DC fan was turned on, the indoor temperature started to rise between 9:00 and 10:00 a.m., when the fan controlling the circulation of the outer air layer reached the operating temperature of 19°C. The indoor temperature increased around 12:00 a.m., when the fan controlling the circulation of the inner air layer reached the operating temperature of 19°C. And the indoor temperature starts to drop after sunset. This phenomenon is basically consistent with the relationship between the outside air layer temperature, the inside air layer temperature and the indoor temperature change as calculated by the simulation, as shown in Figure 4.4.19, for the condition of 140 m³/h. And the higher the rate of DC fan, the greater the slope of the temperature change curve, i.e., the faster the indoor temperature rises. A single fan can provide a maximum ventilation of 70m³/h, so if the ventilation is above 70 m³/h, another fan is required for each internal and external circulation. The power of a single fan is 3.3W, and half of the time is on, so the amount of power added on the day after adding the fan is about 80wh, which has almost no effect on the calculation result. Compared with the situation of no ventilation, 140 m³/h can save 36.03% energy.

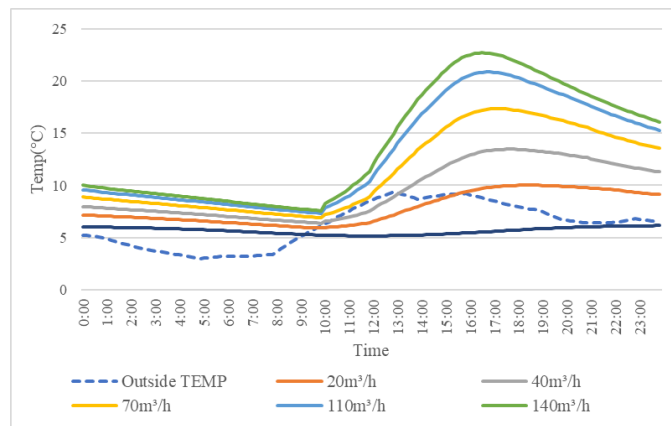


**Figure 4.4.17 Comparison of room temperature with different ventilation rates without heating on January 19<sup>th</sup>**

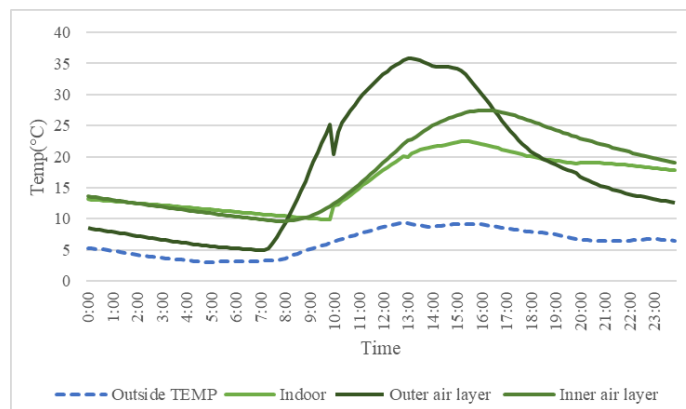


**Figure 4.4.18 Comparison of temperature of different room part with 140m<sup>3</sup>/h ventilation rates without heating on January 19<sup>th</sup>**

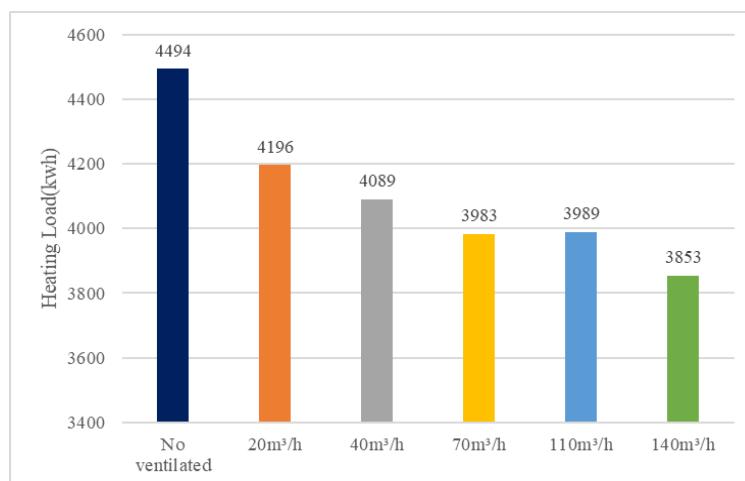


**Figure 4.4.19 Comparison of Air conditioning load with different ventilation rates on January 19<sup>th</sup>**

On February 4, the coldest and overcast day of the year, the average outdoor temperature was only 0.7°C. Solar radiation during the day was minimal. The temperature of both the inner and outer air layers was less than 7°C throughout the day. Although the inner and outer air layers also varied between rising and falling under the change of outdoor climate, the fans were turned off throughout the day under the control of temperature sensing as the air layer temperature did not exceed 19°C throughout the day. Therefore, the trend of temperature change is the same under different ventilation conditions. However, the higher the ventilation, the higher the initial temperature at that time and the higher the average room temperature due to the relatively high initial heat storage. Compared to the case without ventilation, 140m<sup>3</sup>/h can save 0.4% of energy.

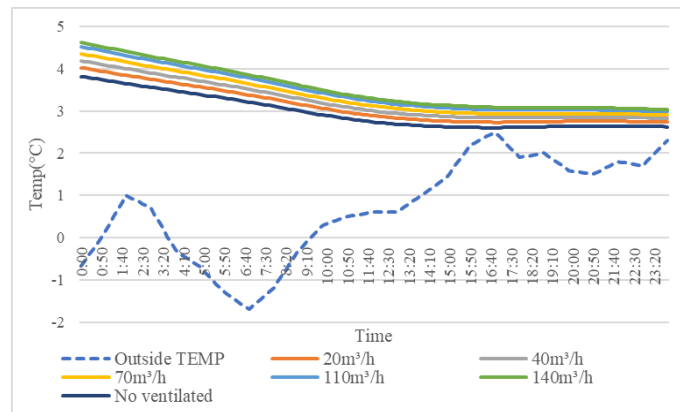


**Figure 4.4.20 Comparison of room temperature with different ventilation rates without heating on February 4<sup>th</sup>**

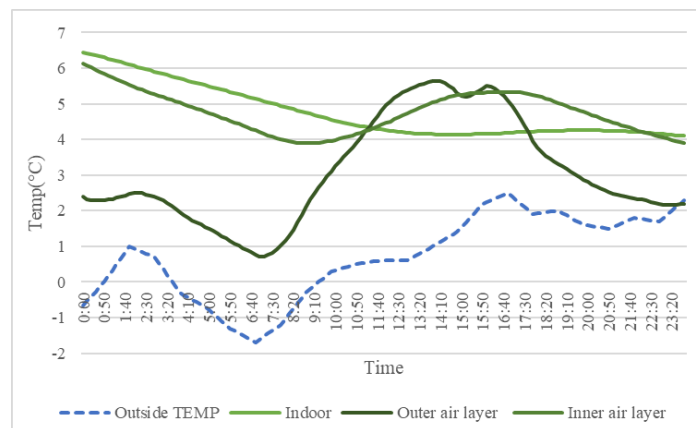


**Figure 4.4.21 Comparison of temperature of different room part with 140m<sup>3</sup>/h ventilation rates without heating on February 4<sup>th</sup>**

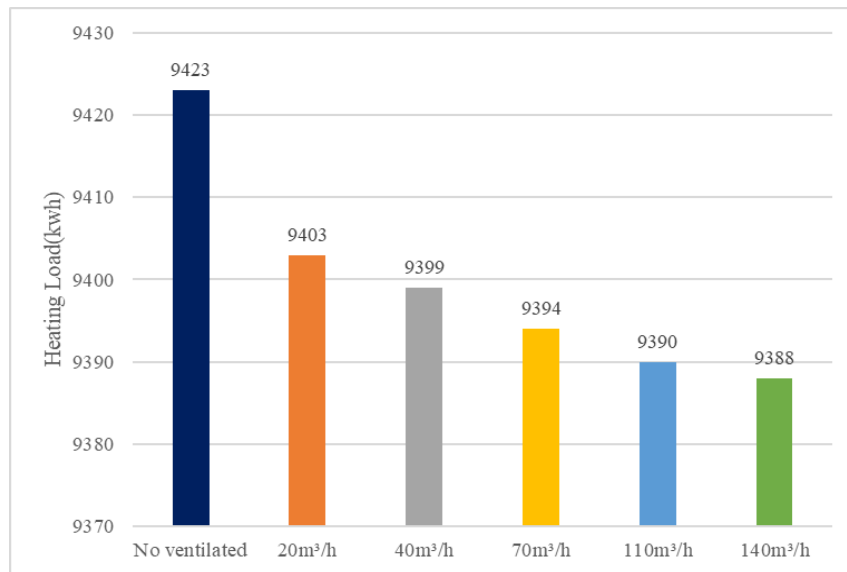


**Figure 4.4.22 Comparison of Air conditioning load with different ventilation rates on February 4<sup>th</sup>**

Combining the total value of indoor air conditioning heat load at different DC fan rates throughout the year, it can be found that under the condition of ventilation below 140 m<sup>3</sup>/h, the greater the ventilation, the smaller the thermal load of the air conditioner. During the whole heating season, compared with the case of no air circulation, the ventilation of 20 m<sup>3</sup>/h, 40 m<sup>3</sup>/h, 70 m<sup>3</sup>/h, 110 m<sup>3</sup>/h, 140 m<sup>3</sup>/h, the energy ratio that can be saved is: 7.6%, 12.6%, 17.2%, 20.5%, and 22%.

Which need to pay attention to is, when the ventilation of the inner and outer circulations is higher than 70 m<sup>3</sup>/h, a single fan cannot apply the required ventilation. Therefore, it is necessary to add 1 fans to maintain the rated air volume for the inner and outer circulations. Even when operating at the highest ventilation of 140 m<sup>3</sup>/h, the DC fans increased energy consumption by only 0.08kwh throughout the day, which has almost no effect on the calculation result.

However, if one calculates the total money expenditure, according to The heating energy cost (HEC) of the building is calculated as:

$$HEC = E_p \times E_h \quad (8)$$

Where  $E_p$  stands for the electricity price per kWh. For the Kitakyushu,  $E_p = 23$  (¥) [3].

The DC fan energy cost (FEC) is calculated as:

$$FEC = E_p \times P \times T \quad (9)$$

Where  $P$  stands for the fan power,  $T$  stands for the fan running time. For this study,  $P = 3.3$  (W) [4].

The total energy cost (TEC) is calculated as:

$$TEC = HEC + FEC + Fp/Y \quad (10)$$

Where  $Fp$  stands for the fan price,  $Y$  stands for the standard lifetime of the fan. For this study,  $Fp = 5480$  (¥),  $Y = 15$  years [4].

Since the cost of a single fan is higher,  $70 \text{ m}^3/\text{h}$  is more economical in terms of total expenses, and  $140 \text{ m}^3/\text{h}$  will cost about 546 yen more per year.

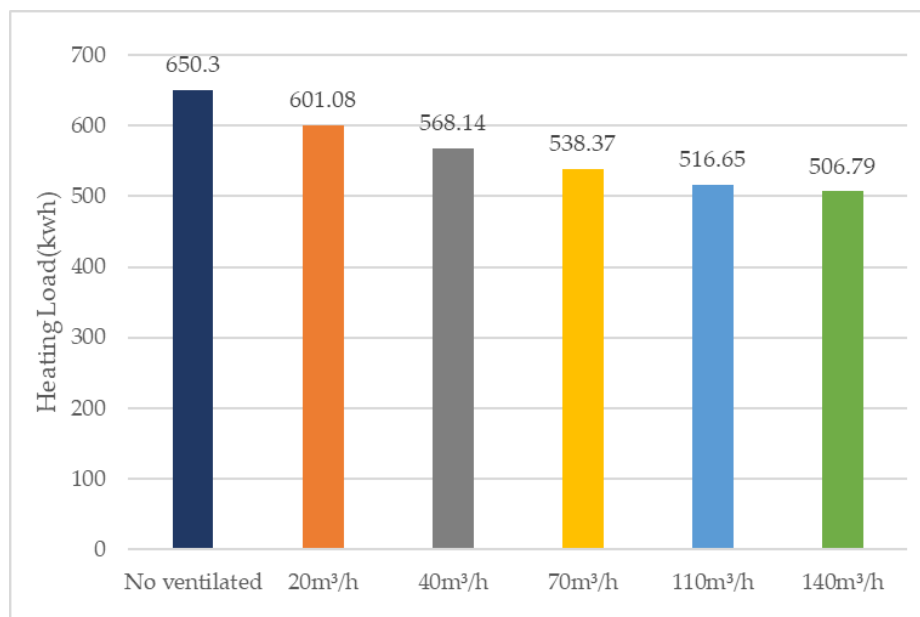


**Figure 4.4.23 Comparison of Air conditioning load with different ventilation rates all over heating season**

#### 4.4.3. The effect of inner wall properties

The inner wall is a new component of the experiment in the study, and there have been few studies on the nature of the inner wall in previous studies so far. The inner wall is set up mainly to insulate to reduce the night-time interior temperature loss through the massive wall with low thermal resistance and glazing surface. This section will focus on the effect of the type and thickness of the interior wall in composite double-circulation Trombe wall on the interior temperature and winter heat load.

##### ① The effect of inner wall materials

With the promotion of highly insulated and sealed houses, central air conditioning systems that integrate ventilation, cooling and heating are gaining attention. In addition, solar thermal utilization is attracting attention as an effective means of reducing energy consumption for cooling/heating and

hot water supply. Therefore, research and development of houses that combine central air conditioning systems and solar energy utilization are necessary for a comfortable thermal environment and energy conservation.

First, the experiment tested the effect of interior wall materials alone, keeping a thickness of 60 mm and using different materials: Styrofoam board, gypsum board, concrete, wood plywood and GW16(Glass wool material with a density of 16 kg/ m<sup>3</sup>) for a simulation experiment without air conditioning to test the effect of inner wall materials.

The parameters of thickness( $\delta$ ), thermal conductivity ( $\lambda$ ), density( $\rho$ ) and specific heat capacity( $c_p$ ) of each material are referred to the following table 4.3.

**Table 4.3 Properties of each material**

Material	$\delta$ (m)	$\lambda$ (W/m K)	$\rho$ (kg/ m <sup>3</sup> )	$c_p$ (J/kg K)
Polystyrene foam	0.06	0.036	27	1100
Rigid polyurethane foam	0.06	0.028	16	840
Gypsum board	0.06	0.220	1039	870
Wooden board	0.06	0.16	380	1880
Concrete	0.06	1.600	2200.0	840

The comparative results are as follows:

In terms of the overall indoor temperature variation throughout the year without the use of air conditioning for heating (Figure 4.4.24), the hottest month of the heating season, November (Figure 4.4.25), and the coldest month of the heating month, January (Figure 4.4.26), the material of the interior wall affects the indoor thermal environment of the composite double-circulation Trombe wall, but the difference between them is not very significant and it can be seen that using concrete gives better results.

Comparing the shorter term, i.e., single day, indoor temperature profiles, here a sunny day (January 19<sup>th</sup> as Figure 4.4.27) and a cloudy day (February 4<sup>th</sup> as Figure 4.4.28) are compared to show the difference between the different materials more clearly. The results of the indoor

temperature change on a sunny day and a cloudy day are consistent, with the interior wall materials used from high to low being: Concrete, Gypsum board, Wooden board, Styrofoam board and GW16. The calculation results of Styrofoam board and GW16 are almost the same and very close.

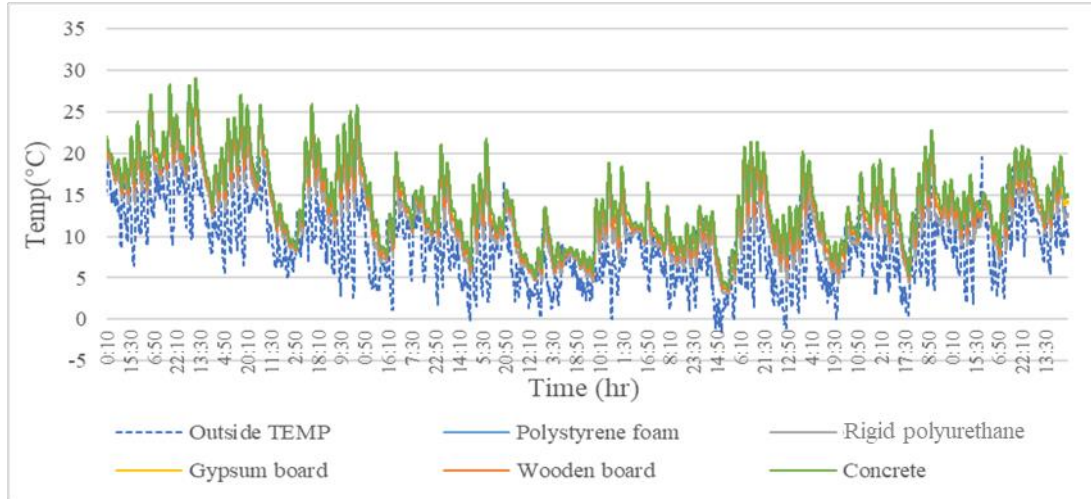


**Figure 4.4.24 Comparison of indoor temperature with different material of inner wall without heating all over heating season**

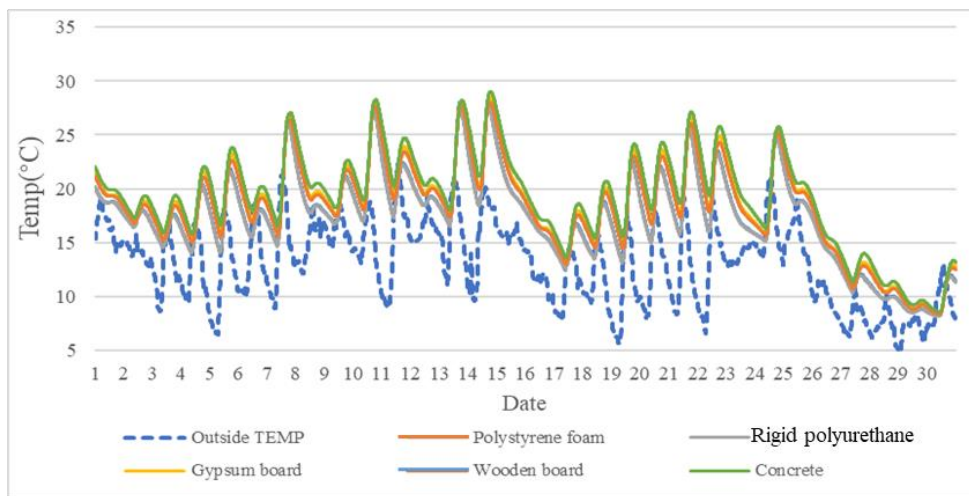


**Figure 4.4.25 Comparison of indoor temperature with different material of inner wall without heating all in November**

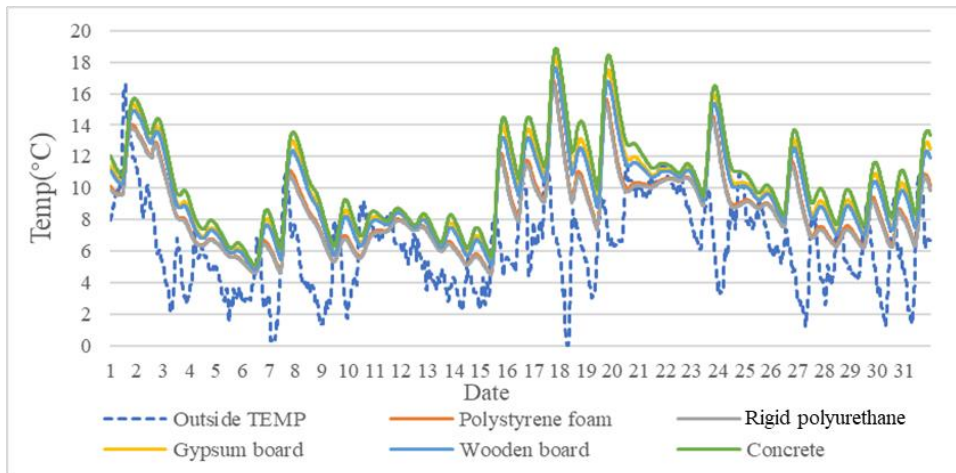


**Figure 4.4.26 Comparison of indoor temperature with different material of inner wall without heating all in January**

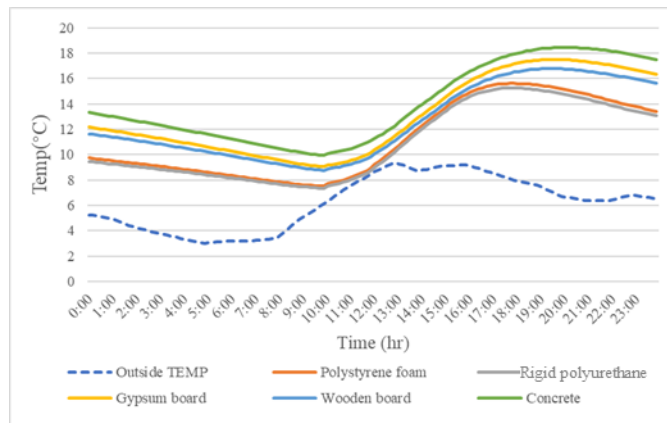


**Figure 4.4.27 Comparison of indoor temperature with different material of inner wall without heating all on January 19th**

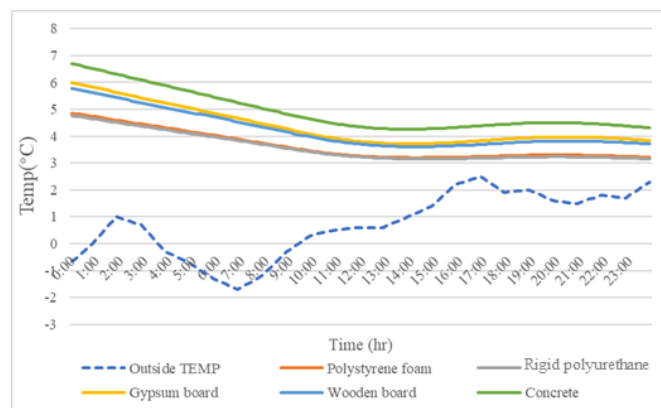


**Figure 4.4.28 C Comparison of indoor temperature with different material of inner wall without heating all on February 4th**

According to the formula for thermal resistance (R).

$$R = \delta/\lambda \quad (11)$$

The thermal resistance of each material can be calculated separately and then, from largest to smallest, as : GW16 2.14 m<sup>2</sup>K/W, Styrofoam board 1.67 m<sup>2</sup>K/W, Wooden board 0.375 m<sup>2</sup>K/W, Gypsum board 0.27 m<sup>2</sup>K/W, and Concrete 0.0375 m<sup>2</sup>K/W. The result of its temperature change corresponds to the calculation of thermal resistance.

The simulation continues by calculating the simulated air conditioning load in residential air conditioning mode and intercepting the air conditioning load for a sunny day on January 19, the coldest day of the year (non-sunny day) and the coldest month of the year as a specific comparison. The results obtained are as follows.

After comparing the single-month air conditioning heat load in November (Figure 4.4.29), the warmest month of winter in Kitakyushu, and January, the coldest month, it was found that the two showed opposite results when air conditioning was used only at night. In the warmer month of November, the higher the thermal resistance, the higher the heat load of the interior wall. The indoor air conditioning heat load of the composite double-circulation Trombe wall with the lowest thermal resistance concrete as the interior wall was 53.5 kwh, followed by Gypsum board and Wooden board. The thermal load of GW16 and Styrofoam board, which are used as building insulation materials with higher thermal resistance, is also higher, 58.9 kwh and 59.2 kwh, respectively, while in cold January, the thermal load of interior walls with high thermal resistance is lower. However, among the insulation materials Styrofoam board and GW16, Styrofoam board has a relatively high thermal resistance but consumes a lower thermal load of 131.4 kwh in the interior, while GW16 consumes 133.9 kwh as an interior wall, followed by Wooden board and Gypsum board. the highest thermal load is consumed by concrete interior walls consumed 141.8 kwh in January.

Then two colder single day indoor air conditioning heat loads were compared, one for a cold sunny day (January 19 in Figure 4.4.31(a)) and the other for a cloudy day (February 4 in Figure 4.4.31(b)). The comparison found that on a sunny day with plenty of solar radiation, similar to the results for a warm November, more energy could be saved by interior wall materials with less thermal resistance. However, the lowest indoor thermal load on that date was for Gypsum board with 3785wh, and the highest thermal load was for GW16 with the lowest thermal resistance. while on cold cloudy days, the results were similar to those of cold January. The lowest air conditioning load is GW16 with the highest thermal resistance, totaling 8839wh, followed by Styrofoam board with 9399wh. the concrete material with the lowest thermal resistance has the highest thermal load of 12107wh.

In summary, the exploration of the interior wall materials for composite double-circulation

Trombe wall revealed that the recommended interior wall materials for the use of composite double-circulation Trombe wall in winter differed for different climatic conditions. In relatively warm climates with sunny days and sufficient solar radiation, materials with low thermal resistance are suitable for interior walls. Conversely, in colder climates with less solar radiation, insulation materials with higher thermal resistance are more suitable to reduce heat loss from the interior.

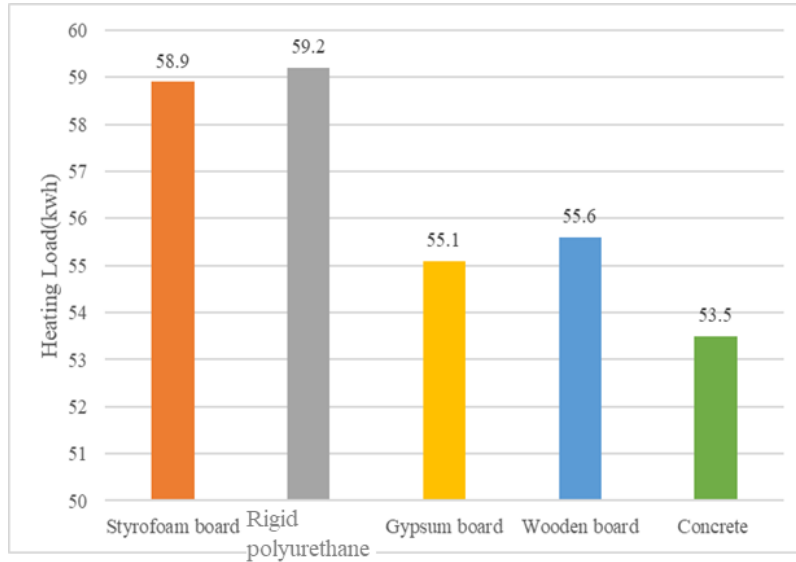


**Figure 4.4.29 Comparison of Air conditioning load with different material of inner wall in November**

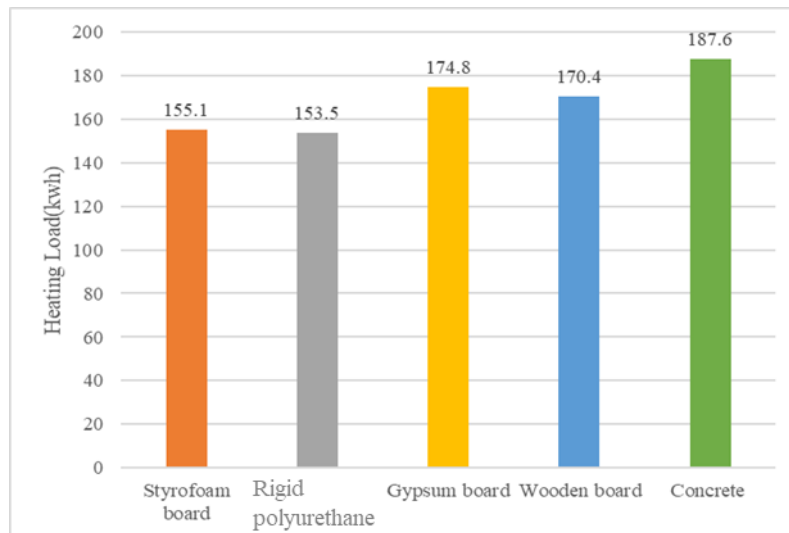


**Figure 4.4.30 Comparison of Air conditioning load with different material of inner wall in January**

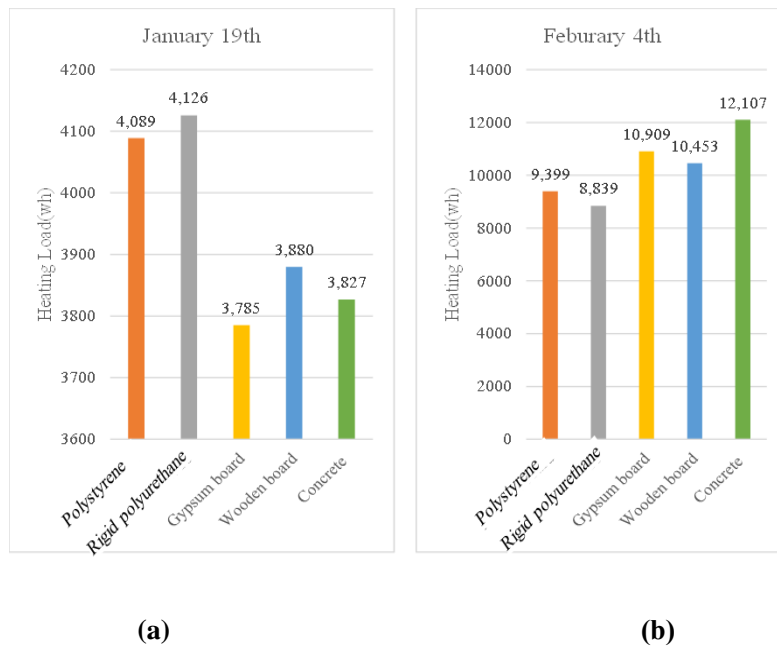


**Figure 4.4.31 Comparison of Air conditioning load with different material of inner wall: (a) on January 19th; (b) on February 4th**

In the Kitakyushu region of Japan, compared with the calculated indoor air conditioning heat load data for the heating season throughout the year in the standard meteorological year (Figure 4.4.32), it is more appropriate to use insulation materials with low thermal resistance such as GW16 and Styrofoam board for the inner wall when only the air conditioning is turned on at night. Because glass wool materials are relatively expensive and do not yield more significant benefits, the use of Styrofoam boards is more appropriate than other materials used in the simulation experiments.

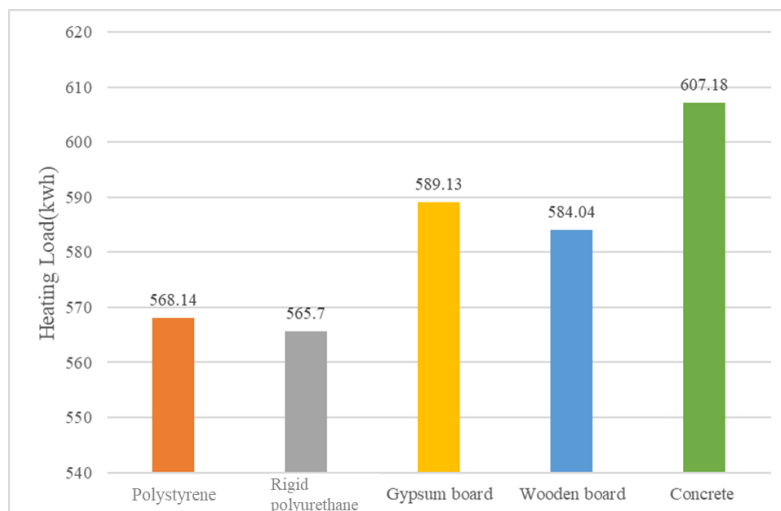


**Figure 4.4.32 Comparison of Air conditioning load with different material of inner wall all over heating season**

## ② The effect of inner wall thickness

This part tests the effect of the thickness of the inner wall, comparing 30mm (single layer), 60mm (double layer), 90mm (triple layer) and 120mm (quadruple layer) Rigid polyurethane panel. According to the calculation in the previous section, the greater the thickness of the material, the greater the thermal resistance. The thermal resistance of 30mm, 60mm, 90mm and 120mm Styrofoam board are 0.84 m<sup>2</sup>K/W, 1.67 m<sup>2</sup>K/W, 2.51 m<sup>2</sup>K/W and 3.34 m<sup>2</sup>K/W respectively.

Comparing the indoor air temperature change curves in November, the warmest month of winter without air conditioning, and January, the coldest month, it can be seen that using the same material, the relationship between the indoor temperature and the thermal resistance of the material (i.e., the thickness of the interior wall) is similar to that of different materials: the lower the thermal resistance (i.e., the smaller the thickness and smaller footprint ratio), the higher the maximum achievable indoor temperature and the greater the fluctuation of temperature. Conversely, the higher the thermal resistance (i.e., the greater the thickness and greater footprint ratio), the lower the maximum achievable indoor temperature and the smaller the fluctuation in temperature. In the warmer months of November, the difference in indoor temperatures caused by different thicknesses of insulation panels is not significant. The difference in indoor temperature variation is greater in the colder months of January.

Comparing the indoor air conditioning heat load of each of the two months in the mode of night air conditioning on (Figure 4.4.35), the warmer November, the higher the indoor air conditioning load caused by the thicker insulation board, the lower the indoor heat load of the smaller thickness of the insulation board. The most energy-efficient panel is the 30mm panel, with an indoor heat load of 58.6 kwh, which is not much different from the highest 120mm panel with an overall heat load of 59.7 kwh, with a difference of only about 1kwh for the whole month, while the opposite is true for the colder month of January: the smaller the proportion of the interior wall, the higher the heat load, and the larger the proportion of the interior wall, the lower the heat load. The larger the proportion of the interior wall, the lower the heat load. The highest heat load is for the 30mm panel with 134kwh and the lowest is for the 120mm panel with 130.5kwh. The overall difference in heat load for the composite double-circulation Trombe wall house with 60mm, 90mm and 120mm panels in January is not significant.

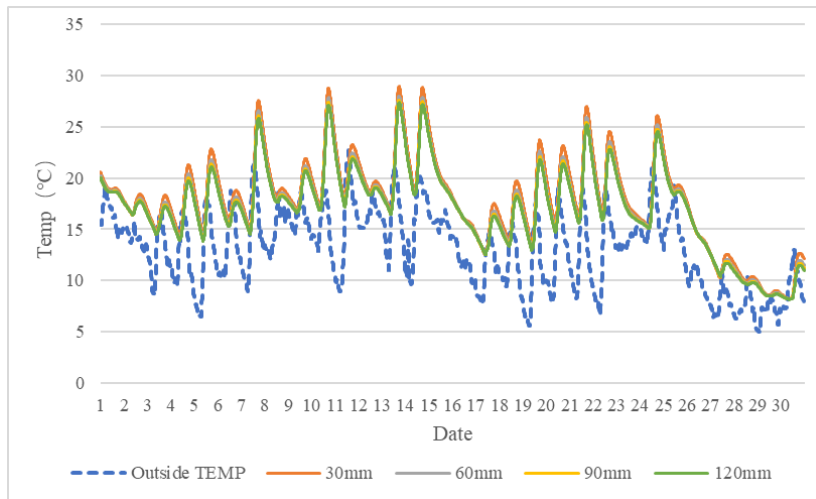


**Figure 4.4.33 Comparison of Air conditioning load with different thickness of inner wall in November**

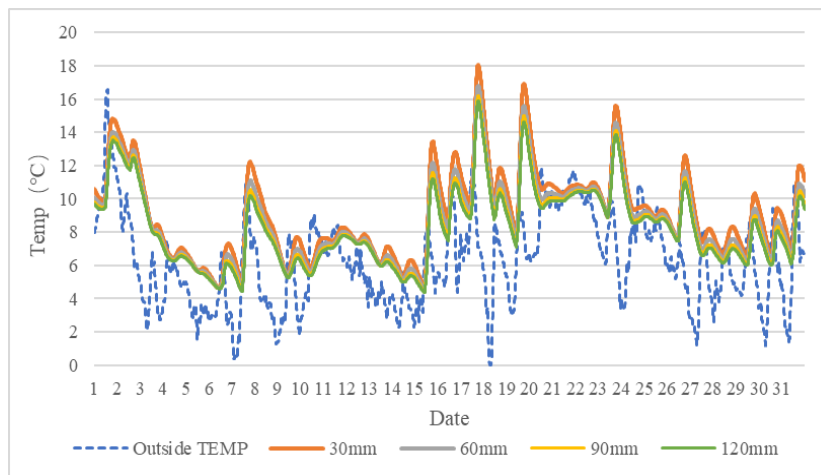


**Figure 4.4.34 Comparison of Air conditioning load with different thickness of inner wall in January**

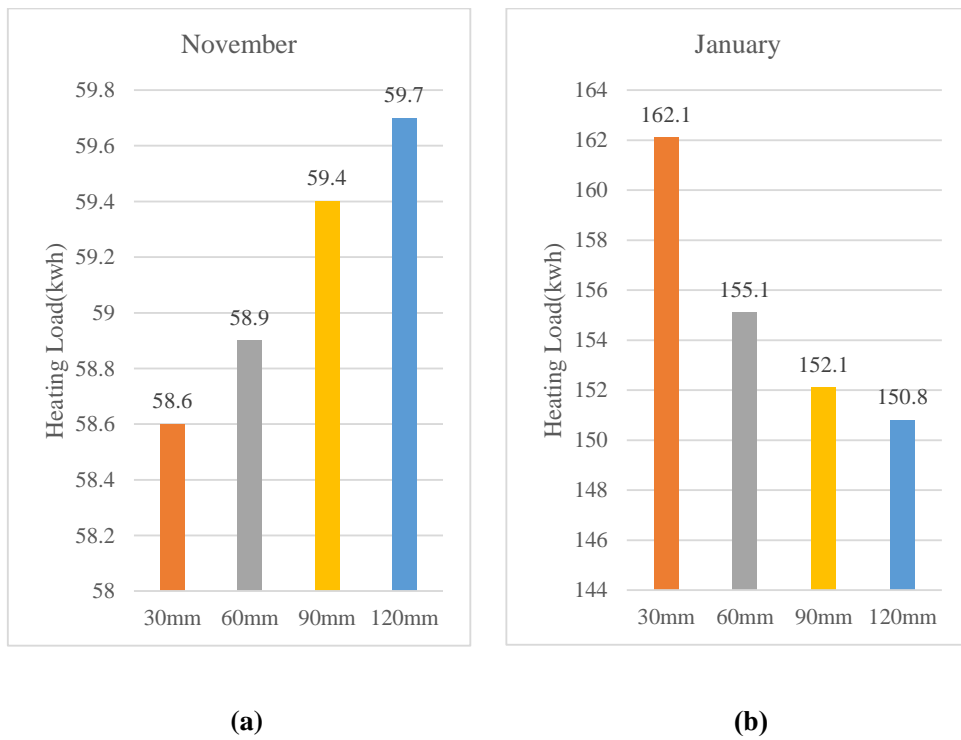


**Figure 4.4.35 Comparison of Air conditioning load with different thickness of inner wall: (a) November; (b) January**

Then two colder single day indoor air conditioning heat loads were compared, one for a cold sunny day (January 19) and the other for a cloudy day (February 4). The comparison found that on a sunny day with plenty of solar radiation, similar to the results for a warm November, more energy could be saved by interior wall materials with thin inner wall.

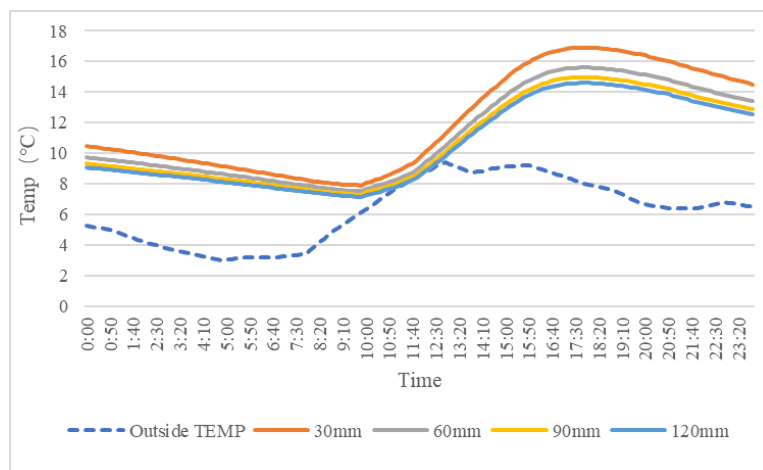


**Figure 4.4.36 Comparison of Air conditioning load with different thickness of inner wall on January 19th**

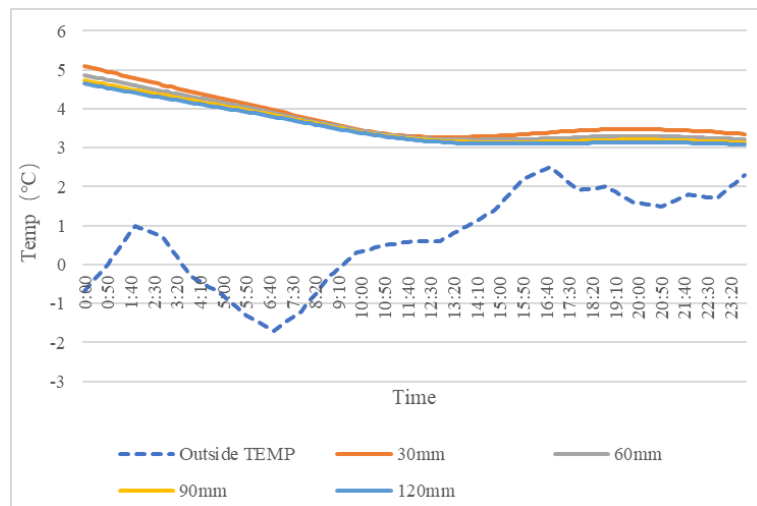


**Figure 4.4.37 Comparison of Air conditioning load with different thickness of inner wall on February 4th**

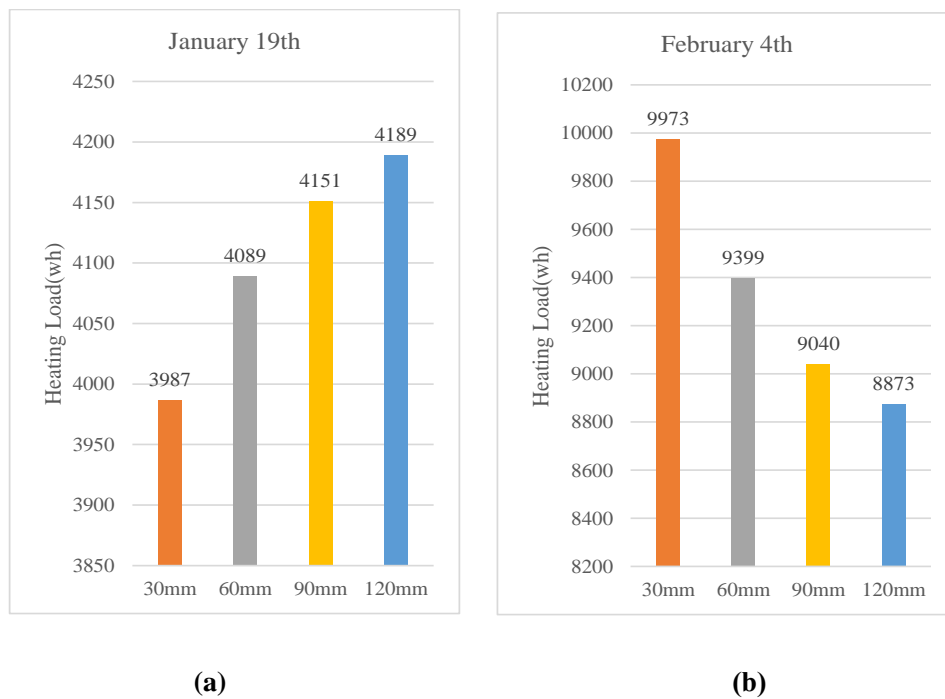


**Figure 4.4.38 Comparison of Air conditioning load with different thickness of inner wall: (a) January 19<sup>th</sup>; (b) February 4<sup>th</sup>**

And a comprehensive comparison of the indoor air conditioning heat load throughout the year under the condition that the air conditioning is turned on at night. The thicker the inner wall, the more energy is saved, using 120mm (4.3% of the total indoor area) with the least heat load of 563.04 kwh, followed by 90mm (3.2% of the total indoor area) with a heat load of 564.76 kwh, and 60mm (2.2% of the total indoor area) with a heat load of 568.14 The maximum heat load of 30mm interior

walls is 577.76 kwh. 60mm, 90mm and 120mm interior walls have a small difference in the annual indoor air conditioning heat load, so from various aspects such as economy and usable area of the room, Calculated from an economic cost perspective.

The total energy cost (TEC) is calculated as:

$$TEC = Ep \times Eh + Fi \times n/Y \quad (12)$$

Where  $F_i$  stands for the insulation panel price,  $n$  stands for the number of insulation panel layers,  $Y$  stands for the standard lifetime of inner wall. For this study,  $F_i=5877(\text{¥})$ ;  $Y = 30$  years [5].

it is more appropriate to use 60mm (2.2% of the total indoor area).

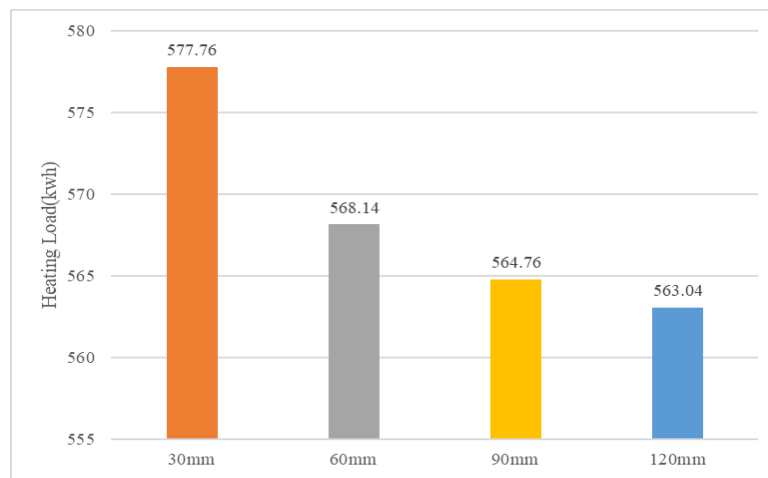


**Figure 4.4.39 Comparison of Air conditioning load with different thickness of inner wall all over heating season**

**Table 4.4 Energy saving statistics of different inner wall thickness**

Thickness (mm)	Ratio to floor area (%)	Heating load (kwh)	Energy cutting (With NH) (%)
30	1.1	577.76	30.9
60	2.2	568.14	32.1
90	3.2	564.76	32.5
120	4.3	563.04	32.7

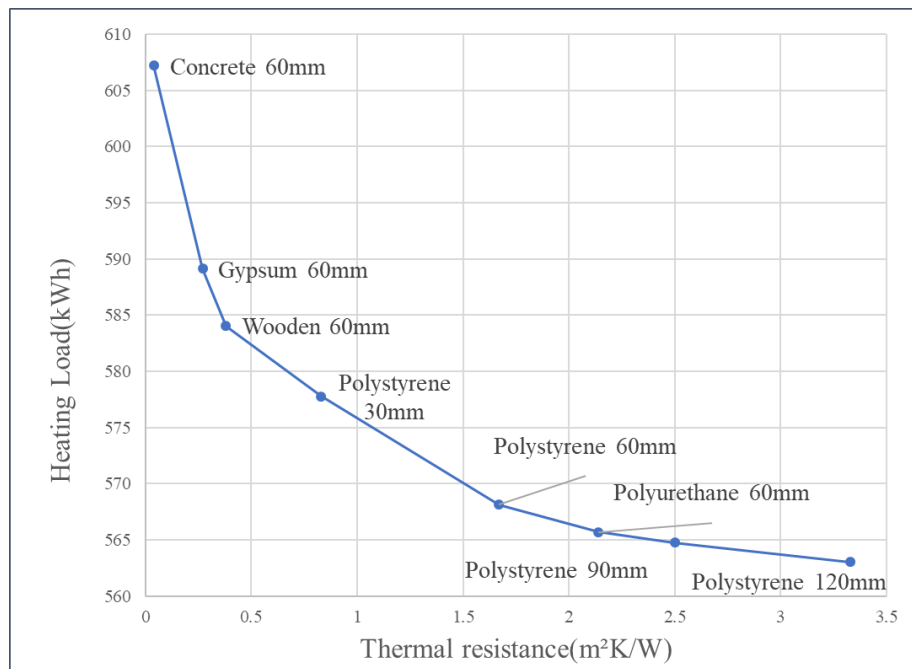


**Figure 4.4.40 Comparison of Air conditioning load with different thermal resistance of inner wall**

#### 4.4.4. The effect of massive wall properties

The massive wall is the core component of the Trombe wall. the nature of the massive wall makes an important contribution to the efficiency of the Trombe wall's heat storage and release capacity. Any material characterized by a high storage capacity can be used to construct a Trombe wall. However, the use of lightweight materials with high storage capacity in relatively small volumes is preferable, such as PCM. Massive wall thickness has been experimented several times in the Trombe wall study. According to some conclusions, construction of a classical Trombe wall with 3.20% of the building floor area can get the best result.[6] The study needs to understand the effect of this parameter on the new composite double-circulation Trombe wall.

Before formally simulating the composite double-circulation Trombe wall, the study simulated the Classic Trombe wall and obtained a graph of the indoor temperature variation without air conditioning. According to the Figure 4.4.41, it was found that in the Classic Trombe wall, the smaller the wall thickness, the more drastic the temperature fluctuation and the faster the heat loss at night. Within a certain range, the greater the wall thickness, the more stable the indoor temperature and the smaller the air conditioning load. In the composite double-circulation Trombe wall house, for the added interior wall used for insulation, the indoor heat is not lost directly through the giant wall, and also the energy radiated directly from the massive wall to the room is missing, so we need to re-evaluate the role of massive wall in the composite double-circulation Trombe wall on building energy consumption.

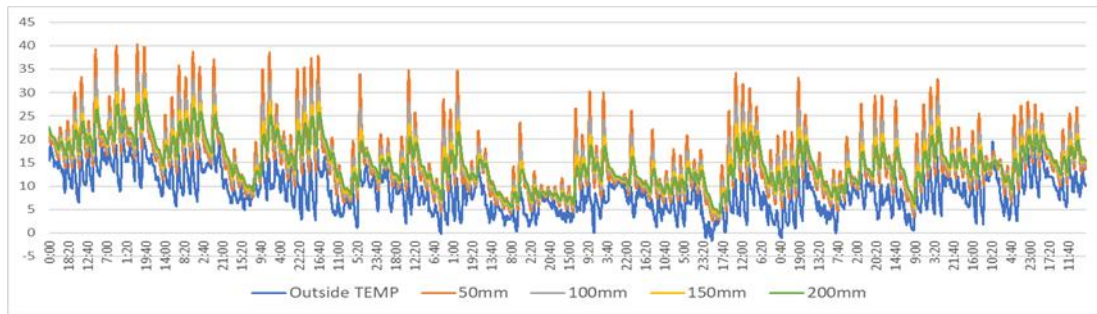


**Figure 4.4.41 Comparison of room temperature with different thickness of massive wall without heating overall heating season of classic Trombe wall**

### ① The effect of massive wall properties

The massive wall in the reference house is built with concrete blocks of 100 mm thickness. For possible further validation in the future and considering the ratio of the massive wall to the house area, the simulation used 50 mm, 100 mm, 150 mm and 200 mm thicknesses as about 1.7%, 3.0%, 5.0%, 6.7% of the building floor area.

Comparing the indoor temperature without air conditioning as Figure 4.4.42, Figure 4.4.43 and Figure 4.4.44, it was found that The same as shown by the temperature fluctuations in the classic Trombe wall house, the smaller the thickness of the massive wall, the higher the maximum indoor temperature that can be achieved. However, at the same time, the minimum temperature at night is significantly lower than that of the thicker massive wall, and the temperature fluctuates more.

The smaller the thickness of the material, the faster the rate of heat transfer. In the daytime with high sunlight radiation, the house with the smallest thickness of massive wall has the fastest indoor temperature rise, but the rate of heat loss at night is also faster. A thicker mass wall stores more heat and loses less heat at night, If the climate is continuously cloudy, the thickness of the smaller mass wall cannot heat the air layer temperature by absorbing solar energy, and the thickness of the larger mass wall house will have a greater indoor temperature than the thickness of the smaller mass wall house even during the daytime. But thicker mass wall also heats up more slowly during the day. Although the composite double-circulation Trombe wall reduces the indoor heat loss at night by adding a layer of inner wall. But the indoor temperature has a direct effect on the temperature of the inner and outer air layers, which is closely related to the heat storage and heat transfer capacity of the massive wall. So the thickness (i.e. floor area) of massive wall is too low or too high, which is not conducive to energy saving effect.

A comparison of indoor heat loads for different months (Figure 4.4.45) confirms this statement. In November, the larger the thickness of the massive wall, the smaller the indoor air conditioning energy consumption, the smallest heat load is 200mm concrete block with 55.2kwh. However, the

overall difference in indoor air conditioning energy consumption between 10mm-200mm massive wall is not significant, and the difference between 100mm and 200mm is only 3.7 kwh. in January, the indoor air conditioning heat load The smallest is 100mm concrete block, with a heat load of 131.4 kwh in a single month, and for the remaining specifications of massive wall thickness, the indoor heat load does not differ much.

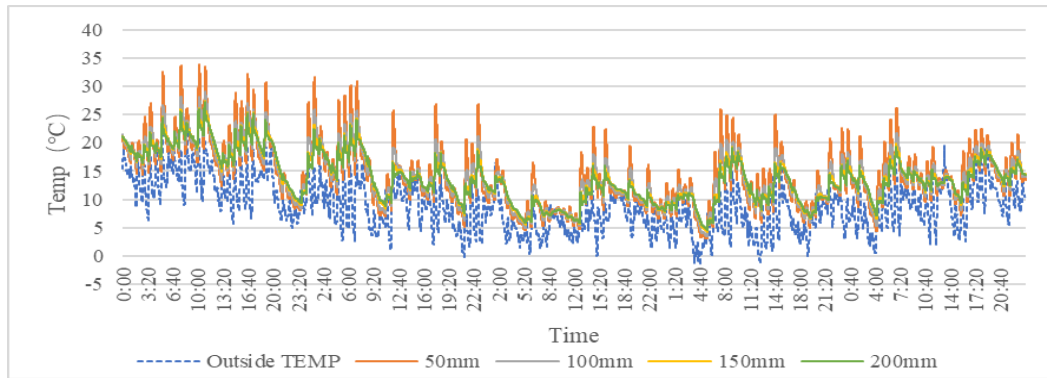


**Figure 4.4.42 Comparison of room temperature with different thickness of massive wall without heating**

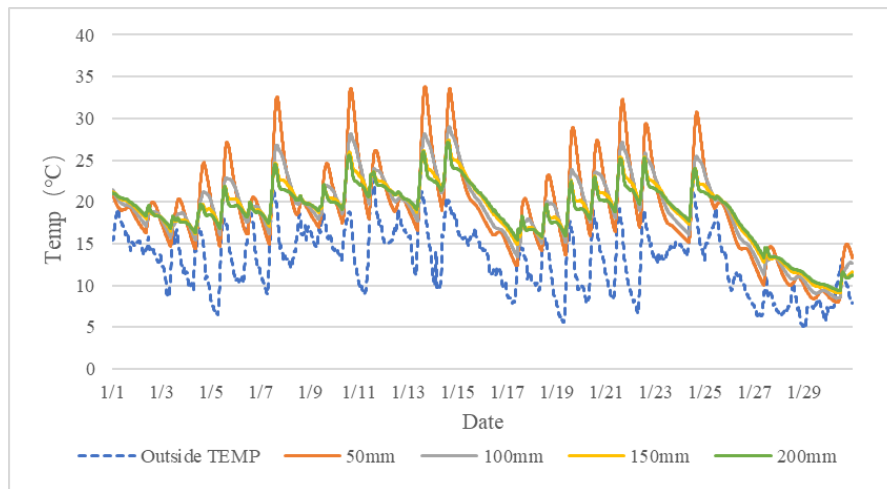


**Figure 4.4.43 Comparison of room temperature with different thickness of massive wall without heating in November**

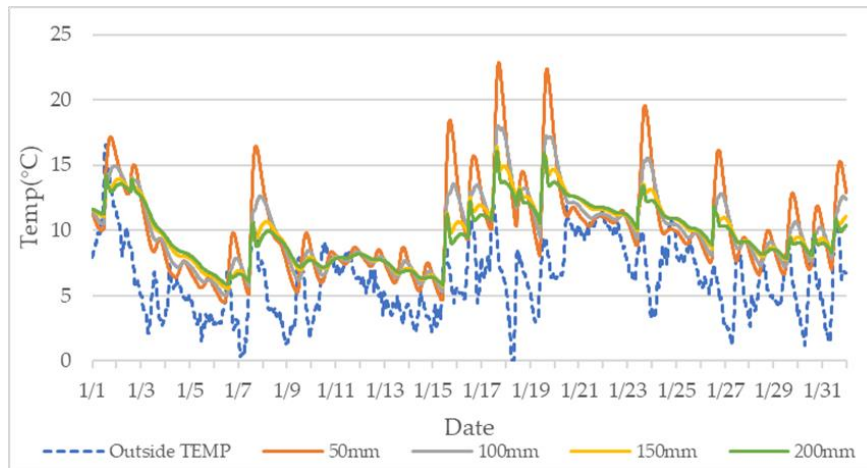


**Figure 4.4.44 Comparison of room temperature with different thickness of massive wall without heating in January**

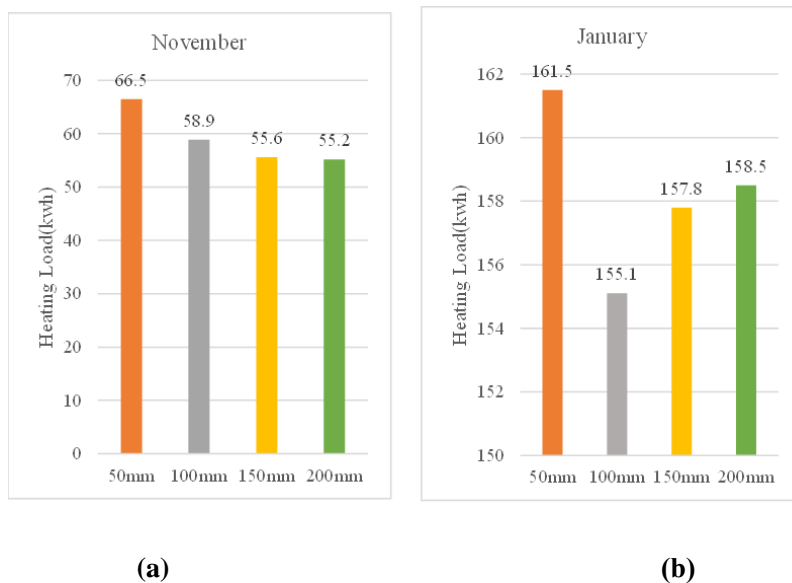


**Figure 4.4.45 Comparison of Air conditioning load with different thickness of massive wall: (a) November; (b) January**

Comparing the results of the comparison of specific heat loads of single day, Walls of thin thickness loses heat quickly due to the rapid drop in temperature at night. However, it is not the case that the thicker the wall, the better the effect. Extracted data from a cold sunny day (January 19th) and a cloudy day (February 4th) for comparison in Figure 4.4.46, and the graph shows that on a cold sunny day, a 100 mm thick massive wall has the lowest heat load, while on a cold, cloudy day, the thicker the massive wall is, the more air conditioning load it can save.

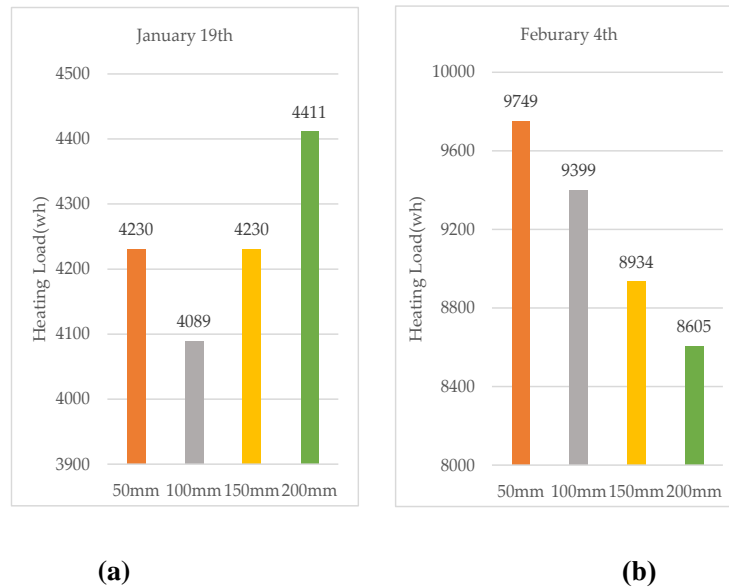


**Figure 4.4.46 Comparison of Air conditioning load with different thickness of massive wall: (a)January 19th; (b)February 4th**

And compare the room temperature change curves of these two days. On January 19, a cold and sunny day, the house with the smallest thickness of 50mm of massive wall could raise the room temperature more quickly when the fan that controls the air circulation inside and outside started to operate. The reason for this is that when comparing the air layer temperatures of different thicknesses of massive walls (Figure 4.4.47), the smaller the thickness of the massive wall, the faster the temperature of the air layer rises after sunrise when solar radiation starts to be absorbed, especially in the inner air layer, and the 50mm massive wall raises the temperature earlier and faster than other thicknesses of the massive wall. So the air temperature delivered to the room through the DC fan is higher, which raises the room temperature faster and higher. However, after sunset, the air layer temperature of the house with the thin thickness of the massive wall drops rapidly and rapidly decreases below the thickness of the larger size of the massive wall. The indoor air temperature did not fall as fast as the air layer, but it was also lower than that of the larger-sized massive wall houses in the latter half of the night. And on February 4, because there was almost no solar radiation all day, the air layer temperature did not reach the standard of DC fan operation, so the fan did not run all day, and the indoor temperature needed to be supported by the residual temperature of the previous day. The thicker the massive wall the higher the base temperature of the house, so the overall temperature was also higher. In areas with cold and rainy days, a thicker massive wall is more suitable.

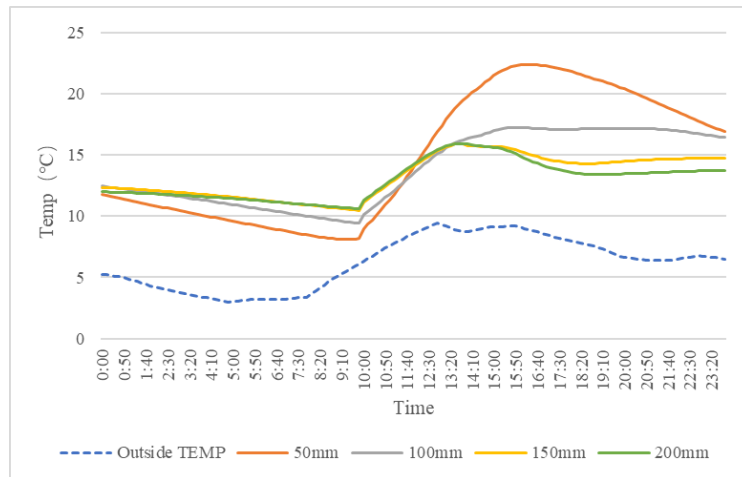
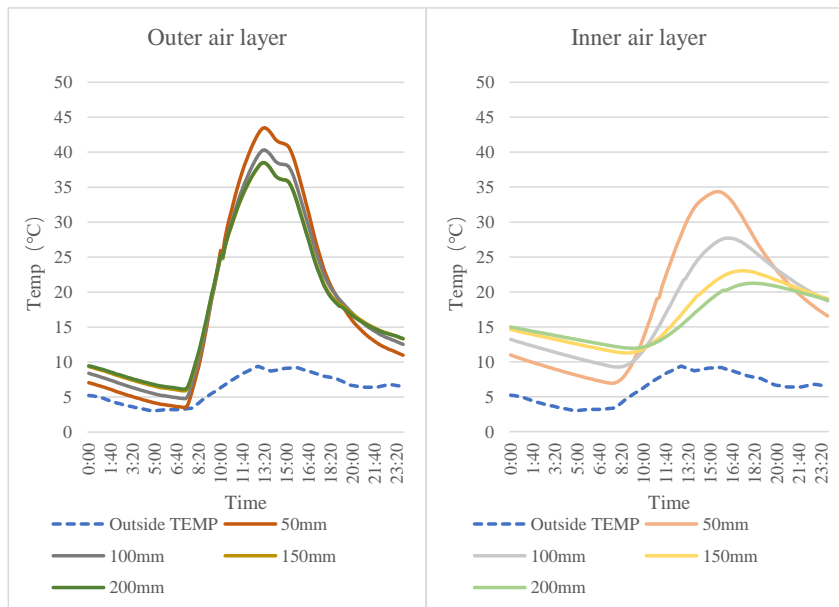


**Figure 4.4.47 Comparison of room temperature with different thickness of massive wall without heating on January 19th**



(a)

(b)

**Figure 4.4.48 Comparison of room temperature with different thickness of massive wall without heating on January 19<sup>th</sup>: (a)Outer air layer; (b) Inner air layer**

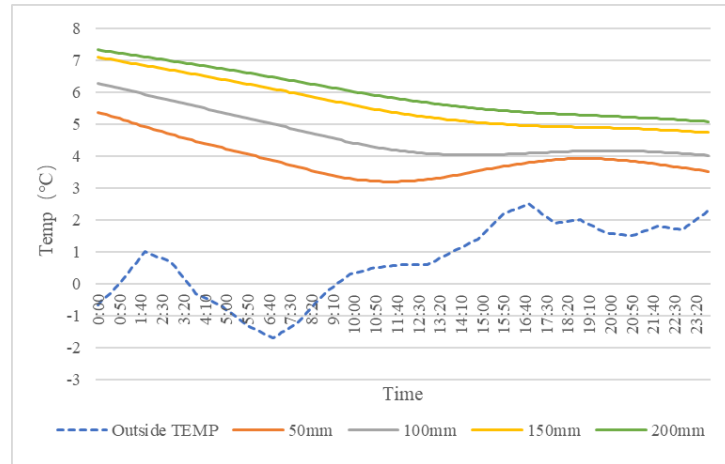


**Figure 4.4.49 Comparison of room temperature with different thickness of massive wall without heating on February 4th**

As shown in Figure 4.4.50, the annual thermal energy consumption of a 100 mm thick massive wall (3.6% of the building floor area) is the lowest in winter climate conditions in Kitakyushu, Japan.

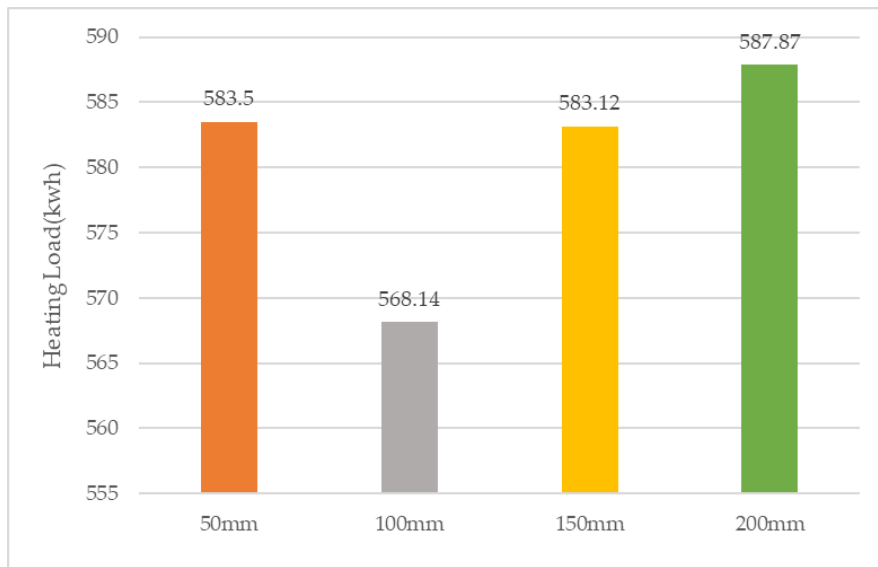


**Figure 4.4.50 Comparison of Air conditioning load with different thickness of massive wall overall heating season**

**Table 4.5 Energy saving statistics of different massive wall thickness**

Thickness (mm)	Ratio to floor area (%)	Heating load	Energy cutting (With NH)
50	3.6	583.5	
100	3.6	568.14	
150	3.6	583.12	
200	3.6	587.87	

		(kwh)	(%)
50	1.8	583.76	30.2
100	3.6	568.14	32.0
150	5.4	583.12	30.3
200	7.2	587.87	29.7

## ② The effect of massive wall materials

The core of the Trombe wall system is the massive wall for heat storage, whose material storage capacity directly affects the temperature of the space in direct contact with it. Therefore, different thermal properties (specific heat, thermal conductivity, etc.) of the material will inevitably affect the efficiency of the Trombe wall system.

In this chapter, the material of the massive wall is not discussed in depth, and the details will be analyzed in Chapter 6.

### 4.4.5. Comprehensive optimization considerations

In the previous comparison, the most obvious energy saving effect is the change of the window type. About the types of glazing, it was found that the Low-E double-glazed window theoretically has the best effect of reducing the building energy consumption. As for ventilation, after calculating the fan power, ventilation rates of 140 m<sup>3</sup>/h still have the best energy saving effect. And use the thickness of 100 mm for massive wall (3.6% of the house floor area) and thickness of 60 mm for inner wall (2.2 % of the house floor area).

To convert the magnitude of the impact of each variable into a more intuitive value for comparison a relative reference result can be calculated from the following equation. Impact factor (HL):

$$HL = \frac{Heatingload_{max} - Heatingload_{min}}{Heatingload_{max} + Heatingload_{min}} \quad (13)$$

Where the Heatingload used for this calculation is the maximum and minimum values of the heat load already calculated in the previous section for each variable range. The final calculation results are shown in the table below. The greatest influence on the performance of the composite double-circulation Trombe wall is the material of the glazing surface, followed by the rate of the

fan. Close, the final impact is not significant, in the selection of materials can be based on economic considerations using cheaper options.

**Table 4.6 Energy saving statistics of different Variables**

Variables		Heating load (kwh)	Energy cutting (With NH) (%)	Impact factor
Glazing types	Max	568.14	32.1%	0.26
	Min	333.34	60.1%	
DC fan rates	Max	650.3	22.3%	0.12
	Min	506.79	39.4%	
Inner wall materials	Max	607.18	27.4%	0.04
	Min	565.7	32.4%	
Inner all thickness	Max	577.76	30.9%	0.01
	Min	564.04	32.6%	
Massive wall thickness	Max	587.87	29.7%	0.02
	Min	568.14	32.1%	

In the previous comparison, in the selection of DC fans, the recommended total indoor ventilation rate from the energy saving point of view is 140 m<sup>3</sup>/h, while 70 m<sup>3</sup>/h is more economical to choose from the total cost point of view. And after combining other optimization conditions, the comparison results of different ventilation efficiencies are shown in Figure 4.4.51. The comparison of indoor temperature on 140 m<sup>3</sup>/h and the annual heat load is also lower on 140 m<sup>3</sup>/h. Also calculating the cost of both, it is found that after considering the optimization conditions in this chapter, the annual cost of 140 m<sup>3</sup>/h ventilation efficiency will save about 129 yen compared to 70 m<sup>3</sup>/h. Therefore, it is more economical and energy-saving to choose 140 m<sup>3</sup>/h.

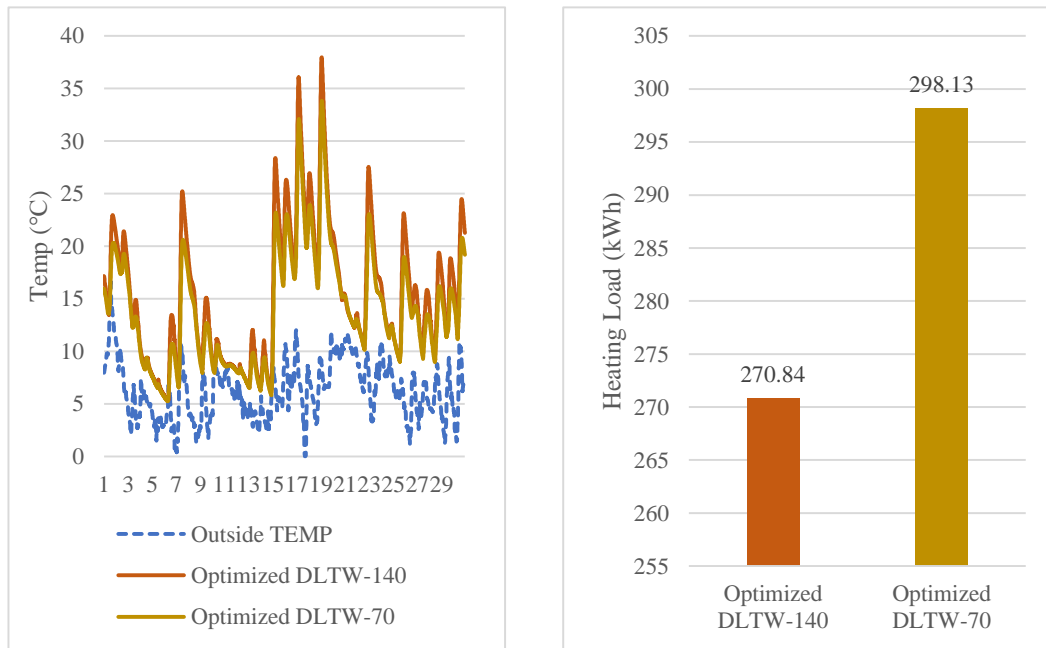


**Figure 4.4.51 Comparison of different DC fan rates**

The final simulated annual air conditioning heat load of this experimental house is about 270.84 kwh, compared to the predicted heat load before optimization, the energy consumption can be saved by more than 52.3% throughout the year.

And in response to the aforementioned problem of low room temperature of this kind of composite double-circulation Trombe wall in the state without air conditioning, after integrating the optimization factors, as shown in the Figure 4.4.52, in January, for example, the optimized composite double-circulation Trombe wall has a significant overall improvement in room temperature compared to the pre-optimized room temperature, and in the daytime with sufficient solar radiation, the room temperature can reach a maximum of about 36.8 °C.

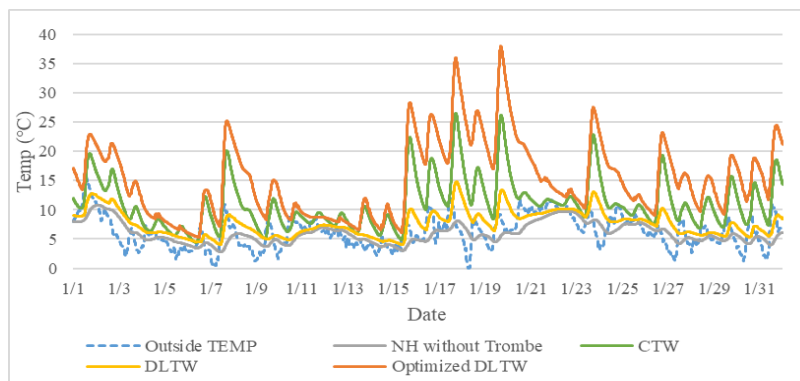


**Figure 4.4.52 Comparison of indoor temperature with different houses in January**

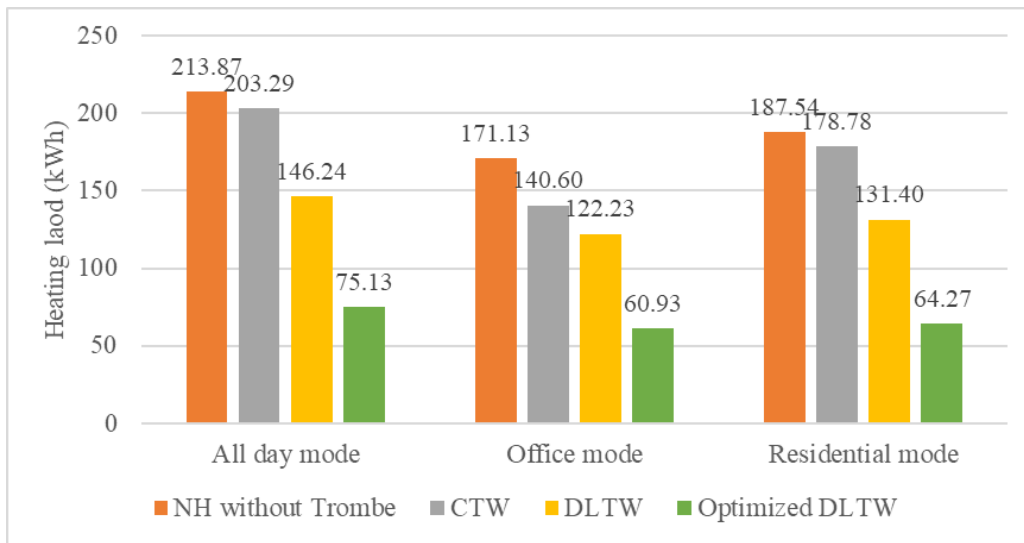


**Figure 4.4.53 Comparison of Air conditioning load with different houses in January**

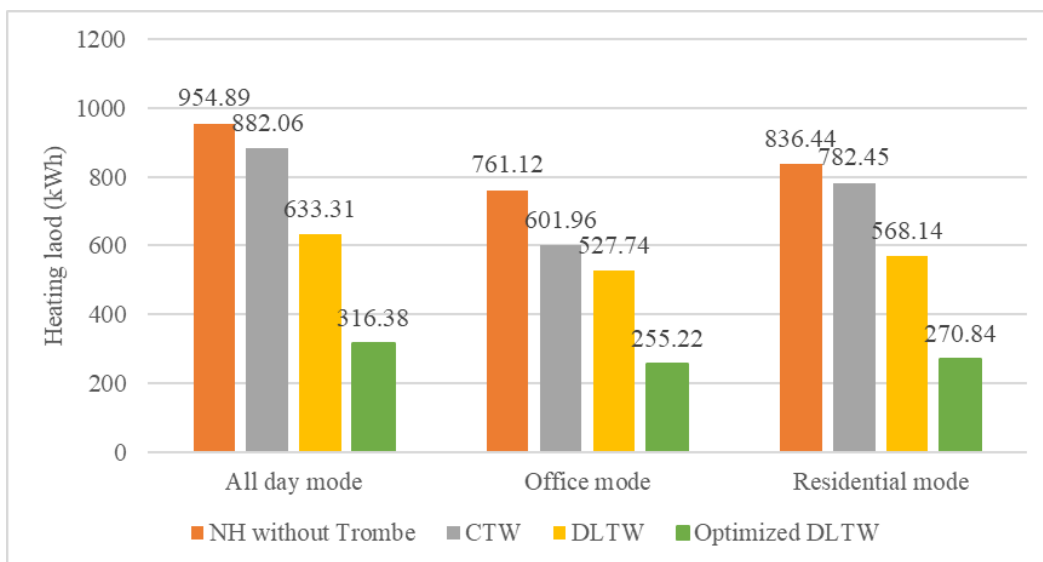


**Figure 4.4.54 Comparison of Air conditioning load with different houses overall heating season**

#### 4.5. Conclusion and discussion

This chapter mainly focuses on a new composite Trombe wall, which adds a layer of thermal insulation wall to the traditional Trombe wall to form two air layers. At the same time, pipes and air vents at upper and down are used to connect the two air layers and the room, so that the composite Trombe wall forms two air circulations as inner and outer. The air circulation is forced to be stable and fast by using temperature-controlled DC fans. The study evaluated the thermal potential of this composite Trombe wall by using THERB for HAM software which has been approved by the

Japanese government as an evaluation method for annual heating and cooling load calculation methods. The following main results were drawn from the numerical simulations performed:

- (a) A composite Trombe wall assisted by a temperature-controlled DC fan can achieve better energy savings compared to a classic Trombe wall with thermal air conditioning. However, the overall room temperature of the composite Trombe wall is smaller than that of the classical Trombe wall in the absence of air conditioning.
- (b) The most obvious energy saving effect is the change of window type. Low-E double-glazing can play a very good role in insulation because of its characteristics, but the effect will be different if the Low-E layer is set in the different positions. Compared to single-glazing, double-glazing with a 3#Low-E layer is expected to save nearly 41.3% of energy. It is expected to save nearly 41.3% of the annual heat load. Energy savings can also be achieved with ordinary multi-panel glass, with double and triple glazing saving 17.2% and 27.9% of energy consumption, respectively. 2# Low-E double-glazing is between triple insulating glass and double insulating glass in terms of energy efficiency.
- (c) Within a certain range, the higher the ventilation volume, the higher the heat load that can be saved. Under existing conditions, a ventilation volume of 140 m<sup>3</sup>/h can save 22% of energy compared to the case with no air circulation.
- (d) The thermal resistance of the inner wall material affects the efficiency of the Trombe wall. In regions with long warm winter periods, materials with lower thermal resistance are suitable, while climates with long cold winter periods are more recommended to use materials with higher thermal resistance. In the Kitakyushu region of Japan, it is more appropriate to use insulation materials with low thermal resistance such as GW16 and Styrofoam board for the inner wall when only the air conditioning is turned on at night. Because glass wool materials are relatively expensive and do not yield more significant benefits, the use of Styrofoam boards is more appropriate than other materials used in the simulation experiments.
- (e) The thickness of the inner wall, i.e., the proportion of the area occupied by the inner wall, also affects the efficiency of the Trombe wall. Simulations show that a Styrofoam board panel as inner wall of 120mm thickness can save most energy. However, since the energy savings are not high, it is recommended to use 60mm Styrofoam board panel for the inner wall thickness from the cost point of view.
- (f) The thickness of the massive wall, i.e., the proportion of the area occupied by the massive wall, also affects the efficiency of the massive wall. Simulations show that a concrete massive wall percentage of about 3% of room area is a better choice.

By integrating optimistic conditions, the annual thermal energy in winter is calculated to be 270.84 kWh, which can save nearly 52.3% of the thermal load compared to the pre-optimization period. It also greatly improves the overall room temperature without the effect of air conditioning. Therefore, the double-circulation Trombe wall assisted by temperature-controlled DC fans is suitable for buildings in hot-summer and cold-winter regions of Japan during the winter heating period.

The basic optimization idea of Trombe wall is to improve the efficiency of solar energy absorption and reduce the heat dissipation of the building. composite double-circulation Trombe wall, assisted by temperature-controlled DC fan, can steadily and quickly transfer the heat from the higher temperature air layer to the lower temperature room, and also avoid the occurrence of siphoning phenomenon. While the double wall setup is for the low thermal resistance of the classical Trombe wall, this setup theoretically hinders the efficiency of heat transfer into the room during the daytime, which is confirmed by the simulation results without air conditioning, but on the whole, this design is promising for research in combination with the air conditioning system to calculate the building heat load. However, researchers would prefer to achieve lower energy consumption or even zero energy consumption. That is why experiments for optimization are necessary.

This experiment is based on the conclusions drawn from the simulation of a virtual model based on the construction of a real reference house. The calculated values of the experiment are all calculated under ideal conditions. The parameters used in the calculation are based on the fact that they can be quickly put into real-life use, so the research will subsequently verify the actual operation of the ideal model based on the scheme proposed by the experimental results. Although the basic module used for the experiment differs somewhat from the actual building rooms used by humans, and applying the Trombe wall to different rooms will produce different values, it can still be calculated certain proportions and trends through the simulation. In future work, we can further investigate about ventilation methods, optimal materials for massive wall, etc. and introduce south-facing transmissible windows to calculate the optimal ratio of windows to Trombe Wall, etc. according to the actual conditions. Re-validation is carried out using the actual building renovation under feasible conditions. Calculation of the total benefit of the whole life cycle from the economic and engineering point of view, discuss its thermal comfort, etc.

## Reference

- [1] ShenJ, Sp Lassue, Zalewski L, Huang D. Numerical study on thermal behavior of classical or composite Trombe solar walls. *Energy and Buildings* 2007;39:962–74.
- [2] Yu, K., Tan, Y., Zhang, T., Jin, X., Zhang, J., & Wang, X. (2019). Experimental and simulation study on the thermal performance of a novel flue composite wall. *Building and Environment*, 151,

126-139.

[3] Electricity prize of Kiatakyushu. <https://denryoku-gas.jp/utility/kyuden/kwh-price>.

[4] <http://kakaku.com/item/K0000913041>

[5] Insulationpanelprize. [http://item.rakuten.co.jp/inaba/10001872/?sid=pc\\_shop\\_recommend&rtg=a5e47df057dac38856da875228662bca](http://item.rakuten.co.jp/inaba/10001872/?sid=pc_shop_recommend&rtg=a5e47df057dac38856da875228662bca)

[6] Zhongting Hu; Wei He; Jie Ji; Shengyao Zhang, A review on the application of Trombe wall system in buildings, Renewable and Sustainable Energy Reviews, Volume 70, April 2017, Pages 976-987

## *Chapter 5*

# ***STUDY ON THE INFLUENCE OF GLAZING SURFACE RATIO ON THE THERMAL PERFORMANCE OF COMPOSITE TROMBE WALL***



**CHAPTER FIVE: STUDY ON THE INFLUENCE OF GLAZING SURFACE RATIO ON THE THERMAL PERFORMANCE OF COMPOSITE TROMBE WALL**

*STUDY ON THE INFLUENCE OF GLAZING SURFACE RATIO ON THE THERMAL PERFORMANCE OF COMPOSITE TROMBE WALL* ..... 5-1

5.1 Overview ..... 5-1

5.2. Influence of glazing surface to massive wall ratio on the thermal performance..... 5-3

    5.2.1. PMV-PPD description of the optimized composite double-circulation Trombe wall system ..... 5-3

    5.2.2. Influence of glazing surface to massive wall ratio on the thermal performance..... 5-8

5.3. Influence of glazing surface to interior area ratio on the thermal performance ..... 5-15

5.4. Conclusion and discussion ..... 5-25

References..... 5-26



## 5.1 Overview

The building envelope plays an important role in maintaining thermal comfort and reducing energy demand. Trombe wall system is an efficient component system for the south (northern hemisphere) façade of a building that can passively utilize solar energy. However, low thermal efficiency and high heat losses are two major drawbacks of these systems [1, 2]. This led researchers to investigate optimizing the components of the Trump wall, integrating other technologies to improve thermal performance, and This led researchers to investigate optimizing the components of the Trump wall, integrating other technologies to improve thermal performance, and suggesting new configurations to be designed to improve heating performance. [3]. The highest loss rates are on the glass surfaces [4] and they have an important role in the solar gain of the Trumbull wall. However, the study of translucent glass surfaces is limited compared to other studies on the parameters and components of Trombe walls.

In the previous chapter, simulation experiments have done a preliminary study of the effect of different types of glass on the thermal efficiency of composite double-circulation Trombe in winter. It was found that the use of a double (multi-layer) glazing system has a significant improvement in performance. The low-e double-circulation glass has better results, but it is related to the location of the low-e film, which is set at position 3# to achieve better results in winter. Moreover, the type of glass has the greatest influence on the Trombe wall compared to other influencing parameters. However, the simulation results on temperature show that the optimized Trombe wall system shows a high risk of overheating.

Indoor thermal comfort is an aspect that cannot be ignored when assessing the performance of a Trombe wall, since the main task of this wall is to maintain a suitable indoor temperature for people. Both winter heating and summer overheating are important issues for the indoor thermal comfort of a Trombe wall.

The American Society of Heating, Refrigeration and Air-Conditioning Engineers (ASHRAE) Standard 55 and the International Organization for Standardization (ISO) Standard 7730 specify air temperature ranges that are satisfactory for most people. These standards are based on the human thermal comfort model, the PMV thermal comfort model, obtained by Professor Fanger and his colleagues in Denmark on the basis of experimental research. This model combines six factors affecting human thermal comfort in human and environmental variables, and the PMV index is the most comprehensive index for evaluating thermal environment so far.

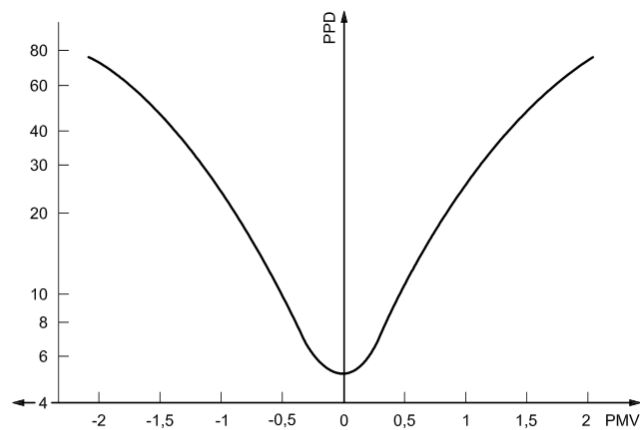
The main index to evaluate the indoor thermal comfort is Predicted Mean Vote (PMV), The PMV is an index that predicts the mean value of the votes of a large group of persons on the 7-point thermal sensation scale (see Table 5.1), based on the heat balance of the human body[5]. Thermal

balance is obtained when the internal heat production in the body is equal to the loss of heat to the environment. In a moderate environment, the human thermoregulatory system will automatically attempt to modify skin temperature and sweat secretion to maintain heat balance [6]. The theory is that when the human body is in a steady-state thermal environment, the greater the thermal load on the human body, the farther the human body deviates from the state of thermal comfort. [7].

The PPD is an index that establishes a quantitative prediction of the percentage of thermally dissatisfied people who feel too cool or too warm. For the purposes of this International Standard, thermally dissatisfied people are those who will vote hot, warm, cool or cold on the 7-point thermal sensation scale given in Figure 5.1.1 and Table 5.2[8]. The recommended value of ISO 7730 for indoor thermal comfort is 10% PPD and PMV between -0.5 and 0.5 [5].

**Table 5.1 Seven-point thermal sensation scale**

Thermal sensation	Cold	Cool	Slightly cool	Neutral	Slightly warm	Warm	Hot
PMV	-3	-2	-1	0	+1	+2	+3



**Key**  
PMV predicted mean vote  
PPD predicted percentage dissatisfied, %

**Figure 5.1.1 PPD as function of PMV [8]**

**Table 5.2 Comparison of PPD and PMV**

PMV	-2	-1	-0.5	0	+0.5	+1	+2
PPD	75%	25%	10%	5%	10%	25%	75%

In a study [9], the authors investigated the thermal comfort and energy performance of Trump wall systems in residential buildings under Mediterranean climate conditions. The heating and cooling requirements were investigated and the insulation level of the system was optimized. The system was optimized. In this regard, the simulated model was validated with experimental data. The validation was carried out with experimental data. Double glazing and single glazing Double glazing and single glazing were evaluated in this study and the results showed the ideal performance of the system in cold periods. [10] A passive solar heating and cooling system is proposed and the study is carried out through a series of numerical simulations in Ansys Fluent 16.0 environment, obtaining a temperature rise of 1.11°C and a temperature drop of 2.27°C in the morning and afternoon. Two options for optimizing the passive heating system were also considered. The first solution involves the use of triple glazing filled with argon gas to reduce the heat loss to the environment. The second solution involved changing the wall material from concrete to brick, which resulted in a temperature increase of 0.40°C next to the storage layer [10].

This section explores whether the area of the glazing surface in an optimized composite double-circulation Trombe can be influenced on energy efficiency and indoor thermal comfort. The thermal comfort is related to the room air temperature, flow rate, relative humidity, average radiant temperature, human metabolism and clothing thermal resistance, which can be estimated in a basic way using the software THERB for HAM. The optimal ratio of glazing surface to interior area is also explored. In the hope of obtaining higher efficiency and more rational usage patterns for Trombe walls.

## **5.2. Influence of glazing surface to massive wall ratio on the thermal performance**

### **5.2.1. PMV-PPD description of the optimized composite double-circulation Trombe wall system**

The composite double-circulation Trombe wall system, which was optimized in the previous section, was first analyzed as a simplified digital spatial model based on a locally built reference house with a wooden structure in Kitakyushu (33.88, 130.70). The overall width of this modeling is 2.70m and the depth is 2.785m. The height of the test space was 3.30m, with 0.31m of overhead below. Its entire south façade consists of a composite Trombe wall system, as illustrated in the figure 5.2.1. The specific structure of Trombe wall is shown in Figure 5.2.2. The structure of the optimization model is shown in Table 5.2 below

Forced ventilation by DC between the air layer and indoor space in the double-circulation Trombe wall: 140m<sup>3</sup>/h both inner circulation and outer circulation, the ventilation temperature is controlled to 19°C, that is, the temperature of the sensing part is higher than 19°C, the DC fan operates, the hot air is sent into the room, and the lower air hole is opened by default to send cold air into the air layer to realize air circulation, and the lower air hole is opened by default to send

cold air into the air layer to realize air circulation. For the time being, do not consider the situation of increased ventilation due to excessive indoor temperature or humidity. The air circulation only needs to meet the necessary amount of ventilation 0.5 times/hour.

The comparison of air conditioning heat load in this section will be compared using residential mode of 20°C: simulates the time of people at home, assuming that they go out to work or entertain at 9:00 every day, back home at 18:00, and the air-conditioning operation time is from 18:00 to 9:00 am.

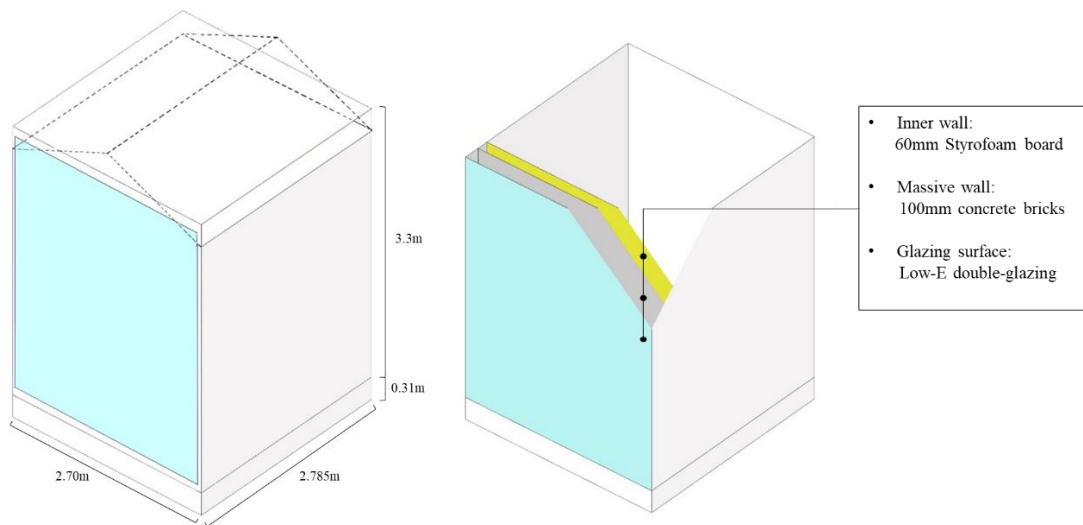


**Figure 5.2.1 Simplification Model of composite double-circulation Trombe wall**

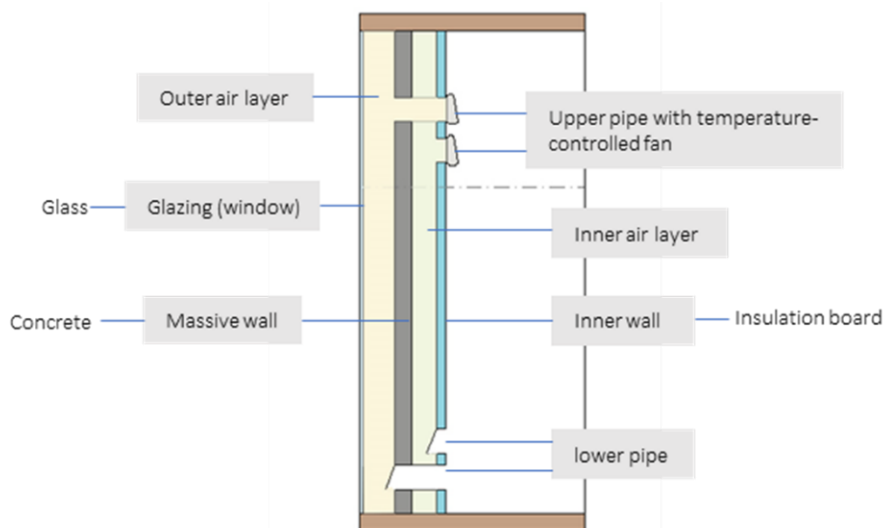


**Figure 5.2.2 Construction of composite double-circulation Trombe wall**

**Table 5.2 Material and structure of each part of the experimental house**

Part	Structure
Exterior wall	Styrofoam board 30mm, Japanese fir 105mm, Galvalume steel plate
Massive wall	Concrete brick 100mm
Inner wall	Styrofoam board 60mm
Floor	Styrofoam board 30mm, Japanese fir 105mm
Roof	Styrofoam board 30mm, Japanese fir 105mm, Gallium steel plate
Ground	Soil
Glazing surface	LOW-E double-circulation Glazing

First, the indoor temperature variation in this composite double-circulation Trombe wall system with and without air conditioning is compared under the optimized conditions. Figure 5.2.3 shows the indoor temperature variation for the whole heating season (November to March), while Figure 5.2.4 and 5.2.5 show the warmest month, November, and the coldest month, January, respectively. It was found that under these conditions, the daytime temperatures were too high, although the interior walls used for insulation were controlled to some extent. Without air conditioning, the maximum indoor temperature reached 49.5°C, exceeded 25°C 31.9% of the time, and exceeded 30°C 16.6% of the time. Especially in the middle and early part of November, even without turning on the air conditioner its indoor temperature was always above 20°C, but it exceeded 30°C or even 40°C a large number of times. Even in January, there are cases of overheating on consecutive sunny days.

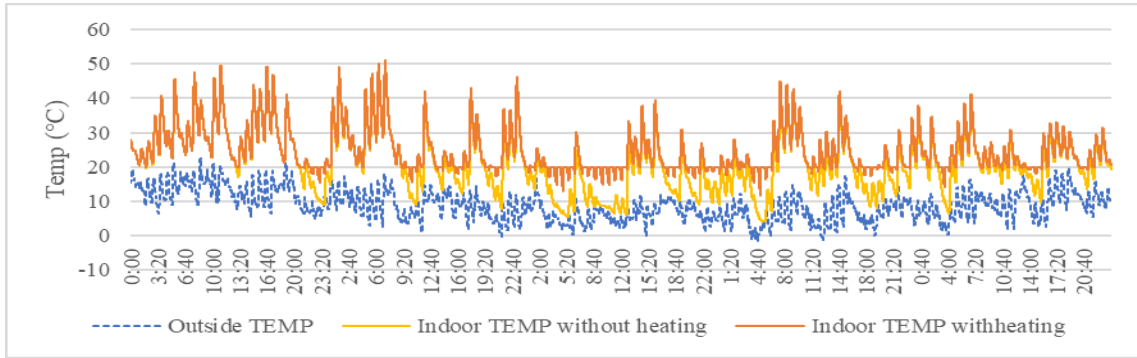


**Figure 5.2.3 Indoor temperature of optimized composite Trombe wall overall heating season**

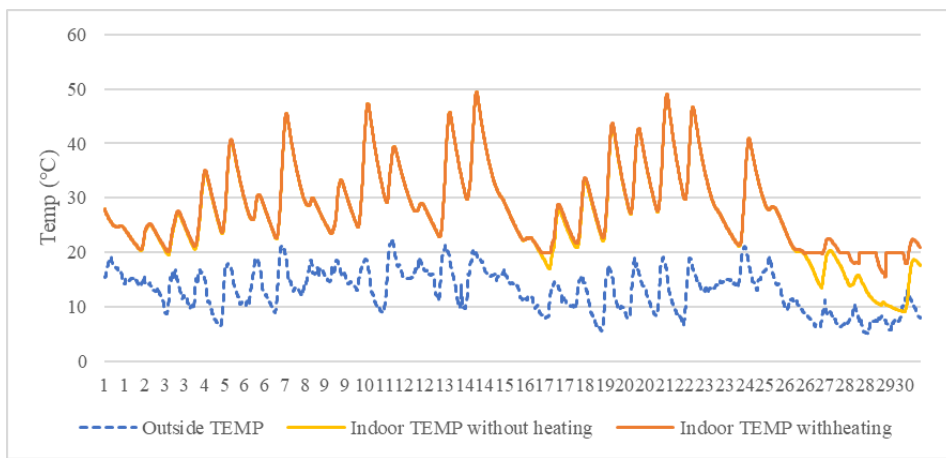


**Figure 5.2.4 Indoor temperature of optimized composite Trombe wall in November**

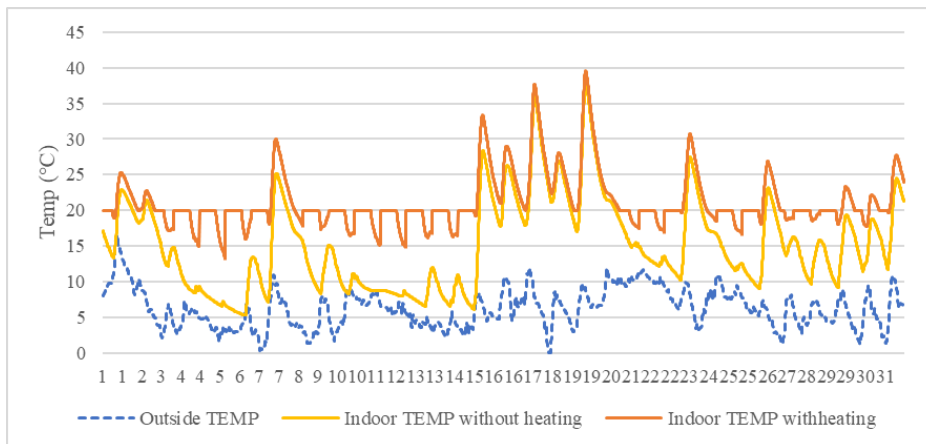


**Figure 5.2.5 Indoor temperature of optimized composite Trombe wall in January**

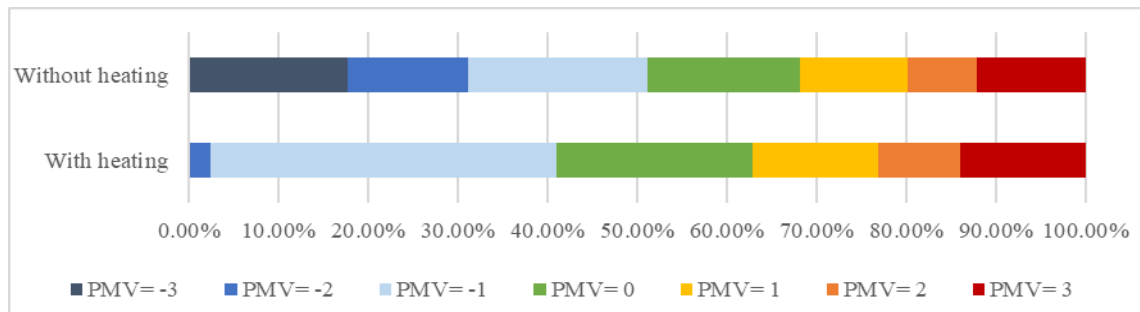
And the results of indoor PMV and PPD estimated by the software THERB for HAM are as follows. the results of PMV calculation are shown in Table 5.4 and Figure 5.2.6. the predicted evaluation of human thermal comfort in winter throughout the year without using air conditioning,

the percentage of time feeling too cold is 17.7%, the percentage of time feeling too hot is 12.1%, and the percentage of PMV values between -0.5 and 0.5 was about 17.4%. In the case of using air conditioning, the predicted human thermal comfort evaluation for the winter season throughout the year, there was no time when it felt too cold, the time when it felt too hot increased by 14.0%, while the percentage of PMV values between -0.5 and 0.5 was about 22.2%.

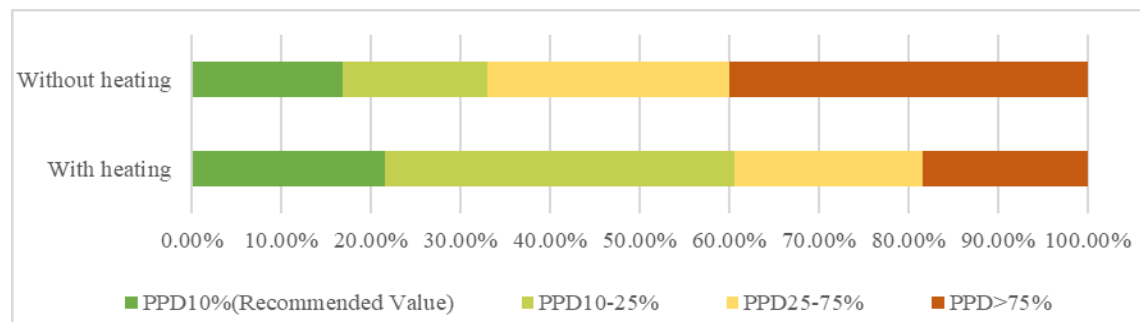
The percentage results of PDD are shown in Figure 5.2.7, and the recommended thermal comfort conditions only accounted for about 20% of the total heating season. Therefore, the purpose of research is to reduce the indoor temperature during the day and improve indoor thermal comfort on the basis of keeping energy consumption as low as possible.

**Table 5.3 PMV Statistics of composite double-circulation Trombe wall**

PMV	-3	-2	-1	0	+1	+2	+3
Without heating	17.7%	13.4%	20.0%	17.0%	11.9%	7.8%	12.1%
With heating	0	2.4%	38.6%	21.8%	14.1%	9.1%	14.0%



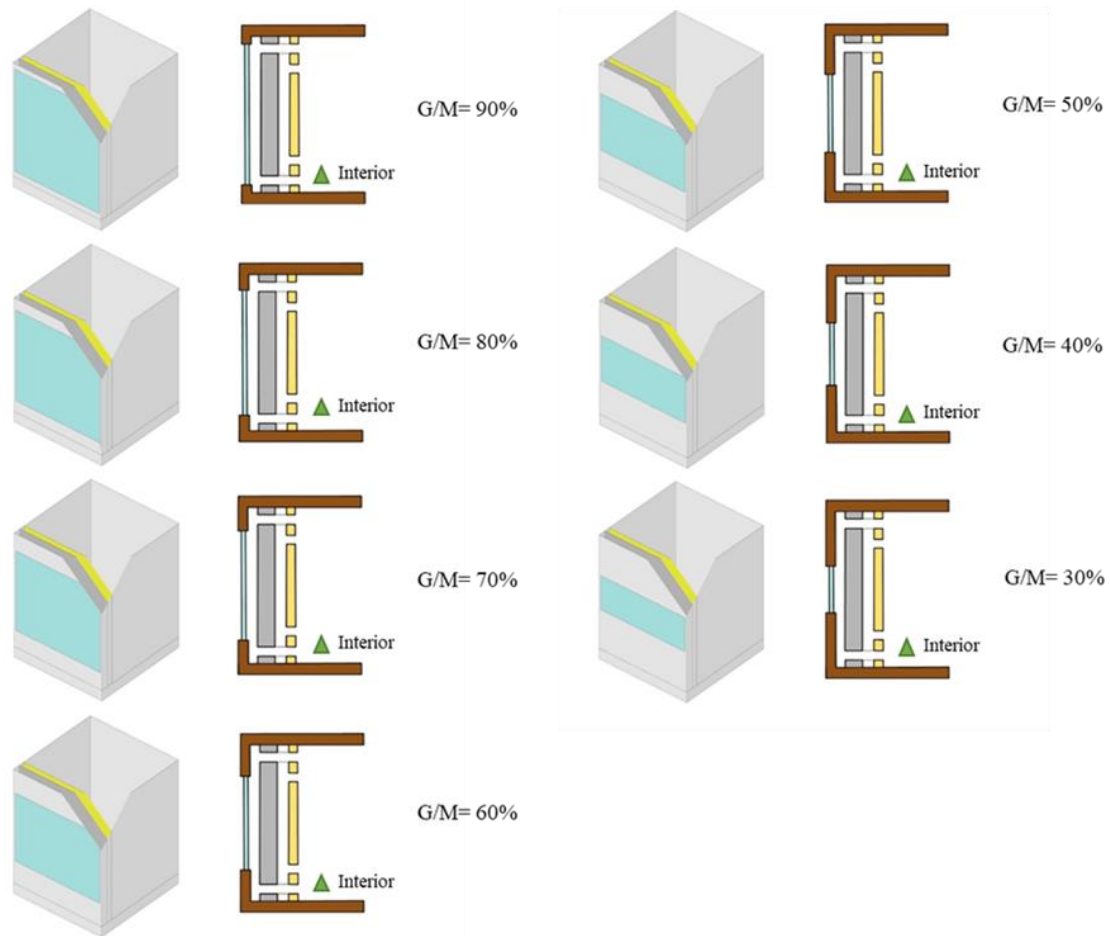
**Figure 5.2.6 PMV Statistics of composite double-circulation Trombe wall**



**Figure 5.2.7 PPD Statistics of composite double-circulation Trombe wall**

### 5.2.2. Influence of glazing surface to massive wall ratio on the thermal performance

The glazing surface in the Trombe wall system is both the main way for the massive wall to obtain solar energy during the day and the main way for heat loss at night. The study will keep the overall volume and footprint of the massive wall unchanged and change the area of the outermost glazing surface, i.e., change the ratio of the glazing surface to the massive wall (G/W). The ratio of the original model glazing surface to the massive wall is about 90%, i.e.,  $G/M=90\%$ . That is,  $G/M=90\%$ . In this stage, the effect of G/M from 30% to 90% on the indoor temperature, i.e., heat load, will be compared. Figure 5.2.8 shows the schematic diagram of the house for different conditions in this study.



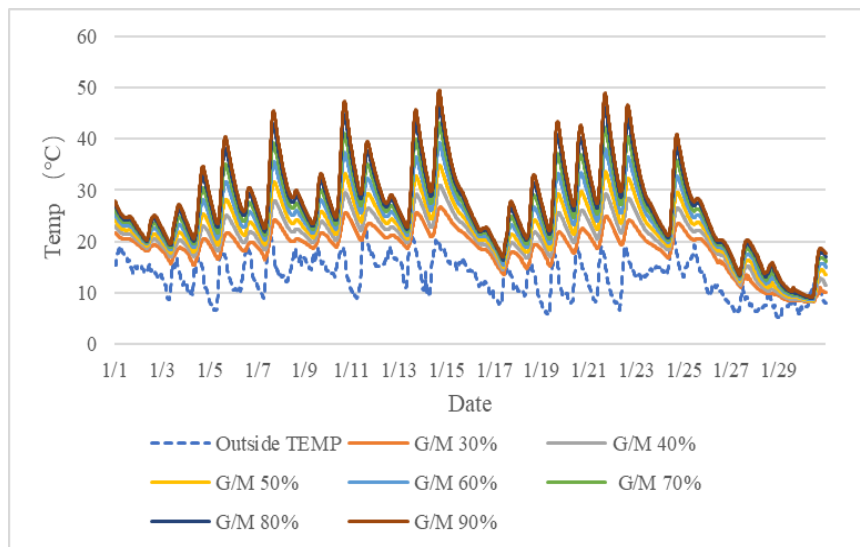
**Figure 5.2.8 Different glazing surface to massive wall ratio houses**

Figure 5.2.9 and Figure 5.2.9 shows the indoor temperature change curve of different glazing surface to the massive wall ratios without heating. Figure 5.2.9 shows the indoor temperature change curve of different glazing surface to the massive wall ratios in warmest month heating season (November) without heating. Figure5.2.10 shows the indoor temperature change curve of different glazing surface to massive wall ratios in coldest month (January) without heating. Comparing the indoor temperature of the composite double-wall Trombe wall model with different glazing surface

to the massive wall ratios without air conditioning, we found that reducing the glazing surface to the massive wall ratio will reduce the overall indoor temperature, and the reduction in daytime will be greater. In the range of 30% to 90%, the indoor temperature of several different window areas at night is not much different. It shows that proper reduction of the glazing surface to the massive wall ratio can indeed control the indoor temperature during the day and improve human thermal comfort.

The comparison results show that reducing the ratio of glazing surface to massive wall does reduce the maximum indoor temperature, with the glazing surface to massive wall ratios ranging from 30% to 50%, and without air conditioning, the indoor temperature is basically higher than the outdoor temperature and hardly overheats throughout the year. However, since the Trombe wall system uses Low-E double glazing, the heat entering the room is greater than the heat consumed from the glass surface, so the increased heat due to the increased surface area of the glass is also greater than the heat lost.

From the predicted statistics of PMV, the room that remained comfortable for the longest time without thermal air conditioning heating was the room with G/M=80%, whose PMV value was between -1 and 1 for 53.8% of the total time, and there was no overheating or overcooling (i.e., PMV between -2 and 2) for 77.8% of the time. The smaller the G/M, the longer the overcooling time and the longer the time to turn on the air conditioner.



**Figure 5.2.9 Indoor temperature of different G/M in November**

CHAPTER5: STUDY ON THE INFLUENCE OF GLAZING SURFACE RATIO ON THE THERMAL PERFORMANCE OF COMPOSITE TROMBE WALL

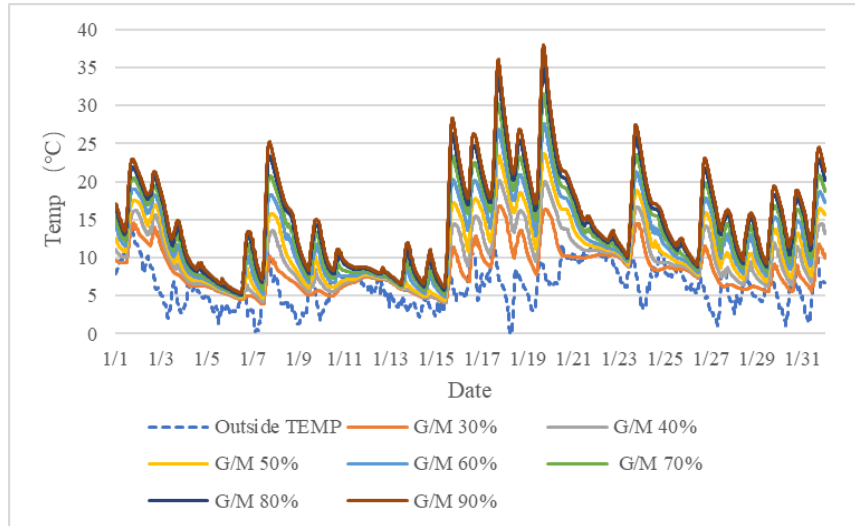


Figure 5.2.10 Indoor temperature of different G/M in January

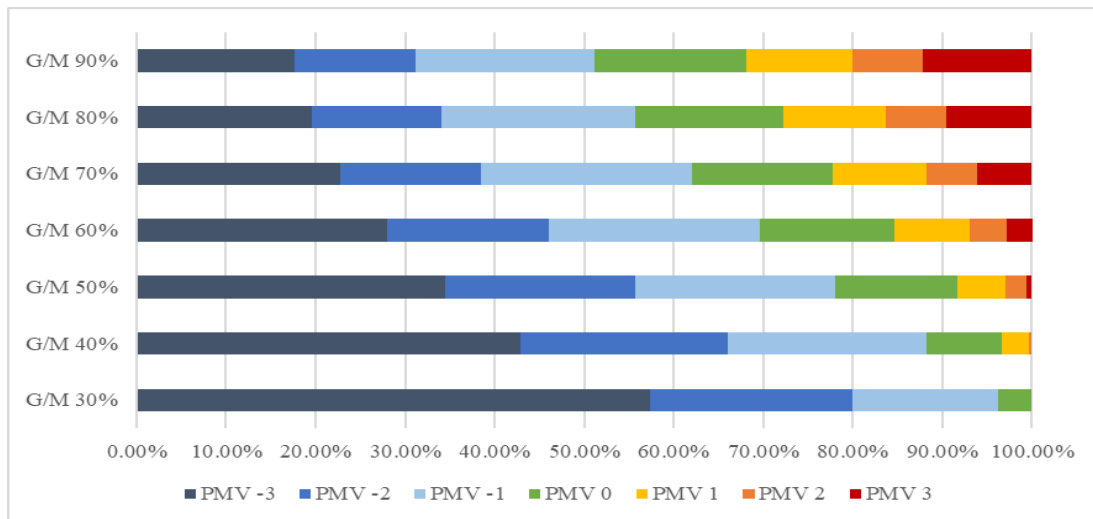


Figure 5.2.11 PMV Statistics of different G/M overall heating season

Table 5.4 Construction of composite double-circulation Trombe wall

PMV	-3	-2	-1	0	+1	+2	+3
G/M 30%	57.4%	22.5%	16.2%	3.7%	1.8%	0	0
G/M 40%	42.9%	23.2%	22.1%	8.5%	3.0%	0.3%	0
G/M 50%	34.5%	21.2%	22.4%	13.6%	5.4%	2.3%	0.6%
G/M 60%	28.0%	18.0%	23.6%	15.1%	8.3%	4.2%	2.9%

G/M 70%	22.8%	15.7%	23.5%	15.8%	10.5%	5.6%	6.1%
G/M 80%	19.6%	15.8%	23.1%	17.9%	12.8%	8.2%	10.9%
G/M 90%	17.7%	13.4%	20.0%	17.0%	11.9%	7.8%	12.1%

Figure 5.2.12 shows the indoor temperature change curve of different glazing surface to the massive wall ratios with heating all over heating season. Figure 5.2.13 shows the indoor temperature change curve of different glazing surface to the massive wall ratios in warmest month heating season (November) with heating. Figure 5.2.14 shows the indoor temperature change curve of different glazing surface to massive wall ratios in coldest month (January) with heating.

The comparison results show that with the air conditioning on in residential mode, i.e., only at night, the glazing surface to the massive wall ratios range from 30% to 90% to keep the room temperature above the outdoor temperature all year round and above 10 degrees C. The total time needed to turn on the air conditioning in November is very small, while in January the G/M The smaller rooms need to be air-conditioned while the larger G/M rooms do not. Figure 5.2.15 compares the indoor air conditioning heat load in residential mode for houses with different G/M in these two months. According to the calculations, in November, the heat load reduction for each 10% increase in glazing surface area in the range of G/M from 30% to 90% compared to the classical Trombe wall are: 46.4%, 58.1%, 65.9%, 71.5%, 74.9%, 77.6% and 79.2%, respectively. And for each 10% increase in glazing surface area starting from G/M=30%, the difference in heat load with the previous level of G/M of the house is: 21.8%, 18.7%, 16.2%, 12.2%, 10.8%, and 6.9%, respectively. In January, the heat load reduction for each 10% increase in glazing surface area in the range of G/M from 30% to 90% compared to the classical Trombe wall are: 34.6%, 41.9%, 48.0%, 53.6%, 58.2%, 62.0% and 64.5%, respectively. And for each 10% increase in glazing surface area starting from G/M=30%, the difference in heat load with the previous level of G/M of the house is: 11.2%, 10.5%, 10.8%, 9.9%, 9.2%, and 6.6%, respectively.

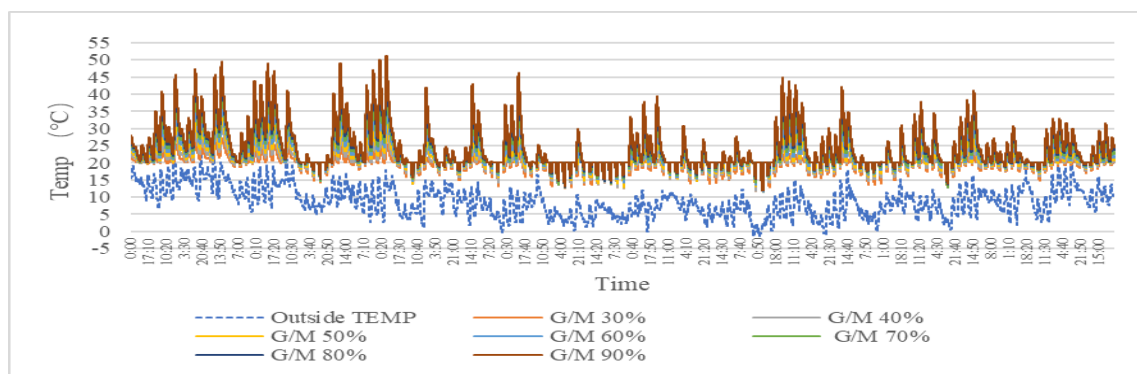


**Figure 5.2.12 Indoor temperature of different G/M overall heating season**

CHAPTER5: STUDY ON THE INFLUENCE OF GLAZING SURFACE RATIO ON THE THERMAL PERFORMANCE OF COMPOSITE TROMBE WALL

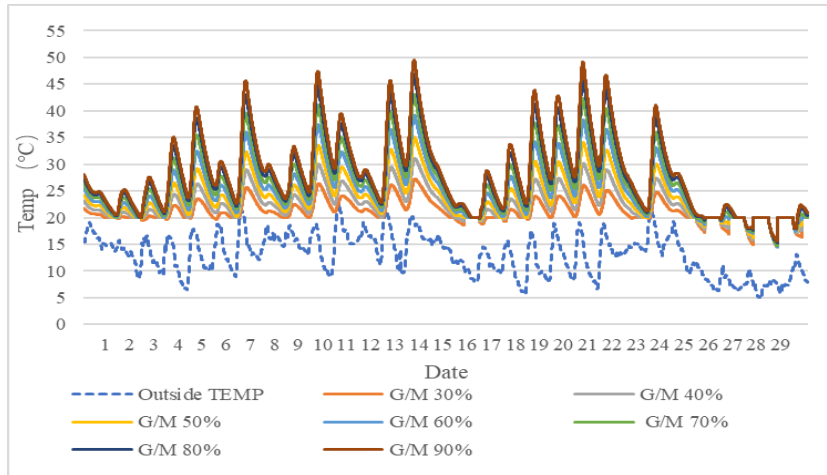


Figure 5.2.13 Indoor temperature of different G/M in November

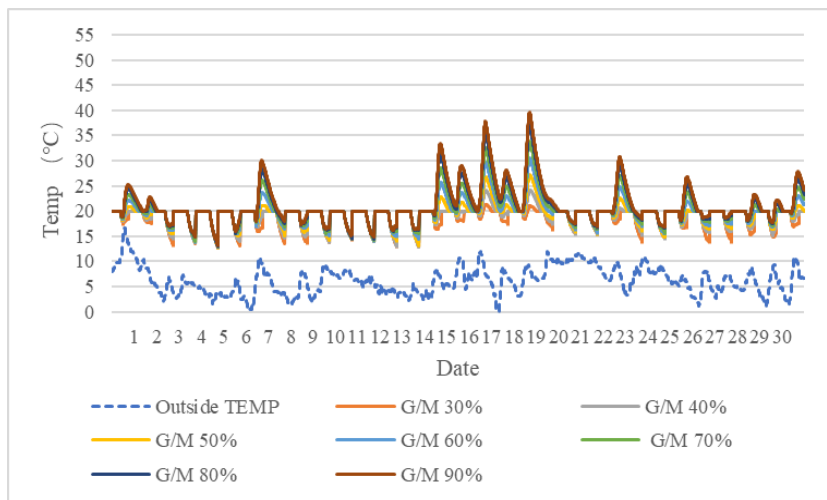


Figure 5.2.14 Indoor temperature of different G/M in January

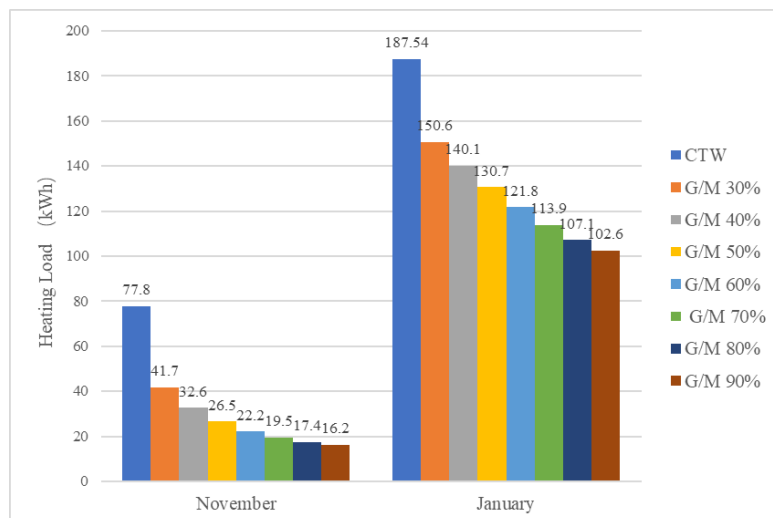


Figure 5.2.15 Construction of composite double-circulation Trombe wall

Analyzed from the perspective of indoor human comfort, the statistics of annual PMV calculations for rooms with different G/M are shown in Table 5.5 and Figure 5.2.16. The overcooling of this Trombe wall system in winter almost disappears when the air conditioner is turned on at night. And the overheating is almost eliminated (less than 1%) in the case of G/M values less than 50%. According to further statistics in Table 5.6, the highest percentage of time with PMV values between -2 and +2 (neither overheating nor overcooling) is G/M=40%, followed by 30% and 50%. the highest percentage of time with PMV values between -1 and +1 is G/M=40%, followed by 30% and 50%. more than 60% of the glazing surface to massive wall ratio there is a relatively large gap between the comfort temperature percentage and below 60%.

And from the analysis of the predicted results of PPD, the highest percentage of G/M ratio in the recommended thermal comfort environment is 60% and 70%, and the highest percentage of G/M ratio in the dissatisfaction below 25% is 40% and 50%. The lowest percentage of dissatisfaction with the spatial thermal environment, i.e., PPD greater than 75%, is G/M = 40%, followed by 50%.

**Table 5.5 PMV Statistics of different G/M overall heating season with heating**

<b>PMV</b>	<b>-3</b>	<b>-2</b>	<b>-1</b>	<b>0</b>	<b>+1</b>	<b>+2</b>	<b>+3</b>
<b>G/M 30%</b>	0.4%	8.6%	79.5%	10.7%	0.9%	0	0
<b>G/M 40%</b>	0.3%	5.9%	70.1%	17.4%	5.4%	0.9%	0
<b>G/M 50%</b>	0.2%	4.8%	61.0%	21.1%	8.6%	3.4%	0.9%
<b>G/M 60%</b>	0.2%	3.8%	52.4%	22.9%	11.4%	5.6%	3.7%
<b>G/M 70%</b>	0.1%	2.8%	46.8%	22.6%	13.2%	6.9%	7.6%
<b>G/M 80%</b>	0.1%	2.5%	41.5%	22.2%	14.4%	8.2%	11.1%
<b>G/M 90%</b>	0	2.4%	38.6%	21.8%	14.1%	9.1%	14.0%

**Table 5.6 PMV Statistics of different G/M overall heating season with heating**

PMV	G/M 30%	G/M 40%	G/M 50%	G/M 60%	G/M 70%	G/M 80%	G/M 90%
-2 ~ +2	99.6%	99.7%	98.9%	96.1%	92.3%	88.8%	86%
-1 ~ +1	91.1%	92.9%	90.7%	86.7%	82.6%	78.1%	74.5%

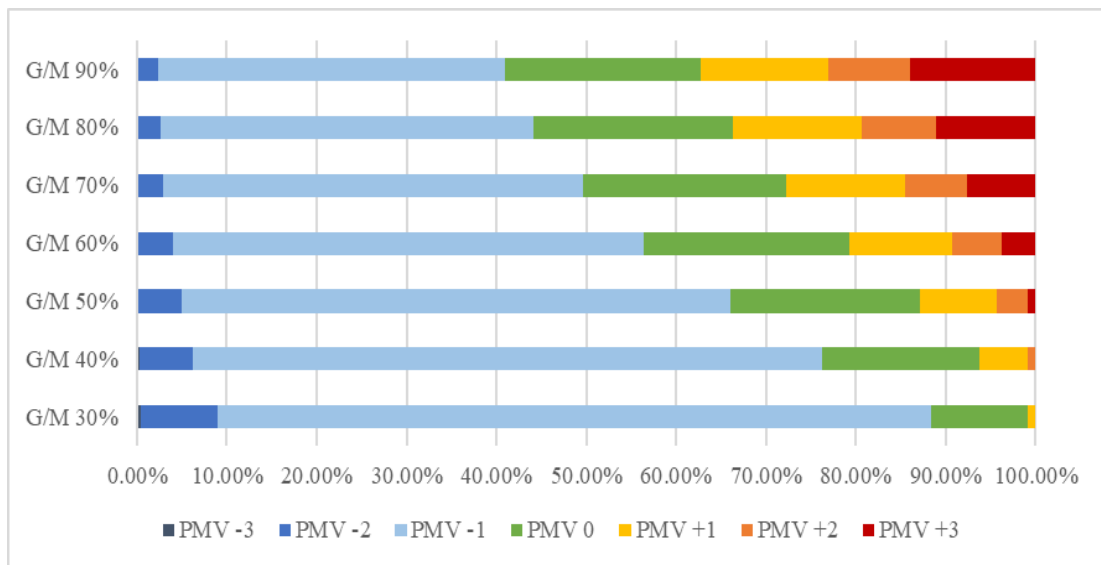


**Figure 5.2.16 PMV Statistics of different G/M overall heating season with heating**

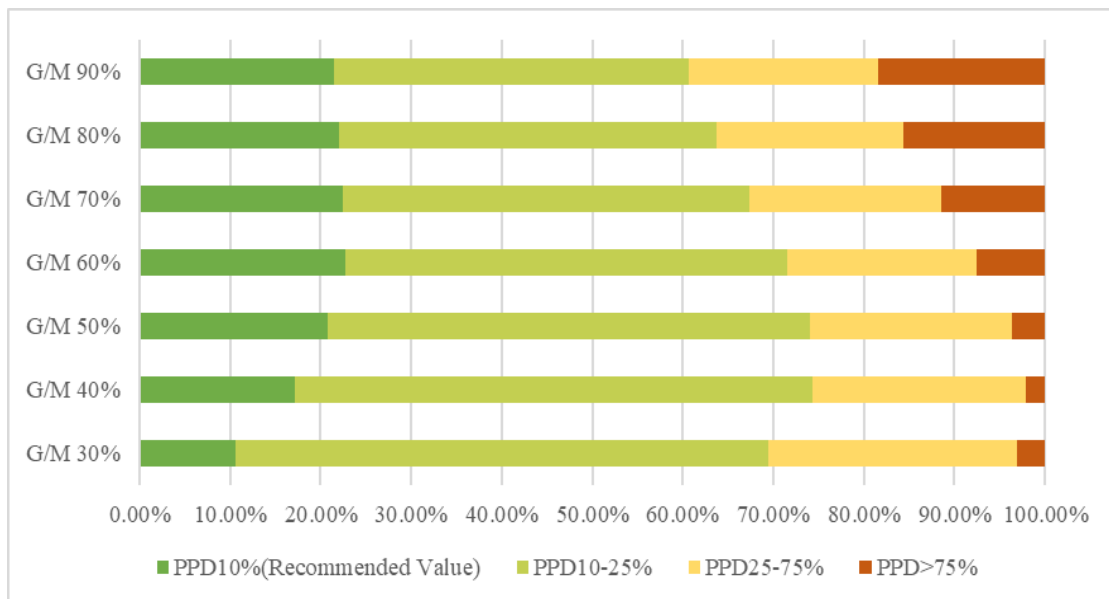


**Figure 5.2.17 PPD Statistics of different G/M overall heating season with heating**

In summary, reducing the area of the glass surface of the optimized composite double-circulation Trombe wall system is indeed effective in controlling the indoor overheating phenomenon. In the case where the space is used as a home during the daytime and it is necessary to prevent the indoor overheating during the daytime, it can be considered to reduce the glazing surface to massive wall ratios, and the most recommended one for thermal comfort is 40%-50% of the glazing surface to massive wall ratios in the experimented modular model. However, the reduction of glazing surface to massive wall ratios is accompanied by a certain amount of increase in sensible heat load, and the reduction in heat loss at night does not offset the reduction in heat absorption during the day. For energy saving reasons alone, a large glazing surface to massive wall ratios setting is recommended. When considering the total energy cost of the house, the difference in average annual cost (winter) between 50% glazing surface to massive wall ratios and 90% glazing surface to massive wall ratios is not significant.

### **5.3. Influence of glazing surface to interior area ratio on the thermal performance**

In the previous part of the experiment, it was concluded that within the composite double-circulation Trombe wall system, if the area of the outer glazing surface is reduced only, the reduction in heat loss at night does not offset the reduction in heat energy radiated by the sun during the day. Therefore, the smaller the percentage of glazing surface, the smaller the overall temperature of the room and the greater the energy consumption for a certain indoor area (volume). Therefore, the composite double-circulation Trombe wall system can be the most efficient in the case of the maximum share of glazing surface during the daytime when there are no special requirements for indoor thermal comfort environment. However, in the previous study, the total indoor area of the subject is about 7.52 m<sup>2</sup>, which is a small unit space with a total volume, and the ratio of glazing surface to floor area (G/F) is close to 1.0. In general, the ratio of glazing surface to indoor area (floor area) of a room used as a residence in a house, in addition to the room area, is less than 1.0 because of the existence of other external walls, windows (different from the glazing surface of the Trombe wall system), and other structures. The ratio of the glazing surface of the Trombe wall system to the interior area (floor area) is generally less than 1.0 because of the presence of other structures such as exterior walls and windows (glazing surface as opposed to the Trombe wall system).

Therefore, in this section, the dimensions of the Trombe wall system in the digital model are maintained, i.e., the dimensions of the glazing surface are kept constant, and the floor area (i.e., interior area) is increased by increasing the length of the simulated house. The indoor thermal comfort is investigated for glazing surface to floor area ratios ranging from 1.0 to 0.3. The specific length and width of the digital model are shown in Table 5.7.

**Table 5.7 Size of different glazing surface to floor area ratios**

<b>G/F</b>	<b>Width (m)</b>	<b>Length (m)</b>	<b>Floor area (m<sup>2</sup>)</b>
1.0	2.70	2.785	7.520
0.9	2.70	3.200	8.640
0.8	2.70	3.600	9.720
0.7	2.70	4.120	11.124
0.6	2.70	4.800	12.960
0.5	2.70	5.760	15.552
0.4	2.70	7.200	19.440
0.3	2.70	9.600	25.920

The indoor temperature without air conditioning was first compared. Figure 5.3.1 represents the indoor temperature variation curve in November, the warmest month of winter. As with the predicted results, the smaller the ratio of glazing surface to floor area ratios (G/F), the smaller the peak indoor temperature available, and a G/F below 0.7 can keep the indoor temperature below 30°C throughout the month, and a G/F below 0.4 can keep the indoor temperature below 30°C throughout the month. Figure 5.3.2 shows the indoor temperature variation curve in January, the month with the lowest annual temperature. In January, despite the low outdoor temperature, the room still receives sufficient solar radiation during the daytime on sunny days, and the indoor temperature still exceeds 30°C when G/F is above 0.7. In addition, although the difference in maximum indoor temperatures of the composite double-circulation Trombe wall system with different G/F ratios was large during the day, the difference in indoor temperatures of different G/F ratios became smaller at night, especially when there were continuous cloudy days, such as from January 11 to January 13, the room temperatures of all G/F ratios continued to drop to almost the same minimum temperature. However, the indoor temperature of each room can basically be maintained at a level higher than the outdoor temperature.

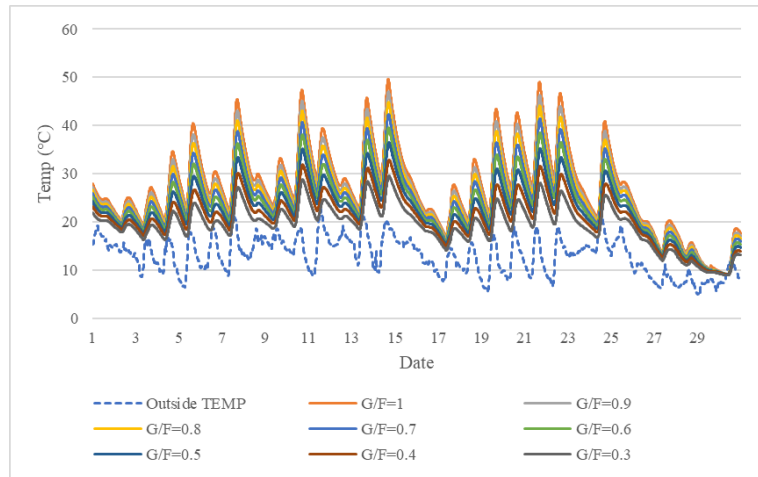


**Figure 5.3.1 Indoor temperature of different G/F in November**

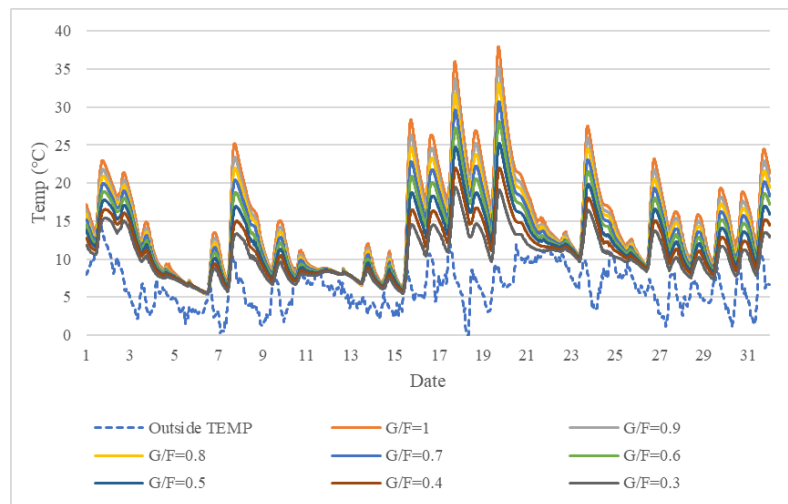


**Figure 5.3.2 Indoor temperature of different G/F in January**

While analyzing the indoor comfort situation from the calculated predicted values of PMV-PPD, Table 5.7, and Figure 5.3.3 show the predicted values of PMV for different houses, and the percentage of the total hours of different PMVs in the heating season. In the state without air conditioning on, the recommended comfort level, i.e.  $PMV=0$ , the highest proportion of hours in different G/F is when  $G/F=1.0$ , accounting for 17.0% of the total hours, and the lower the proportion of G/F, the longer the time when the room is too cold, and vice versa, the longer the time when it is too hot. Table 5.8 calculates the percentage of time in different rooms in more comfortable (PMV values between -1 and +1) and no abnormal state (PMV values between -2 and +2), the more comfortable indoor thermal environment state maintained the longest time is  $G/F = 0.9$ , accounting for 49.7%. The next highest to lowest G/F was 0.8, 1.0, 0.7, 0.6, 0.5, 0.4, and 0.3. The shortest percentage of time in the overheated or overcooled indoor condition was  $G/F=0.8$  and 0.7, and the percentage of time in the non-abnormal condition was 71.7%.

**Table 5.7 PMV Statistics of different G/F overall heating season without heating**

PMV	-3	-2	-1	0	+1	+2	+3
G/F=1.0	17.70%	13.40%	20.00%	17.00%	11.90%	7.80%	12.20%
G/F=0.9	19.30%	15.00%	22.00%	16.40%	11.30%	6.60%	9.40%
G/F=0.8	20.90%	16.50%	23.10%	15.80%	10.50%	5.80%	7.40%
G/F=0.7	23.10%	18.70%	23.30%	15.20%	9.60%	4.90%	5.20%
G/F=0.6	26.00%	21.30%	23.40%	14.60%	7.60%	4.10%	3.00%
G/F=0.5	30.10%	24.60%	22.50%	13.10%	5.90%	2.50%	1.30%
G/F=0.4	35.50%	28.40%	21.20%	9.90%	3.50%	1.40%	0.10%
G/F=0.3	44.70%	30.00%	18.30%	5.40%	1.60%	0	0

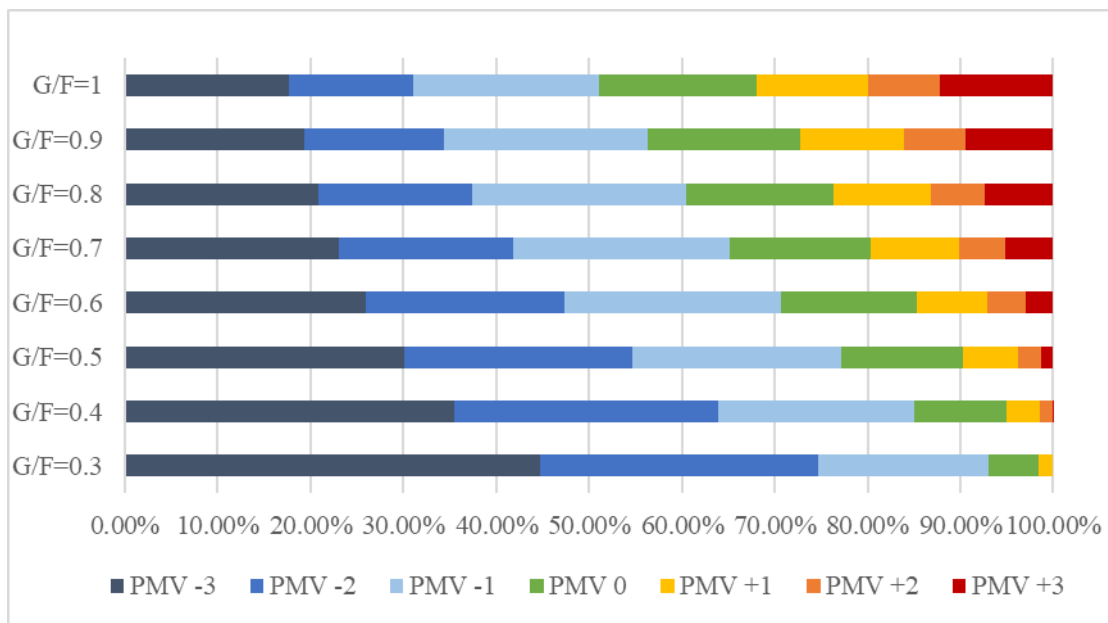


**Figure 5.3.3 PMV Statistics of different G/F overall heating season without heating**

**Table 5.8 PMV Statistics of different G/F overall heating season without heating**

PMV	G/F							
	1	0.9	0.8	0.7	0.6	0.5	0.4	0.3
-2 ~ +2	70.1%	71.3%	71.7%	71.7%	71.0%	68.6%	64.4%	55.3%
-1 ~ +1	48.9%	49.7%	49.4%	48.1%	45.6%	41.5%	34.6%	25.3%

Figure 5.3.4 shows the PPD evaluation values calculated from the simulations. Without air conditioning, the smaller the G/F ratio is, the greater the percentage of time that it is too cold leads to a higher dissatisfaction with thermal comfort. The overall evaluation is relatively good for conditions with G/F ratio greater than 0.7, but the percentage of time with poor thermal comfort (PPD greater than 75%) is still close to 40%.

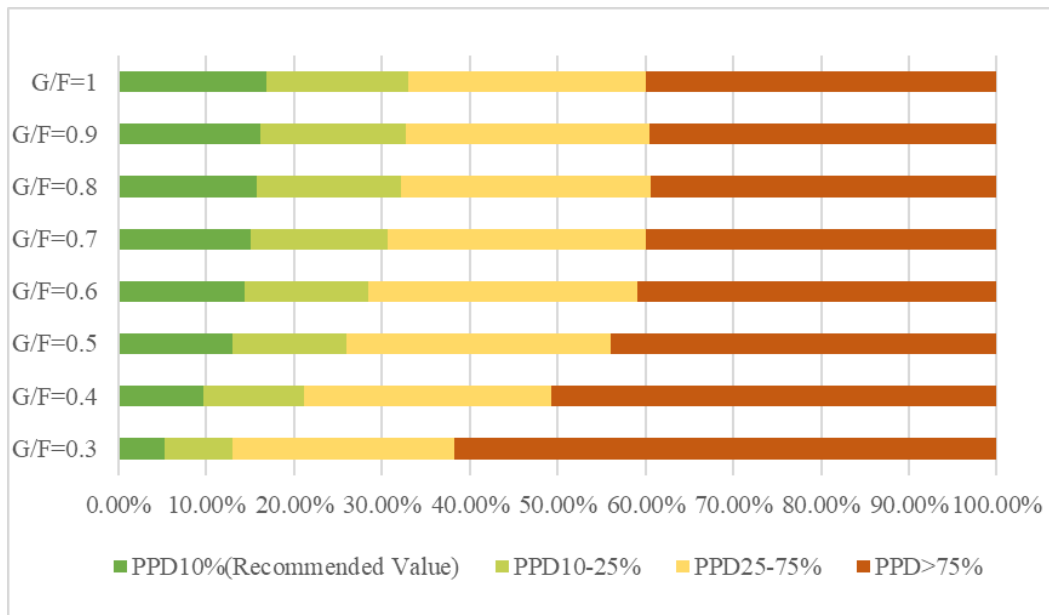


**Figure 5.3.4 PPD Statistics of different G/F overall heating season without heating**

The analysis of the room with the air conditioner turned on at night and the air conditioner set at 20°C. Figure 5.3.5 shows the indoor temperature variation in November, the month with the highest average daily temperature during the heating season. In November, the outdoor temperature is higher, the climate is dry and sunny with more days, and solar radiation is relatively abundant, so there are only a few days when the indoor temperature is below 20°C at night and requires air conditioning operation. Rooms with a high G/F ratio in that month are prone to indoor temperatures exceeding 30°C, especially when the G/F ratio is greater than 0.5. Figure 5.3.6 shows the indoor temperature variation curve for January, the month with the lowest average daily temperature

throughout the year.

In January, due to the presence of multiple consecutive rainy days, indoor temperatures below 20°C occurred during the daytime when the air conditioning was not turned on, but except for a few days (e.g., the afternoon of January 5 and January 6), room temperatures were maintained above 15°C for different G/F ratios, and indoor temperatures for different glazing surface to floor area ratios. The differences were not significant. Throughout January, the indoor air temperature was consistently higher than the outdoor level even when the air conditioner was not turned on all day. On consecutive sunny days, such as from January 15 to January 20, the indoor temperature in the composite double-circulation Trombe wall house with a G/F ratio greater than 0.6 exceeded 30°C. The peak temperature in the room with a G/F ratio greater than 0.8 exceeded 35°C.

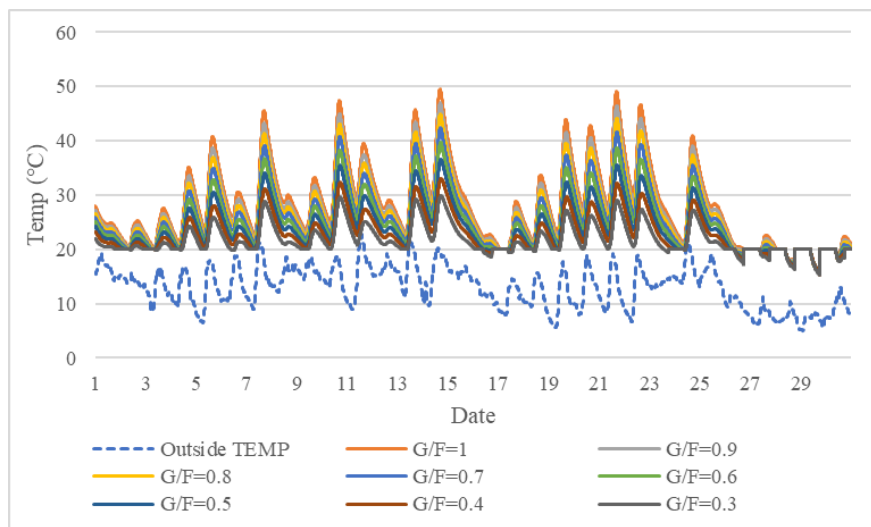


**Figure 5.3.5 Indoor temperature of different G/F in November with heating**

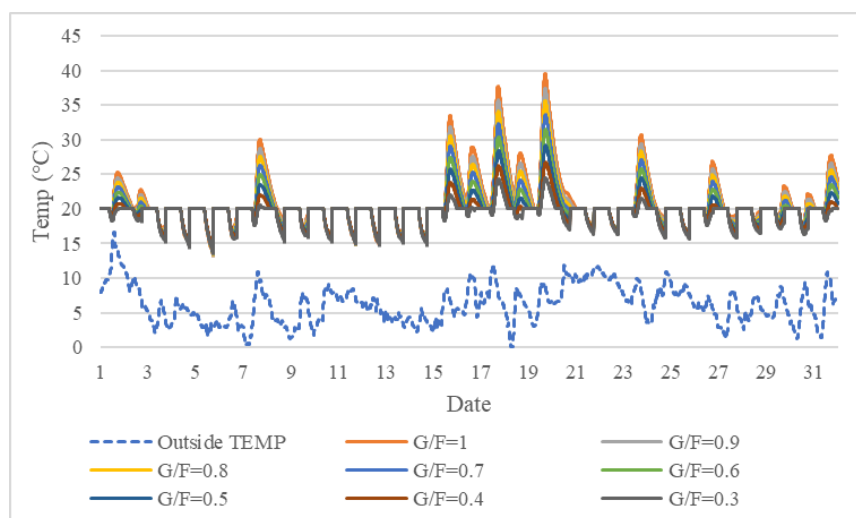


**Figure 5.3.6 Indoor temperature of different G/F in January with heating**

The analysis calculates the indoor air conditioning heat load for these two months because the

total value of its air conditioning load is bound to increase as the indoor area increases, so in addition to simulating the total value of the air conditioning load for each month, the air conditioning load per unit area, i.e., per square meter of floor area, is also calculated. Figure 5.3.7 shows the heat load statistics for November. From the total value, the ratio of G/F will increase for every 0.1 decrease in the proportion of heat load required to consume more. Combined with the temperature change curve, the smaller the ratio of G/F, the more the room will enter a state where the indoor temperature is less than 20°C first, and the longer the air conditioner will run. Therefore, the energy consumption of air conditioning per unit area will also increase with the decrease of glazing surface to floor area ratios, and the increase will become larger when G/F is greater than 0.5. The situation in January (Figure 5.3.8) is also similar to that in November.

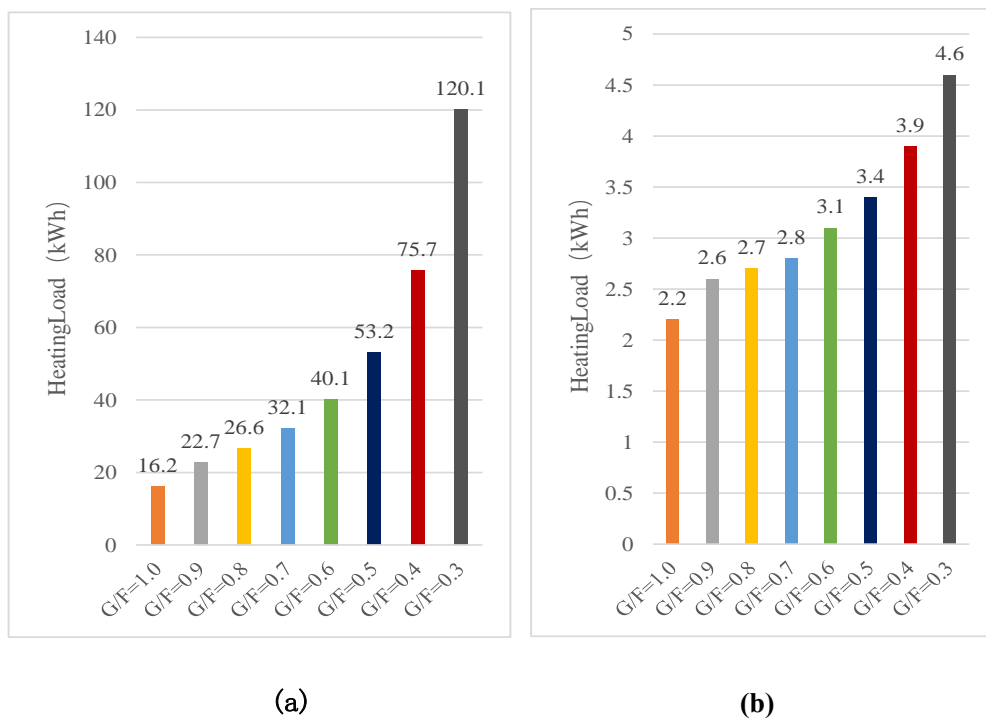


**Figure 5.3.7 Heating load of different G/F in November: (a) Total heating load; (b) Heating load per unit area**

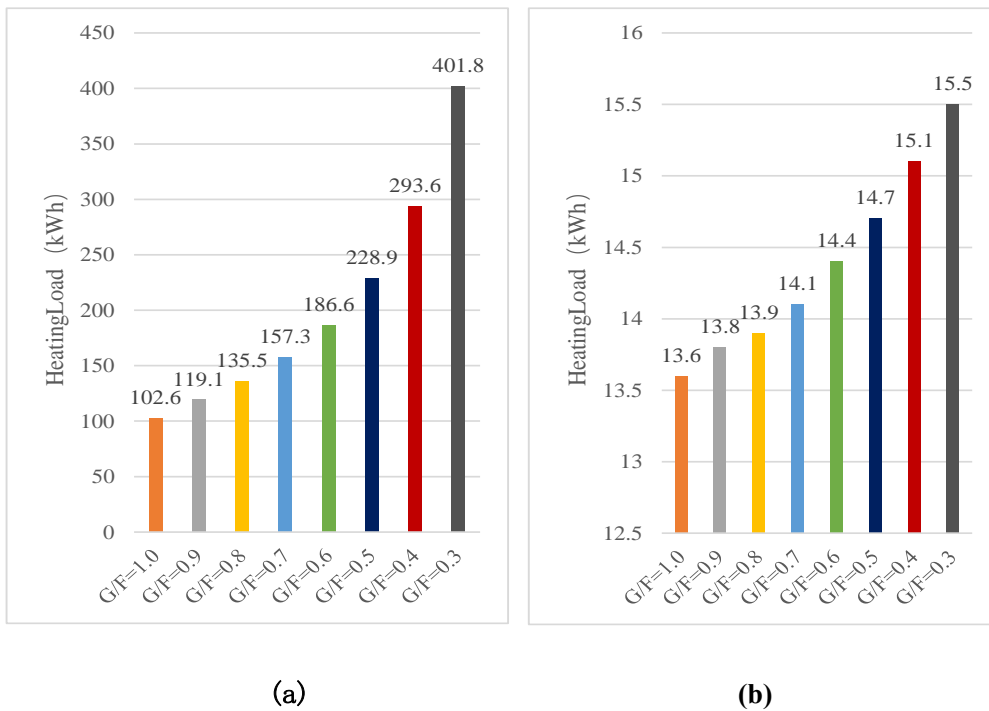


**Figure 5.3.8 Heating load of different G/F in January: (a)Total heating load; (b) Heating load per unit area**

While analyzing the indoor comfort from the calculated predicted values of PMV-PPD, Table 5.9, and Figure 5.3.3 show the predicted values of PMV for different houses, and the total percentage of hours in the heating season for different PMVs are counted. The overall room temperature is increased because the air conditioner is turned on inside the house at night, and during the daytime, despite the fact that on individual days, the room temperature will be below 20°C, but the overcooling is eliminated. At the recommended comfort level, i.e. PMV=0, the highest proportion of hours in different G/F was G/F=0.7, accounting for 23.0% of the total hours. Turning on the air conditioner can only eliminate the phenomenon of overcooling, but it will increase the proportion of overheating situation to some extent, and the higher the proportion of G/F, the longer the overheating time. When the G/F ratio is less than 0.4, the percentage of PMV= +3 is 0, i.e., no overheating occurs in the room.

Table 5.10 calculates the time share of different rooms in more comfortable (PMV value between -1 and +1) and no abnormal state (PMV value between -2 and +2), the longest time of maintaining the more comfortable indoor thermal environment state is G/F=0.3, accounting for 94.6%. the higher the ratio of G/F, the smaller its time share The shortest time share of indoor overheating state is G/F= 0.3 and 0.4, no non-abnormal state.

**Table 5.9 PMV Statistics of different G/F overall heating season with heating**

CHAPTER5: STUDY ON THE INFLUENCE OF GLAZING SURFACE RATIO ON  
THE THERMAL PERFORMANCE OF COMPOSITE TROMBE WALL

PMV	-3	-2	-1	0	+1	+2	+3
G/F=1	0	2.40%	38.60%	21.80%	14.10%	9.10%	14.00%
G/F=0.9	0	2.40%	42.10%	22.00%	14.30%	8.00%	11.20%
G/F=0.8	0	2.50%	45.40%	22.30%	13.50%	7.30%	9.00%
G/F=0.7	0	2.60%	49.10%	23.00%	12.20%	6.40%	6.70%
G/F=0.6	0	2.80%	53.70%	22.90%	11.10%	5.20%	4.30%
G/F=0.5	0	3.00%	59.10%	22.40%	9.30%	4.40%	1.80%
G/F=0.4	0	3.80%	67.00%	19.70%	7.00%	2.50%	0
G/F=0.3	0	5.10%	74.90%	15.30%	4.40%	0.30%	0

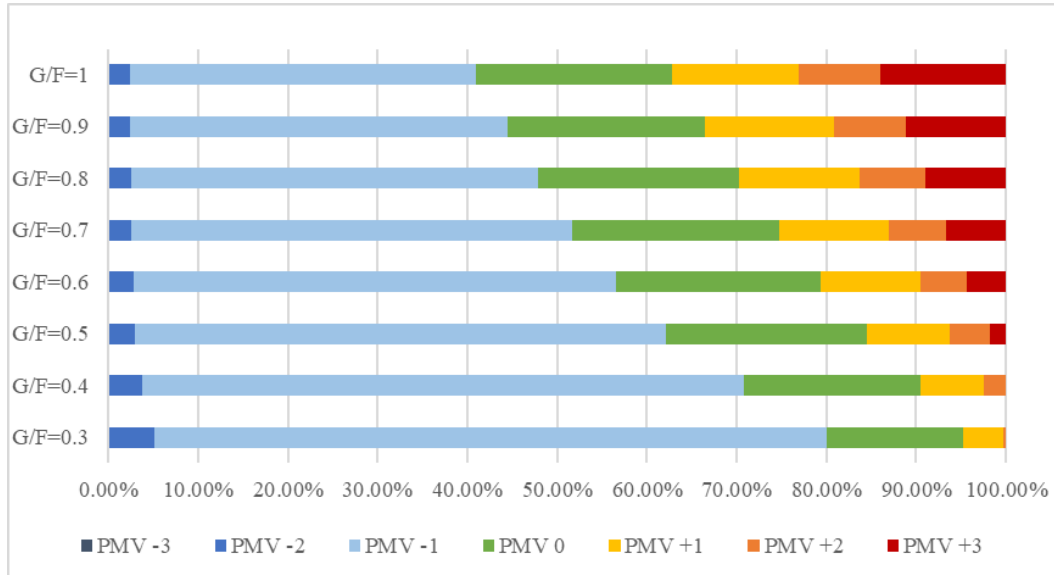


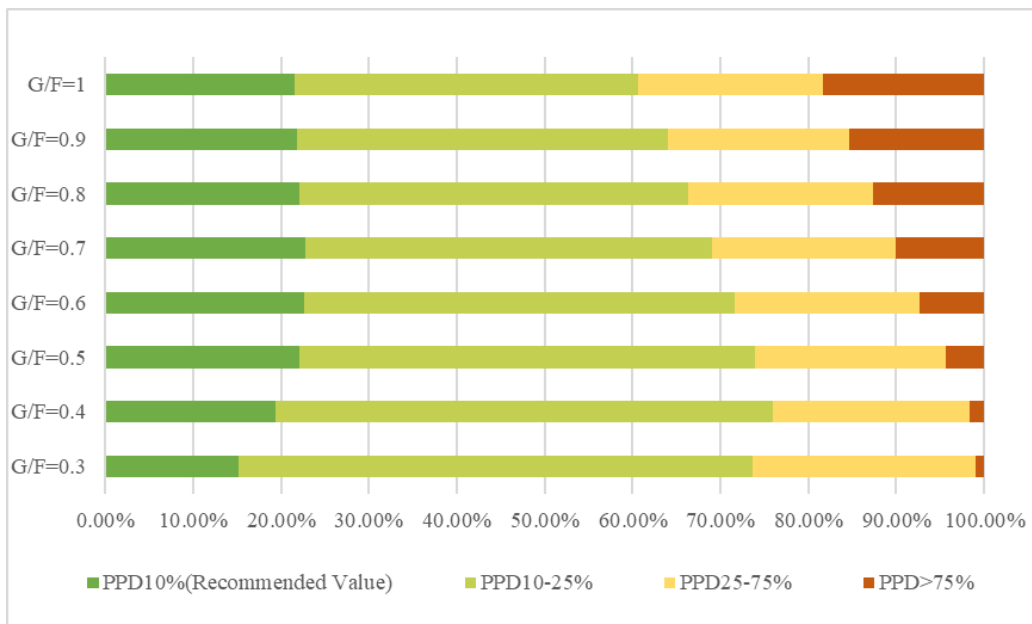
Figure 5.3.9 PPD Statistics of different G/M overall heating season with heating

**Table 5.10 PMV Statistics of different G/F overall heating season with heating**

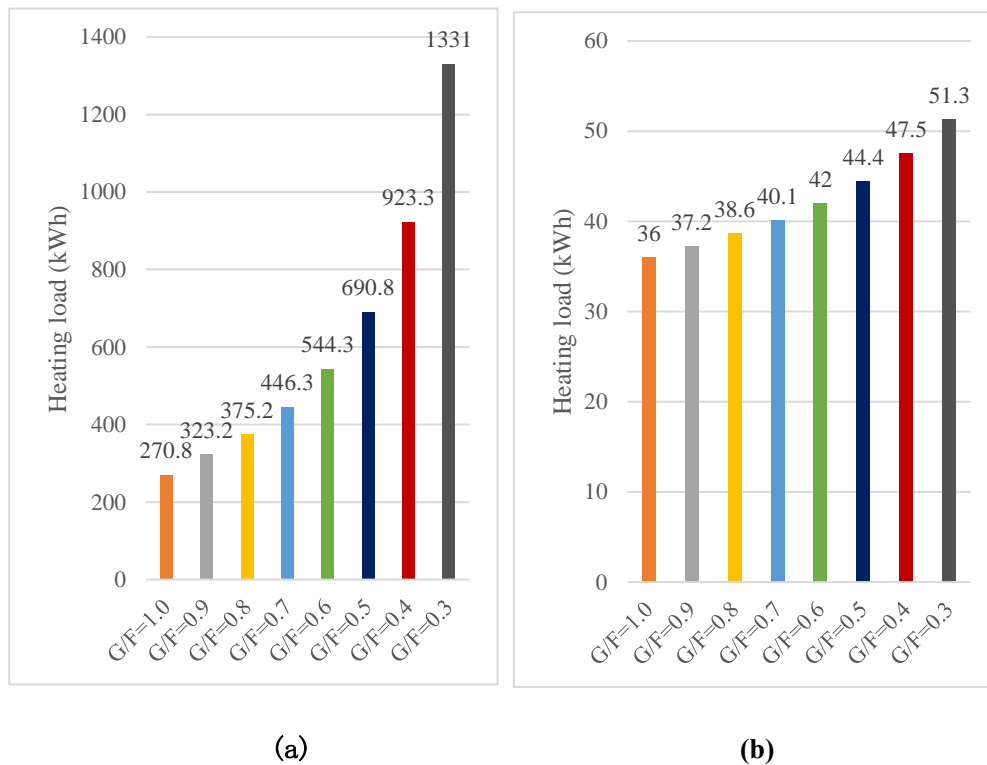
PMV	G/F							
	1	0.9	0.8	0.7	0.6	0.5	0.4	0.3
-2 ~ +2	86.0%	88.8%	91.0%	93.3%	95.7%	98.2%	100%	100%
-1 ~ +1	74.5%	78.4%	81.2%	84.3%	87.7%	90.8%	93.7%	94.6%

Figure 5.3.4 shows the PPD rating values calculated from the simulations. With the air conditioning on at night, the smaller the G/F ratio, the smaller the percentage of PPD greater than 75%. the longest percentage of time with PPD less than 75% glazing surface to floor area ratios are 0.3 and 0.4. the longest percentage of time with PPD less than 25% is G/F = 0.4. while the room is in a comfortable environment (i.e. PPD is less than 10%) is G/F=0.7.

In terms of the total value of heat load, for every 0.1 decrease in the ratio of heat load, the heat load to be consumed will increase. Therefore, the energy consumption of air conditioning per unit area also increases with the decrease of the ratio of glass area to floor area. However, since glazing surface to massive wall ratios are already the highest efficiency ratios, all composite double-circulation Trombe walls under current conditions have the highest efficiency status. Therefore, in combination with the analysis of indoor thermal comfort, a ratio of G/F value less than 0.4 is recommended in the case where the user has a requirement for indoor thermal comfort.



**Figure 5.3.10 PPD Statistics of different G/F overall heating season with heating**



**Figure 5.3.11 Heating load of different G/F in heating season: (a)Total heating load; (b) Heating load per unit area**

#### 5.4. Conclusion and discussion

This Chapter focuses on the effect of the proportion of glazing surface in an optimized composite Trombe wall system on indoor thermal comfort in winter. In general, few studies have considered indoor overheating in winter, and the discussion of indoor thermal comfort is generally in summer. However, indoor overheating in summer can generally be solved by air conditioning and cooling, while natural high temperatures during the daytime in winter due to Trombe wall systems, if occurring unmanaged, can be hazardous to plants and animals that may be present indoors, as well as to incapacitated humans. This situation is relatively riskier for homes, so the researcher believes that this topic is worth exploring. In the conclusion of the study using the current model, the greater the ratio of glazing surface to massive wall, the higher the efficiency of the entire composite Trombe wall system, especially since the optimized glazing surface uses low-E double glazing for the winter season, and the heat loss value at night has almost no effect.

In the second half of this chapter the influence of the glazing surface on the ratio of the room floor area (also equivalent to the ratio of the composite double-circulation Trombe wall system) on the peak room temperature and thermal comfort is discussed. The recommended ratio for experimental conditions without risk of overheating is below 0.4. The recommended ratios provided in the conclusions of this study were simulated under specific experimental conditions for the

benefit of different users. It is important to note that the general rooms, both office and residential, have additional transparent windows that can transmit light and can be opened, which is different from the glazing surface of the Trombe wall system across the massive wall. According to the comparison and speculation of sunroom in the previous section, after the addition of the window component, the peak temperature of the room will increase further during the daytime on a sunny day without curtains or other shading devices. Therefore, when considering the proportion of Trombe wall, users should also pay attention to the priority of energy saving or thermal comfort.

In addition, the proportion of glazing surface and the proportion of windows, glass curtain wall or other components of the house also involves the discussion of the aesthetics of the building facade, which is difficult to improve because of the fixed components of the Trombe wall. If we understand the impact of the proportion of the glazing surface on the thermal performance and thermal comfort, we can be inspired in the design of the building.

## References

- [1] Omrany H, Ghaffarianhoseini A, Ghaffarianhoseini A, Raahemifar K, Tookey J. Application of passive wall systems for improving the energy efficiency in buildings: a comprehensive review. *Renew Sustain Energy Rev* 2016;62:1252–69.
- [2] Hu Z, He W, Ji J, Zhang S. A review on the application of Trombe wall system in buildings. *Renew Sustain Energy Rev* 2017;70:976–87.
- [3] Sergei K, Shen C, Jiang Y. A review of the current work potential of a trombe wall. *Renew Sustain Energy Rev* 2020;130:109947.
- [4] Hern´andez-L´opez I, Xam´an J, Ch´avez Y, Hern´andez-P´erez I, Alvarado-Ju´arez R. Thermal energy storage and losses in a room-Trombe wall system located in Mexico. *Energy* 2016;109:512–24.
- [5] ISO, 2005. ISO 7730:2005 Ergonomics of the thermal environment — Analytical determination and interpretation of thermal comfort using calculation of the PMV and PPD indices and local thermal comfort criteria
- [6] ISO, 2003. ISO 15099:2003 Thermal performance of windows, doors and shading devices-Detailed calculations. International Standards Organization.
- [7] Zhu Yingxin. *Built Environment: China Construction Industry Press*, 2010
- [8] ISO, 2005. ISO 7730:2005 Ergonomics of the thermal environment — Analytical determination and interpretation of thermal comfort using calculation of the PMV and PPD indices and local thermal comfort criteria

[9] Stazi F, Mastrucci A, di Perna C. The behaviour of solar walls in residential buildings with different insulation levels: an experimental and numerical study. *Energy Build* 2012;47:217–29.

[10] BŁOTNY, Jagoda; NEMŚ, Magdalena. Analysis of the Impact of the Construction of a Trombe Wall on the Thermal Comfort in a Building Located in Wrocław, Poland. *Atmosphere*, 2019, 10.12: 761.

[11] <https://findpro.jp/glass/low-e#h2-5>

## *Chapter 6*

# ***NUMERICAL STUDY OF COMPOSITE TROMBE WALL IN SUMMER AND INFLUENCE OF MASSIVE WALL MATERIALS***



**CHAPTER SIX: NUMERICAL STUDY OF COMPOSITE TROMBE WALL IN  
SUMMER AND INFLUENCE OF MASSIVE WALL MATERIALS**

<i>NUMERICAL STUDY OF COMPOSITE TROMBE WALL IN SUMMER AND INFLUENCE OF MASSIVE WALL MATERIALS</i> .....	6-1
6.1 Overview .....	6-1
6.2. The effect of ventilation mode in summer .....	6-1
6.2.1. Optimized composite Trombe wall system in summer .....	6-1
6.2.2. The effect of different ventilation mode.....	6-6
6.3. The effect of massive wall material .....	6-19
6.3.1. The effect of massive wall material in summer.....	6-23
6.3.2. The effect of massive wall material in winter .....	6-26
6.3.3. Conclusion .....	6-36
6.4. Discussion .....	6-38
Reference .....	6-39



## **6.1 Overview**

The climate in Kitakyushu, Japan, is hot in summer and cold in winter, and there is a huge difference between the summer and winter climates. Although Kitakyushu, as a coastal city, has a relatively mild climate in summer, the maximum temperature can still reach over 30°C. Therefore, it is still necessary to install indoor cooling measures to reduce the indoor temperature and maintain a comfortable thermal environment for human beings.

In the previous paper, after a series of optimization comparisons, a relatively economical and optimized result was obtained for this study in winter. However, in theory, the use of thermal storage walls is likely to lead to overheating of the room in summer. In particular, the optimized composite double-circulation Trombe wall with Low-E glass is likely to aggravate the overheating situation. So it is a question to be explored whether this Trombe wall is possible to be used all year round. If it can be easily and economically retrofitted to achieve effective energy savings in summer, its applicability and universality can be greatly increased.

This chapter will focus on the ventilation pattern of the composite Trombe system in summer and the material of the massive wall, so that the Trombe wall system can be used in both winter and summer.

## **6.2. The effect of ventilation mode in summer**

### **6.2.1. Optimized composite Trombe wall system in summer**

The simulation experiment compares a normal house without Trombe wall (NH), a Sunroom without Trombe wall (SR), a classic Trombe wall (CTW) and an optimized composite double-circulation Trombe wall (DLTW) in summer (take August as an example).

Based on the outdoor temperature and the temperature status of different houses, it can be deduced that in a meteorological standard year in Kitakyushu, the first half of August has several rainy or cloudy days, while the second half of the month has continuous sunny days and high temperatures, and the air conditioner generally needs to be turned on indoors to maintain human comfort.

Take August, when the temperature is high, as an example, from the performance of indoor (main activity space) temperature without air conditioning (the results are shown in the figure 6.2.1.), the house equipped with Trombe wall has significantly higher indoor temperature than outdoor because of the solar heat collection effect of massive wall, and it is easy to be overheated (above 30°C) for a long time, and the optimized composite Trombe wall, although the thermal performance in winter has The optimized composite Trombe wall, although the thermal performance in winter is significantly improved, in summer, however, without any improvement measures, the indoor

temperature will be above 27°C while maintaining the original temperature control fan operation rate.

Comparatively, the ordinary house without Trombe wall (having an envelope with good insulation measures), which performs the worst in winter. But it has the lowest overall indoor temperature without direct sunlight, which can even be lower than the outdoor temperature. Also, the temperature fluctuation is relatively smooth in terms of the temperature dynamic change curve. It is the best performance among the four types of houses. The sunroom, on the other hand, because of the direct sunlight into the room during the day, is consistent with the situation in winter, and there is a substantial warming of the room and the temperature is obviously overheated. At night, it also cannot dissipate heat well because of the small temperature difference between indoor and outdoor.

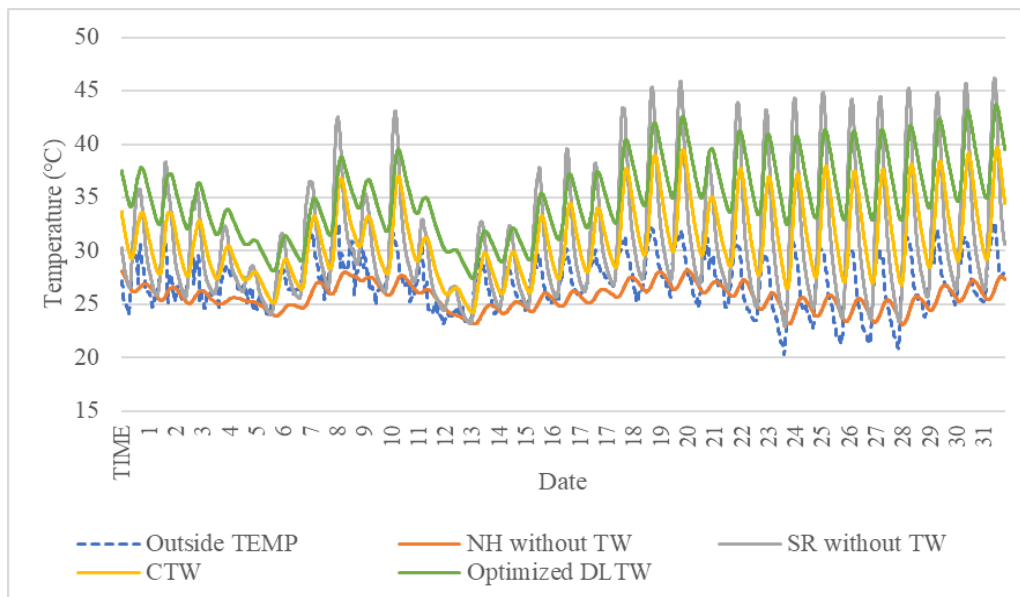


**Figure 6.2.1 Comparison of indoor temperature of different types of houses in August**

And one of the sunny days in August with a maximum temperature above 30°C, August 19, was selected for analysis (in figure 6.2.2). Without using air conditioning for cooling, at night, the indoor temperature of each house decreases due to the temperature difference between indoor and outdoor, until it starts to warm up after sunrise due to solar radiation. The lowest room temperature at night is in the normal house without Trombe wall, followed by the sunroom without Trombe wall, which has the fastest temperature loss. Both types of houses with Trombe walls have high room temperatures, especially the modified Low-E double-glazing houses with Trombe walls because they do not lose heat easily and always have high room temperatures. The trend and magnitude of temperature change in the house with Trombe wall is more consistent in the daytime sunroom because of the rapid increase in indoor temperature due to direct sunlight. A well-insulated opaque

house, in summer, the indoor temperature tends to be almost flat.

Equation based on two criteria for the evaluation of temperature fluctuations :

Thermal load levelling (TLL)

$$TLL = \frac{T_{r\ max} - T_{r\ min}}{T_{r\ max} + T_{r\ min}} \quad (1)$$

Thermal load levelling (f)

$$f = \frac{T_{w\ inside\ max} - T_{w\ inside\ min}}{T_{w\ outside\ max} - T_{w\ outside\ min}} \quad (2)$$

Comparing the indoor temperature fluctuation index of each type of room in summer (August), the maximum outdoor temperature in Kitakyushu in August was 32.9°C and the minimum was 20.3°C according to the calculation.

In the normal house without Trombe wall, the monthly maximum indoor temperature is 28.2°C and the minimum is 23.12°C. Thermal load levelling (TLL<sub>nh</sub>) is calculated to be 0.10 and thermal load levelling (f<sub>nh</sub>) is 0.40. In the sunroom without Trombe wall, the monthly maximum indoor temperature is 46.22°C and the minimum is 22.93°C. The thermal load levelling (TLL<sub>sr</sub>) is 0.34 and the thermal load levelling (f<sub>sr</sub>) is 1.85. In the classical Trombe wall house, the monthly maximum indoor temperature is 39.68°C and the minimum is 24.19°C. Thermal load levelling (TLL<sub>ctw</sub>) is calculated to be 0.24 and thermal load levelling (f<sub>ctw</sub>) is 1.23. In the Optimized composite Trombe wall house, the monthly maximum indoor temperature is 44.31° C and the minimum is 27.47° C. Thermal load levelling (TLL<sub>dltw</sub>) is calculated to be 0.23 and thermal load levelling (f<sub>dltw</sub>) is 1.34.

Subsequently, one day was randomly selected from the consecutive sunny days in late August, comparing the indoor temperature fluctuation index of each type of room in August 19th, the maximum outdoor temperature in Kitakyushu in August was 32.2°C and the minimum was 25.4°C according to the calculation.

The maximum indoor temperature in the normal house without Trombe wall is 28.07°C and the minimum is 26.23°C. Thermal load levelling (TLL<sub>nh</sub>) is calculated to be 0.03 and thermal load levelling (f<sub>nh</sub>) is 0.27. In the sunroom without Trombe wall, the maximum indoor temperature is 45.34°C and the minimum is 27.36°C. The thermal load levelling (TLL<sub>sr</sub>) is 0.25 and the thermal load levelling (f<sub>sr</sub>) is 2.64. The maximum indoor temperature of the classical Trombe wall is 39.02°C and the minimum is 29.62°C. Thermal load levelling (TLL<sub>ctw</sub>) is calculated to be 0.14 and thermal load levelling (f<sub>ctw</sub>) is 1.38. The maximum indoor temperature of the Optimized composite Trombe wall is 42.47°C and the minimum is 34.55°C. Thermal load levelling (TLL<sub>dltw</sub>) is calculated to be

0.10 and thermal load levelling ( $f_{dlw}$ ) is 1.16.

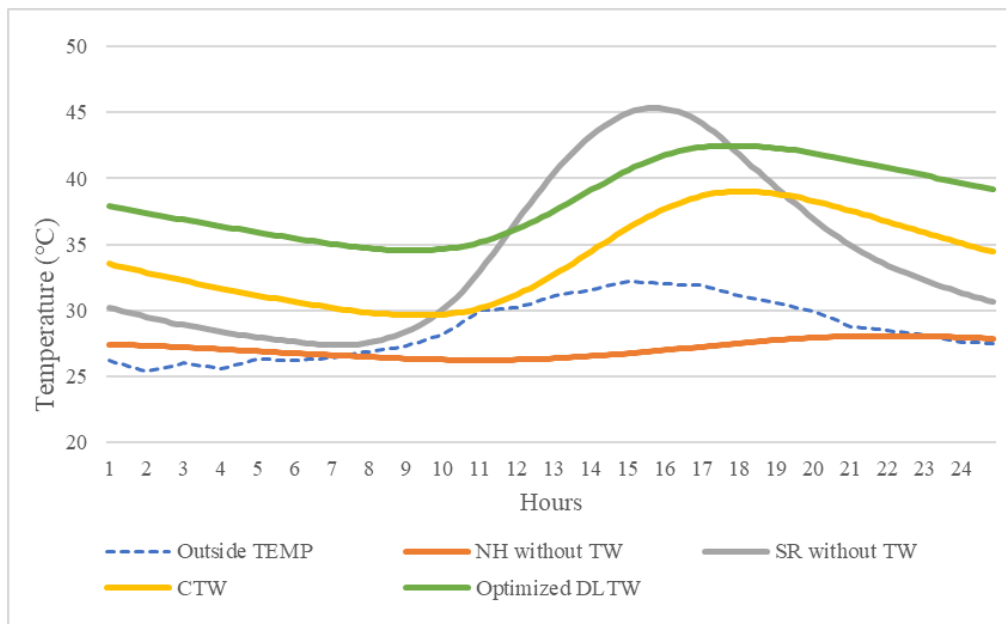


**Figure 6.2.1 Comparison of indoor temperature of different houses on August 19th**

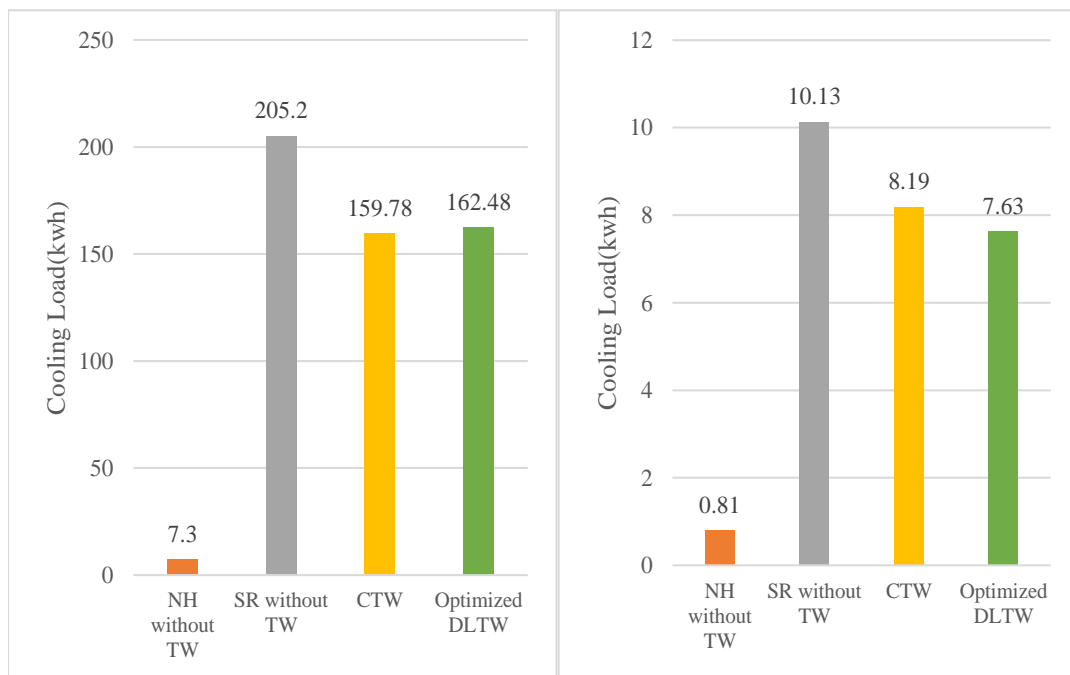
Consistent with the results of the observational analysis, the normal house without Trombe wall has the lowest Thermal load levelling and the least fluctuation. The sunroom without Trombe wall has the highest Thermal load levelling and the highest fluctuation. The magnitude of indoor temperature variation in summer is very similar for the classical Trombe wall house and the optimized Composite double-circulation Trombe wall house.

The simulation experiment continued with a refrigeration air conditioner in the room, with the temperature set to 26°C and the on time turned on for the whole day. The calculated air conditioning load of the main indoor space with air conditioning on was compared, and the results are shown in the figure 6.2.3 and figure 6.2.4.

The cooling load of the normal house without Trombe wall is the lowest, with only 20.6 kwh for the whole year and 7.3 kwh for the whole month of August. the air-conditioning load of the sunroom without Trombe wall is the highest, with 619.51 kwh for the whole summer and 205.2 kwh for the single month of August. while the air-conditioning load of the house with Trombe The summer air conditioning loads of the two types of houses with Trombe walls are relatively similar. In terms of the cooling load values for a longer period of time, i.e., for the whole year and for a single month in August, the load of the house with the classic Trombe wall is relatively low, asking 416.92 kwh and 159.78 kwh, respectively. while the optimized composite double-circulation Trombe wall has a cooling load of 474.99 kwh in summer last year and a cooling load of 162.48 kwh in a single month in August. The single-month cooling load was 162.48 kwh. Because the optimized composite double-circulation Trombe wall has a slightly lower Thermal load levelling

than the classical Trombe wall. So there is also a situation that the cooling load of the single-day double-circulation Trombe wall is lower than that of the classical Trombe wall. For example, on a single day of August 19, the composite double-circulation Trombe wall has about 0.5kwh lower air conditioning load than the classic Trombe wall.

Combined with the overall analysis of the winter heat load, the energy consumption of an ordinary house without Trombe wall is very low in summer, but its winter performance is poor and it is difficult to do both. The sunroom without Trombe wall obviously has high energy consumption and high variation of room temperature in both winter and summer. A house with a Trombe wall, on the other hand, can increase the room temperature and save a lot of energy in winter, but it can cause overheating in summer. According to the previous analysis, a composite Trombe wall before improvement has relatively small fluctuations in room temperature with the addition of a layer of insulation. After the improvement, the overall indoor temperature has been significantly increased, but at the same time the magnitude of indoor temperature variation has also increased. There is a significant improvement in the energy-saving effect in winter, but also increases the difficulty of cooling in summer.



**(a)** **(b)**  
**Figure 6.2.3 Comparison of cooling load of different houses: (a) In August; (b) On August 19th**

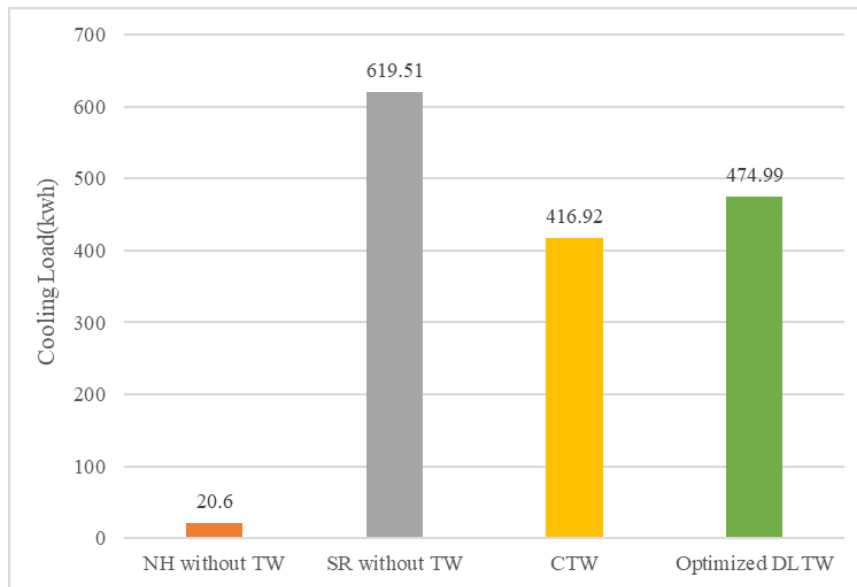


**Figure 6.2.4 Comparison of cooling load of different houses overall cooling season**

### 6.2.2. The effect of different ventilation mode

This study expected that the optimized Composite double-circulation Trombe wall would also perform well in summer, but with the current construction and usage, it is clear that the Trombe wall does not perform well in summer. According to Sodha et al. [1,2], the principles and basic measures of passive cooling of buildings are as follows.

#### (1) Reduction of solar and convective heat input

The following measures can be taken, orientation, setting shading by neighboring building, shading by vegetation, shading by overhangs textured facades, reflecting surfaces, and shelter against hot winds.

(2) **Reduction of heat transmission:** The following measures can be taken, increase thermal insulation, air cavities.

(3) **Increase of heat loss by radiation:** The following measures can be taken, enlarged surface area, movable elements.

(4) **Increase of heat loss by convection:** The following measures can be taken, Outdoor wind management, indoor natural ventilation, Indoor forced ventilation, Earth air tunnel flowing water.

#### (5) Increase of heat loss by evaporation

For the current winter optimized composite double-circulation Trombe wall, the main heat transfer in the heating season is the hot air transfer from the upper vents. According to the design

principle of (2) reducing heat transfer, the main heat transfer path of composite Trombe wall can be cut off, i.e. closing the upper and lower vents (close the DC fans) . And play the role of heat insulation of interior wall insulation board.

First of all, study propose the following three basic application of summer application schemes with closing the upper and lower vents and fans as shown in figure 6.2.5. The thermal conductivity is  $0.036(\text{W/m K})$ , and the thermal insulation board material with good thermal insulation performance is the same as the inner wall in the simulated condition. Set indoor external ventilation, every two hours, i.e.,  $12\text{m}^3/\text{h}$ .

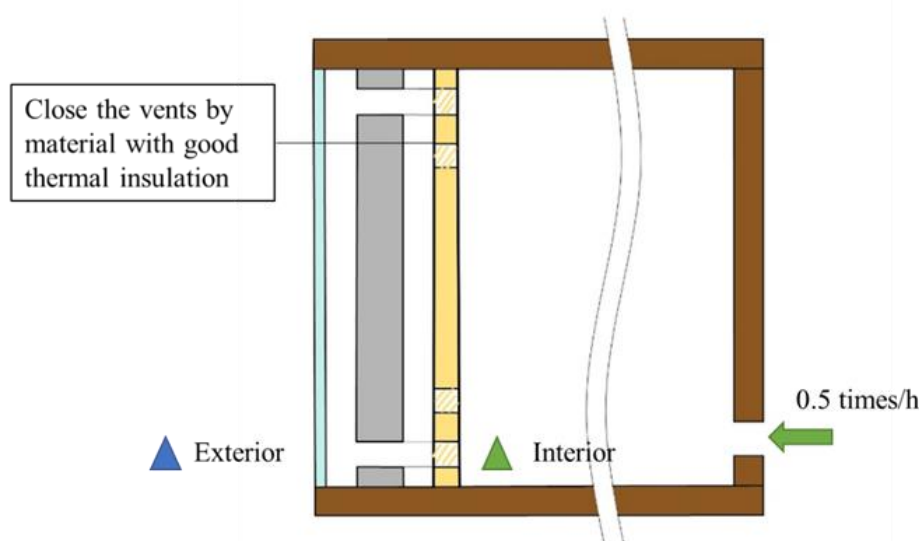
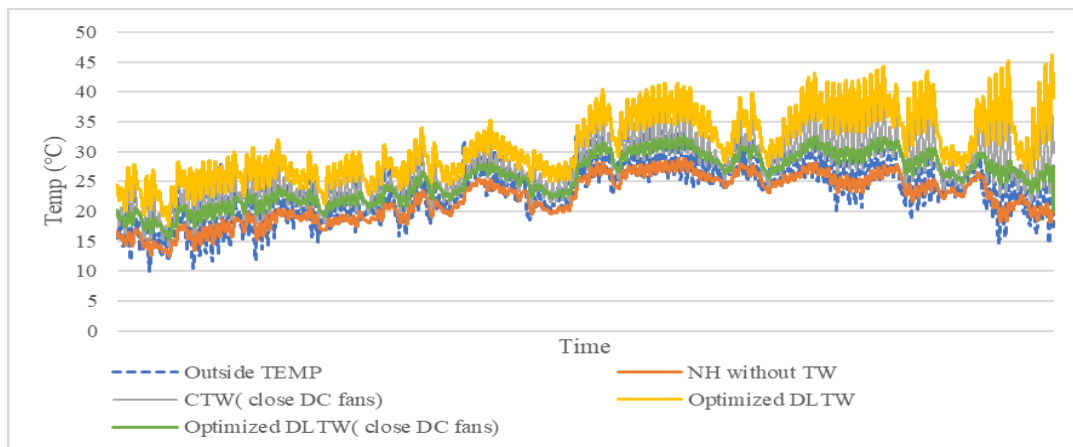


**Figure 6.2.5 The section of composite double-circulation Trombe wall (close the DC fans)**

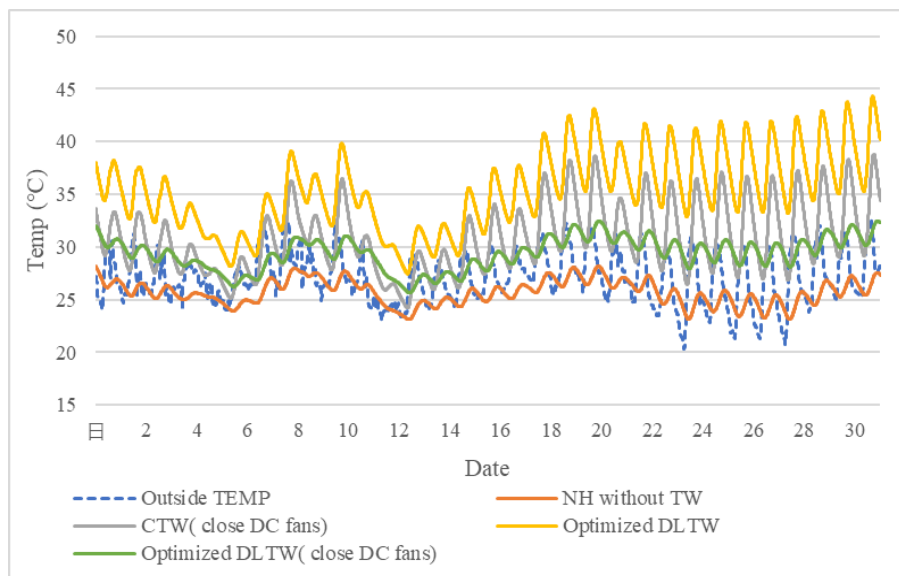
As a comparison, the Normal house without Trombe wall, the best performer in the previous section, was selected for the study, while the classic Trombe wall was compared under the same conditions, i.e., simulated with the upper and lower vents and DC fans turned off.

Figure 6.2.6 shows the variation of indoor temperature in summer throughout the year without air conditioning, and Figure 6.2.7 shows the fluctuation of indoor temperature in August, the hottest month. The comparison shows that even though the classical Trombe wall blocks the convection and propagation of hot air, it cannot block the direct heat transfer and heat radiation through the massive wall, and it still generates high temperatures of  $30^{\circ}\text{C}$  or even  $35^{\circ}\text{C}$  or more during the day. In the composite Trombe wall system, the interior wall is used to block the main heat transfer path, and the indoor temperature is effectively reduced, and the fluctuation is significantly reduced. However, the overall indoor temperature of the composite double-circulation Trombe wall system is still about  $5^{\circ}\text{C}$  higher than that of a normal house without Trombe wall. The indoor temperature change curve of a single day on August 19 (Figure 6.2.8) shows a more obvious comparison,

although the indoor temperature in the classic Trombe wall system drops to lower than that in the composite Trombe wall system with DC fans turned off before sunrise, the indoor temperature gradually rises to more than 35°C degrees after sunrise due to the rapid After sunrise, the indoor temperature gradually rises above 35°C due to the rapid transfer of solar heat radiation from the massive wall. The indoor temperature in the composite double-circulation Trombe wall system with DC fans turned off varies similarly to the normal house without Trombe wall, but is always higher than the normal house without Trombe wall.



**Figure 6.2.6 Comparison of indoor temperature of different houses overall cooling season**



**Figure 6.2.7 Comparison of indoor temperature of different houses in August**

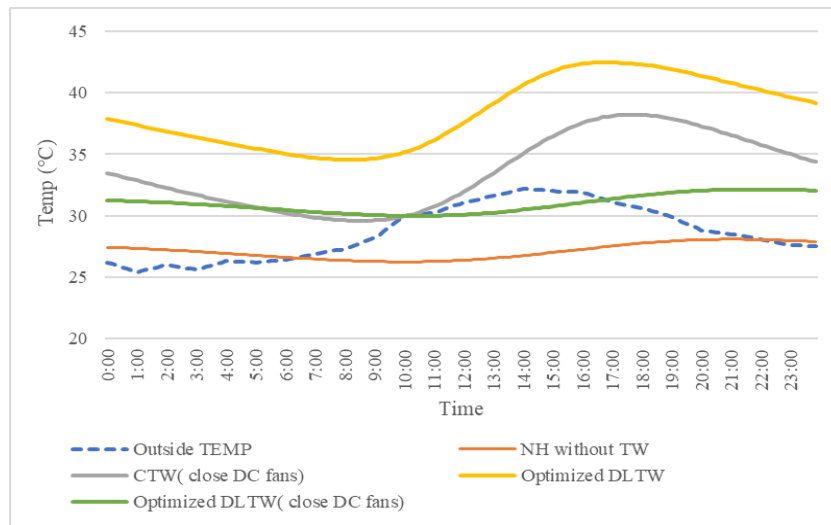


**Figure 6.2.8 Comparison of indoor temperature of different houses on August 19<sup>th</sup>**

The reason for this can be seen in Figure 6.2.9, which shows the change of indoor temperature and the temperature of the two air layers in the optimized DLTW (close DC fans) system. normal house without Trombe wall has a direct contact with the outdoor air on the south façade. In contrast, the south facade of the composite double-circulation Trombe wall house is separated from the outside by two air layers, and the graph shows that the inside and outside air layers of the composite double-circulation Trombe wall system with the temperature-controlled fans turned off maintained high temperatures for almost the entire month of August. The average temperature was over 45°C and the maximum temperature was over 60°C. Although the composite double-circulation Trombe wall system has an inner wall as insulation, the material used is not perfectly insulated, and heat is still transferred to the room through the insulation panels, causing the room temperature to rise.

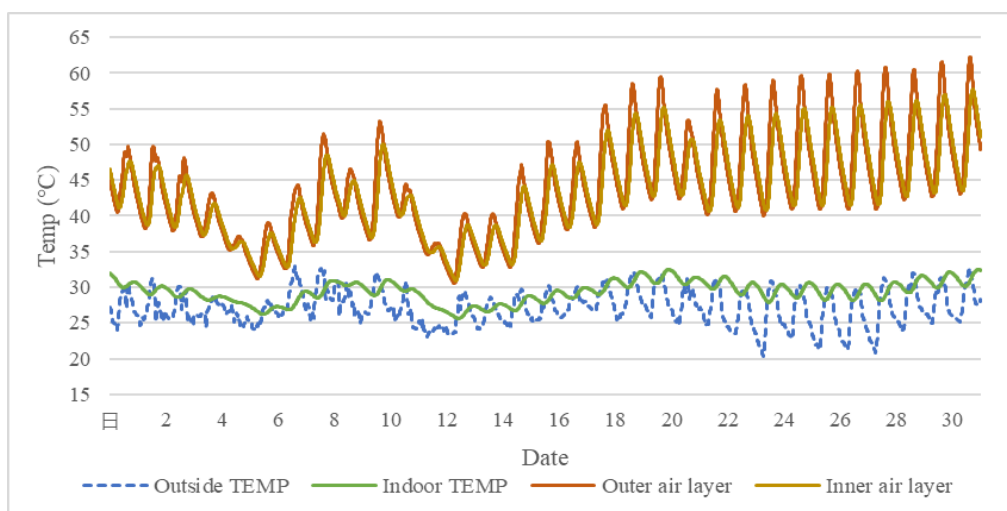


**Figure 6.2.9 Comparison of different part temperature of optimized DLTW (close DC fans) in August**

Figure 6.2.10 shows the indoor air conditioning load in August, the hottest month, when the indoor air conditioning is turned on all day, and Figure 6.2.11 shows the total indoor air conditioning load for the whole cooling season. The comparison of the results shows that the air conditioning loads of both the classic Trombe wall system and the composite double-circulation Trombe wall system decrease after the DC fans are turned off. the load of the composite double-circulation Trombe wall system decreases very significantly after the vents are turned off. The load of the composite double-circulation Trombe wall system decreases significantly after turning off the vents, by 74.4% in August compared to before turning off the temperature-controlled fans. However, this is still higher than the performance of a normal house without Trombe wall in summer. The study needs to be further optimized to reduce the indoor air conditioning load of the composite double-circulation Trombe wall system.

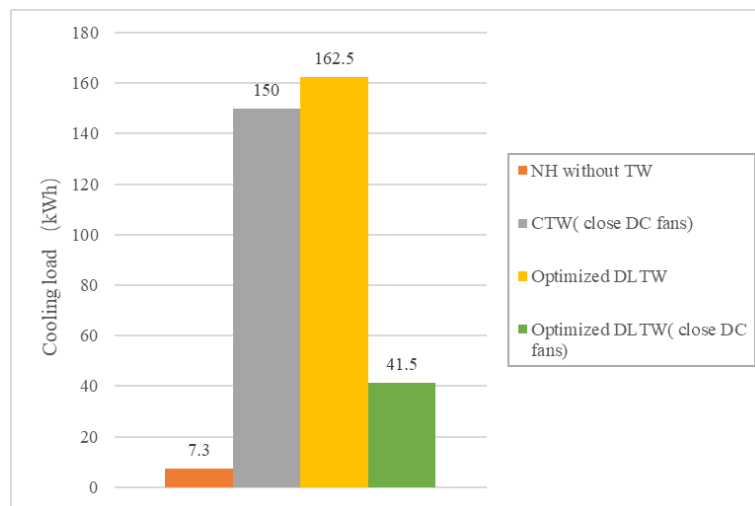


**Figure 6.2.10 Comparison of cooling load of different houses in August**

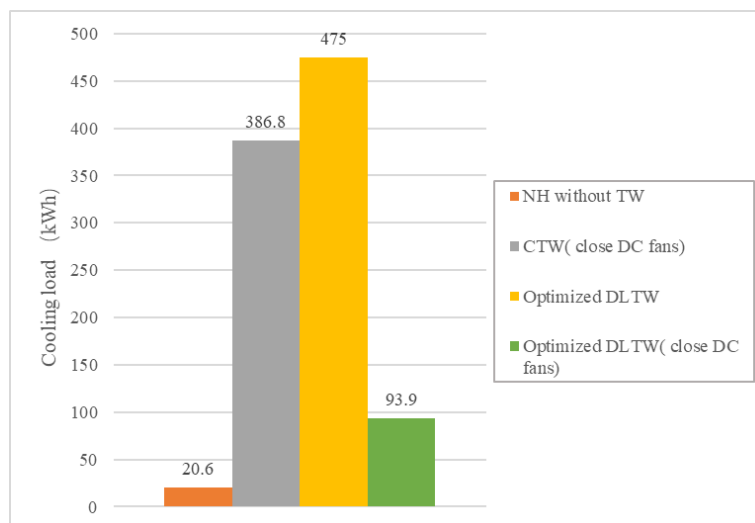


**Figure 6.2.11 Comparison of cooling load of different houses overall cooling season**

Through the previous study, it was found that in the composite double-circulation Trombe wall system, a relatively good reduction of energy consumption can be achieved by cutting off the air circulation between the room and the air layer in the same ventilation mode as in winter, i.e., by turning off vents and temperature-controlled DC fans. However, the high air temperature in the air layer makes the overall indoor temperature also increase to some extent. All to further reduce the summer indoor temperature, one of the ways is to reduce the air layer temperature. Figure 6.2.12 shows the temperature change curves of the inside and outside air layer temperatures before and after turning off the fan for the August composite double-circulation Trombe wall system. The comparison reveals that after turning on the fan, the air temperature of the inner and outer air layers decreases due to the air flow. The overall air temperature in the inner and outer air layers after turning on the fan is lower than that with the fan turned off. So the experiment can try to reduce the air layer and indoor air temperature at the same time by turning on the fan and changing the ventilation of the fan.

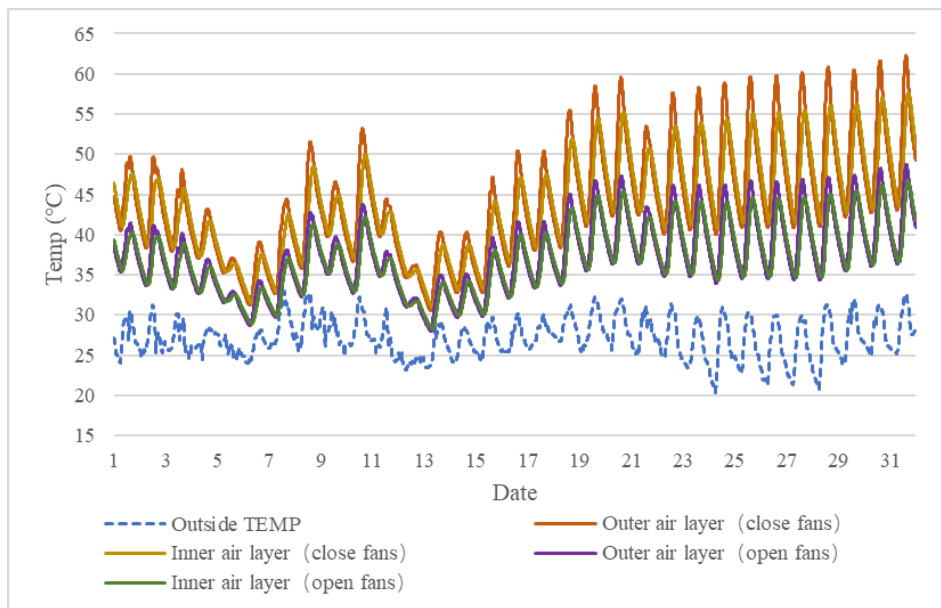


**Figure 6.2.12 Comparison of different part temperature of optimized DLTW in August**

According to the discussion of summer Trombe wall system in the review[3], there are two main countermeasures for air circulation and ventilation in summer (mainly in the classic Trombe wall system), one is as shown in Fig. 6.2.13(a), where indoor air enters the air layer through measures such as fans, and then the air is dissipated through the surface of the massive wall to the massive. The air is then dissipated through the surface of the massive wall and the hot air is discharged to the outside, which is called Indoor-air layer-outdoor mode here. The other one is as shown in Fig. 6.2.13 (b), where the air from the air layer surface enters the air layer from the bottom of the glazing surface without passing through the room, dissipates heat from the surface of the massive wall and discharges the hot air from above, which is called the Outdoor-air layer-outdoor mode.

In classic Trombe wall system, (a) for mild climates, the cooling-based Trombe wall acts as a natural ventilation when the outdoor temperature is lower than the indoor temperature. (b) for hot climates, it acts as an insulating material to reduce the heat gain in the room when the outdoor temperature is higher than the indoor temperature.

As for the composite Trombe wall system, because there are two air layers inside and outside, ventilating different air layers may have different effects, and because the inner wall itself is an insulation material, the effect of both modes in the composite Trombe wall system may be different from that of the classical Trombe wall, so the study needs to be discussed on a case-by-case basis.

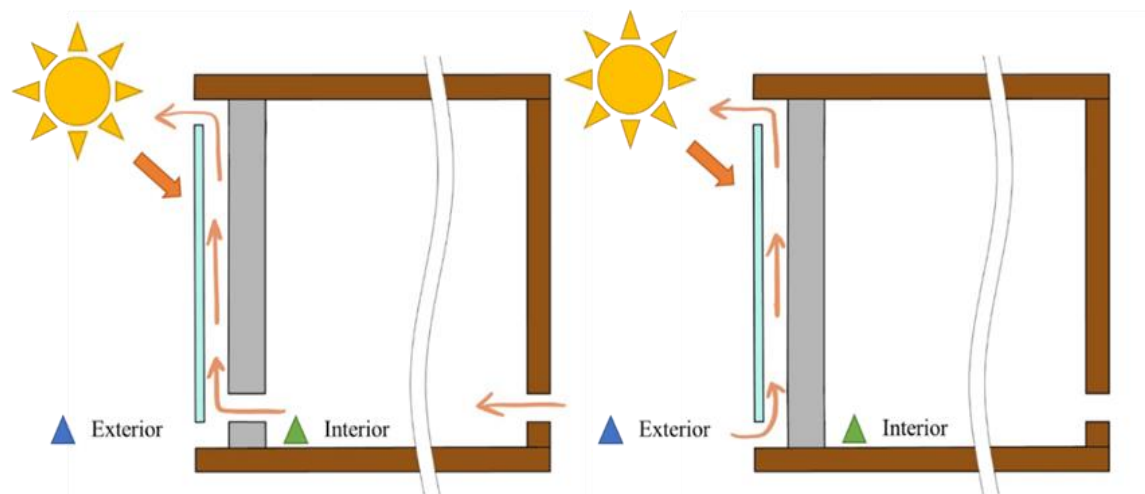


**Figure 6.2.13 Trombe wall summer ventilation countermeasures: (a) Indoor-air layer-outdoor mode; (b)Outdoor-air layer-outdoor mode**

The study designed 6 different air circulation methods for the optimized composite double-circulation Trombe wall based on the above reference, as shown in Figure 6.2.14.

Among them, Type A: outside-air layer-outdoor mode with only outer air layer ventilation; Type B: outside-air layer-outdoor mode with outside air layer ventilation only; Type C: Indoor-air layer-outdoor mode with inner-air layer ventilation only; Type D: Outdoor-air layer-outdoor mode for inside air layer ventilation only; Type E: indoor-air layer-outdoor mode with both inside and outside air layer ventilation; Type F: outdoor-air layer-outdoor mode with both inside and outside air layer ventilation. All types indoor ventilation is once every two hours, i.e.,  $12\text{m}^3/\text{h}$ . The air circulation between all air layers is controlled by a DC fan with a maximum winter efficiency of  $140\text{m}^3/\text{h}$ .

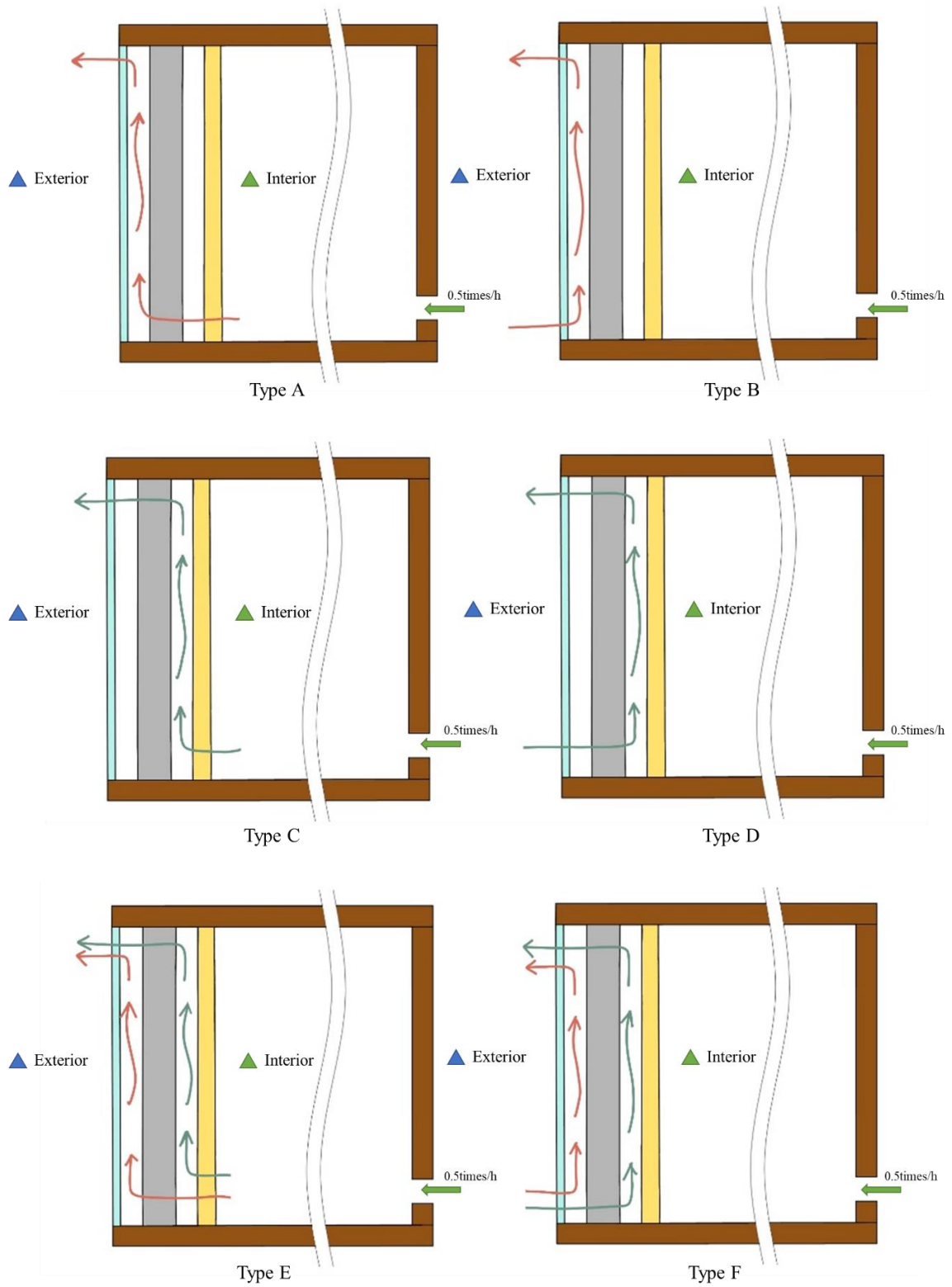
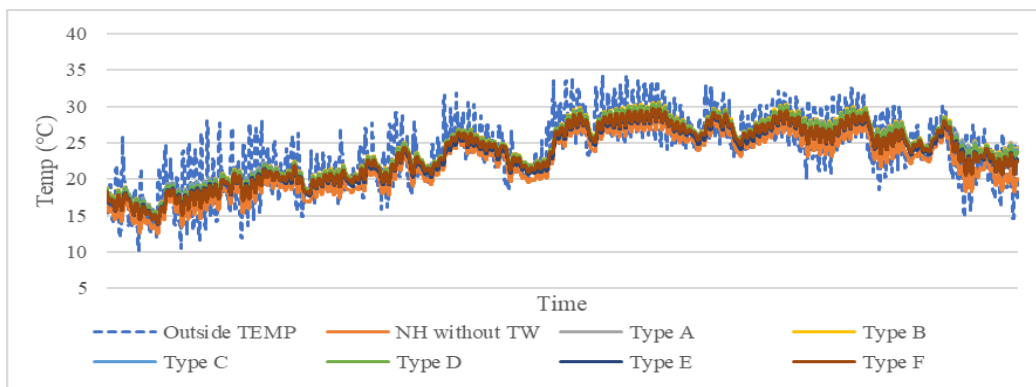
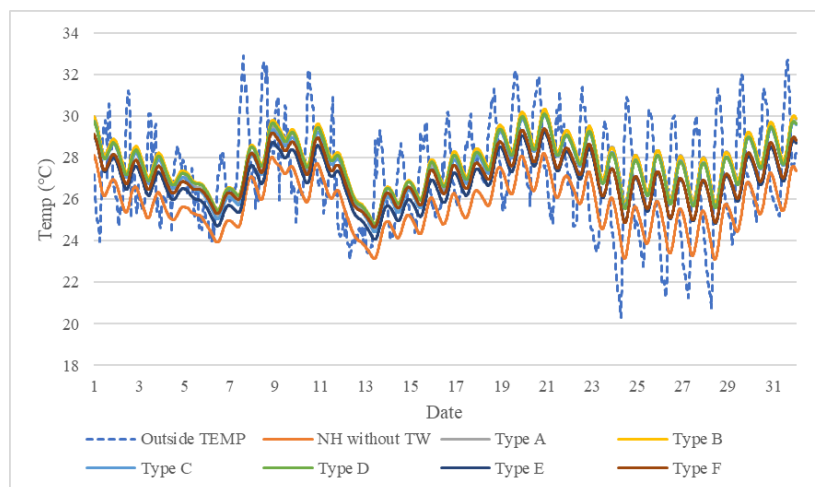


Figure 6.2.14 Different types of ventilation mode in summer

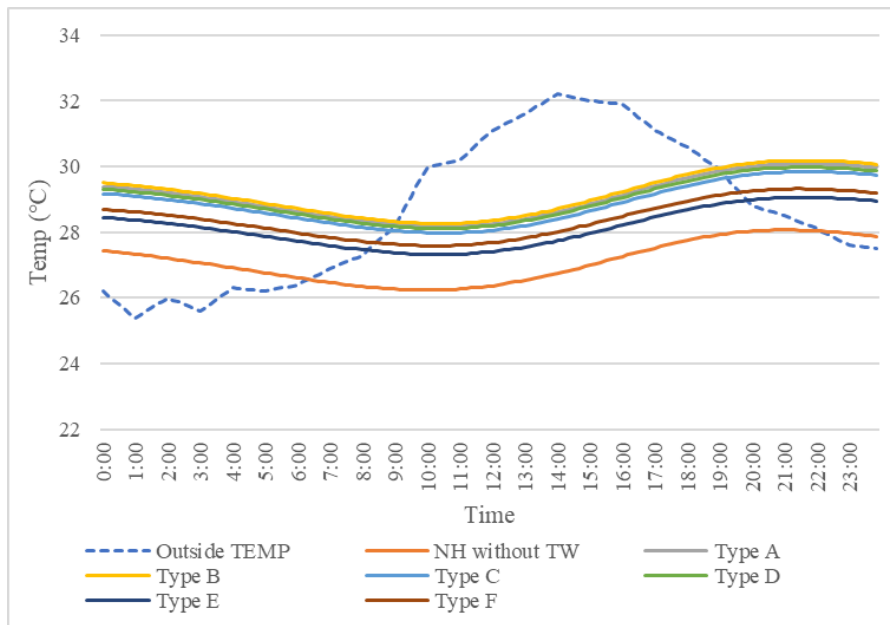
Figure 6.2.15 shows the variation of indoor air temperature for different types of fan ventilation patterns throughout the summer without turning on the air conditioner. Figure 6.2.16 shows the variation of indoor air temperature for different types of fan ventilation modes throughout the summer in August. In terms of overall comparison, the indoor air temperature for Type E and Type F, which both turn on the inner and outer air layer fans, is lower than that of the modes that turn on only the inner layer or only the outer layer fan. Figure 6.2.17 takes a sunny day in August and shows more clearly that simultaneous ventilation of the inner and outer air layers is more effective than ventilation with only the outer air layer on or only the inner air layer on. The indoor air temperature in the ventilation mode with only the inner or outer air layer on is from high to low: Type B (outer-air layer-outdoor mode), Type A (inner-air layer-outdoor mode), Type D (outer-air layer-outdoor mode), Type C (inner-air layer-outdoor mode), That is, Type C (Indoor-air layer-outdoor mode with inner-air layer ventilation only;) is more effective. In the case of simultaneous ventilation of both inside and outside air layers, Type E (indoor-air layer-outdoor mode with both inside and outside air layer ventilation) has lower indoor temperature and better effect.



**Figure 6.2.15 Comparison of indoor temperature of different ventilation mode in summer**



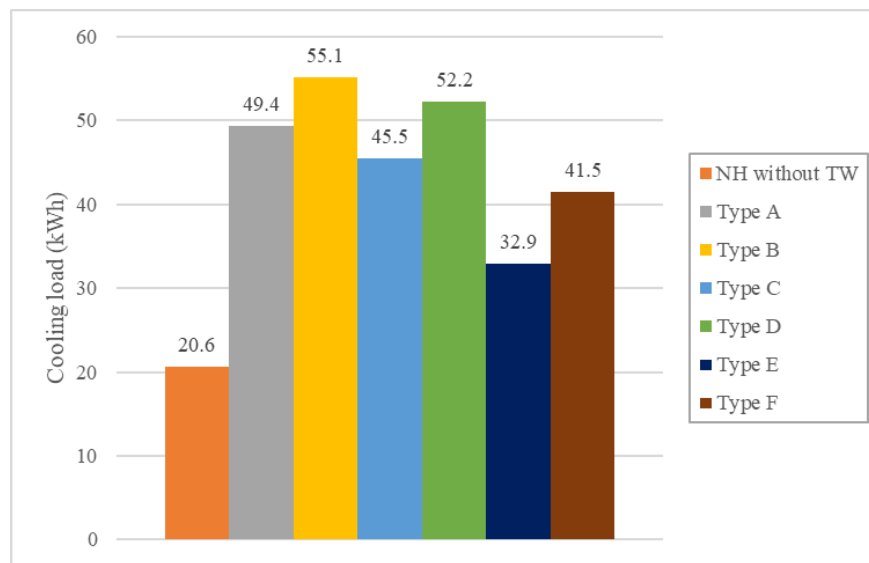
**Figure 6.2.16 Comparison of indoor temperature of different ventilation mode in August**



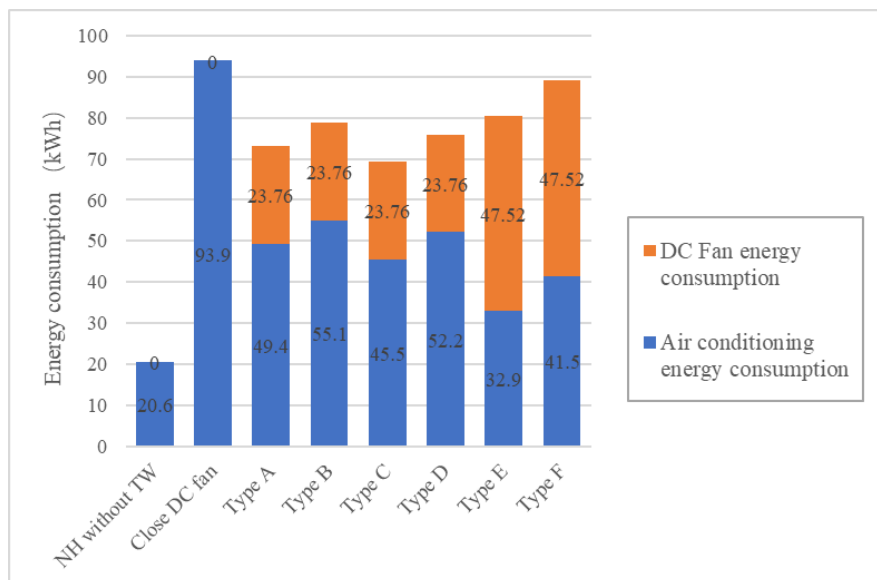
**Figure 6.2.17 Comparison of indoor temperature of different ventilation mode on August 19th**

Figure 6.2.18 shows the total value of the indoor air conditioning load for different types of fan ventilation modes throughout the summer cooling period. The comparison reveals that Type E and Type F, the two modes with both internal and external air circulation on, consume relatively less air conditioning load, with the most energy-efficient being Type E with 32.9kWh of annual air conditioning cooling, followed by Type F with a total of 41.5kWh. Type C in the mode with only internal air circulation on or only external air circulation on consumes the least amount of energy at 45.5kWh.

However, with the low energy consumption of the air conditioner and the net difference not being significant, the energy consumption of the DC fan is also not negligible. The power of a single fan is 3.3W, and if the fan is on all day long as the air conditioner, it consumes about 2.4kWh per fan per month. Compared to a house without Trombe wall and a house with a composite double-circulation Trombe wall system with fans turned off, the total annual summer energy consumption plus the total fan energy consumption is shown in Figure 6.2.19. After adding the energy consumption of the fans, the lowest energy consumption is for Type C, which consumes 69.26 kWh for the whole summer, followed by Type A, which consumes 73.16 kWh. The total energy consumption of Type E increases to 80.42 kWh because two additional fans are needed.



**Figure 6.2.18 Comparison of cooling load of different ventilation mode in summer**



**Figure 6.2.19 Total energy consumption of different types of ventilation overall cooling season**

Subsequently, the total energy consumption of air conditioning plus fans was calculated and simulated for each month (May to September), and the results showed that in May, there was no air conditioning load generated in several modes, i.e., whether the fans were turned on or not, the indoor temperature throughout May was less than 26°C, and a more comfortable temperature could be achieved without turning on the air conditioning. Turning on the fan in May will instead increase the fan energy consumption, and it is recommended to adopt the mode of not turning on the fan in May. The results for June are shown in Figure 6.2.20. The need to turn on the air conditioner is also

minimal throughout June, and the lowest total energy consumption is 3.3 kWh without turning on the fan, which basically keeps the room temperature low even without turning on the fan. The total energy consumption in July is shown in Figure 6.2.21. As the temperature rises, the overall indoor temperature also rises gradually, and the time needed for air conditioning cooling grows, so the role of the fan becomes more significant at this time. The situation in August is similar to that of July, with the lowest energy consumption type being Type C, with a total of 14.0 kWh. In July and August, not turning on the fan increases the total energy consumption. In September, although the outdoor temperature starts to cool down gradually, the total energy consumption with the fan on is still less than the air conditioning cooling load with the fan off, with the lowest energy consumption being Type C with 11.5kWh and Type A with 10.9 kWh.

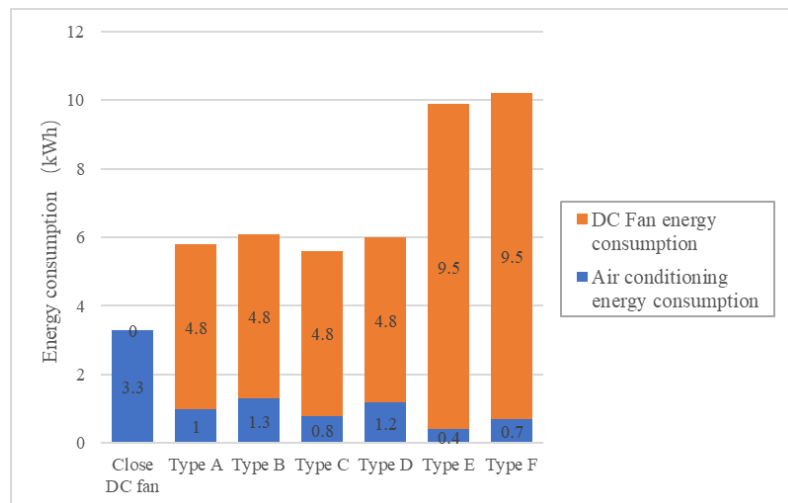


**Figure 6.2.20 Total energy consumption of different types of ventilation in June**

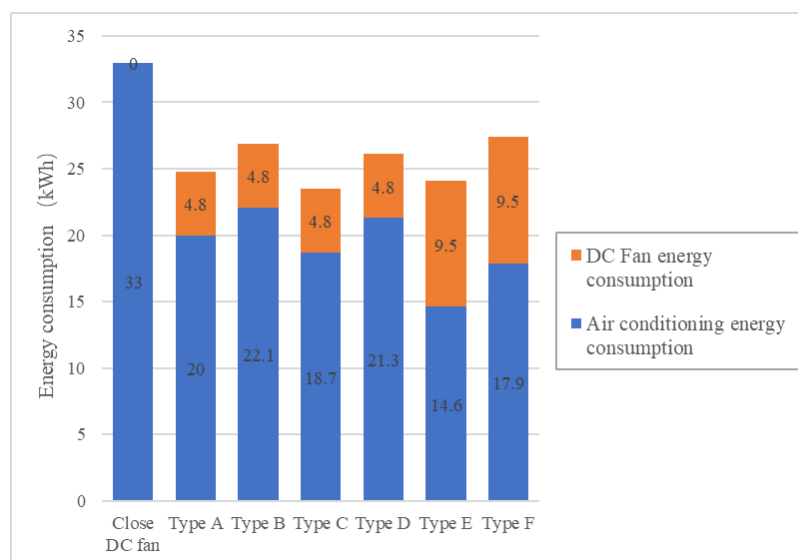


**Figure 6.2.21 Total energy consumption of different types of ventilation in July**

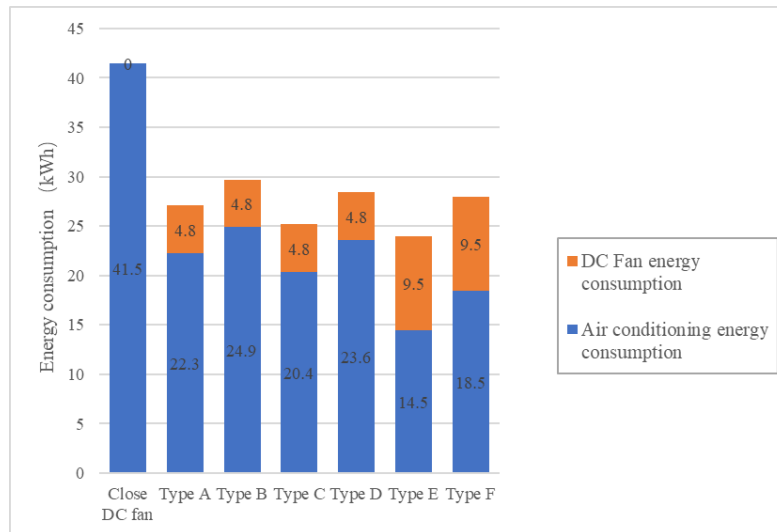


**Figure 6.2.22 Total energy consumption of different types of ventilation in August**

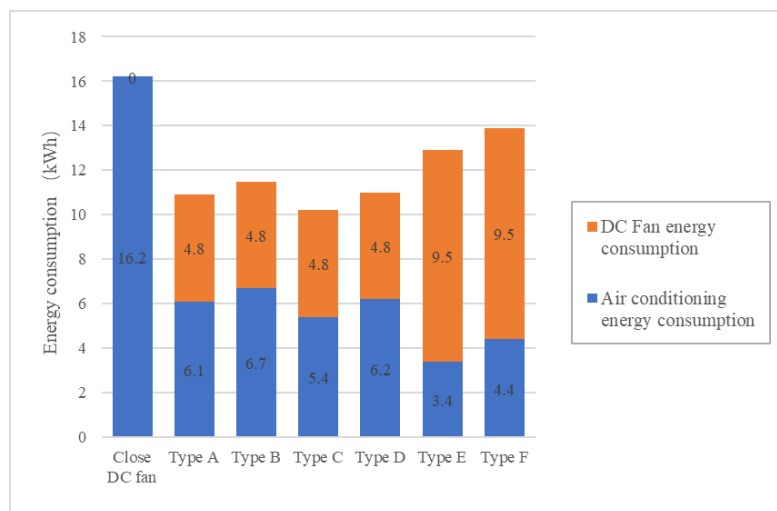


**Figure 6.2.23 Total energy consumption of different types of ventilation in September**

Considering the simulation situation in different months, the fan is more recommended to adopt the ventilation method of indoor-air layer-outdoor. In May and June, the fan can be left on, in August, the Type E ventilation is used for both the inner and outer air layers, and in July and September, the fan for the outer ventilation can be turned off and the Type C ventilation is used. The total combined consumption is 61.0kWh, as shown in Figure 6.2.23, which is still higher than the normal house without Trombe wall, but can save 35.0% of energy compared to the fan-off mode.

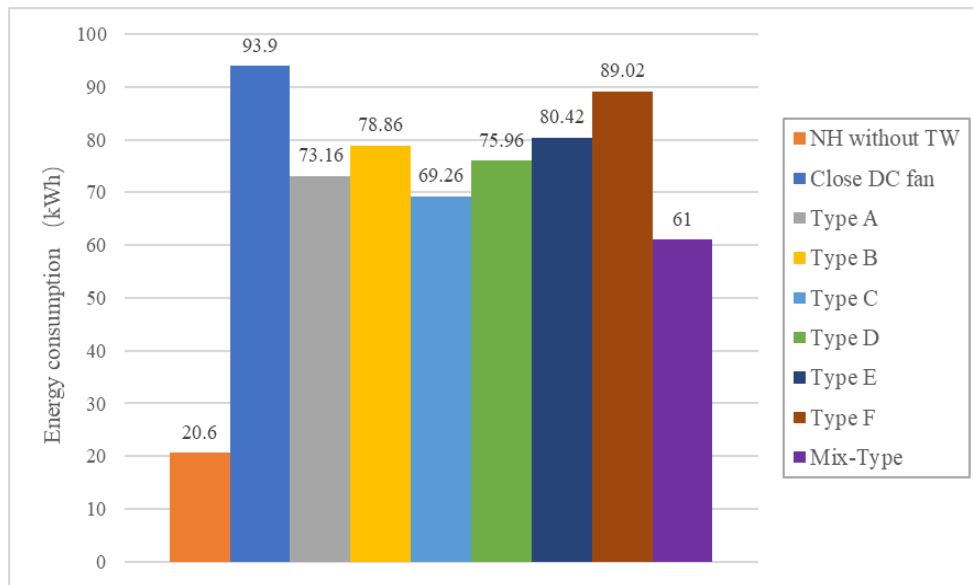


**Figure 6.2.23 Total energy consumption of different types of ventilation overall cooling season**

### 6.3. The effect of massive wall material

The heat transfer from the surface of massive wall is mainly radiant. In the composite trombe wall system, the massive wall directly transfers heat to the air layer, which indirectly exchanges air with the room through air circulation. In summer, the study wanted to change the characteristics of the massive wall to reduce its heat absorption. And in winter, it is necessary to reduce its heat loss. In the review, there is to improve the performance of Trombe wall system by using water wall, the high specific heat capacity can theoretically reduce the night time heat loss of the wall and also slow down the heating rate during the day. As the most common high specific heat capacity material in nature, water has a high specific heat capacity of 4200 J/kgK at 20°C, which is more than four times that of concrete. As a fluid, water generates thermal convection during the temperature rise, accelerating the heat transfer efficiency.

And in the choice of massive wall material for Trombe wall system, phase change material is a hot research topic in recent years. A PCM Material (Phase Change Material) is a substance that changes the state of a substance and provides latent heat when the temperature is constant. The process of transforming physical properties is called a phase change process, in which case the phase change material will absorb or release a large amount of latent heat.

Latent heat storage can be achieved through liquid→solid, solid→liquid, solid→gas and liquid→gas phase changes. However, only solid→liquid and liquid→solid phase changes are practical for PCMs. Although liquid-gas transitions have a higher heat of transformation than solid-liquid

transitions, liquid→gas phase changes are impractical for thermal storage because large volumes or high pressures are required to store the materials in their gas phase. Solid-solid phase changes are typically very slow and have a relatively low heat of transformation. [4] However, this PCM cannot be applied directly, and the problem of preventing its leakage needs to be solved in the encapsulation.

The commonly used encapsulation methods are (a) direct mixing, i.e., the phase change material is directly mixed into the layer of gypsum, cement, concrete, and insulation material, which is a relatively simple encapsulation method. For example, Athienitis et al [5] infiltrated the phase change material

For example, Athienitis et al [4] infiltrated the phase change material into gypsum board and then used the phase change material gypsum board in a passive solar test house. Neeper [6] infiltrated different ratios of fatty acids and paraffin wax into gypsum board to make a phase change gypsum board and studied the thermal properties of this phase change board. Li et al [7] dissolved an organic phase change material n-nineteen alkane and cement into water in the ratio of 1:4 and 1:1 by mass, respectively, and the phase change material would be dispersed into the pores of cement after drying to obtain a phase change material composite board.

(b) macroscopic encapsulation, that is, the phase change material is encapsulated inside a metal tube, plastic bag, etc., . For example, Medina et al [8] encapsulated the phase change material into copper tubes and then placed these copper tubes into the frame wall. Bontemps et al [9] used glass containers to encapsulate the phase change material. Zalewski et al [10] used polymer polyolefin material to encapsulate the phase change material in a brick-like structure. Silva et al [11] filled the phase change material into a steel capsule and then placed the capsule into the hole of the porous brick.

(c) Microscopic encapsulation. The phase change material is encapsulated in a microcapsule made of polymeric material with a small diameter (generally less than 1000  $\mu\text{m}$ ), which can better solve the leakage problem of phase change material.

In this section, a theoretical discussion is made on the materials of the massive wall, and water and PCM are selected as the materials of the massive wall, in comparison with the original Trombe wall system using 100mm concrete blocks. The aim was to optimize the use of composite Trombe wall in both summer and winter.

In the selection of PCM usage and location, the usage method was adopted from (a) and (b) above, in which (a) method, the PCM was mixed into the concrete block with 25% PCM, while (b) method reduced the PCM to a single layer of 40mm material in the simulation, which was laminated to different locations of the concrete. For the simulation method of water as the main material is also simplified as the whole sealed in a 3mm thick glass container, where the natural convection heat

transfer coefficient of water is taken as  $200 \text{ W}/(\text{m}^2 \cdot \text{K})$  and the thermal conductivity is taken as  $0.59 \text{ W}/(\text{m} \cdot \text{K})$  at standard atmospheric pressure of  $20^\circ\text{C}$ . The specific way is shown in Figure 6.3.1.

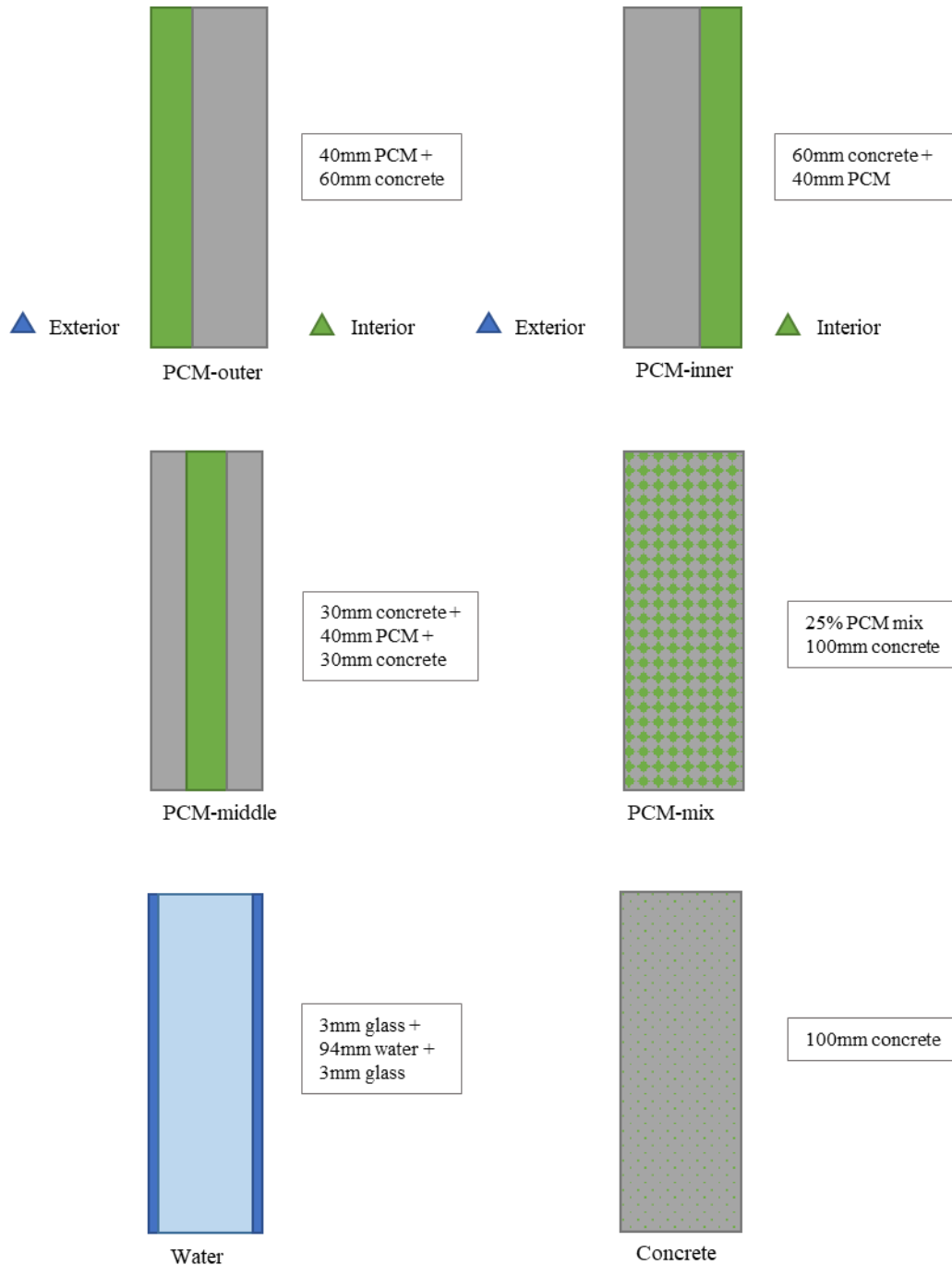


**Figure 6.3.1 Different massive wall material**

As for the selection of the phase change temperature of PCM, in general, the highest efficiency can be achieved when the phase change material can complete the phase change process once in a day. Figure 6.3.2 shows the temperature fluctuation curves of the interior side and exterior side surfaces of the massive wall for the most energy-efficient usage mode in the optimized composite

double-circulation Trombe wall system during the cooling and heating seasons. It is found that the surface temperature of the massive wall differs greatly from the expected one due to the different air circulation in the air layer of the Trombe wall system in summer and winter, and the maximum temperature in winter is much higher than that in summer, but the temperature fluctuates sharply, and the cooling at night or on cloudy days is obvious, and the temperature difference between day and night is large. In contrast, the fluctuation range in summer is small and the overall surface temperature of the wall is more stable under the action of the fan.

Table 6.1 shows the average surface temperature of the massive wall for each month in winter and summer, and it is found that the overall average temperature is close to each other despite the huge difference in temperature profile trends between winter and summer. In the case of using only a single layer of phase change material, the phase change temperature of the material can be considered to be around 30°C.

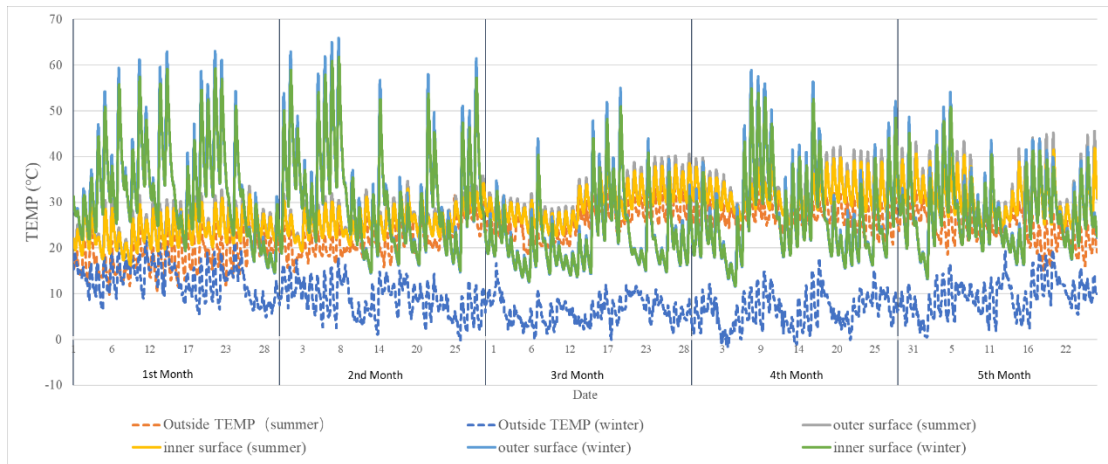


**Figure 6.3.2 Massive wall surface temperature in summer and winter**

**Table 6.1 Massive wall surface average temperature statistics**

	Summer		Winter	
	Outer Ave. TEMP	Inner Ave. TEMP	Outer Ave. TEMP	Inner Ave. TEMP
<b>May</b>	24.6°C	23.9°C	<b>Nov</b>	33.8°C
<b>June</b>	26.6°C	26.0°C	<b>Dec</b>	31.4°C
<b>July</b>	30.8°C	30.1°C	<b>Jan</b>	23.2°C

<b>Aug</b>	32.6°C	31.8°C	<b>Feb</b>	28.4°C	27.6°C
<b>Sept</b>	31.4°C	30.5°C	<b>Mar</b>	28.1°C	27.5°C
<b>Ave</b>	29.1°C	28.4°C	<b>Ave</b>	29.0°C	28.3°C

According to the statistical table in Chapter 2, eutectic inorganic hydrated salt (66.6%CaCl<sub>2</sub>·6H<sub>2</sub>O+33.4% MgCl<sub>2</sub>·6H<sub>2</sub>O) is selected as PCM with material phase transition temperature of 27.5°C, will be used as the massive wall material for this phase of the experiment, the phase transition temperature range is 26-29 °C and the reference parameters of this material are shown in Table 6.2.

**Table 6.2 PCM (66.6%CaCl<sub>2</sub>·6H<sub>2</sub>O+33.4% MgCl<sub>2</sub>·6H<sub>2</sub>O) material properties**

Parameters	Unit	Value
Melting Point	°C	27.5
Latent heat of fusion	J/kg	127000
Specific heat (solid)	J/kg·K	1568
Specific heat (liquid)	J/kg·K	2130
Specific weight (solid)	kg/m <sup>3</sup>	1802
Specific weight (liquid)	kg/m <sup>3</sup>	1562
Thermal conductivity (solid)	W/m·k	0.95
Thermal conductivity (liquid)	W/m·k	0.54

### 6.3.1. The effect of massive wall material in summer

First of all, for the summer season, Figure 6.3.3 shows the indoor temperature variation for different massive wall materials from May to September during the supply cooling season. As a whole, the materials in comparison have little effect in the summer, and in May, the indoor

temperature is even slightly elevated due to the exotherm during the PCM phase change due to the initial low temperature. Figure 6.3.4 shows the variation of indoor air temperature in August, and it can be noticed that PCM plays a role in the days from August 7 to August 9, and from August 15 to August 18. The effect is relatively more obvious in September (as shown in Figure 6.3.5). In contrast, the use of PCM as a material is more advantageous than the use of water as the main material of massive wall, and the use of mixing PCM into concrete blocks is relatively more efficient in terms of temperature performance in September.

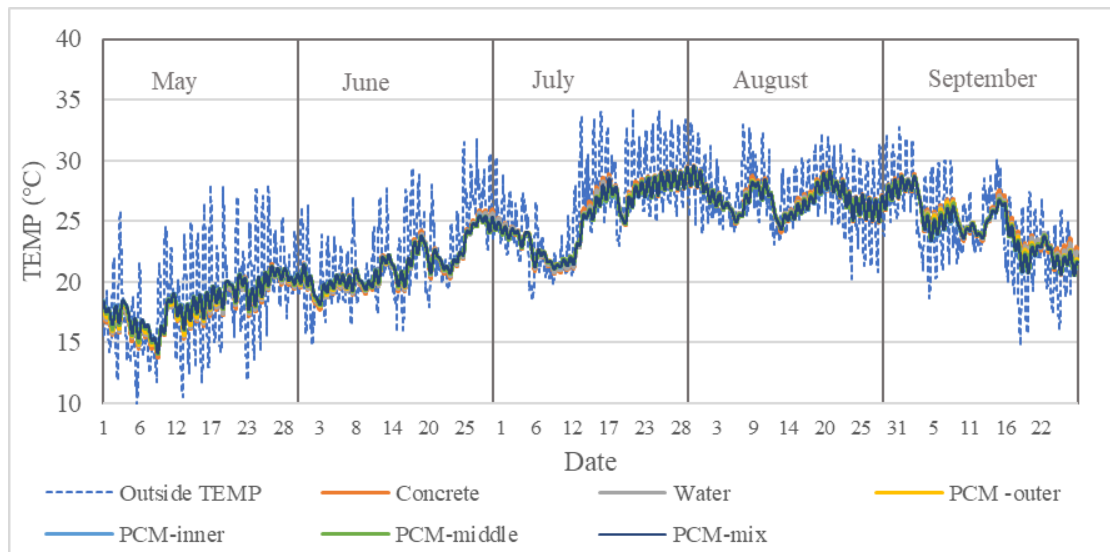


**Figure 6.3.3 Indoor temperature of different massive wall material in summer**

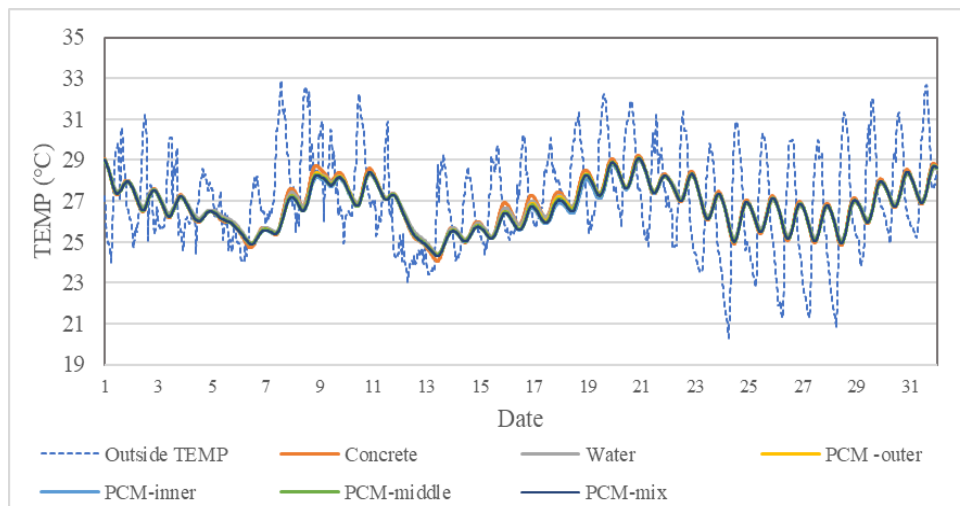


**Figure 6.3.4 Indoor temperature of different massive wall material in August**

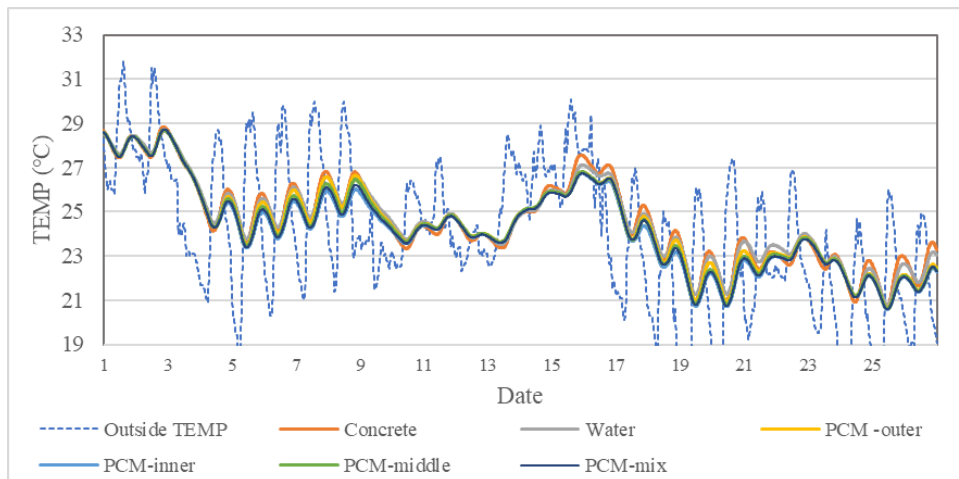


**Figure 6.3.5 Indoor temperature of different massive wall material in September**

Compare the energy consumption of different massive wall houses with air conditioning set to cool at 26°C throughout the day. Figure 6.3.6 shows the total energy consumption of air conditioning plus DC fans consuming electricity in August, the month with the highest summer temperature. The comparison reveals that using PCM as the material of massive wall has some energy saving effect in hot weather, and the effect of using static water inside the glass container under the closure is not significant. among the different placement of PCM, setting it on the interior side of the massive wall has relatively better effect. The next method of setting PCM mixed into concrete material. Figure 6.3.7 shows the total energy consumption of indoor air conditioning and DC fans throughout the summer. The overall energy consumption of several methods using PCM is similar, and the best comparison is on the outdoor side of the massive wall, but the energy savings is only about 6% compared to the concrete block.

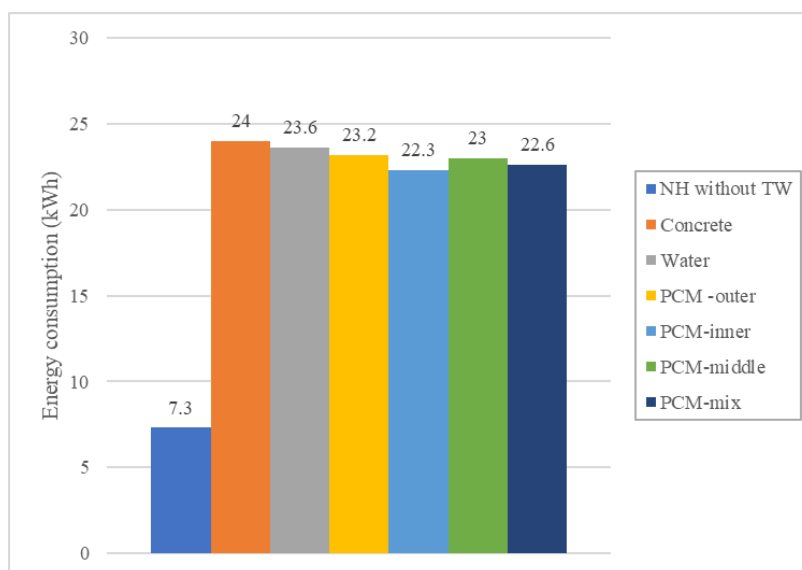


**Figure 6.3.6 Total energy consumption of different massive wall material in August**

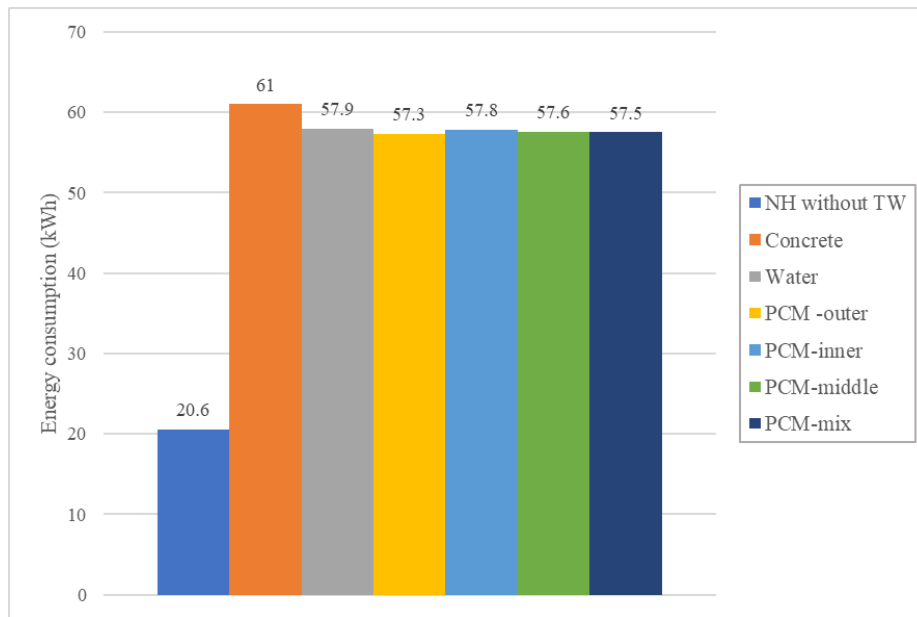


**Figure 6.3.7 Total energy consumption of different massive wall material in summer**

From the overall point of view, the effect of using static water or PCM as the massive wall material is not satisfactory in summer using the optimized composite double-circulation Trombe wall, one reason may be that the material, location and proportion of PCM is not suitable for this model. Another reason may be that the glazing surface of the optimized composite double-circulation Trombe wall is made of Low-E double-glazing glass, and the low-e film is in position 3#, in which the heat entering the room is much larger than the heat lost from the room, and this kind of glass itself is not suitable for summer use, which affects the results of the simulation experiment to some extent. To a certain extent, it affects the simulation experiment results.

### 6.3.2. The effect of massive wall material in winter

Comparing the winter situation, Figure 6.3.8 shows the indoor temperature fluctuations for the entire winter heating period, without air conditioning on, from November to March, under different massive wall materials. The comparison shows that the effect of using PCM is more obvious in winter, and the overall fluctuation of indoor temperature is reduced. The peak temperature under a large amount of solar radiation during the day was reduced, while the minimum temperature at night was increased. However, if we encounter continuous cloudy days with low solar radiation, the Trombe wall system has difficulty storing heat, as shown in Figure 6.3.10 between January 9 and January 15. During this period, the weather is continuously cloudy and rainy, the solar radiation is hardly available during the daytime, and the outdoor temperature gradually decreases. With PCM, it is still possible to keep the indoor temperature at a relatively high level during the first few days, but the overall decrease will be gradual until January 14 and January 15, when the indoor temperature drops below 10°C and is similar for all materials.

Figure 6.3.9 shows the variation of indoor temperature in a warmer November without air conditioning. The comparison shows that both the use of static water and PCM can suppress the high indoor temperatures during the day to some extent. For example, from November 5 to 6, and from November 20 to 21, the maximum temperature dropped from above 40 degrees Celsius to about 30 degrees Celsius. Figure 6.3.10 shows the situation in January, the coldest month. The comparison revealed that the composite Trombe wall system using static water as the primary material for the massive wall was slightly more effective than concrete blocks in colder climates, but was expected to be less efficient than with PCM. In several cases where PCM is used as the mass wall, the better results are PCM set on the outside surface of the room (PCM-outer) and PCM set on the middle layer (PCM-middle). the efficiency of PCM set on the inner layer and mixed such as concrete is relatively poor. Single are higher than using static water and concrete blocks.

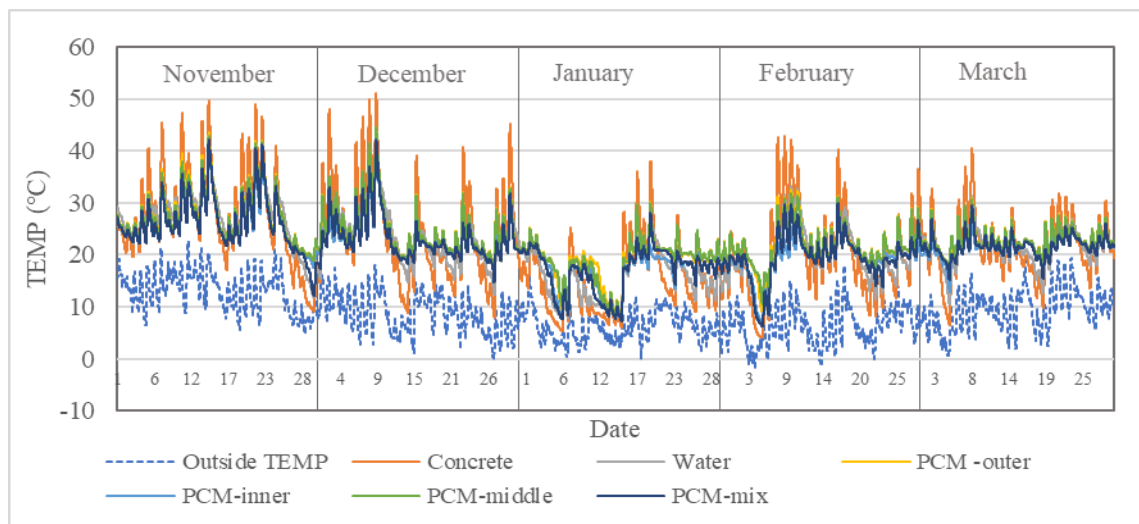


**Figure 6.3.8 Indoor temperature of different massive wall material in winter**

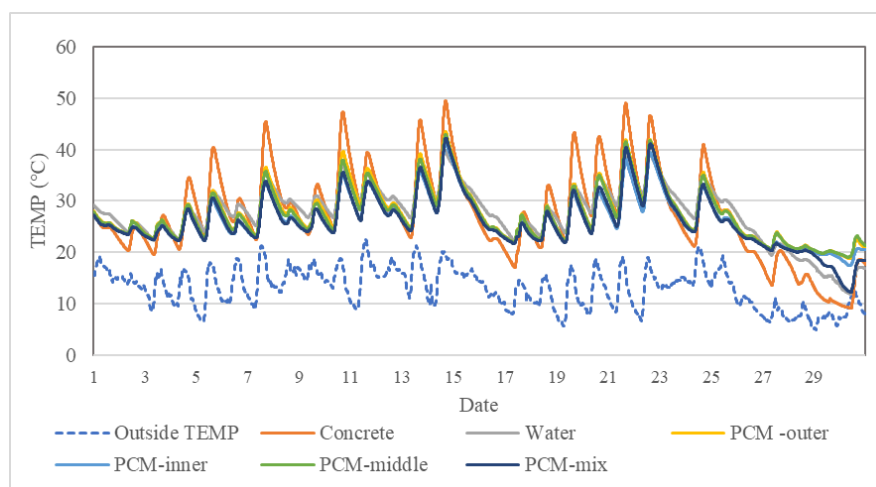


**Figure 6.3.9 Indoor temperature of different massive wall material in November**

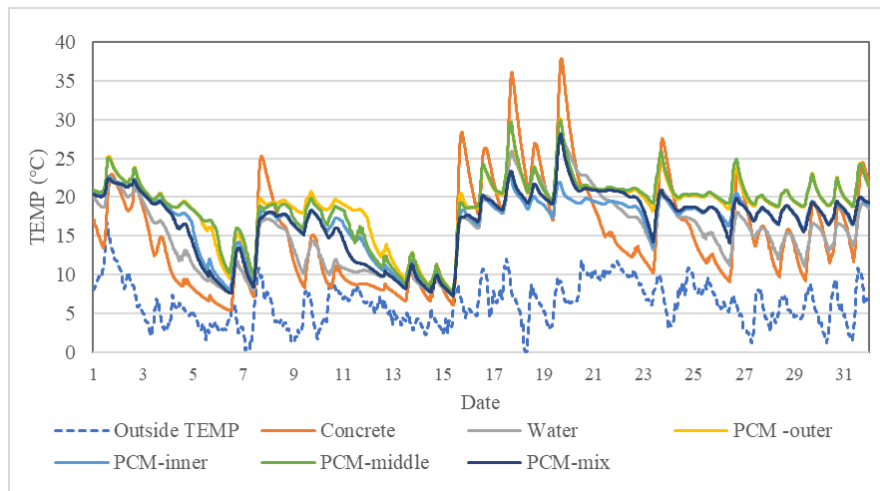
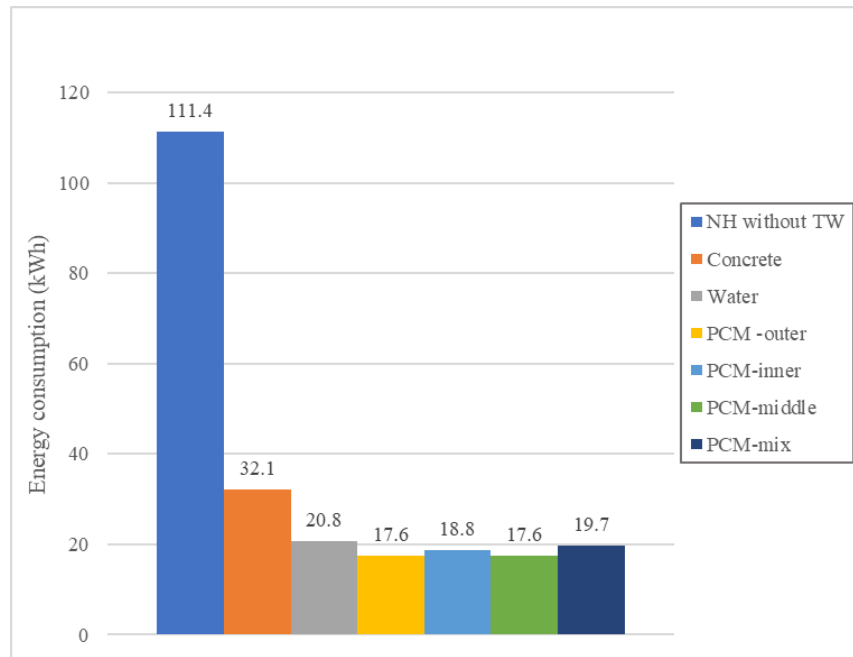


**Figure 6.3.10 Indoor temperature of different massive wall material in January**

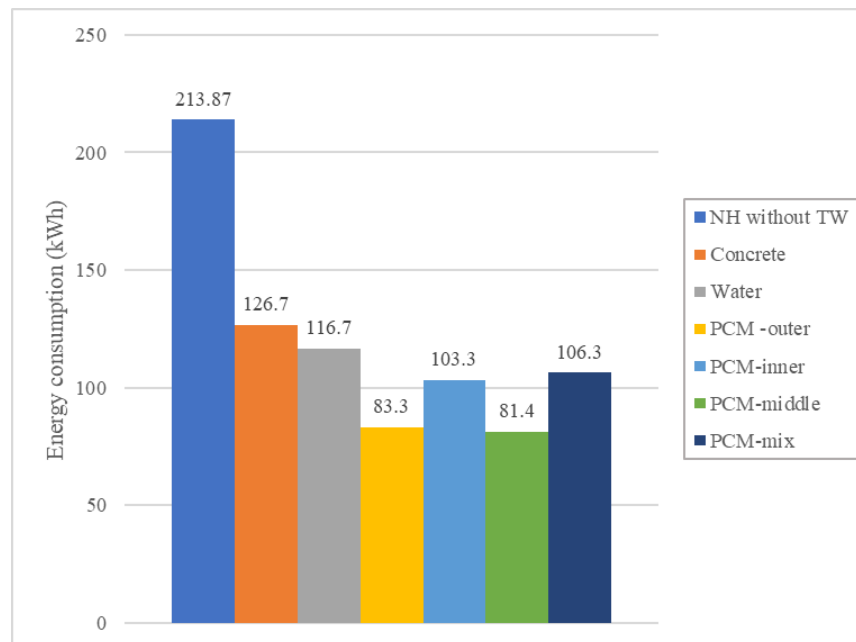
And comparing these two months, the energy consumption of turning on the room air conditioner all day long and the air conditioner temperature is set to 20°C, and adding the temperature-controlled DC fan (here the temperature control of the fan is set to 19°C, and the operation will be suspended if the temperature control point is less than 19°C, but the energy consumption of the fan is still calculated with the energy consumption of running all day long, except for the reference room where the Trombe wall system is not applicable, the energy consumption of the fan in a single month (transport is calculated with 9.5 kWh). Figure 6.3.11 shows the energy consumption comparison for the warmer month of November. It can be noticed that the air conditioning does not run for a long time in November and the difference in the total indoor energy consumption with the composite Trombe wall system is not very large. The use of static water and PCM as the massive wall material both have some energy saving effect. The best results in November are PCM-outer and PCM-middle, i.e. PCM set on the outside of the room of the massive wall and set between the concrete blocks, both with a total power consumption of 17.6 kWh. compared to the original house with concrete blocks, saving 45.3% of energy consumption. Compared with the reference house without Trombe wall, the energy consumption is 84.2%. The PCM-inner, where the PCM is installed on the interior side of the massive wall, has a total energy consumption of 18.8 kWh. The two methods of mixing the PCM into the concrete at 25% and using a glass container filled with static water perform relatively poorly, but both are better than using concrete blocks directly.

Figure 6.3.11 shows the comparison of energy consumption for the colder January months. The use of static water and PCM as the massive wall material both showed some energy savings. The best result in November is PCM-middle, with a total power consumption of 81.4kWh in both cases. Compared to the original house with concrete blocks, there is a 35.8% energy saving. Compared to the reference house without Trombe wall, it saved 61.9% of energy consumption. The PCM-outer is the next one, with a total energy consumption of 83.3 kWh, which is 34.3% less than in the

original concrete block house. The energy consumption of PCM-inner and PCM-mix is similar, with 103.3 kWh and 106.3 kWh, respectively. The water wall performs relatively poorly, but outperforms the direct use of concrete blocks, saving 7.9% of energy compared to the house with concrete blocks. The energy savings are 45.4% compared to the reference house without Trombe wall.



**Figure 6.3.11 Total energy consumption of different massive wall material in November**



**Figure 6.3.12 Total energy consumption of different massive wall material in January**

Two special representative days were selected individually for the analysis of indoor temperatures. One is January 19, which is a colder sunny day with an average daily temperature of 6.2 degrees Celsius, but with plenty of sunlight and solar radiation during the day. As can be seen in Figure 6.3.13(a), the interior of the different massive wall materials all started to rise after sunrise, with the concrete wall rising the fastest until the interior temperature rose to its highest point of over 35 degrees Celsius (interior overheating) just before sunset. However, the concrete walls also showed the fastest decrease in indoor temperature after sunset. The starting temperature of the concrete wall was the highest at 0:00 that day, but the indoor temperature of the concrete wall dropped to the lowest point until sunrise due to the low outdoor temperature at night and the absence of solar radiation. the indoor temperature of the house with PCM as the massive wall material rose slower than concrete during the day due to the solid to liquid phase change process that occurs in PCM during the day, and this phase change process heat absorption slows down the temperature rise of the wall as well as the air layer. Similarly, after sunset, the opposite exothermic phase change process occurs, which inhibits the rapid temperature drop to some extent. The overall interior of the house with water as massive wall material is gentler, unlike PCM, water is due to the large specific heat, its warming and cooling rate is slower. the curve of PCM-inner also shows a gentle on that day, but the indoor temperature can also be maintained almost above 20 °C.

Another representative day was on February 4 (as shown in Figure 6.3.13(b)), which was a cloudy day with an average daily temperature of only 0.7°C. Since the daytime does not provide a lot of solar radiation and the temperature-controlled DC fan stops running when the air layer temperature falls below 19°C, almost all types of indoor heat are continuously lost on that day, combined with the comparison of the internal and external air layer temperatures of the Trombe wall system with different materials for the massive wall shown in Figure 6.3.14, the concrete wall, the The internal and external air layers of the water wall and PCM-mix wall were below 19°C throughout the day, and the fans stopped running throughout the day, and the indoor air temperature always dropped steadily. Although the concrete wall was able to collect some heat even during the cloudy day because of its low thermal resistance, it was also unable to heat the air layer above 19°C, i.e. the fan was turned off and no heat transfer from the air layer to the room could take place. The initial indoor temperature of the concrete wall is the lowest, so the overall temperature is also the lowest. the temperature of the inner air layer of PCM-inner is higher than 19°C from 0:00 to 7:00, so its inner air circulation is turned on at that time, and the indoor heat loss is accompanied by a certain amount of heat input through the air circulation, and the rate of decline is slow. after 7:00, the fan that controls the air supply to the inner air layer is turned off, and the indoor temperature decreases faster. the fan of PCM The inner air layer fan of PCM-middle stopped working at about 20:00 at night, and the outer air layer fan stopped supplying air at about 16:00 in the afternoon, which corresponds to the first acceleration of the indoor temperature drop at 16:00, and the second decline and acceleration of the drop at 20:00. In contrast, the inner and outer air layer of PCM-middle is higher

than 19°C almost all day, the fan is always on, and the inner and outer air layers transfer heat at the same time, so the indoor temperature drops slowly and can maintain a relatively high temperature. However, in case of continuous rainy days, it is assumed that the indoor temperature of PCM-middle will continue to drop to a level similar to that of other types of houses.

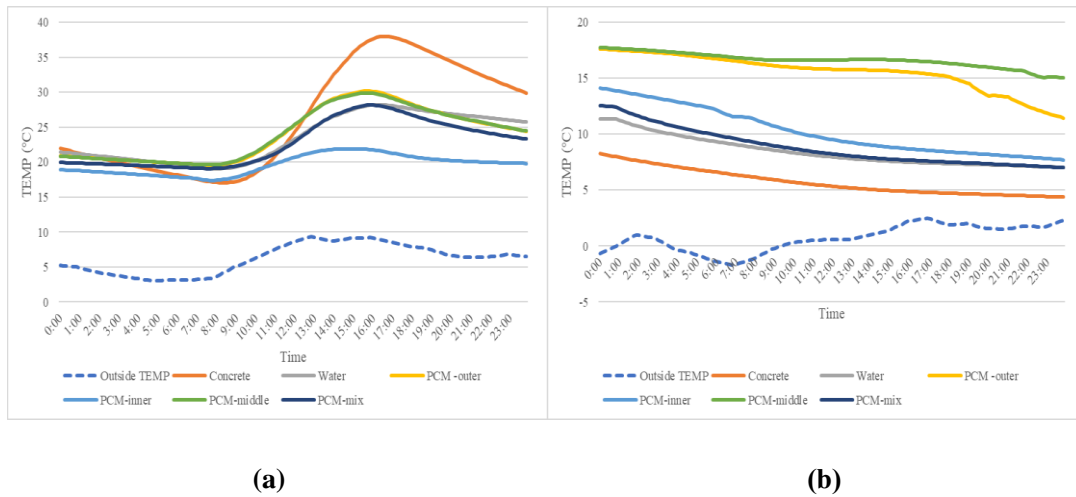


**Figure 6.3.13 Indoor temperature of different massive wall material: (a) On January 19<sup>th</sup>; (b) On February 4<sup>th</sup>**

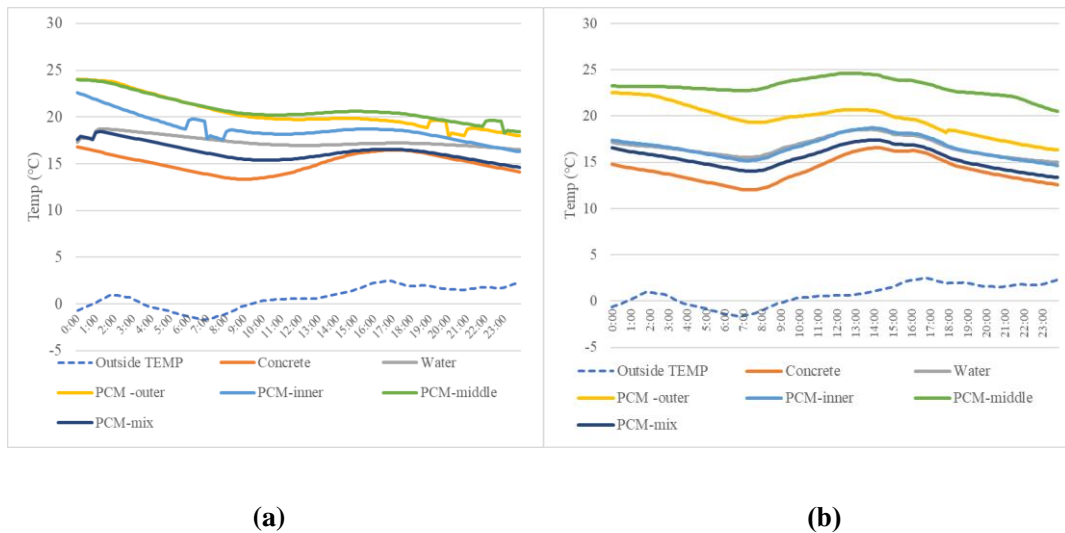


**Figure 6.3.14 Air layer of different massive wall material on February 4th: (a) Inner air layer; (b) Outer air layer**

Figure 6.3.15 shows the air conditioning heat load versus the total fan energy consumption for the entire heating season (here the fan energy consumption is calculated as being on all day and the total energy consumption for five months is 47.5 kWh). The use of static water and PCM as the massive wall material both have some energy saving effect. In terms of the overall year, the best result is PCM-middle, with a total power consumption of 237.0 kWh for both. Compared to the

original concrete block house, there is a 34.9% energy saving. Compared to the reference house without Trombe wall, it saved 75.2% of energy consumption. The PCM-outer is the next one, with a total energy consumption of 241.2 kWh, which is 33.7% less than in the original concrete block house. The energy consumption of PCM-inner and PCM-mix is similar, with a total of 289.4 kWh and 294.6 kWh respectively. The water wall performs relatively poorly, but better than the direct use of concrete blocks, with a total energy consumption of 306.7 kWh, a saving of 15.7% compared to the concrete block house. 15.7% of energy consumption compared to the concrete block house. The energy saving is 67.9% compared to the reference house without Trombe wall.

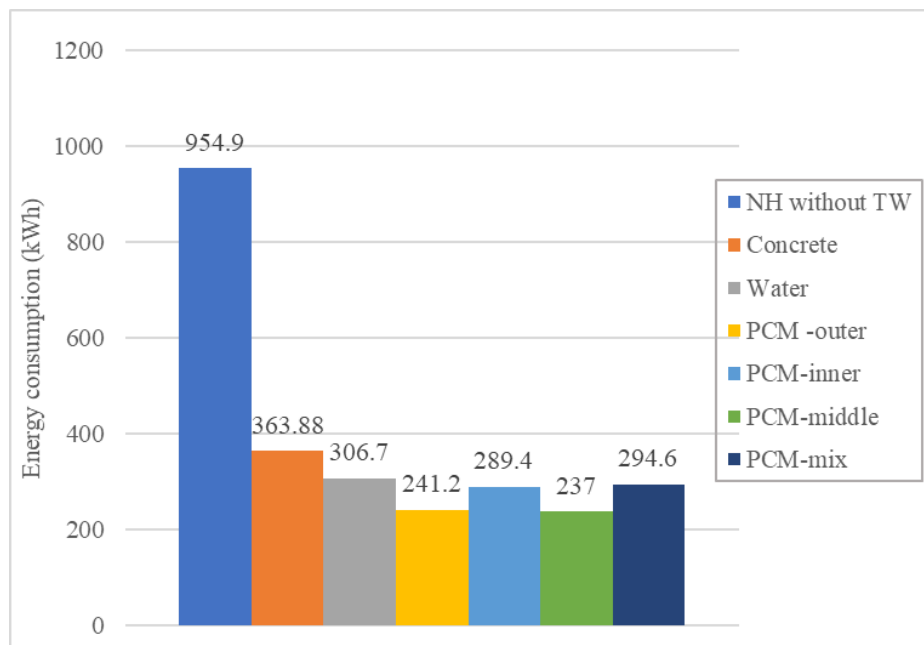


**Figure 6.3.15 Total energy consumption of different massive wall material in winter**

In the optimization of the massive wall to composite Trombe wall with concrete material, although in terms of energy consumption, a large amount of thermal load was saved, but in the final optimization results, the phenomenon of overheating in the room (the maximum temperature in the room exceeded 40 degrees Celsius or even approached 50 degrees Celsius) occurred in part of the daytime, which was not possible for a part of the overheating phenomenon to be cooled by the There is a risk for some users who cannot cool down the overheating phenomenon. Therefore, the improvement of the overall thermal comfort of the room is one of the issues of the composite Trombe wall system. In the previous comparison of indoor temperature, it was found that the peak temperature of the room was less than that of the concrete wall using glass-filled static water as the main material and using the addition of PCM. Further research experiments will be conducted to see if changing the material of the massive wall can eliminate the indoor overheating condition.

Figure 6.3.16 shows the indoor temperature variation curves for different massive wall materials

from November to March when the air conditioner is turned on all day and the temperature is controlled at 20°C. Since the air conditioner was turned on all day, the indoor temperature was kept above 20°C throughout the heating season. The comparison reveals that the state of indoor temperature exceeding 40°C occurs in every month for concrete wall, which is especially obvious in November and December, while the peak temperature decreases with water wall and PCM, but still exceeds 40°C. Figure 6.3.17 shows the graph of indoor temperature change in November when the average daily outdoor temperature was the highest. Concrete walls had 9 days in November when the maximum temperature exceeded 40°C, while it dropped to 3 days after changing the massive wall material, adopting water walls or adding PCM. Figure 6.3.18 shows the indoor temperature change in January, the month with the lowest average daily temperature of the year. From the graph, it is found that the concrete wall still has the indoor temperature over 30°C. Under the continuous sunny weather conditions, such as January 19, the indoor temperature is even close to 40°C in the state of turning on the air conditioner, and the PCM-middle with the second highest indoor temperature is 8.7°C lower than the concrete wall. But the overall maximum temperature will still exceed 30°C.

In the compared conditions, the highest temperature peak when the concrete wall, followed by PCM-outer and PCM-middle, is about 5°C lower than the peak of the concrete wall, however, the heat load comparison is also lower than the concrete wall.

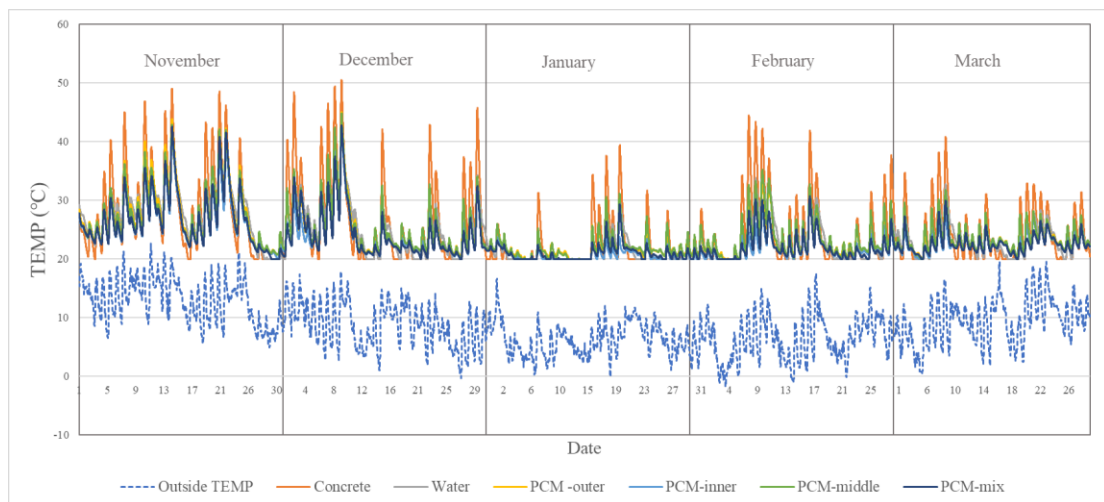


**Figure 6.3.16 Indoor temperature of different massive wall material in winter with heating**

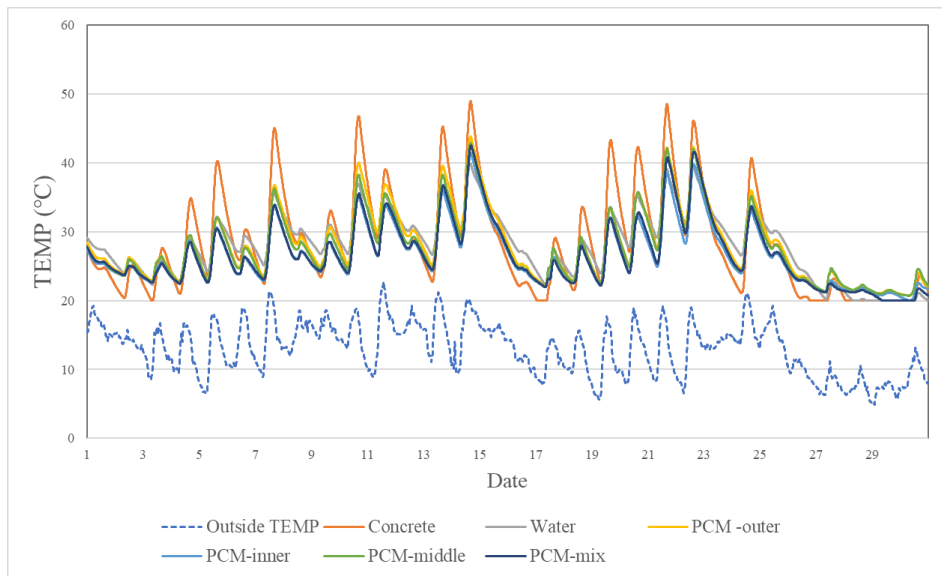


**Figure 6.3.17 Comparison of indoor temperature of different massive wall material in November with heating**

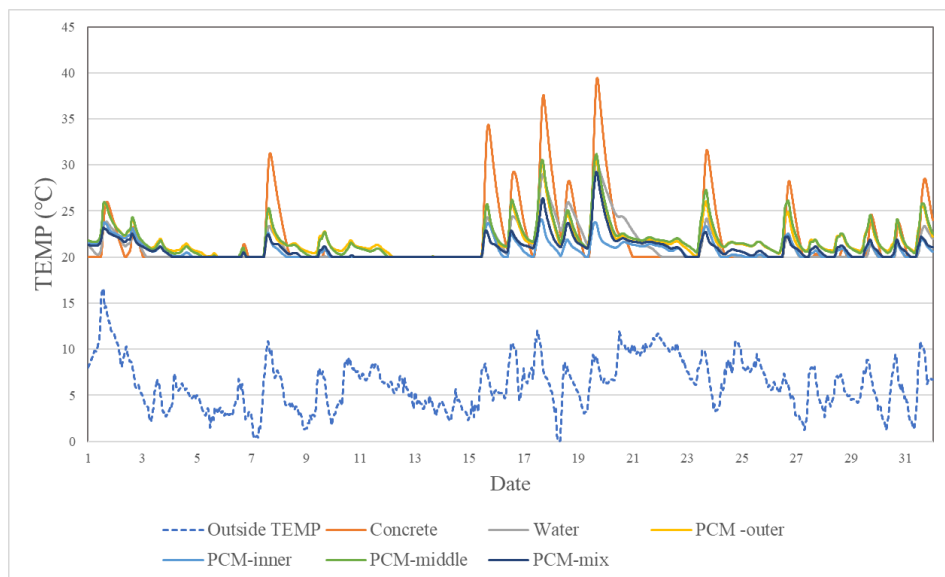


**Figure 6.3.18 Comparison of indoor temperature of different massive wall material in January with heating**

The evaluation of indoor thermal comfort of composite double-circulation Trombe wall system with different massive wall materials requires more specific values for analysis. Table 6.3 and Figure 6.3.19 show the indoor thermal comfort of different houses in the state of turning on the air conditioner all day, with the PMV value as the performance. Since the air conditioning was set to turn on all day, the indoor temperature of all houses was higher than 20°C, so there was no indoor thermal environment of overcooling, and their PMV was evaluated as greater than -1 (the actual calculated value was greater than -0.6). The lowest percentage of overheating time is PCM-inner

with 3.4% of the total time, followed by PCM-mix with 3.8%, and PCM-outer and PCM-middle with 6.2% and 6.3%, respectively. The most severe overheating was in the concrete walls, and changing the materials all improved their overheating, reducing the overheating time by more than 50%. Among all types, the highest percentage of PMV=0 makes PCM-outer, accounting for 57.3% of the total time. And the largest percentage of PMV values between -1 and +1 are PCM-inner and PCM-mix, accounting for 92.0% and 91.1%, respectively.

Figure 6.3.20 shows the predicted statistics of the PPD simulation for the indoor thermal environment with different massive wall materials. Since the air conditioner heating eliminates the indoor overcooling condition, the distribution of the dissatisfaction values of PPD is similar to the statistics of PMV. "The longest percentage of time with PPD less than 25% is PCM-outer, i.e., the condition where PCM is set at the exterior surface of the concrete massive wall indoor side, accounting for 56.8%. 86.3%. The use of water walls outperformed concrete walls, but not as much as the condition where PCM was set. Concrete wall has the worst thermal comfort in the comparison of several materials. Changing the material of the massive wall and using PCM did improve the thermal comfort of the interior.

**Table 6.3 PMV Statistics of different massive wall material with heating**

PMV	-3	-2	-1	0	+1	+2	+3
Concrete	0	0	38.50%	23.30%	14.80%	9.30%	14.10%
Water	0	0	30.80%	32.80%	18.70%	10.30%	7.40%
PCM -outer	0	0	11.80%	57.30%	17.40%	7.30%	6.20%
PCM-inner	0	0	24.30%	54.70%	13.00%	4.60%	3.40%
PCM-middle	0	0	13.30%	54.60%	18.20%	7.60%	6.30%
PCM-mix	0	0	23.40%	55.30%	12.40%	5.10%	3.80%

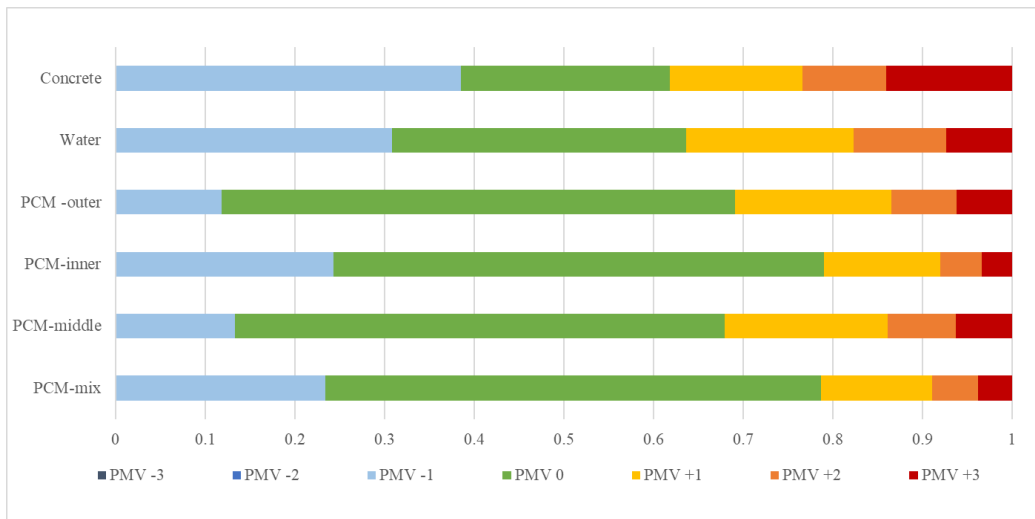


**Figure 6.3.19 PMV Statistics of different massive wall material with heating**

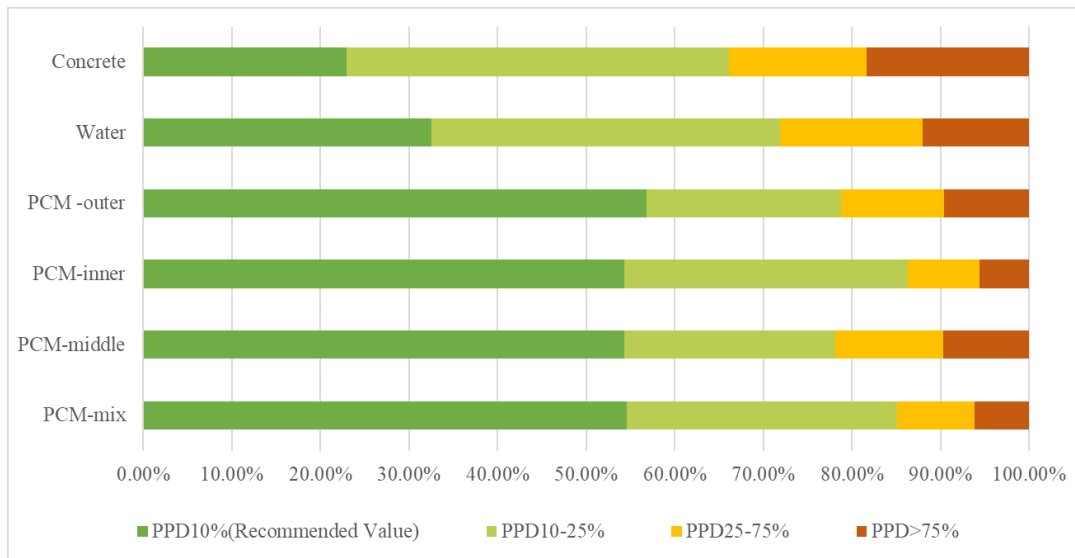


**Figure 6.3.20 PPD Statistics of different massive wall material with heating**

### 6.3.3. Conclusion

Combining the air conditioning load and fan energy consumption for cooling in summer and heating in winter (fans are calculated at 47.5 kWh in winter and 14.3 kWh in summer), the two total energy consumptions in the interior of the house with composite double-circulation Trombe wall system with different massive wall materials are shown in Figure 6.3.21. Although the total energy consumption of the composite double-circulation Trombe wall system is higher than the total energy consumption of normal house without Trombe wall (NH without TW) in summer, the efficiency of the optimized composite Trombe wall system is still much higher than that of NH without TW due to the good energy efficiency in winter. TW. According to the statistics, the total energy consumption of NH without TW is 975.5 kWh, the total energy consumption of concrete as massive wall material

is 424.9 kWh, that of water wall is 364.6 kWh, that of PCM-outer is 298 kWh, that of PCM-inner is 347.2 kWh, that of PCM-middle is 294.6 kWh, and that of PCM-mix is 352.1 kWh. The lowest total energy consumption is PCM-middle, which consumes 69.8% less energy than normal house, while PCM-outer and PCM-middle have similar energy-saving effects, consuming 69.4% less energy than normal house. PCM-inner, PCM-mix, water massive wall and concrete massive wall can reduce energy consumption by 64.4%, 63.9%, 62.6% and 56.4%, respectively.

Combined with the indoor thermal comfort environment in winter (indoor temperature is always below 26°C in summer when the air conditioner is turned on all day, such as summer is not discussed), the material and setting method of massive wall with the highest thermal comfort is PCM-inner, followed by PCM-mix, PCM-outer, PCM-middle, water massive wall and concrete massive wall from high to low. Combining the above two evaluations, under the experimental conditions, the most recommended one is PCM-inner, i.e., PCM (40mm 66.6%CaCl<sub>2</sub>·6H<sub>2</sub>O+33.4% MgCl<sub>2</sub>·6H<sub>2</sub>O) is set on the interior side surface of the massive wall.

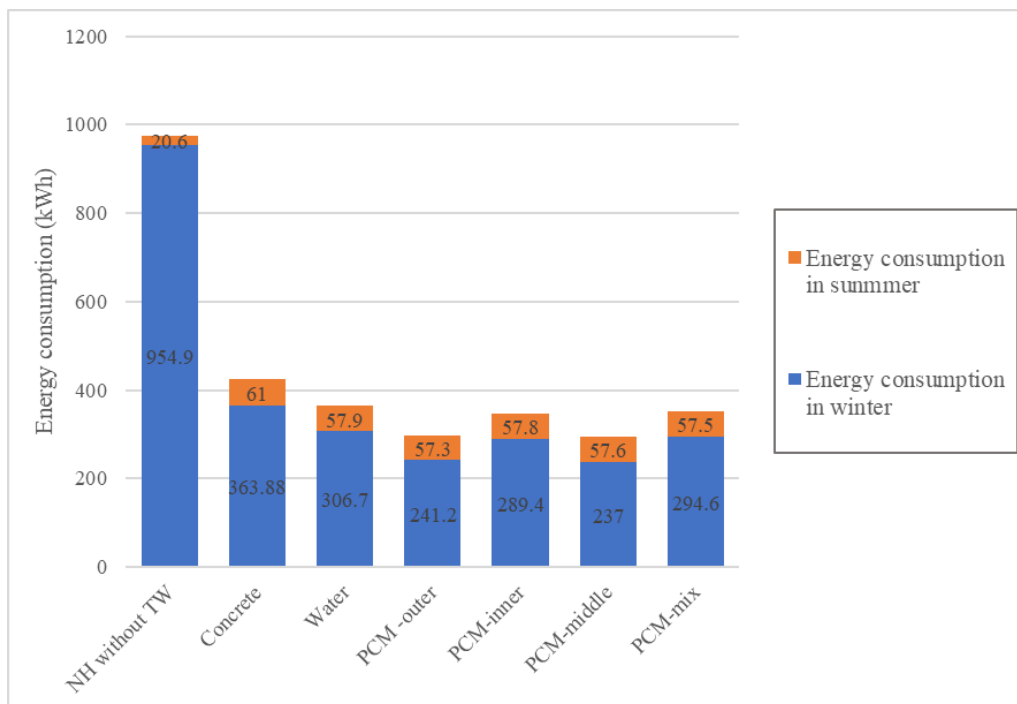


**Figure 6.3.21 Total energy consumption of different massive wall material**

**Table 6.4 Year-round statistics for different massive wall materials**

Material	Summer (kWh)	Winter (kWh)	Total (kWh)	Cut (%)	PPD <25% (winter)
NH without TW	20.6	954.9	975.5	-----	-----
Concrete	61	363.9	424.9	56.4%	66.1%
Water	57.9	306.7	364.6	62.6%	71.9%
PCM -outer	57.3	241.2	298.5	69.4%	78.8%
PCM-inner	57.8	289.4	347.2	64.4%	86.3%
PCM-middle	57.6	237	294.6	69.8%	78.1%
PCM-mix	57.5	294.6	352.1	63.9%	85.1%

#### 6.4. Discussion

This section discusses the countermeasures of the optimized composite Trombe wall for use in summer in the Kitakyushu region of Japan, and the thermal performance of different massive wall materials in summer in winter. The main object of reference in summer is a well-insulated shaded space that is impervious to light. Although the experiment was optimized to reduce energy consumption in comparison with itself, there is still a gap compared with the reference house. The summer countermeasures discussed in this chapter are mainly through changes in the existing conditions, i.e., adjusting the ventilation of the fan, without adding or subtracting other components in the composite Trombe wall system. The study speculates that one of the reasons why the composite Trombe wall system has difficulty in further reducing energy consumption in summer is the use of low-E double glazing for the glazing surface, which is suitable for winter use. In future studies of the composite Trombe wall for summer use, it may be possible to consider adding, subtracting, or replacing components where practical. For example, removing the glazing surface (in case the glazing surface can be opened, so that the massive wall is in direct contact with the outdoor environment); adding shading measures to the glazing surface, such as adding louvers, wings or overhanging parts, and also considering trying to make the low-E double glazing suitable

for winter use upside down. -E double glazing is inverted, so that the low-E film is located in 2# position to play the role of heat insulation.

And in this chapter, in the discussion of massive wall materials, only a single PCM type and ratio were tried, and although good results were achieved in winter, the results in summer were not as expected. In future research, experiments can be conducted on the phase change interval of multiple PCMs, and the thickness or mixing ratio of PCMs can be changed, and the dependent components can be changed (e.g., using metal filling, or set on other materials such as gypsum, insulation board). Experiments can also be performed with double-circulation PCM, i.e., two PCMs with different phase change temperatures, for winter and summer, respectively.

In addition, the discussion of materials in this chapter is mainly theoretical numerical simulation, and further empirical measurements are needed to verify the accuracy of its calculation method.

## Reference

- [1] Sodha M, Bansal N, Kumar K, Mali A. Solar passive building. United Kingdom: Persanon Press; 1986.
- [2] HU, Zhongting, et al. A review on the application of Trombe wall system in buildings. *Renewable and Sustainable Energy Reviews*, 2017, 70: 976-987.
- [3] Saadatian O, Chin L, Sopian K, Salleh E, Ludin N. Solar walls: the neglected components of passive designs. *Advanced in Environment, Biotechnology and Biomedicine* 2012:120–6.
- [4] Kenisarin, M; Mahkamov, K (2007). "Solar energy storage using phase change materials". *Renewable and Sustainable Energy Reviews*. 11 (9): 1913–1965.
- [5] Athienitis AK, Liu C, Hawes D, et al. Investigation of the thermal performance of a passive solar test-room with wall latent heat storage [J]. *Building and Environment*, 1997, 32(5) :405 -410.
- [6] Neepser D A. Thermal dynamics of wallboard with latent heat storage | J]. *Solar Energy*, 2000, 68(5): 393 - 403.
- [7] Li H, Liu X, Fang G Y. Preparation and characteristics of n-nonadecane/cement composites as thermal energy storage materials in buildings [J]. *Energy and Buildings*, 2010, 42(10); 1661 — 1665.
- [8] Medina M A, King J B, Zhang M. On the heat transfer rate reduction of structural insulated panels (SIPs) outfitted with phase change materials (PCMs) [J]. *Energy*, 2008, 33(4) :667 — 678.
- [9] Bontemps A, Ahmad M, Johannes K, et al. Experimental and modelling study of twin cells with latent heat storage walls[J]. *Energy and Buildings*, 2011, 43(9): 2456 - 2461.
- [10] Zalewski L, Joulin A, Lassue S, et al. Experimental study of small-scale solar wall integrating

phase change material[J]. Solar Energy, 2012, 86(1): 208-219.

[11] Silva T, Vicente R, Soares N, et al. Experimental testing and numerical modelling of masonry wall solution with PCM incorporation; a passive construction solution[J]. Energy and Buildings, 2012,49(2). 235 - 245.

## *Chapter 7*

# ***CONCLUSION, DISCUSSION AND FUTURE WORK***



**CHAPTER 7: CONCLUSION, DISCUSSION AND FUTURE WORK**

*CONCLUSION, DISCUSSION AND FUTURE WORK* ..... 7-1

7.1 Conclusion ..... 7-1

7.2. Discussion and future work..... 7-4



## 7.1 Conclusion

This research mainly focuses on a new composite Trombe wall, which adds a layer of thermal insulation wall to the traditional Trombe wall to form two air layers. At the same time, pipes and air vents at upper and down are used to connect the two air layers and the room, so that the composite Trombe wall forms two air circulations as inner and outer. The air circulation is forced to be stable and fast by using temperature-controlled DC fans. The study evaluated the thermal potential of this composite Trombe wall by using THERB for HAM software which has been approved by the Japanese government as an evaluation method for annual heating and cooling load calculation methods.

A composite Trombe wall assisted by a temperature-controlled DC fan can achieve better energy savings compared to a classic Trombe wall with thermal air conditioning. However, the overall room temperature of the composite Trombe wall is smaller than that of the classical Trombe wall in the absence of air conditioning.

The most obvious energy saving effect is the change of window type. Low-E double-glazing can play a very good role in insulation because of its characteristics, but the effect will be different if the Low-E layer is set in the different positions. Compared to single-glazing, double-glazing with a 3#Low-E layer is expected to save nearly 41.3% of energy. It is expected to save nearly 41.3% of the annual heat load. Energy savings can also be achieved with ordinary multi-panel glass, with double and triple glazing saving 17.2% and 27.9% of energy consumption, respectively. 2# Low-E double-glazing is between triple insulating glass and double insulating glass in terms of energy efficiency. Within a certain range, the higher the ventilation volume, the higher the heat load that can be saved. Under existing conditions, a ventilation volume of 140 m<sup>3</sup>/h can save 22% of energy compared to the case with no air circulation. The thermal resistance of the inner wall material affects the efficiency of the Trombe wall. In regions with long warm winter periods, materials with lower thermal resistance are suitable, while climates with long cold winter periods are more recommended to use materials with higher thermal resistance. In the Kitakyushu region of Japan, it is more appropriate to use insulation materials with low thermal resistance such as GW16 and Styrofoam board for the inner wall when only the air conditioning is turned on at night. Because glass wool materials are relatively expensive and do not yield more significant benefits, the use of Styrofoam boards is more appropriate than other materials used in the simulation experiments. The thickness of the inner wall, i.e., the proportion of the area occupied by the inner wall, also affects the efficiency of the Trombe wall. Simulations show that a Styrofoam board panel as inner wall of 120mm thickness can save most energy. However, since the energy savings are not high, it is recommended to use 60mm Styrofoam board panel for the inner wall thickness from the cost point of view. The thickness of the massive wall, i.e., the proportion of the area occupied by the massive wall, also affects the efficiency of the massive wall. Simulations show that a concrete massive wall percentage

of about 3% of room area is a better choice.

In winter, the selection of the material of the massive wall, compared to the concrete material of the massive wall, the use of static water in a glass jar or a material with a suitable phase change temperature (PCM) not only reduces the heat load of the air conditioner, but also reduces the peak temperature of the room during the day. At the same time, the thermal efficiency of the Trombe wall varies depending on where the PCM is set. From the viewpoint of energy saving, the most efficient one is setting PCM (40mm 66.6% CaCl<sub>2</sub>-6H<sub>2</sub>O+33.4% MgCl<sub>2</sub>-6H<sub>2</sub>O) in the middle of concrete slab (PCM-middle), which can save 69.8% more energy than normal house without Trombe wall.

The choice of Glazing surface ratio requires a larger choice of glazing surface to massive wall ratios (G/M) if the efficiency of the Trombe wall is given priority. If there is a demand for indoor thermal comfort, a lower glazing surface to ratios ratio can be chosen. Due to the smaller size of the numerical model used for the experiments, the glazing surface to floor area ratios (G/F) are consequently reduced considering the actual room usage area. The results of the simulation experiments show that the value of glazing surface to floor area ratios decreases and the heat load per unit area of the room grows while keeping the ratio of G/M at the maximum, i.e., the highest efficiency of the Trombe wall, and the value of G/F at less than 0.4 without adding other room components (e.g., windows, etc.), the overheating of the room The situation is improved.

To convert the magnitude of the impact of each variable into a more intuitive value for comparison a relative reference result can be calculated from the following equation. Impact factor (IF):

$$IF = \frac{Heatingloadcut_{max}-Heatingloadcut_{min}}{Heatingloadcut_{max}+Heatingloadcut_{min}} \quad (1)$$

According to the calculation results in Table 7.1, under the base conditions of this study (based on a field-built wooden house in the Yahata area of Kitakyushu, Japan), the most influential factor on the simulated installation of the composite double-circulation Trombe wall system in the study house is the nature of the glazing surface, including the material (glass type) selection and setting ratio, etc. Choosing the right type of glass, setting direction, setting ratio, etc. can greatly improve the efficiency of the Trombe wall system and have a significant effect on the reduction of energy consumption in the house, especially the reduction of heat load in winter. The second is the rate of DC fan. The use of temperature-controlled assisted DC fan to force air to the inner and outer air layers of the composite double-circulation Trombe wall system is one of the innovations of the design, and the efficiency of the fan also has an important impact on the efficiency of the Trombe wall. The choice of material for the massive wall in winter also has an impact on the composite double-circulation Trombe wall system. The use of special materials such as PCM not only reduces energy consumption, but also reduces the peak indoor temperature and improves thermal comfort. Similarly, the choice of material for the inner wall is also important, and the recommended choice

of material is different for different climatic conditions. And the impact of massive wall and inner wall on the energy efficiency of composite double-circulation Trombe wall system under the current experimental conditions is relatively small.

**Table 7.1 Energy saving statistics of different Variables in winter**

Variables		Heating load (kwh)	Energy cutting (With NH) (%)	Impact factor
Glazing types	Max	568.14	32.1%	0.30
	Min	333.34	60.1%	
DC fan rates	Max	650.3	22.3%	0.27
	Min	506.79	39.4%	
Inner wall materials	Max	607.18	27.4%	0.08
	Min	565.7	32.4%	
Inner all thickness	Max	577.76	30.9%	0.03
	Min	564.04	32.6%	
Massive wall thickness	Max	587.87	29.7%	0.04
	Min	568.14	32.1%	
Glazing surface to massive wall ratios*	Max	513.11	34.4%	0.31
	Min	270.84	65.4%	
Massive wall materials**	Max	383.90	56.4%	0.11
	Min	237.00	69.8%	

\* This part of the study is based on the optimized composite Trombe wall system

\*\* This part of the study is based on an optimized composite Trombe wall system and the air conditioning mode is all-day mode

In the study of the summer thermal performance of the Trombe wall system, the use of the winter fan operation scheme leads to severe indoor overheating and generates high energy consumption. However, due to the thermal insulation of the inner wall in the composite double-circulation Trombe wall system, a relatively stable indoor temperature can be maintained in summer after the direct heat transfer is blocked by turning off the fan, and changing the ventilation of the fan can further reduce the indoor energy consumption. Under the experimental conditions, the total energy consumption is lowest in May and June when the fan can be left on, and from July to September when only the inner-air layer-outer ventilation is used.

## 7.2. Discussion and future work

In this study, optimization predictions were performed using the establishment of numerical model simulations based on a field-built reference room for experiments. The limitation of this study is that the space of the experimental room is small, so the results are only a relative result and cannot be directly put into practical applications for discussion. Similarly, the range of values selected for the comparison conditions chosen is small due to the small volume of the laboratory. The numerical comparison of the variables does not necessarily reflect the optimal solution in the real case. Another important point to note is that the general rooms, both office and residential, have additional transparent windows that can transmit light and can be opened, which is different from the glazing surface of the Trombe wall system across the massive wall. According to the comparison and speculation of sunroom in the previous section, after the addition of the window component, the peak temperature of the room will increase further during the daytime on a sunny day without curtains or other shading devices. Therefore, when considering the proportion of Trombe wall, users should also pay attention to the priority of energy saving or thermal comfort.

In the summer experiment, although the experiment was optimized to reduce energy consumption compared to itself, it still falls short compared to the reference house. The summer countermeasures discussed in this chapter are mainly through changing the existing conditions, i.e. adjusting the ventilation of the fans, without adding or reducing other components in the composite Trombe wall system. This study speculates that one of the reasons why composite Trombe wall systems struggle to further reduce energy consumption in the summer is the use of low-e double glazing for the glazing surfaces, which is suitable for use in the winter. In future studies of composite Trombe walls for summer use, consideration could be given to adding, reducing, or replacing components where feasible. For example, removing the glass face (where the glass face can be opened, leaving the massive wall in direct contact with the outdoor environment); adding shading measures to the glass

face, such as adding blinds, wings, or overhanging sections, and also considering trying to make low-E double glazing suitable for winter use inverted. -E double glazing inverted so that the low-e film is located in position 2# to provide insulation.

In the discussion of massive wall materials, only a single PCM type and ratio was attempted, and while good results were achieved in winter, the results in summer were not as good as desired. In future research, experiments can be conducted with multiple PCM phase change intervals, which can vary the thickness or mixing ratio of PCM and change the slave composition (e.g., using metal fillers, or set on other materials, such as gypsum or insulation board). Experiments can also be performed with double-layered PCM, i.e., with two PCMs having different phase change temperatures, in winter and summer, respectively.

At the same time, the continued prevalence of COVID-19 poses new challenges for future building design and environmental engineering. In the initial stage of building design, more epidemic prevention and isolation are added. For aerosol-borne diseases like COVID-19, the use of high temperature and air circulation between air layers, or the installation of other disinfection and sterilization equipment can also be considered in the Trombe wall system to purify the indoor air environment.